7. POSTCLOSURE SAFETY ASSESSMENT – CONTAMINANT TRANSPORT

This chapter, together with Chapter 8, presents an illustrative postclosure safety assessment for a used fuel repository located in the sedimentary rock of the Michigan Basin. This chapter focusses on liquid-borne contaminant transport, where 'contaminant' includes both radionuclides and stable elements. Chapter 8 focusses on gas transport.

The purpose of a postclosure safety assessment is to determine the potential effects of the repository on the health and safety of persons and the environment during the postclosure period. The assessment timeframe is one million years based on the time period needed for the radioactivity of the used fuel to decay to essentially the same level as that in an equivalent amount of natural uranium. This timeframe is also within a reasonable extrapolation of the geological stability of these rocks. However, due to the very good retention properties of the sedimentary rock, the peak impacts may occur beyond one million years. Analyses presented here include an approximate extension beyond one million years to demonstrate that the peak impacts remain well below the interim acceptance criteria.

The assessment is conducted by applying computer models to a range of analysis cases. The analysis cases here examine the Normal Evolution Scenario and some of the Disruptive Scenarios identified in Chapter 6, together with a series of sensitivity studies performed to examine the importance of various model features and assumptions.

The assessment is arranged as follows:

- Section 7.1 – Interim Acceptance Criteria: four sets of interim acceptance criteria are presented against which the radiological and non-radiological impacts on persons and the environment assessed.
- Section 7.2 – Scope: provides a detailed description of the analysis cases together with the rationale for their selection. Included is a brief discussion of items excluded from the scope but which might otherwise be included in a licence submission.
- Section 7.3 – Conceptual Model: discusses the conceptualization of the repository evolution.
- Section 7.4 – Computer Code: introduces the main computer codes used.
- Section 7.5 – Analysis Methods and Key Assumptions: the computer code representations created for this study are described in detail. Some numerical data are presented to provide context.
- Section 7.6 – Results of Radionuclide and Chemical Toxicity Screening Analysis: discusses the set of potentially significant radionuclides and chemical elements included in the study.
- Section 7.7 – Results of Detailed 3D Groundwater Flow and Transport Analysis: discusses 3D simulations of groundwater flow and radionuclide transport for I-129, Cs-135, U-234 and U-238.
- Section 7.8 – Results of System Model: discusses deterministic and probabilistic (i.e., Monte Carlo) simulations of radionuclide release, transport and impact for all radionuclides of potential interest identified in Section 7.6.

- Section 7.9 – Disruptive Scenarios: describes the analysis and presents results for those Disruptive Scenarios included in the scope of this study.
- Section 7.10 – The Effects of Glaciation on the Normal Evolution Scenario: uses results of the regional glaciation modelling studies described in Chapter 2 to draw conclusions on the likely effects of glaciation on the dose consequences for the Normal Evolution Scenario.
- Section 7.11 – Other Considerations: describes two complementary indicators for radiological safety, results for the radiological protection of the environment, and results for the protection of persons and the environment from hazardous substances (including results for one complementary indicator).
- Section 7.12 – Summary and Conclusions.

7.1 Interim Acceptance Criteria

This section presents interim acceptance criteria applicable to the postclosure safety assessment. These criteria are used to judge the acceptability of analysis results.

CNSC Guide G-320 (CNSC 2006) identifies the following categories of acceptance criteria:

1. Radiological protection of persons;
2. Protection of persons from hazardous substances;
3. Radiological protection of the environment; and
4. Protection of the environment from hazardous substances.

Interim acceptance criteria defined for each category are discussed in the following sections. These criteria are consistent with current Canadian and international practice; however, it is recognized that the criteria used in a licence application will need to be accepted by the CNSC at that time, and may be different from the specific values identified here.

7.1.1 Interim Acceptance Criteria for the Radiological Protection of Persons

The main objective of the postclosure safety assessment is to provide reasonable assurance that the regulatory radiological dose limit for public exposure (1 mSv/a) will not be exceeded. To account for the possibility of exposure to multiple sources, a dose constraint below the regulatory limit is adopted.

For the Normal Evolution Scenario, the interim dose acceptance criterion is:

- An annual individual effective dose rate of 0.3 mSv/a with the calculation performed to encompass the time of maximum predicted impact to the average adult member of the critical group.

The 0.3 mSv/a dose constraint is consistent with recommendations of the International Commission on Radiation Protection (ICRP) and IAEA guidance (ICRP 2007, ICRP 2013, IAEA 2006) and is significantly less the average Canadian individual dose rate of 1.8 mSv/a received from background radiation (Grasty and LaMarre 2004).

At this dose level, there is no clear evidence for adverse health effects (NRC 2006, CNSC 2011). However, the Linear-No-Threshold model recommended by international agencies (ICRP 2013) and adopted by Canadian regulators assumes that any dose exposure results in some increase in health risk, notably cancer. This dose constraint ensures that the health risks are small in comparison to the risk from natural background radiation, and to the risk of cancer from all causes.

Calculating the exposure of an adult member of the critical group is consistent with ICRP recommendations which recognize that any exposures are expected to occur in the distant future, any exposure would be associated with levels of radionuclides in the environment that change slowly over the time scale of a human life time, and the calculated exposures at long times have inherent uncertainties (ICRP 2013). Effective dose rates are calculated using the dose coefficients from ICRP 72 (ICRP 1995), which are based on a human model that includes male and female organs to ensure it includes all radionuclide sensitivities.

For Disruptive Scenarios, the interim acceptance criteria are:

- An annual individual effective dose rate target of 1 mSv/a for credible chronic[1] release scenarios with the calculation performed for the average adult member of the critical group; and
- Acceptability of any scenario with the calculated annual individual effective dose rate for chronic releases exceeding 1 mSv/a to be examined on a case-by-case basis taking into account the likelihood and nature of the exposure, uncertainty in the assessment and conservatism in the dose criterion. Where the probability of exposure can be quantified without excessive uncertainty, a measure of risk will be calculated based on the probability of exposure and the consequent health effects. This is compared with a reference risk value of 10^{-5}/a.

A dose rate of 1 mSv/a corresponds to the current radiological limit for exposure of the public. This is less than the 1.8 mSv/a. average natural background dose rate for Canadians.

The reference health risk value of 10^{-5}/a is consistent with ICRP (2013) and IAEA (2006). Based on the ICRP probability coefficient of 0.057 per Sv for stochastic effects (e.g., cancers or hereditary effects) (ICRP 2007), this corresponds to a health risk about a factor of 10 lower than the risk from the natural background dose rate.

Regulatory document G-320 (CNSC 2006) and ICRP (2013) recognize that inadvertent human intrusion into a repository could result in doses greater than 1 mSv/a since human intrusion by definition bypasses the repository barriers. The risk from human intrusion is made low by the site selection criteria which require the facility to be located deep underground in an area known not to have economically exploitable natural resources or potable groundwater resources at repository depth. Institutional controls will also reduce risk in the short-term, when the hazard is highest.

[1] Chronic refers to a release that is sustained over many years.

7.1.2 Interim Acceptance Criteria for the Protection of Persons from Hazardous Substances

For this category, the interim acceptance criteria are based on Canadian guideline values for concentrations in environmental media relevant to human health and environmental protection, supplemented as needed.

The values are shown in Table 7-1. The criteria are based on federal and provincial guideline concentrations for surface water, groundwater, soil and sediment, and in particular Canadian Council of the Environment (CCME 2007 a, b, c and CCME 2002). In cases where federal guidelines do not currently exist, Ontario Ministry of the Environment guidelines (MoE 2011a, MoEE 1994) and Oregon Department of Environmental Quality (ODEQ, 2001) have been adopted as interim acceptance criteria. Depending on the actual site location, the applicable provincial guidelines would be used.

The values have been reviewed to determine the effect of updates to the original source documents. All values remain conservative.

Estimated environmental concentrations of contaminants are compared with the above interim acceptance criteria. Additive effects are not considered in this stage. If any concentrations exceed the criteria in the Normal Evolution Scenario, these contaminants are assessed further in a tiered approach with decreased conservatism in the models. If any concentrations exceed these criteria for Disruptive Scenarios, acceptability is judged on a case-by-case basis taking into account the likelihood and nature of the exposure, uncertainty in the assessment and conservatism in the criteria.

Table 7-1: Interim Acceptance Criteria for the Protection of Persons and the Environment from Non-Radiological Impacts

Chemical Hazard Criteria					
Element	**Background Groundwater [µg/L]**	**Potable Groundwater [µg/L]**	**Surface Water* [µg/L]**	**Soil [µg/g]**	**Sediment [µg/g]**
Ag	0.3	1.2	0.1	0.5	0.5
Al	-	-	5	50	-
Ba	610	1000	4	210	-
Be	0.5	4	11+	2.5	-
Bi	-	-	150	20	-
Cd	0.5	2.1	0.017	1	0.6
Ce	-	-	22	53	19000
Co	3.8	3.8	0.9	19	50
Cr	11	50	1	0.4	26
Cs	-	-	450	-	-
Cu**	5	69	5	62	16
Eu	-	-	10.1	50	4700
Hg	0.1	0.29	0.004	0.16	0.17
La	-	-	10.1	50	4700
Mo	23	70	40	2	-
Nd	-	-	1.8	50	7500
Ni	14	100	25	37	16
P	-	-	4	-	-
Pb	1.9	10	1	45	31
Pd	-	-	200	-	-
Pr	-	-	9.1	50	5800
Sb	1.5	6	20+	1	3
Se	5	10	1	1	-
Sm	-	-	8.2	5	-
Sr	-	-	1500	33000	-
Te	-	-	20	250	-
U	8.9	20	5	1.9	-
V	3.9	6.2	6	86	-
Y	-	-	6.4	50	1400
Zr	-	-	4	97	-

Notes: '-' indicates that there are no defined criteria for that element in the given medium.

* Surface water values differ from groundwater values because the surface water values protect biota and humans, whereas groundwater values protect humans only (i.e., biota (other than microbes) do not live in groundwater). Differences arise for Be and Sb because different references are used for different values.

** The Cu value is for water with a $CaCO_3$ content > 20 mg/L

+: These values are greater than their associated groundwater values because of different source documents.

Detailed information on the individual source documents is available in Gobien et al. (2013)

7.1.3 Interim Acceptance Criteria for the Radiological Protection of the Environment

For radiological protection of the environment, the interim acceptance criteria are based on dose benchmarks developed for the assessment of priority substances in relation to discharges of radionuclides from nuclear facilities.

No-Effect Concentrations are derived from Estimated No Effect Values (ENEVs) for the most limiting indicator species relevant to the Southern Canadian Deciduous Forest ecosystem, the Boreal Forest ecosystem and the Inland Tundra ecosystem. For every indicator species, the radionuclide concentration that corresponds to the ENEV is calculated for each medium (i.e., surface water, soil, and sediment) assuming zero radionuclide concentration in other media. The lowest concentration from all indicator species is then selected as the No-Effect Concentration for that radionuclide. The interim acceptance criteria are shown in Table 7-2.

If any radionuclide concentration exceeds the No-Effect Concentration in the Normal Evolution Scenario, an Ecological Risk Assessment will be carried out for that radionuclide, taking into account uncertainties and potential need for the effect of several radionuclides to be summed into account. If any concentration exceeds the No-Effect Concentration in Disruptive Scenarios, then acceptability will be judged on a case-by-case basis taking into account the likelihood and nature of the exposure, uncertainty in the assessment and conservatism in the dose criterion.

The ENEVs are based on the dose benchmarks from Environment Canada / Health Canada (EC/HC 2003) or lower; and the transfer factors are based on literature review. The analysis is summarized in Garisto et al. (2008). It is recognized that there has been a substantive effort over the past few years to obtain new data in this area, and that the parameter values will need to be reconsidered as new information becomes available. Criteria will also need to be provided for other radionuclides of potential interest; however, the basic concept of comparing media concentrations with benchmark values remains a plausible approach for non-human biota. Note that the NWMO has an ongoing work program in which different methods, including the ERICA method (Brown et al. 2008), are being investigated for defining these criteria. When this work matures, the acceptance criteria will be updated.

Table 7-2: Interim Acceptance Criteria for the Radiological Protection of the Environment

Radionuclide	Media		
	Water (Bq/L)	Soil (Bq/kg)	Sediment (Bq/kg)
Cl-36	2.8×10^{0}	3.8×10^{-1}	4.1×10^{4}
I-129	3.2×10^{0}	2.4×10^{3}	1.2×10^{6}
Cs-135	2.1×10^{-3}	8.5×10^{0}	3.5×10^{5}
Tc-99	8.0×10^{-1}	4.3×10^{1}	3.0×10^{6}
Ra-226	5.9×10^{-4}	2.5×10^{2}	9.3×10^{2}
Np-237	5.8×10^{-2}	5.0×10^{1}	1.1×10^{3}
U-238	2.3×10^{-2}	4.2×10^{1}	1.1×10^{4}
Pb-210	4.3×10^{0}	3.7×10^{3}	6.3×10^{3}
Po-210	7.0×10^{-3}	3.0×10^{1}	5.6×10^{3}

7.1.4 Interim Acceptance Criteria for the Protection of the Environment from Hazardous Substances

For this category the criteria defined in Section 7.1.2 also apply because the values selected are the lowest values relevant to either human health or the environment.

7.2 Scope

This section presents the scope of work addressed in this chapter.

The scope is developed for consistency with the objectives of the pre-project review. As such, analysis cases are limited to those needed to provide a demonstration of the overall approach and the main analysis needed to reach possible conclusions for the hypothetical site. Items excluded from the scope but which might be included in a licence submission as part of a more comprehensive assessment are discussed in Section 7.2.4.

The scope is defined taking into account the discussion of the Normal Evolution Scenario and the Disruptive Scenarios in Chapter 6 together with experience gained from previous postclosure studies performed for other hypothetical sites and conceptual designs.

Results for all scenarios and their associated sensitivity cases are measured against the interim acceptance criteria for the radiological protection of persons provided in Section 7.1.1.

Results for the Reference Case (see below) of the Normal Evolution Scenario and selected sensitivity cases are also measured against the criteria for the protection of persons from hazardous substances provided in Section 7.1.2, the criteria for the radiological protection of the environment provided in Section 7.1.3, and the criteria for the protection of the environment

from hazardous substances provided in Section 7.1.4. Comparisons are also done for the Disruptive Scenario with the most significant consequences.

7.2.1 Analysis Cases for the Normal Evolution Scenario

The Normal Evolution Scenario is based on a reasonable extrapolation of the site and repository. It accounts for anticipated significant events, in particular glaciation.

Chapter 5 presents information describing why the used fuel containers are expected to remain intact over the time scale of interest. No releases are anticipated for very long times, during which radioactivity in the used fuel decays to levels similar to that of a natural uranium ore body.

However, given the large number of containers, it is possible that some containers could be placed with undetected defects. In particular, a simple estimate of the likelihood of undetected defects arising in the copper shell welding and inspection process (i.e., 1/5000, Maak et al. 2001), indicates that statistically there could be three containers with defects placed in the repository. While these statistics have been conservatively estimated, for the Normal Evolution Scenario it is assumed that three containers with undetected defects are present.

Recognizing that the geosphere characteristics at a candidate site and the design of the repository may be different from the assumed reference conditions, a number of sensitivity cases are also examined to illustrate the function of the various engineered and natural barriers. Both deterministic and probabilistic simulations are performed.

In the deterministic simulations, parameters are varied about a Reference Case of the Normal Evolution Scenario, where the Reference Case has the following attributes:

- Geosphere properties as per Chapter 2;
- Used fuel inventories as per Chapter 3;
- Repository design as per Chapter 4;
- Three containers each with an undetected defect placed in the repository at the position with the shortest groundwater transport time to the well;
- Defect radius = 1 mm, no evolution of the defect size with time;
- No other container failures occur;
- Groundwater fills the defective containers 10,000 years after the containers are placed in the repository (Gobien et al. 2013);
- Constant temperate climate and steady-state groundwater flow;
- Self-sufficient farming family growing crops and raising livestock on the surface above the repository;
- Drinking and irrigation water for the family obtained from a 219 m deep well that penetrates the entire thickness of the Guelph formation located along the main pathway for contaminants released from the defective containers;
- The well is pumping at a rate of 1307 m^3/a. This is sufficient for drinking water and irrigation of household crops;

- A small amount (tens of metres) of surface erosion occurs in the first one million years[2]
- Input parameters that are represented by probability distributions are set to either the most probable value (when there is one) or to the median value otherwise.

The sensitivity cases are shown in Table 7-3 and listed below. The table includes a description of the variation from the Reference Case assumptions for each case together with a brief rationale for the case selection.

The sensitivity cases are:

- Fuel dissolution rate increased by a factor of 10;
- Instant release fractions set to 0.10 for all radionuclides;
- Container defect area increased by a factor of 10;
- No solubility limits in the container;
- No sorption in the Engineered Barrier System (EBS);
- Geosphere hydraulic conductivities increased by a factor of 10;
- Geosphere diffusivities increased by a factor of 10;
- No sorption in the geosphere;
- 100 m surface erosion in the first one million years (Hallet 2011);
- Overpressure in the Shadow Lake formation;
- Hydraulic conductivity of the excavation damaged zones (EDZ) increased by a factor of 10; and
- Low sorption in the geosphere with coincident high solubility limits in the container.

For the probabilistic simulations, random sampling is used to simultaneously vary all input parameters for which probability distribution functions are available. The radionuclide release and transport parameters are varied with the fixed reference geosphere adopted in the system model. This case is also described in Table 7-3.

An assessment based on the results of the regional glaciation modelling studies described in Chapter 2 is used to discuss the anticipated effects of glaciation.

Results are developed for one complementary radiological indicator.

Results are also generated to address the radiological protection of the environment, and the protection of persons and the environment from hazardous substances. A complementary indicator of safety for hazardous substances is also evaluated.

[2] This amount of erosion is neglected in the analysis simulations because of its anticipated negligible effect. A sensitivity case considers the effect of 100 m of surface erosion.

Table 7-3: Sensitivity Cases for the Normal Evolution Scenario

Uncertainty	Reference Case Assumption*	Sensitivity Case Assumption	Rationale
Fuel			
Dissolution Rate	Generated via a model that takes into account the effects of radiolysis and chemical dissolution. No credit for the effect of H_2 gas on suppressing dissolution. With this model, ~22% of the fuel dissolves in the first one million years.	The dissolution rate is increased by a factor of 10. With this increase, all of the fuel dissolves in the first one million years.	The fuel is an important barrier to the release of radionuclides because most radionuclides are contained within the fuel matrix. As the fuel dissolves in the long term these radionuclides become available for transport. The factor of 10 increase roughly corresponds to the 95th percentile value, thereby accounting for uncertainties.
Instant Release Fractions	Most radionuclides have no instant release. Instant release fractions for selected radionuclides are: Cl = 0.06 Cs = 0.04 I = 0.04 Np, Pu, Th, U = 0.00	Instant release fractions for all radionuclides are set to 0.10.	Some radionuclides in the used fuel are present initially in the fuel sheath gap and grain boundaries and are therefore available for release early after contact with water. This fraction of the inventory is referred to as the instant release fraction. Assigning an instant release fraction to all radionuclides (including actinides) ensures the results are bounding.
Container			
Defect Area	Defect Radius = 1.0 mm Defect Area = 3.14 mm^2	The defect area is increased by a factor of 10.	The container is an important barrier to the release of radionuclides. The size of the defect can influence the rate at which radionuclides escape the container and enter the buffer. Since the Reference Case assumes a constant defect size, this case provides information on the sensitivity of results to a larger defect. Defects of greater size (~ 30 mm^2) are unlikely to be missed during inspection.

Uncertainty	Reference Case Assumption*	Sensitivity Case Assumption	Rationale
Solubility Limits	Solubility limits are determined externally from thermodynamic data and specified as input. Solubility limits (mol/m^3) for selected radionuclides are: Np = 1.7×10^{-6} Se = 3.4×10^{-6} Th = 1.4×10^{-4} U = 4.5×10^{-6} Cl, Cs, I = no limit The solubility limits are increased in the Reference Case by a factor of ten above the values listed here to account for uncertainties in groundwater chemistry and thermodynamic data.	Solubility limits for all radionuclides are set to 2000 mol/m^3. This is equivalent to having no solubility limit.	The concentration of a dissolved radionuclide is one of the parameters that affect the rate of radionuclide release from the defective container. While some radionuclides are highly soluble (e.g., I and Cl), others are not (e.g., Pu and U). Removal of all solubility limits provides information on the importance of this parameter to the overall dose consequence.
Buffer, Backfill and Seals (i.e., the Near Field)			
Sorption in the EBS	Use of linear equilibrium sorption model. Sorption coefficients from SKB reviews and Vilks (2011) have been adopted where similar materials and conditions exist. Some elements are non-sorbing (e.g., Cl and I) while others are highly sorbing in the saline reducing environment (e.g., Np, Th, and U). Sorption on iron oxides, from corrosion of the steel inner vessel of the container, is conservatively neglected.	Sorption coefficients for all near field barrier components including the shafts are set to zero. Sorption coefficients in the geosphere are maintained at their Reference Case values.	The clay-based seals have a high surface area and can sorb radionuclides released into the groundwater from the containers. Under saline conditions, ion exchange absorption is not important, but surface complexation sorption is still active. Disregarding sorption provides information on the importance of this process to the overall dose consequence.

Uncertainty	Reference Case Assumption*	Sensitivity Case Assumption	Rationale
Geosphere			
Geosphere Conductivity	Reference Case hydraulic conductivity profile as defined in Chapter 2.	A factor of 10 increase relative to the Reference Case.	Geosphere hydraulic conductivity is an important parameter controlling groundwater flow and advective radionuclide transport in the sedimentary rock formations. The sensitivity case examines the effect of higher hydraulic conductivity on the advective component of radionuclide transport.
Sorption in the Geosphere	Use of linear equilibrium sorption model. Limestone and shale sorption coefficients based on Vilks (2011). Some elements are non-sorbing (e.g., Cl and I) while others are highly sorbing in the saline reducing environment (e.g., Np, Th, and U). Colloid transport is not important under diffusion-dominant and highly saline transport conditions, so it is not included.	The geosphere sorption coefficients for all elements are set to zero. All other near field sorption coefficients (i.e., buffer, backfill and seals) are maintained at their Reference Case values.	Radionuclides can be sorbed onto the surfaces of the host rock minerals, thereby retarding their transport to the surface. Under saline conditions, ion exchange absorption is not important, but surface complexation sorption is still active. Setting the sorption coefficients to zero provides information on the relative importance of sorption in the geosphere.
Geosphere Diffusivity	Reference Case effective diffusion coefficients vary from layer to layer. Anion and neutral species are assumed to have the same diffusion coefficients. This conservatively ignores anion exclusion. Cations are assumed to have an effective diffusion coefficient three times greater than neutral and anions due to surface diffusion.	A factor of 10 increase relative to the Reference Case.	Geosphere diffusivity is an important parameter controlling radionuclide transport in low hydraulic conductivity sedimentary rock formations. The sensitivity case examines the effect of higher diffusion coefficients on radionuclide transport.

Uncertainty	Reference Case Assumption*	Sensitivity Case Assumption	Rationale
Hydraulic Conductivity of EDZ	The excavation damaged zones, which also consider potential thermal damage, are defined with higher hydraulic conductivity than the surrounding rock. Hydraulic Conductivity (K/K_{rock}) for selected areas are: Rooms and drifts: Inner EDZ = 1000; Seal EDZ = 1000; Outer EDZ = 100 Shafts: Inner EDZ = 100; Seal EDZ = 100; Outer EDZ = 10	Hydraulic conductivity of all excavation damaged zones increased by a factor of 10.	The excavation damaged zone is a region of rock damaged during the construction process; potential thermal damage is also taken into account. The EDZ has higher hydraulic conductivity than the surrounding intact rock and could be a pathway for radionuclide transport. EDZ values reflect the likelihood of connected damage paths aligned with bedding planes. There is a possibility of some self-sealing due to shale swelling or salt precipitation. Increasing the hydraulic conductivity provides information on the importance of these damage zones to the transport and subsequent release of radionuclides to the surface.
Erosion	Tens of metres of erosion in the first one million years. This is neglected in the Reference Case due to its anticipated negligible effect.	100 m erosion in the first one million years.	Repeated glaciations over one million years could remove a significant amount of the formations closest to the surface.
Overpressure in the Shadow Lake Formation	No overpressure.	158 m above hydrostatic conditions.	Overpressure in formations below the repository could result in increased advective flow to the surface. This case examines the significance of this effect.
Low Sorption Geosphere with Coincident High Solubility Limits	Geosphere sorption is as described above in the “Sorption in the Geosphere” sensitivity case. Solubility limits are as described above in the Fuel “Solubility Limits” sensitivity case.	“Low” / “High” means the values are set to three sigma values in the conservative direction.	This case determines the effect of simultaneous pessimistic assumptions affecting the solubility and geosphere barrier.

Uncertainty	Reference Case Assumption*	Sensitivity Case Assumption	Rationale
Combined			
Simultaneous Variation of all Probabilistically Defined Parameters	Input parameters represented by probability distributions are set to either the most probable value (when there is one) or to the median value otherwise.	Monte Carlo analysis in which all input parameters represented by probability distributions are simultaneously varied. An important caveat is that these probabilistic simulations are performed in the fixed geosphere of the system model.	Many of the modelling parameters are uncertain or have a natural degree of variability and as such are more generally characterized by a range or distribution of values. Varying all such parameters simultaneously provides information on the overall range or uncertainty in the results.

Note: * A detailed description of the input data is available in Gobien et al. (2013).

7.2.2 Analysis Cases for Disruptive Scenarios

Disruptive Scenarios postulate the occurrence of unlikely events leading to possible penetration of barriers and abnormal loss of containment.

Chapter 6 describes the set of Disruptive Scenarios applicable to the conceptual design and hypothetical geosphere in this study. These have been identified through consideration of the features, events and processes that are important to this repository system, and through consideration of the key barriers. The scenarios are:

- Inadvertent Human Intrusion;
- All Containers Fail. A base case with failure at 60,000 years is considered together with a sensitivity case with failure occurring at 10,000 years;
- Shaft Seal Failure;
- Abandoned Repository;
- Poorly Sealed Borehole;
- Undetected Fault;
- Severe Erosion; and
- Container Failure[1].

The first three scenarios are within the scope of this illustrative safety assessment. Table 7-4 describes each of these three scenarios and includes a description of the parameters changed from the Reference Case and the rationale for the scenario selection. It is recognized that for an actual site, the full set of scenarios would need to be evaluated.

The consequences of gas generation caused by corrosion of steel in the defective containers are assessed for the All Containers Fail scenario because this event produces the greatest amount of gas. This assessment is described in Chapter 8.

With respect to the Undetected Fault Scenario, it is anticipated that any large fractures intercepting the repository not identified during site characterization would be discovered during construction such that appropriate mitigating measures could be taken. These measures could include grouting and possible rerouting of the repository layout to avoid large transmissive features.

The Abandoned Repository scenario considers the consequences if the repository is abandoned and the shafts are not sealed. It implies a near-future loss-of-society.

The Poorly Sealed Borehole scenario is a Disruptive Scenario because it creates a pathway that bypasses the low-permeability geosphere. However, as long as the boreholes are kept sufficiently far from the repository footprint, this scenario is unlikely to be important due to the small size of the borehole and the limits of diffusive transport. It would be analyzed as part of a real site, when the borehole distances are known.

---

[1] This considers delayed but substantive failure of a few containers due to unexpected in-situ conditions, and is different from the Normal Evolution Scenario which considers a small defect initially present in some containers.

The Severe Erosion scenario considers the possibility of high erosion at the repository due to glaciation. The Normal Evolution Scenario evaluated in this report assumes a small amount of net erosion (tens of metres) in the Reference Case, with a sensitivity case examining the effect of 100 m erosion. Whether a case with more erosion should be considered would need to be assessed in the context of a specific site, and would be factored into the selection of repository depth.

Although a detailed analysis of the Container Failure Scenario is outside the scope of this study, the peak dose arising from this event is anticipated to be significantly less than that associated with the All Containers Fail Scenario due to the much reduced number of affected containers.

All scenarios are analysed with deterministic methods only since the basic parameters defining the scenarios are chosen conservatively.

7.2.3 Analyses for Miscellaneous Modelling Parameters

Some additional cases were simulated in the course of the analysis to check various FRAC3DVS-OPG modelling parameters. These cases are discussed in Table 7-5 and listed below:

- Increased spatial resolution to confirm model convergence. This is achieved by comparing contours and mass fluxes between the Site-Scale and Repository-Scale models.
- Increased and decreased number of time steps to confirm that model results are not sensitive to temporal resolution.

As will be discussed in later sections, changes to spatial and temporal resolution have no material effect on the results.

Table 7-4: Analysis Cases for Disruptive Scenarios

Disruptive	Reference Case Assumption*	Disruptive Case Assumption	Rationale
Inadvertent Human Intrusion	Not Applicable	The engineered and natural barriers are bypassed via the drilling of a borehole into the repository. The borehole intersects a used fuel container and used fuel material is brought to the surface. The variant case, in which the borehole thereafter remains open, is not considered.	Institutional controls and knowledge of the repository can be lost in the future. This scenario examines the potential consequences to the drill crew and a future resident on the site for a stylized intrusion event.
All Containers Fail	Three containers each with an undetected defect (radius = 1 mm) are placed in the repository at the location with the shortest groundwater transport time to the well. Groundwater fills the defective containers 10,000 years after the containers are placed in the repository.	*Base Case* All containers fail 60,000 years after repository closure and no containers fail prior to this time. The radionuclide release model takes no credit for the presence of the container. As such, the release of radionuclides from the slowly dissolving fuel to the near field is limited only by the buffer properties. *Extreme Case* Identical to the above, except the time of container failure is 10,000 years.	The containers are anticipated to last for a period in excess of one million years, based on the copper corrosion barrier, sturdy mechanical design and favourable site attributes, including geochemical stability. This scenario considers common cause failure of all containers. The base case considers failure at 60,000 years. This corresponds to the likely timeframe for an ice sheet to cover the site, and it is possible that some unanticipated effect of the ice sheet might cause failure, such as beyond-design mechanical loading or unexpected changes in groundwater chemistry. An extreme case with failure at 10,000 years provides information on the sensitivity of results to the assumed failure time.

Disruptive	Reference Case Assumption*	Disruptive Case Assumption	Rationale
Shaft Seal Failure	The shaft is filled with a combination of bentonite / sand (70:30), concrete and asphalt with the following hydraulic conductivities (m/s): Bentonite / Sand = 1.6×10^{-11} Concrete = 1.0×10^{-10} Asphalt = 1.0×10^{-12}	*Base Case* The hydraulic conductivity of all shaft seal materials is set to 10^{-9} m/s from the time of repository closure. *Extreme Case* The hydraulic conductivity of all shaft seal materials is further increased by an additional factor of 100. A hydraulic conductivity of 10^{-7} m/s is about equivalent to that of fine silt and sand. An important caveat is that the locations of the defective containers and the well are the same as in the Reference Case. In future studies these locations may need to be moved to ensure the most conservative consequence is obtained.	This scenario examines the effects of significant degradation in shaft seal. For conservatism, this degradation is assumed to occur at the time of repository closure.

Note: * A detailed description of the input data is available in Gobien et al. (2013).

Table 7-5: Modelling Parameter Cases

Modelling Parameter	Description	Modelling Case Assumption	Rationale
Spatial Resolution and Time Step Size	User determined in the Reference Case.	Spatial resolution in the FRAC3DVS-OPG model is increased by over 10-fold. Time step control in the FRAC3DVS-OPG model is adjusted to change the number of time steps, with the changes resulting in a factor of 2 decrease in one simulation and a factor of 3 increase in another.	Increasing the spatial resolution and the number of time steps provides information on whether the model results are numerically converged.

7.2.4 Analysis Exclusions

As noted earlier in Section 7.2, the scope of the postclosure safety assessment is defined for consistency with the objectives of the pre-project review. As such, the analysis cases are limited to those needed to provide a demonstration of the overall approach and to those needed to reach preliminary conclusions for the hypothetical site.

This section lists scope items that do not appear in this report but which might otherwise be included in a postclosure safety assessment for a licence submission. These are:

- Fracture Uncertainty. In principle a sedimentary rock site may have features that provide high confidence that there are no significant fractures near the repository. For a real site, there will be some uncertainty regarding the existence (and location) of any such fractures. These uncertainties can be reduced through site selection and repository location and depth, and any residual uncertainties can be handled through the adoption of conservative assumptions and / or Disruptive Scenarios (such as the Undetected Fault Scenario) within the postclosure analysis.

- Variable Climate Analysis. The effects of permafrost and glaciation are not explicitly determined in this assessment. Instead, the results of regional glaciation modelling studies described in Chapter 2 are used to draw inferences about the likely effects of glaciation on the dose assessment for the Normal Evolution Scenario.

- Additional Disruptive Scenarios. As described in Section 7.2.2, a reduced number of Disruptive Scenarios is evaluated here. However, the full list of Disruptive Scenarios anticipated for a licence submission is identified.

- Alternative Critical Groups. Other potential critical groups may be considered for a candidate site depending on communities nearby that could be interested in potential impacts - for example, downstream communities and / or First Nation lifestyles.

7.3 Conceptual Model

This section describes the conceptual model associated with key processes occurring in the repository with defective containers present. The presence of defective containers leads to releases of contaminants that eventually enter the biosphere. These biosphere releases have potential impacts on humans and non-human biota living nearby.

The conceptual model describes the release, migration and fate of contaminants through the identification of key features, events and processes. The model is used to guide the development and application of the computer codes used in the postclosure safety assessment.

Figure 7-1 illustrates the general conceptual model. There are four main elements:

- The used fuel containers;
- The engineered barrier system;
- The geosphere; and
- The biosphere.

Each of these is discussed below. The discussion is aligned with the Reference Case of the Normal Evolution Scenario which, as noted in Section 7.2.1, assumes a constant temperate climate.

For simplicity, the descriptions of conceptual models are given in terms of radionuclides but the models also can be applied to simulate the behaviour of potentially hazardous chemical elements, except that for chemical elements there is no radioactive decay and in the biosphere there is no food chain and no dose rate calculations. Instead, protection of the environment is ascertained by comparison of calculated chemical element concentrations in various biosphere media to the criteria outlined in Table 7-1.

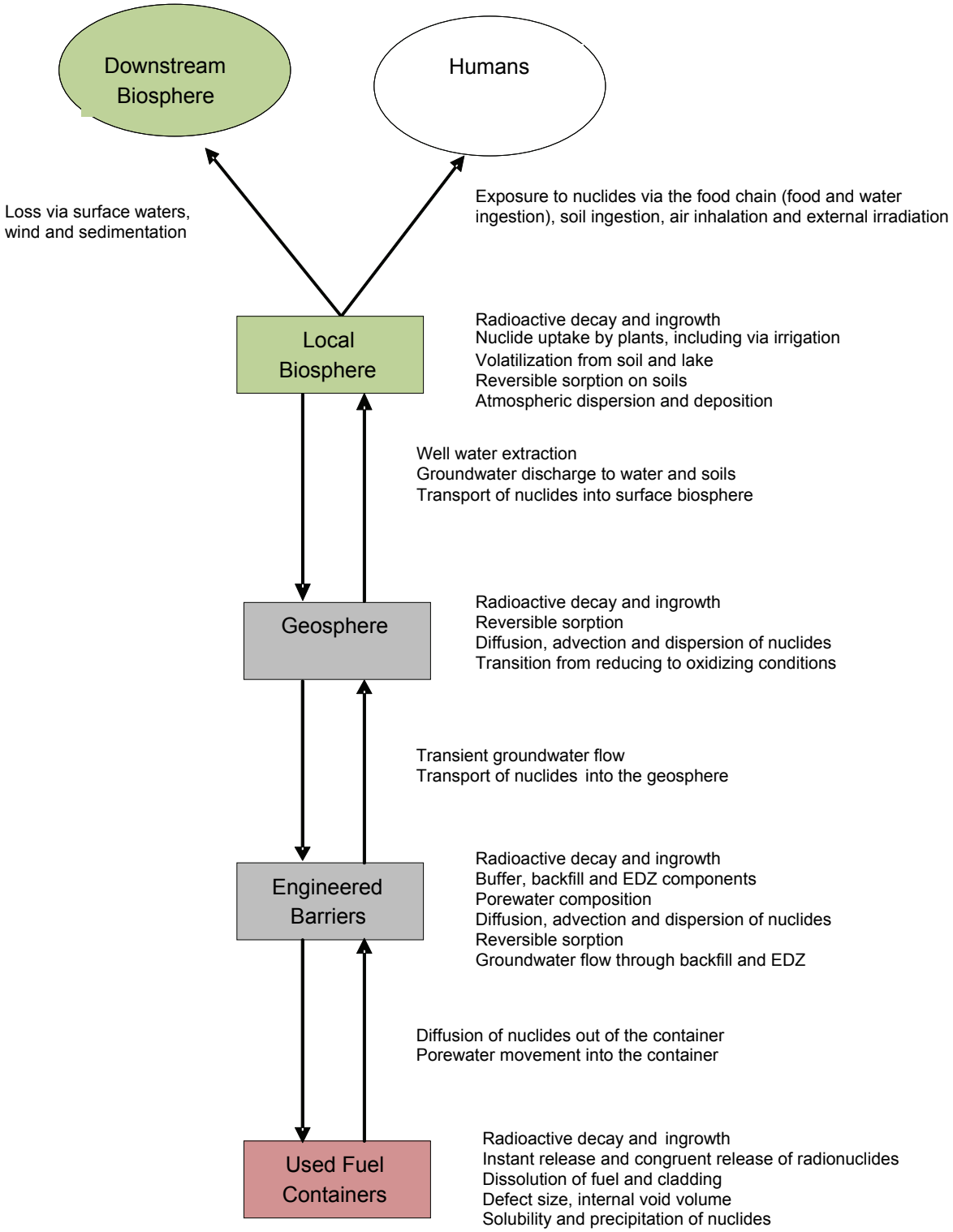

Figure 7-1: General Conceptual Model for Defective Containers

7.3.1 Used Fuel Containers

The principal fuel components and processes for the used fuel containers and waste form are shown in Figure 7-2.

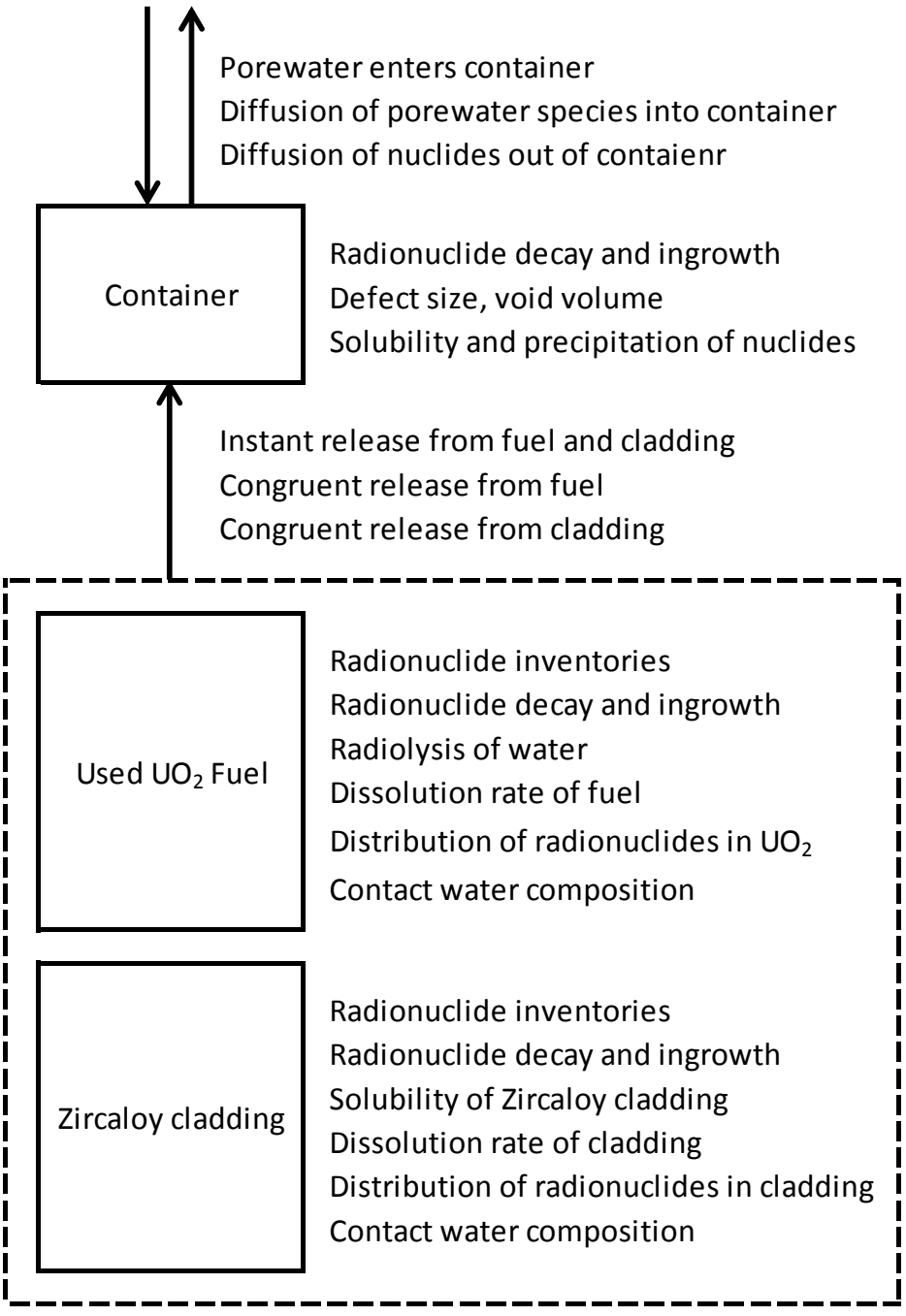

Figure 7-2: Conceptual Model for the Waste Form and Container

The container has a copper outer shell with a steel inner vessel for structural support.

The inner steel vessel is not specifically included in the conceptual model, except that it is assumed present to maintain the void volume inside the container. In practice, the steel components in any breached container would corrode, producing H_2 gas and iron oxides. Although H_2 could substantially reduce the dissolution rate of the UO_2 fuel, this effect is conservatively ignored. Similarly, formation of iron oxides would provide a high surface area for adsorption of some of the radionuclides released from the fuel. These effects are also ignored.

The reference waste form is a standard CANDU 37-element fuel bundle with a burnup of 220 MWh/kgU and an average fuel power during operation of 455 kW as discussed in Chapter 3. The repository holds 4.6 million bundles.

After water enters the container, the Zircaloy cladding could prevent water from contacting the fuel for some time. However, the cladding is neglected in the fuel dissolution model and it is assumed that water contacts all the fuel as soon as the container fills with water.

The temperature at the container surface reaches a peak value of about 120ºC at 10 years after container placement, decreases to about 80ºC at 100 years, decreases slowly to about 70ºC at 10,000 years and reaches ambient conditions at around 100,000 years (Guo 2010). To account for uncertainties in chemical element solubility values at these higher temperatures, reference solubility values are increased by a factor of 10.

The waste form has two distinct components: the UO_2 fuel and the Zircaloy cladding. Releases of radionuclides from these two waste forms are modelled separately.

Radionuclides within the UO_2 fuel are released by two mechanisms which operate on very different time scales (Grambow et al. 2010) as discussed immediately below.

Instant Release from Fuel

Initially, there will be a comparatively rapid release of a small fraction (typically a few percent) of the inventory of a selected group of radionuclides that are either very soluble (such as C-14, Cl-35, Cs-137 and I-129) or gaseous (such as Xe), and that are residing in the fuel sheath gap or at grain boundaries which are quickly accessed by water. This release process is referred to as “instant-release”; and is modelled assuming a certain fraction of the radionuclide inventory in the fuel is released at the time water contacts the fuel.

Ferry et al. (2008) have shown that the instant release fractions do not change with time due to, for example, athermal diffusion of radionuclides induced by alpha-particle recoil displacements.

The instant release fractions used in this assessment are given in Section 7.5.4.1.

Fuel Dissolution

The second and slower release process comprises release of radionuclides from the UO_2 fuel matrix as the matrix itself corrodes or dissolves (called "congruent dissolution").

At the fuel-water interface the alpha dose rate, which exceeds the gamma and beta dose rates for most of the fuel history (Figure 7-3), is the main contributor to radiolysis, producing molecular

oxidants such as H_2O_2. Other potential sources of oxidants, such as any O_2 trapped in the porewater, will already have been consumed by corrosion processes (e.g., corrosion of the Cu shell) before the fuel cladding is breached because these corrosion reactions are relatively fast (King and Kolar 2006). In principle, the radiolytically produced oxidants will also be consumed by reaction with container materials rather than by reaction with used fuel; however, for alpha radiolysis, the oxidants (e.g., H_2O_2) are only produced within 20 μm of the fuel-water interface (Garisto 1989), so they are much closer to the fuel than to the container and thus more likely to react with the fuel.

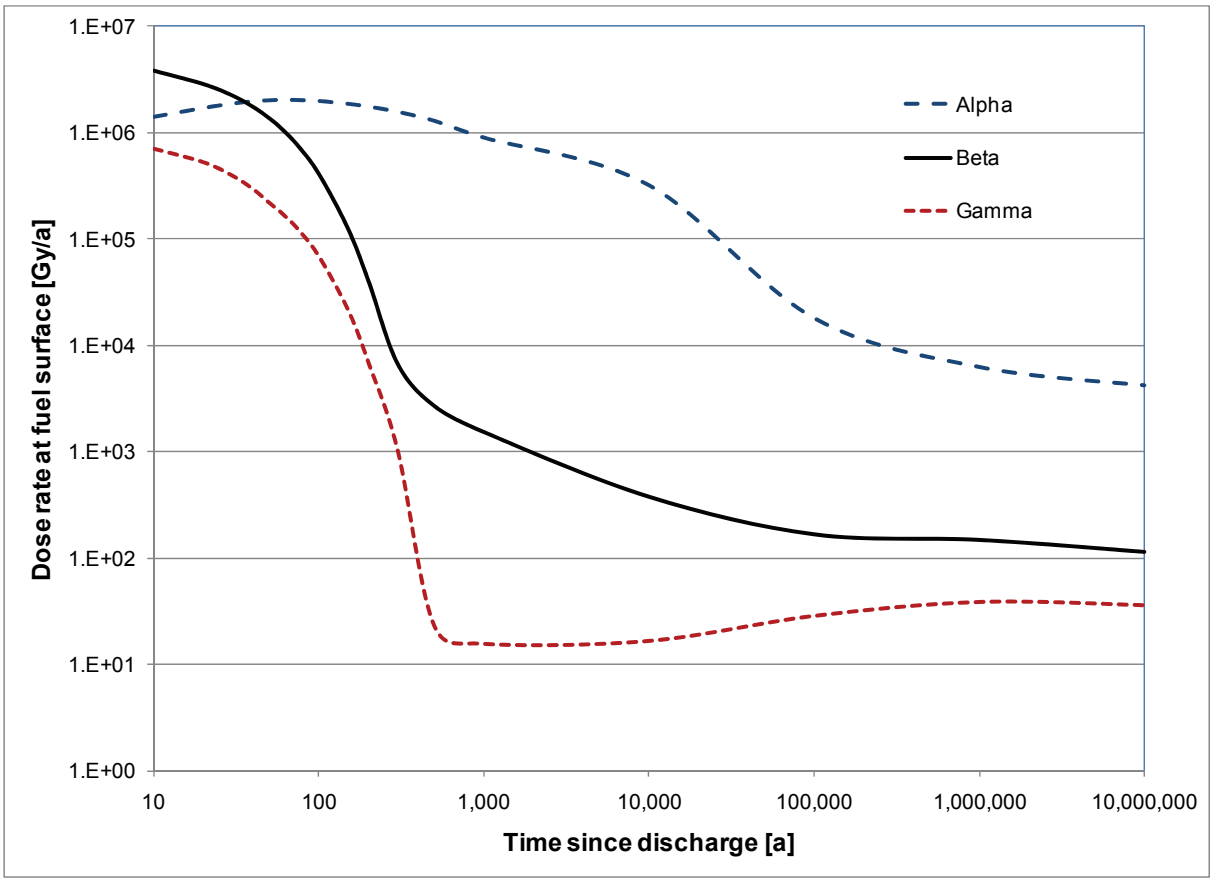

Figure 7-3: Radiation Dose Rate in Water at the Fuel Surface (220 MWh/kgU Burnup)

Oxidative dissolution of the fuel continues as long as the alpha radiation field is sufficiently high. Eventually, after about 10 million years (Gobien et al. 2013), chemical dissolution of the fuel dominates according to the reaction,

$$UO_2 + 2H_2O \rightarrow U(OH)_4 \qquad (7\text{-}1)$$

This is a very slow process, as illustrated by the existence of uranium ore bodies that are millions or billions of years old.

The UO_2 dissolution rate would be affected by build up of hydrogen gas inside the steel vessel generated by anaerobic corrosion of the steel. Experimental evidence shows that the dissolution rate drops by several orders of magnitude in the presence of even modest pressures of hydrogen gas (Shoesmith 2008). This is likely due to the activation of hydrogen by various mechanisms to produce the strongly reducing $H^{\bullet}$ radical, which in turn scavenges radiolytic oxidants and suppresses fuel corrosion (Shoesmith 2008 and references therein). While this hydrogen effect will suppress fuel dissolution, it is conservatively ignored in the current assessment.

The fuel dissolution rate used in this assessment is shown in Section 7.5.4.1.

Radionuclide Releases from Zircaloy

All radionuclides trapped in the Zircaloy cladding, except for C-14, are assumed to be released congruently as the cladding dissolves. The cladding dissolution rate is calculated using a solubility-limited dissolution model, and dissolution continues until the cladding completely dissolves. For C-14, there is evidence that a fraction of the C-14 in the Zircaloy is released as soon as water contacts the cladding (Gobien et al. 2013).

Section 7.5.2 shows that C-14 is not a potentially significant radionuclide for liquid-borne contaminant transport. The dose consequences associated with gaseous transport are described in Chapter 8.

7.3.2 Engineered Barrier System

Chapter 4 provides a detailed description of the conceptual repository and engineered barriers assumed in this study.

The dense 100% bentonite layer that surrounds the container:

1. Prevents groundwater flow near the container;
2. Mechanically supports the container; and
3. In conjunction with the high groundwater salinity, prevents microbial activity that could cause corrosion of the copper shell.

The buffer has a sufficiently low hydraulic conductivity that transport through it is diffusion dominant (i.e., the advective velocity is negligible). In contrast, advection is possible in the access tunnel backfill if sufficient hydraulic gradients are present, as it has a higher hydraulic conductivity.

The excavation damaged zone (or EDZ) extends around the perimeter of excavated spaces and is modelled as a uniform porous medium. Excavation damaged zones along placement rooms, which are narrower, may be less permeable than damage zones along the larger drifts and cross-cuts. As a conservative estimate, the placement room EDZ has been assigned the same hydraulic conductivity as the drift and cross-cut EDZ.

The design includes seals at the entrance of each placement room and seals spaced throughout the access drifts and cross cuts. These seals are composed of concrete and clay bulkheads that interrupt the tunnel and placement room EDZs. An additional smaller EDZ associated with excavation of the seals is also assigned the same hydraulic conductivity as the drifts and cross-cut EDZ. These features are modelled as uniform porous media.

Groundwater contacting the fuel must pass through the buffer. Initially, the composition of this contact water is similar to the buffer porewater composition which depends strongly on the minor mineral components of the buffer (e.g., the calcite and gypsum contents (Muurinen and Lehikoinen 1999, Curti and Wersin 2002)). After some time, these minor mineral components are all dissolved and the contact water composition resembles the geosphere porewater composition.

This time evolution in contact water composition is not explicitly taken into account; rather, two contact water compositions are defined. The first composition is geosphere porewater equilibrated with buffer minerals, and the second composition is geosphere porewater equilibrated with buffer minerals and the steel insert of the container. These compositions are used for the calculation of chemical element solubilities and the highest calculated solubility is used in the safety assessment calculations.

The composition of the groundwater and the diffusion and sorption coefficients for the buffer and backfill material assumed in this assessment are shown in Section 7.5.

7.3.3 Geosphere

Chapter 2 provides a description of the hypothetical geosphere assumed in this study.

The principal components of the conceptual model are shown in Figure 7-4. The geosphere is assumed to be continuous and relatively uniform, lacking the presence of permeable fractures or fault zones. The rock mass is assigned an effective hydraulic conductivity in accordance with properties for the different geological units assumed to be present.

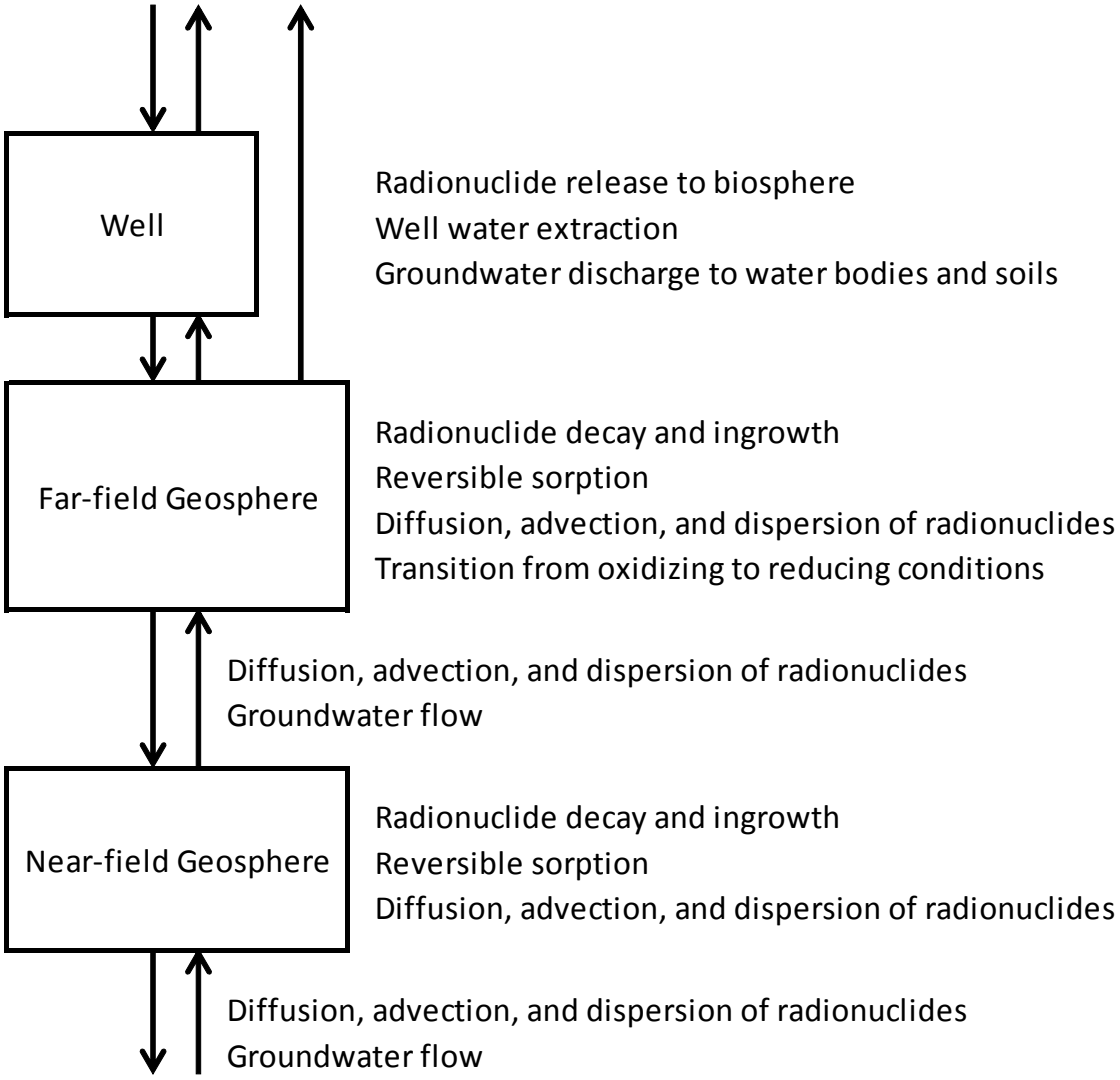

Figure 7-4: Conceptual Model for the Geosphere

Flow boundary conditions are derived from the Regional Model described in Chapter 2. The Regional Model includes the representation of density driven flow to account for the effect on the flow field of highly saline brines at greater depths. Section 7.5.3.1 contains a detailed discussion of how the model boundary conditions are obtained.

The hydrogeological model includes a 219 m deep well spanning the entire 71 m thickness of the Guelph formation, supplying water at the specified reference rate of 1307 m^3/year (i.e., the rate required to meet the needs of the critical group). At this flow rate, the influence of the well on the overall groundwater flow field is small, although the flow field near the well is affected by drawdown. According to the Regional Model (Chapter 2), groundwater in the Guelph formation

is slightly saline, so using a deep well in this formation, rather than the shallower permeable formations, is conservative with respect to contaminant uptake at the well.

In the near-field geosphere (i.e., around the repository), chemically reducing conditions prevail. The temperature in the near field will initially be warmer than in the surrounding geosphere due to radioactive decay, with the maximum temperature reached within about 5,000 years (Guo 2010) and with ambient temperatures returning within about 100,000 years. Generally, the rock mass around the repository would be about 40^{o}C for about 10,000 years. For the contaminant transport times estimated in this study, however, the bulk of the transport occurs under close to ambient conditions. Therefore 25^{o}C values are used for transport parameters.

The physical properties of the rock are described in Chapter 2. The diffusion and sorption coefficients assumed for the rock at repository level are given in Section 7.5.

7.3.4 Biosphere

The main features of the biosphere model are illustrated in Figure 7-5.

The model includes only the local biosphere near the repository, since doses to the critical group living near the repository should be higher than for any individual living further away. In general, radionuclides are lost from the local biosphere by outflow with water, by radioactive decay, by atmospheric dispersion and by leaching into deep soil or sediments.

The local biosphere has the characteristics of a temperate climate region of Southern Ontario. As noted earlier in Section 7.2.4, a constant temperate climate is assumed. While the properties of the biosphere could vary with time due to global warming in the near term, or due to other natural or human-induced changes, the assumption of a constant biosphere provides a convenient and clear measure of the potential impacts, which can be readily related to what is currently acceptable.

In the long term, it is assumed that glaciation will resume with consequent significant effects as a result of the glaciation itself and the related climate change. The anticipated effects of glaciation on the dose assessment for the Normal Evolution Scenario are discussed in Section 7.10.

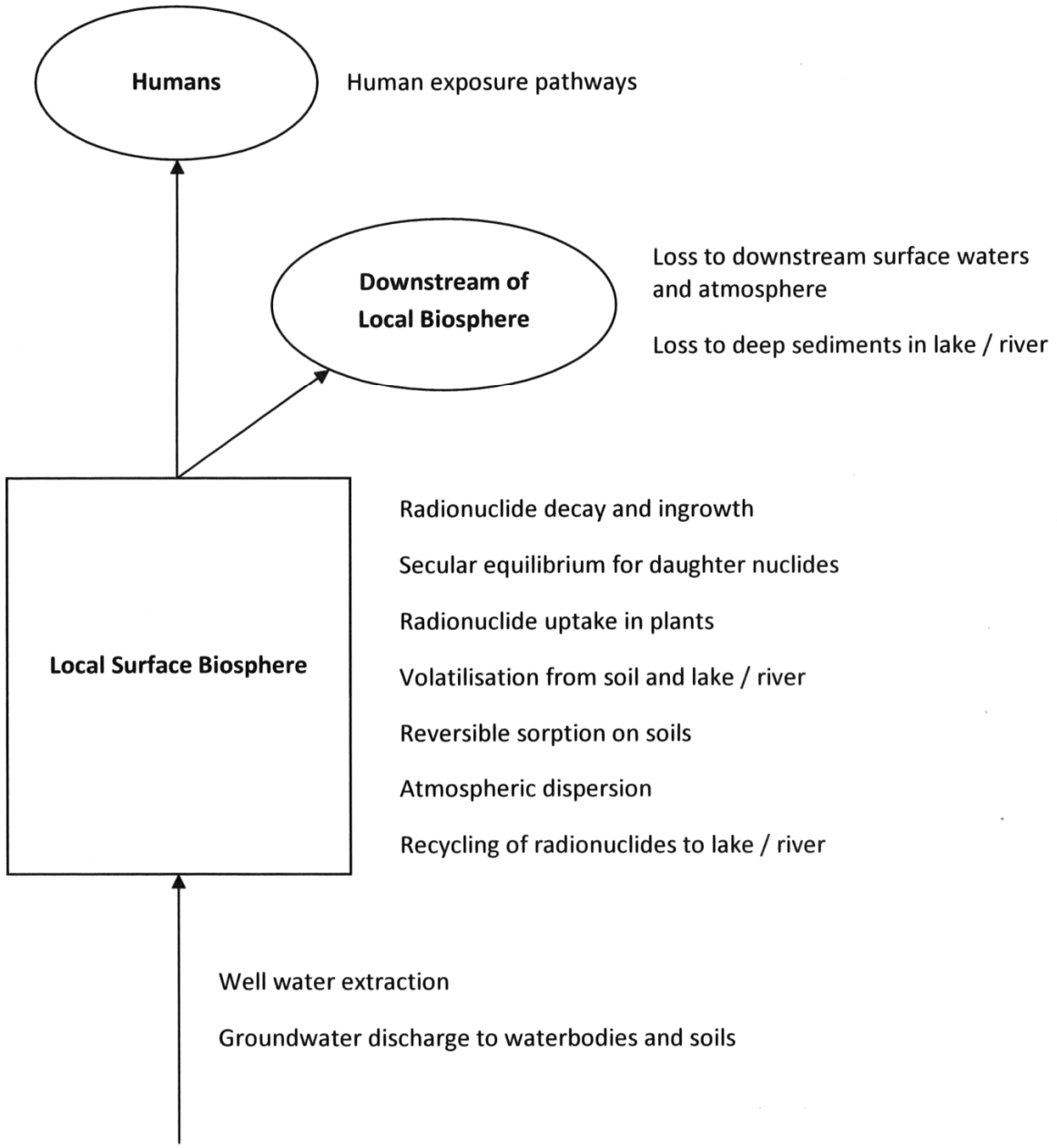

Figure 7-5: Conceptual Model for the Constant Biosphere

Following international practice, the site is assumed occupied by a group of people (i.e., the "critical group") that behaves in a plausible manner but with lifestyle characteristics that maximize their exposure to any radionuclides entering the biosphere. It is assumed that the members of the critical group spend all their lives in the local biosphere and obtain all their food, water, fuel and building materials from the local vicinity.

The characteristics of the critical group will change with climate; however, since a constant temperate climate is assumed, a self-sufficient farming family is selected as the critical group.

This group uses a well that intercepts the contaminant plume from the repository, and grows its own crops and raises animals. Their food includes plants grown in a garden, domesticated animals and fish. This lifestyle is more self-sufficient than current habits and will lead to higher estimates of impacts. Note that future safety assessments may consider additional lifestyles.

Plants growing near the repository can become contaminated directly by atmospheric deposition of radionuclides that reach the biosphere and become volatilized (e.g., I-129) or suspended due to aerosol formation (all nuclides). Plants can also become contaminated due to root absorption of groundwater discharge, irrigation with contaminated surface water (edible crops), and with radionuclides that are deposited to the soil from the atmosphere.

In this site, a deep groundwater well is assumed to intercept the radionuclide plume in the Guelph formation. Radionuclides released from the repository reach the local surface biosphere via the well. Radionuclides not intercepted by the well would be diluted to lower concentrations than in the well by the flow in the aquifer and carried to other locations not represented in the model domain. Section 7.5.3.1 shows that 93.7% of the contaminant plume is captured by the well, so that any dose associated with the remaining aquifer radionuclides would be considerably less than that associated with the well water.

The biosphere model:

- describes the movement of radionuclides through soil, plants and animals, and the atmosphere in the surface environment near the repository;
- calculates the concentrations of radionuclides in water and air in the local habitat of the critical group; and
- calculates radiological dose rates to an individual in the critical group caused by ingestion and inhalation of radionuclides and by external exposure to radiation from radionuclides in the environment (air immersion, water immersion, building materials and groundshine).

A schematic representation of the environmental transfer model is shown in Figure 7-6. The dose model uses the concentration of radionuclides in the various biosphere compartments (well, soil, plants, animals and air) to calculate the annual dose to a member of the critical group.

The internal exposure pathways considered are:

- soil-to-man;
- soil-to-plant-to-man;
- soil-to-plant-to-animal-to-man;
- soil-to-animal-to-man;

- air-to-man;
- air-to-plant-to-man;
- air-to-plant-to-animal-to-man;
- air-to-animal-to-man;

- water-to-man;
- water-to-plant-to-man;
- water-to-animal (including fish)-to-man; and
- water-to-plant-to-animal-to-man.

The external exposure pathways considered are:

- air immersion;
- water immersion (bathing or swimming if a suitable water body is nearby);
- groundshine (exposure to radiation from contaminated soil); and
- building materials (exposure to radiation from building materials).

These exposure pathways are similar to those considered in the guidelines used to calculate derived release limits for normal operation of a nuclear facility (CSA 2008).

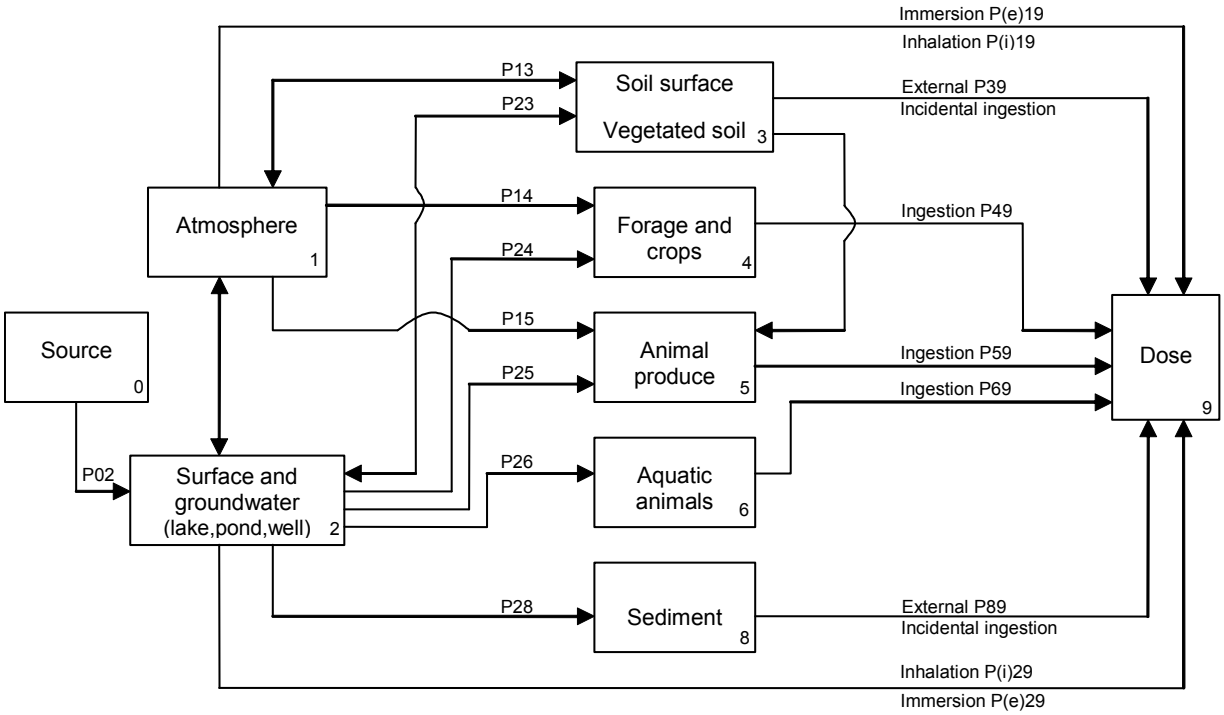

Notes: The nomenclature is from CSA (2008) and the Pij represent transfer parameters from compartment i to compartment j. The biosphere model includes all these environmental transfers and exposure pathways. The building material exposure pathway is not shown here since it is not included in the CSA (2008) dose model.

Figure 7-6: Environmental Transfer Model Showing Critical Group Exposure Pathways

7.4 Computer Codes

The conceptual model for contaminant transport is numerically represented in a suite of computer codes used in postclosure safety assessment modelling.

Figure 7-7 identifies the codes used and their interrelationship. Information from used fuel characteristics, engineering design and site characterization is used to develop site-specific input parameters.

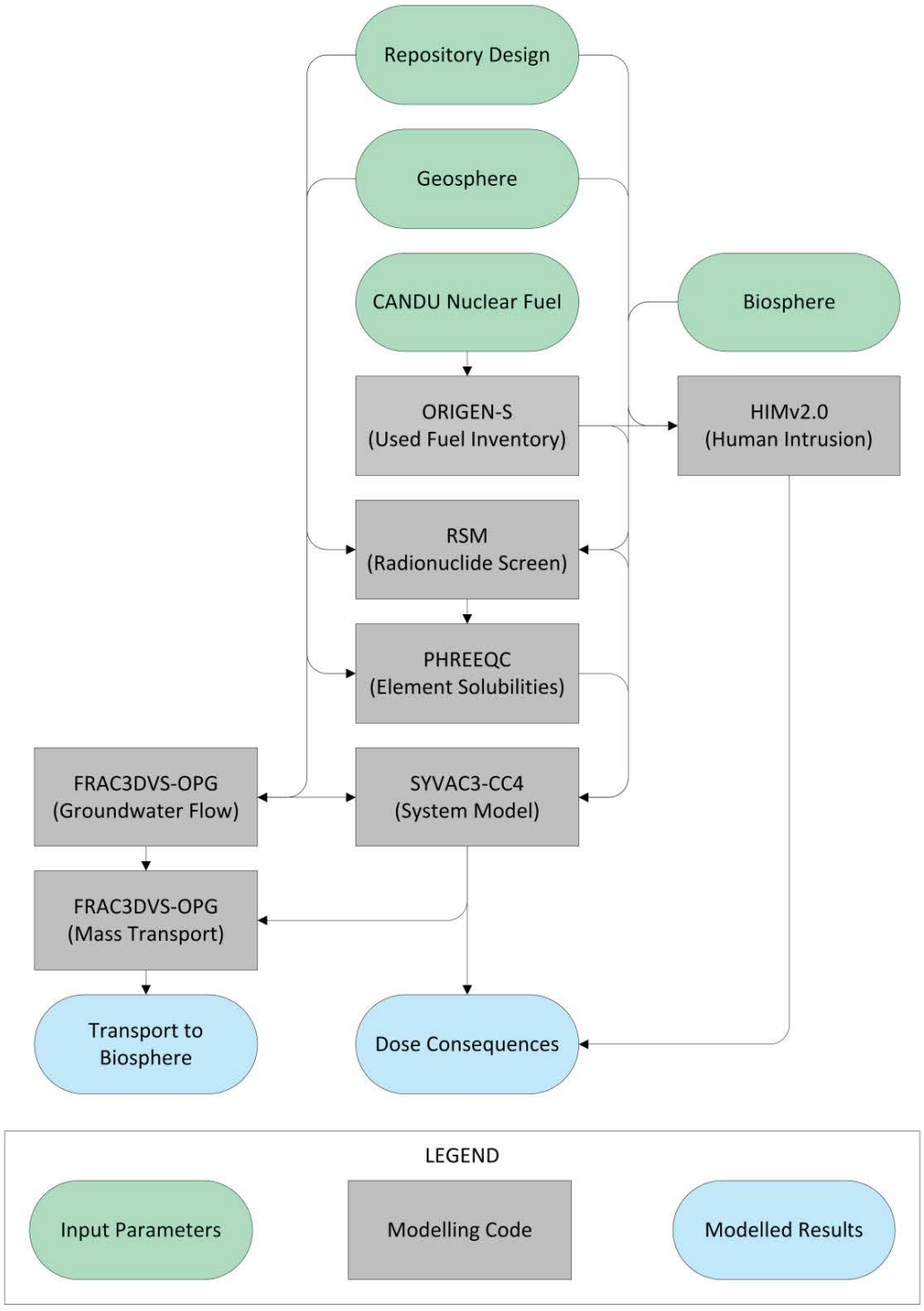

Figure 7-7: Main Computer Codes

ORIGEN-S is a CANDU-industry standard code used to calculate radionuclide inventories in the fuel and Zircaloy cladding at the time of placement, based on a defined reactor exposure scenario (Hermann and Westfall 1995, Tait et al. 1995).

ORIGEN-S was used to derive the used fuel inventories used in this study (see Chapter 3).

PHREEQC is a widely used and tested open source computer program developed by the United States Geological Survey (Parkhurst and Appelo 1999). PHREEQC is based on an ion-association aqueous model and is designed to perform a wide variety of low-temperature aqueous geochemical calculations.

In this assessment, PHREEQC Version 2.17 has been used for solubility and speciation calculations. The ThermoChimie v.7.b thermodynamic dataset was used, as described in Gobien et al. (2013).

RSM (Radionuclide Screening Model) is a project-specific simple model of groundwater transport of radionuclides from container to humans via a well. Through a conservative choice of input parameters, a large input set of radionuclides can be screened so as to objectively identify which are worth analyzing using more detailed models. RSM incorporates data for all radionuclides with half-lives longer than 0.1 years as well as radionuclides with half-lives longer than one day if they have a parent with a half-life longer than 0.1 years.

Table 7-6 provides more information on RSM.

SYVAC3-CC4 is the reference system model for the assessment of radionuclide release, transport, decay, biosphere transfer and dose assessment. It has been developed for a deep geological repository concept based on used fuel placed in durable containers, surrounded by engineered barrier material and located deep underground. The code can perform both deterministic and probabilistic calculations.

Table 7-7 provides more information on SYVAC3-CC4.

FRAC3DVS-OPG is the reference groundwater flow and transport code. This is a commercially available 3D finite-element / finite-difference code (Therrien et al. 2010). FRAC3DVS-OPG supports both equivalent porous medium and dual porosity representations of the geologic media.

Table 7-8 provides more information on FRAC3DVS-OPG.

HIMv2.0 is a project-specific code that assesses the consequences of the Inadvertent Human Intrusion Scenario. The model considers a scenario in which a used fuel container is unknowingly intersected by a drilled borehole, resulting in used fuel being brought directly to surface. Dose consequences are estimated for the drill crew and for a resident subsequently using the contaminated area.

Table 7-9 provides more information on HIMv2.0.

Table 7-6: RSM, Version RSM110

Parameter	Comments
Components:	
SYVAC3	Executive module, Version SV3.10.1
RSM	System model, Version RSM 1.10
Main Documents	*RSM Version 1.1 - Theory* (Goodwin et al. 2001) *RSM Version 1.1 Verification and Validation* (Garisto 2001)
Main Features	- Linear decay chains - Radionuclide release by instant release and by congruent dissolution - UO_2 dissolution calculated from user-supplied time-dependent data - Precipitation in container when user-supplied solubility limits exceeded - Durable containers, some fail with small defects - 1D buffer and backfill layer that surrounds the container and inhibits groundwater flow and radionuclide transport - Repository model based on one room containing failed container(s) - Linear sequence of 1D transport segments that connect the repository to a well. Transport segments are user-supplied; transport is solved considering diffusion, advection/dispersion and sorption - Dose impacts to a self-sufficient human household that uses well water, based on conservative model for drinking, immersion, inhalation and ground exposure. Effect of other ingestion pathways is included through a user-input multiplier - Ability to represent all input parameters with a probability density function (PDF) and to run Monte-Carlo type simulations - Time-independent material properties and biosphere characteristics - Database of all radionuclides with half-lives longer than 0.1 years as well as radionuclides with half-lives longer than one day if they have a parent with a half-life longer than 0.1 years

Table 7-7: SYVAC3-CC4, Version SCC4.09.1

Parameter	Comments
Components:	
SYVAC3	Executive module, Version SV3.12
CC4	System model, Version CC4.09.1
ML3	SYVAC3 math library, Version ML3.03
SLATEC	SLATEC Common Mathematical Library, Version 4.1
Main Documents	*SYVAC3-CC4 Theory Manual (NWMO 2012)* *SYVAC3-CC4 User Manual (Kitson et al. 2012)* *SYVAC3-CC4 Verification and Validation Summary (Garisto and Gobien 2013)*
Main Features	- Linear decay chains - Radionuclide release by instant release and by congruent dissolution - UO_2 dissolution rate calculated using radiation dose-rate based model - Precipitation in container when user-supplied solubility limits exceeded - Durable container, but some fail due to small defects - Cylindrical buffer and backfill layer that surrounds the container and inhibits groundwater flow and radionuclide transport - Multiple sector repository connected to the geosphere at sector-specific nodes chosen considering the local groundwater flow - Geosphere network of 1D transport segments that connect the repository to various surface discharge locations, including a well - Transport considers diffusion, advection / dispersion and sorption - Biosphere model that calculates field soil concentrations, well water concentrations, and uses a surface water body as a final collection point - Dose impacts to a self-sufficient human household that uses water body or well water, locally grown crops and food animals, local building materials and heating fuel - Dose impacts to generic non-human biota - Flow-based models in repository and geosphere, concentration-based models in biosphere - Generally time-independent material properties and characteristics for the biosphere and geosphere model. Transitions from one geosphere (or biosphere) state to another at specific times can be accommodated - Ability to represent all input parameters with a probability density function and to run Monte-Carlo type simulations

Table 7-8: FRAC3DVS-OPG, Version 1.3

Parameter	Comments
Components:	
FRAC3DVS-OPG	Main code, Version 1.3
Main Documents	*A Three-dimensional Numerical Model Describing Subsurface Flow and Solute Transport* (Therrien et al. 2010)
Main Features	- Linear decay chains - 3 D groundwater flow and solute transport in saturated and unsaturated media - Variable density (salinity) fluid - 1D hydromechanical coupling - Equivalent porous medium or dual-continuum model; fractures may be represented as discrete 2D elements - Finite-element and finite-difference numerical solutions - Mixed element types suitable for simulating flow and transport in fractures (2D rectangular or triangular elements) and pumping / injection wells, streams or tile drains (1D line elements) - External flow boundary conditions can include specified rainfall, hydraulic head and flux, infiltration and evapotranspiration, drains, wells, streams and seepage faces - External transport boundary conditions can include specified concentration and mass flux and the dissolution of immiscible substances - Options for adaptive time-stepping and sub-gridding

Table 7-9: HIMv2.0

Parameter	Comments
Components:	
AMBER	Executive Code, Version 5.5
HIMv2.0	Main Model Version
Main Documents	*Human Intrusion Model for the Fourth and Fifth Case Studies: HIMv2.0 (Medri 2012)*
Main Features	- Linear decay chains - Dose consequences by external, inhalation and ingestion pathways to drill crew and site resident - Surface contamination decreases with time due to radioactive decay and soil leaching - Time-independent material properties and biosphere characteristics - Includes data for potentially relevant radionuclides

7.5 Analysis Methods and Key Assumptions

This section describes the analysis approach and the manner in which the FRAC3DVS-OPG and SYVAC3-CC4 models are used in the analysis.

Data for selected parameters are also given to provide context. Gobien et al. (2013) should be consulted if more details are required.

7.5.1 Overall Approach

The general approach for conducting the postclosure safety assessment is as follows:

1. Conduct Radionuclide and Chemical Hazard Screening

Used nuclear fuel initially contains hundreds of radionuclides and chemically hazardous stable elements; however, most are short lived and / or present in very small amounts. Following placement in a deep geological repository, only a small subset poses a potential risk to humans and the environment. The RSM code is used to identify this subset for more detailed assessment.

The methods used for performing the screening analysis are described in Section 7.5.2.

2. Perform 3D Groundwater Flow and Radionuclide Transport Modelling

Detailed 3D steady-state hydrogeological modelling is performed with FRAC3DVS-OPG to determine the groundwater flow field near the repository.

Once the flow field is determined, detailed 3D diffusive and advective radionuclide transport calculations are performed to determine radionuclide transport for I-129, Cs-135, U-234 and U-238. These radionuclides are typically the most important in terms of potential radiological impact or in representing a range of low-sorption to high-sorption species. Radionuclide releases from the defective containers are provided from the SYVAC3-CC4 container release model and imposed as a source term on the FRAC3DVS-OPG mass transport calculation.

Dose consequences cannot be determined because the FRAC3DVS-OPG code does not have biosphere and dose models. Transport results are therefore expressed in units of Bq/a.

Due to the large size of the modelled environment, three different nested models are created. These are:

- Regional Model - described in Chapter 2, this model encompasses a large region with an east-west extent of 152 km, a north-south extent of 179 km, and extending deep into the Precambrian basement rock. This model was used to determine the boundary conditions for the Site-Scale Model, as described in Section 7.5.3.1.

  No repository features are incorporated at this scale of resolution (1 km by 1 km, horizontally).

- Site-Scale Model – the domain includes the repository and a section of the surrounding geosphere. The portion of the regional flow system into which groundwater flow from the repository travels and discharges is not included.

  The model is used to determine the most conservative source location (i.e., the container location with the most rapid contaminant transport to a conservatively located water-supply well). Reference Case and various sensitivity simulations are performed to determine radionuclide transport to the well. The model also supplies boundary conditions to the Repository-Scale Model.

  A simplified representation of the repository and the Engineered Barrier System (EBS) is included at this scale of resolution; however, individual containers are not modelled.

- Repository-Scale Model - the model domain is a small section of the repository surrounding the defective containers and the adjacent geosphere.

  Reference Case and various sensitivity simulations are performed to corroborate results of the Site-Scale Model and to provide a more complete understanding of repository component functions.

  The model incorporates a high level of detail and individual containers are represented at the source location.

Figure 7-8 illustrates the spatial relationships for the Site-Scale and Repository-Scale models.

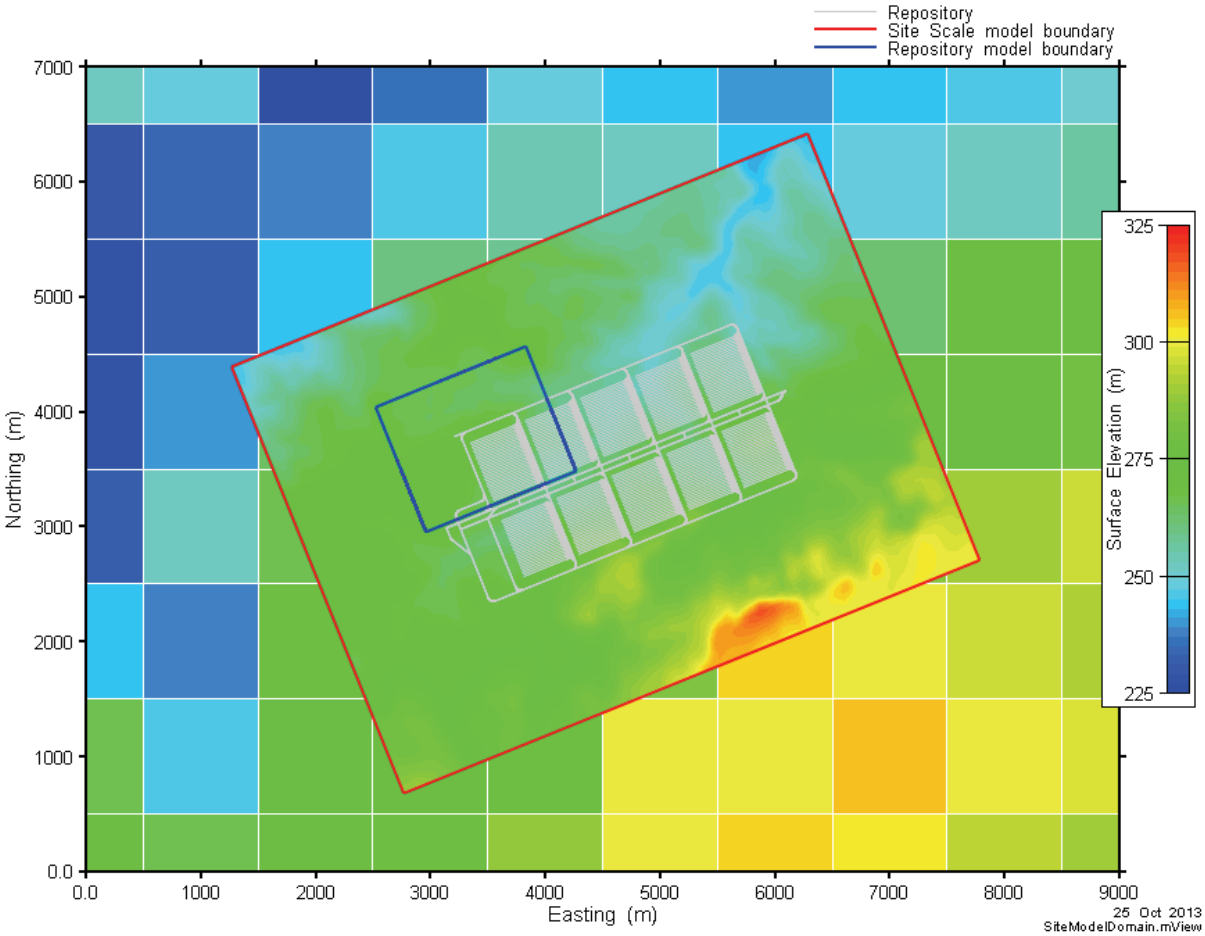

Figure 7-8: FRAC3DVS-OPG Site-Scale and Repository-Scale Model Domains

The nested models are also used to obtain a description of the groundwater flow field for use in subsequent SYVAC3-CC4 system modelling. To provide data for confirming that the resulting SYVAC3-CC4 system model is appropriate for use, radionuclide transport calculations (taking into account both diffusion and advection) for I-129, Cs-135, U-234 and U-238 are performed with FRAC3DVS-OPG. Results are generated for radionuclide transport out of a virtual volume around the placement room containing the defective containers and for transport to the biosphere.

The methods used in this phase of the assessment are described in Section 7.5.3.

3. Perform System Modelling

The 3D groundwater flow field generated with FRAC3DVS-OPG is used to guide development of the geosphere model in the SYVAC3-CC4 system model.

The SYVAC3-CC4 geosphere model is verified by comparing the radionuclide transport results with radionuclide transport results from FRAC3DVS-OPG. These comparisons are performed for I-129, Cs-135, U-234 and U-238, as these represent the key radionuclides for groundwater transport, as well as provide a test of the two models for species that cover a range of sorptions as well as a simple decay chain.

All other aspects of the system model - used fuel, container, near-field and biosphere are defined by the scenario and by input data.

The dose consequences for the Reference Case and for various deterministic sensitivity cases are determined for the full suite of radionuclides of interest.

The SYVAC3-CC4 system model is also used for the probabilistic safety assessment, assuming a fixed geosphere. The radionuclide inventory, release and transport properties are varied about the Reference Case values, as are the characteristics of the biosphere and dose receptor.

The methods used in this phase of the assessment are described in Section 7.5.4.

7.5.2 Radionuclide and Chemical Hazard Screening Model

This section describes how the radionuclide and chemical hazard screening is performed.

Section 7.5.1 shows how this fits into the overall assessment approach. Note that because the Inadvertent Human Intrusion Disruptive Scenario bypasses the geosphere barrier, the screening assessment described here does not apply and a separate case-specific screening assessment is required. This separate assessment is described in Section 7.9.1.

The screening uses the RSM model. RSM closely resembles the SYVAC3-CC4 system model used to perform the primary dose assessment; however, some simplifications are incorporated to ensure conservative results are obtained. The following discusses the RSM model in terms of its key features and whether they differ from those in the SYVAC3-CC4 model.

- Solubility limits, diffusion coefficients, sorption coefficients and decay constants are the same.
- The radionuclide source term is the same.
- The container release model is the same.
- The near field model (representing the engineered barriers) is represented by a simple one dimensional pathway consisting of a 0.63 m thick bentonite buffer. The bentonite properties are identical to those in the SYVAC3-CC4 model.
- The geosphere model is similar in that it is based on a one dimensional diffusion-dispersion-advection transport model; however, unlike the detailed geosphere model in SYVAC3-CC4, only a single fast transport pathway is represented. This pathway is composed of five zones

corresponding to the primary sedimentary layers between the repository and the Guelph aquifer. The incorporated layers are: Cobourg, Georgian Bay, Queenston, Manitoulin, and Cabot Head.

All failed containers share the same transport pathway.

The properties used to represent the five geosphere zones are shown in Table 7-10. These properties are selected to ensure a conservative representation of the transport time to the surface. The model assumes that the advective velocity in the geosphere is zero in all layers due to the extremely low permeability of the various rock types.

Table 7-10: Screening Model Geosphere Zone Properties

Geosphere Zone	Material Type	Length (m)	Diffusion Coefficient in Water (m^2/a)	Porosity (-)	Tortuosity (-)
1	Cobourg	25.4*	0.13	0.015	0.03
2	Georgian Bay	154.3	0.13	0.07	0.014
3	Queenston	77.6	0.13	0.073	0.02
4	Manitoulin	15.6	0.13	0.028	0.006
5	Cabot Head	15.8	0.13	0.116	0.03

Note: * the repository is located in approximately the middle of this layer

- The biosphere model is greatly simplified. Both codes use the same critical group based on a self-sufficient farming family living on the site; however, SYVAC3-CC4 incorporates the biosphere model in Figure 7-6 with explicit modelling of various pathways while RSM has a more limited set of exposure pathways. RSM calculates doses from water ingestion, groundshine, air immersion and air inhalation. The plant ingestion dose rate is estimated

  The following assumptions are also incorporated in the biosphere model to ensure conservative results:

  - The well demand is set to that corresponding to a single person, excluding irrigation. This ensures the minimum amount of dilution.
  - The surface soil is a small irrigated garden large enough to support only a single person. This maximizes the soil concentration.
  - Contaminant concentrations in any surface water present are set equal to those in the well. This maximizes the surface water concentrations.

Prior to running the model, a pre-screening is done. All radionuclides with half-lives longer than 0.1 years as well as radionuclides with half-lives longer than one day if they have a parent with a half-life longer than 0.1 years are included. This results in a total of 251 distinct radionuclides and 96 stable elements remaining in the used fuel and zirconium fuel sheath for further consideration.

The RSM model is then run for the suite of analysis cases shown in Table 7-11, with the cases selected to bound the cases described in Section 7.2 (i.e., the sensitivity cases included in the safety assessment). For each case listed in Table 7-11, the screening assessment conservatively assumes failure of all containers. All RSM cases are run for a 10 million year simulation time.

For the radiological dose assessment, the set of radionuclides that together contribute 0.1% or less of the total peak dose rate are screened out.

For the chemical hazard assessment, all stable chemically hazardous elements whose peak groundwater, surface water or soil concentration exceed 10% of their associated interim acceptance criterion are screened in.

Finally, the results are compared with previous Canadian and international case studies to verify that all important radionuclides and elements are included. Section 7.6 describes the results of the screening assessment.

Table 7-11: Cases Considered for the Radionuclide and Chemically Hazardous Element Screening Assessment

Case	Description
Base Case	The "All Containers Fail Scenario" with all parameter values set to their median values.
No Sorption	The "All Containers Fail Scenario" with sorption coefficients for the geosphere and engineered sealing materials set to zero and all other parameters maintained at their Base Case values.
High Solubility	The "All Containers Fail Scenario" with solubility limits for all species set to an arbitrarily high value of 2000 mol/m^3 and all other parameters maintained at their Base Case values.
High Instant Release Fraction	The "All Containers Fail Scenario" with instant release fractions for all elements set to 10% and all other parameters maintained at their Base Case values.
10x Diffusion Coefficient	The "All Containers Fail Scenario" with all diffusion coefficients in the engineered sealing materials and geosphere increased by a factor of 10 and all other parameters maintained at their Base Case values.

7.5.3 Detailed Flow and Transport Models

This section provides descriptions of the two nested models illustrated in Figure 7-8 and used in the FRAC3DVS-OPG groundwater and radionuclide transport calculations. Section 7.5.1 describes how this fits into the overall assessment approach.

All flow modelling is steady-state. This is consistent with the Reference Case assumption of constant climate. Small changes in climate may affect the shallow groundwater system, but would not affect the deep geosphere. The effects of large changes in climate associated with glacial cycles are discussed separately in Section 7.10.

The reference groundwater composition at repository depth is shown in Table 7-12. The flow modelling assumes a freshwater fluid, and the justification and methodology behind this assumption are discussed near the end of Section 7.5.3.1.

Table 7-12: Groundwater Composition for the Cobourg Formation (Repository Level)

Composition	SR-270 EQ	SR-270 NF
pH	6.3	8.1
Environment	Reducing	Reducing
Eh (mV)	-200	-535
Density (g/L)	1.192	1.192
Solutes (mg/L)		
Na	50,025	48,673
K	12,486	3,482
Ca	32,494	37,285
Mg	8,173	9,940
HCO_3	135	3
SO_4	1,784	1,813
Cl	168,058	168,744
Br	1,698	1,703
Sr	1,198	1,200
Li	5	5
F	1	1
I	3	3
B	80	80
Si	4	10
Fe	30	579
NO_3	10	10
PO_4	-	-
TDS (mg/l)	276,184	273,531

Notes: SR-270 EQ is equilibrated with minerals in the bentonite and SR-270 NF is equilibrated with both the carbon steel insert and bentonite.

TDS – Total Dissolved Solids

From Gobien et al. (2013)

Element solubilities are shown in Table 7-13. These have been calculated for the two groundwater compositions shown above at 25°C, with the higher of the resulting values selected. To account for higher temperatures and uncertainties associated with non-homogeneity in material composition, the solubility values shown in Table 7-13 are increased by a factor of 10 in the safety assessment calculations.

Elements not listed are assigned a solubility of 2000 mol/m^3 to ensure precipitation does not occur.

Table 7-13: Element Solubilities

Element	Value (mol/m^3)	GSD	Distribution Type
C	2.2	3.2	Lognormal
Cu	2.6×10^{-2}	3.2	Lognormal
Np	1.7×10^{-6}	3.2	Lognormal
Pa	3.2×10^{-5}	10	Lognormal
Ra	1.7×10^{-2}	3.2	Lognormal
Se	3.4×10^{-6}	3.2	Lognormal
Sn	9.1×10^{-5}	3.2	Lognormal
Tc	4.4×10^{-6}	3.2	Lognormal
Th	1.4×10^{-4}	3.2	Lognormal
U	4.5×10^{-6}	3.2	Lognormal
Zr	1.8×10^{-5}	3.2	Lognormal
Other	2000	-	Constant

Note: From Gobien et al. (2013)

Data for effective diffusion coefficients, sorption coefficients, and material porosities are shown in Table 7-14 through Table 7-16. These data are described in Gobien et al. (2013). Note that the effective diffusion coefficients are conservative, in some cases exceeding the estimated free-water diffusion coefficient (e.g., dense backfill blocks). Sorption coefficients are taken from data generated using high salinity water.

For creating input files for FRAC3DVS, tortuosity is calculated based on the effective diffusivity and porosity values reported in Table 7-14 and Table 7-16, according to the following formula:

$$\tau = \frac{D_e}{\varphi D_o} \qquad (7\text{-}2)$$

where τ is tortuosity;
D_e is effective diffusion coefficient (m^2/a, Table 7-14);
φ is porosity (Table 7-16); and
D_o is free water diffusion coefficient (m^2/a).

Table 7-14: Data for Effective Diffusion Coefficients, Reference Case Values

Effective Diffusion Coefficients (Vertical) (m^2/a)			
Material	**Neutral and Anionic Species**	**Cationic Species**	**$D_{e.H} : D_{e,V}$**
Drift	3.79×10^{-2}	1.14×10^{-1}	1
Unit G	2.71×10^{-5}	8.14×10^{-5}	2
Unit F	2.59×10^{-4}	7.76×10^{-4}	2
Unit E	2.97×10^{-4}	8.90×10^{-4}	2
Unit B and C	7.26×10^{-4}	2.18×10^{-3}	2
Unit A-2 Carbonate	7.57×10^{-5}	2.27×10^{-4}	2
Unit A-1 Upper Carbonate	4.29×10^{-4}	1.29×10^{-3}	1
Unit A-1 Carbonate	1.14×10^{-5}	3.41×10^{-5}	2
Unit A-1 Evaporite	1.89×10^{-6}	5.68×10^{-6}	2
Unit A0	1.89×10^{-6}	5.68×10^{-6}	2
Guelph	1.83×10^{-3}	5.49×10^{-3}	1
Fossil Hill	2.71×10^{-6}	8.14×10^{-6}	2
Cabot Head	1.96×10^{-4}	5.87×10^{-4}	2
Manitoulin	9.47×10^{-6}	2.84×10^{-5}	2
Queenston	6.31×10^{-5}	1.89×10^{-4}	2
Georgian Bay / Blue Mountain	5.18×10^{-5}	1.55×10^{-4}	2
Cobourg	2.34×10^{-5}	7.01×10^{-5}	2
Sherman Fall	1.39×10^{-5}	4.17×10^{-5}	2
Kirkfield	2.65×10^{-5}	7.95×10^{-5}	2
Cobokonk	1.70×10^{-5}	5.11×10^{-5}	2
GullRiver	1.64×10^{-5}	4.92×10^{-5}	2
Shadow Lake	8.20×10^{-5}	2.46×10^{-4}	2
Placement Room Bentonite (Homogenized Backfill)	1.28×10^{-2}	3.72×10^{-2}	1
Tunnel Seal Bentonite (Compacted Bentonite)	9.47×10^{-3}	1.58×10^{-2}	1
Shaft Bentonite/Sand	9.47×10^{-3}	1.58×10^{-2}	1
Tunnel Dense Backfill	6.31×10^{-2}	1.89×10^{-1}	1
Low Heat High Performance Concrete (LHHPC), degraded	3.94×10^{-3}	1.18×10^{-2}	1
Shaft Asphalt	3.16×10^{-6}	9.47×10^{-6}	1
Shaft Soil Backfill	7.89×10^{-3}	2.37×10^{-2}	1

Note: All elements are either neutral or anions, with the exception of Cs which is treated as a cation.
All material properties are defined for 25°C except for Placement Room Bentonite which is defined for 70°C

Table 7-15: Data for Sorption Coefficients (K_d), Reference Case Values

Sorption Coefficients (m^3/kg)				
Element	**Bentonite**	**Dense Backfill**	**Limestone**	**Shale**
Am	0.23	0.070	0.020	0.23
Cs	4.0×10^{-3}	1.2×10^{-3}	3.6×10^{-4}	0.060
Cu	7.0×10^{-3}	2.1×10^{-3}	2.0×10^{-4}	1.0×10^{-4}
Nb	0.10	0.030	0	0.050
Np	4.3	1.3	2.6	1.2
Pa	0.020	6.0×10^{-3}	0.014	0.014
Pb	1.0×10^{-3}	3.0×10^{-4}	0	0.030
Pu	0.50	0.15	0.020	0.20
Th	40	12	2.6	1.2
U	40	12	2.6	1.2
Zr	0.050	0.015	0	0.010
Other	0	0	0	0

Note: To be conservative, sorption coefficients for concrete and asphalt are assumed to be zero.
Data are from Gobien et al. (2013)

Table 7-16: Data for Material Porosity

Material	Porosity (-)
Drift	0.200
Unit G	0.172
Unit F	0.100
Unit E	0.100
Unit B and C	0.165
Unit A-2 Carbonate	0.120
Unit A-1 Upper Carbonate	0.070
Unit A-1 Carbonate	0.019
Unit A-1 Evaporite	0.007
Unit A0	0.032
Guelph	0.057
Fossil Hill	0.031
Cabot Head	0.116
Manitoulin	0.028
Queenston	0.073
Georgian Bay / Blue Mountain	0.070
Cobourg	0.015
Sherman Fall	0.016
Kirkfield	0.021
Cobokonk	0.009
GullRiver	0.022
Shadow Lake	0.097
Tunnel Seal Bentonite (Compacted Bentonite)	0.481
Placement Room Bentonite (Homogenized Backfill)	0.413
Shaft Bentonite/Sand	0.411
Tunnel Dense Backfill	0.194
Concrete (LHHPC), degraded	0.100
Shaft Asphalt	0.020
Shaft Soil Backfill	0.200

7.5.3.1 Site-Scale Model

The Site-Scale Model is used to investigate the mass flows to the well and surface environment for I-129, Cs-135, U-234 and U-238 released from failed containers in the repository. The source containers are placed in the location with the shortest transport time and the maximum I-129 mass transport to the well. The model supplies boundary conditions for use in the Repository-Scale Model, and examines sensitivity cases investigating the effect on transport of the EDZ hydraulic conductivity, geosphere hydraulic conductivity and overpressure in the Shadow Lake formation. Spatial and temporal convergence testing is also done with this model.

The model domain is specified as the repository footprint together with approximately 1200 m of surrounding geosphere that encompasses the repository influenced flow domain. A new coordinate system is established, with the new system rotated 158 degrees counter-clockwise, so that the X axis follows the middle of Access Drift 1. This allows natural finite-difference discretization of the generally orthogonal repository features.

Figure 7-9 shows the coordinate system and model boundaries.

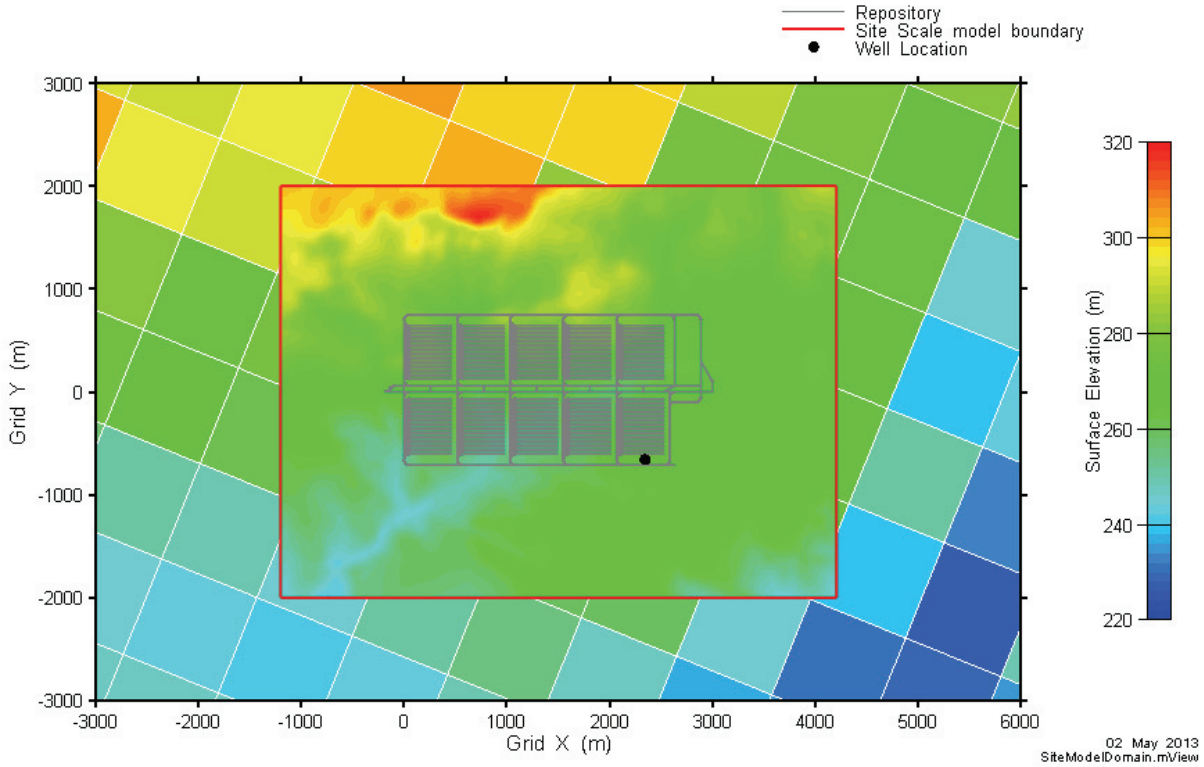

Figure 7-9: Site-Scale Model - Coordinate System and Domain Boundary

Domain Discretization

The repository is about 500 m below ground surface (mBGS). Since the surface elevation varies slightly across the repository, the horizontal depths are also defined in terms of an

absolute measure of metres above sea level (mASL). The floor of the hypothetical repository is located at an average elevation of -237 mASL.

Unlike the Regional Model (see Chapter 2), which is discretized with constant 1000 m by 1000 m square elements, the Site-Scale Model uses variable element sizes in X, Y, and Z directions to incorporate repository related features with good geometric fidelity. The maximum element area is 50 × 50 m in the corners of the grid. The smallest XY dimension is 1.25 × 1.5 m, and is used to incorporate the shaft excavation damaged zone and tunnel seal features. This results in grid layers containing 148,635 elements.

Vertical discretization is driven by the requirement to incorporate geosphere and repository features as well as shaft sealing materials. Eighty layers are incorporated, yielding a total of 11.7 million elements. Figure 7-10 presents elemental volumes. Individual element edges are not shown due to the density of the elements.

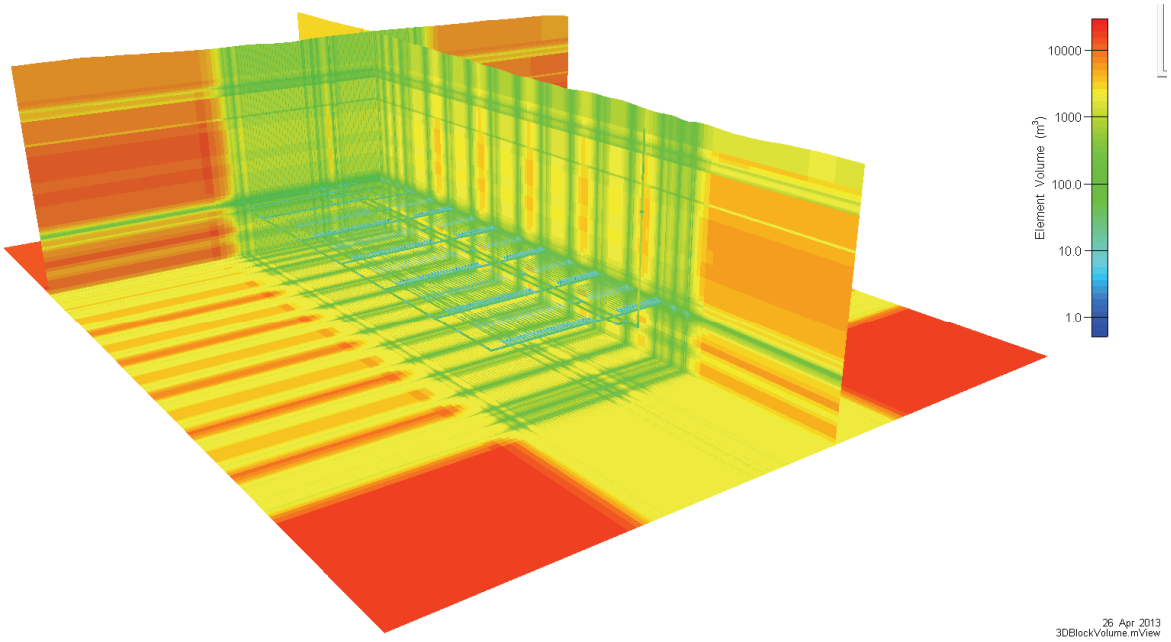

Figure 7-10: Site-Scale Model Element Volume

Hydraulic Conductivity Profile

The bulk rock properties are described as a layered system dipping towards the southwest. Hydraulic conductivity is generally lower in the deeper formations, as discussed in Chapter 2. Hydraulic conductivities and model discretization are shown in Table 7-17. Reference Case values are used in all simulations except for the sensitivity study that examines the effect of a factor of 10 increase in geosphere hydraulic conductivity.

Table 7-17: Geosphere Hydraulic Conductivity and Layering

Formation	Average Thickness (m)	Hydraulic Conductivity (m/s)*			Model Layers
		Reference Case (K_h)	Sensitivity Case	Anisotropy K_h:K_v	
Drift	40.64	1.0×10^{-7}	1.0×10^{-6}	2	5
Unit F	60.30	5.0×10^{-14}	5.0×10^{-13}	10	6 shared
Unit E		2.0×10^{-13}	2.0×10^{-12}	10	
Unit B and C		4.0×10^{-13}	4.0×10^{-12}	10	
Unit A-2 Carbonate	15.39	3.0×10^{-10}	3.0×10^{-9}	10	3
Unit A-1 Upper Carbonate	3.11	2.0×10^{-7}	2.0×10^{-6}	1	1
Unit A-1 Carbonate	22.12	9.0×10^{-12}	9.0×10^{-11}	10	4
Unit A-1 Evaporite	4.19	3.0×10^{-13}	3.0×10^{-12}	10	1
Guelph	71.57	3.0×10^{-8}	3.0×10^{-7}	1	5
Fossil Hill	6.86	5.0×10^{-12}	5.0×10^{-11}	10	1
Cabot Head	15.82	9.0×10^{-14}	9.0×10^{-13}	10	1
Manitoulin	15.53	9.0×10^{-14}	9.0×10^{-13}	10	1
Queenston	77.52	2.0×10^{-14}	2.0×10^{-13}	10	4
Georgian Bay and Blue Mountain	154.40	4.0×10^{-14}	4.0×10^{-13}	13	10
Cobourg	46.32	2.0×10^{-14}	2.0×10^{-13}	10	23
Sherman Fall	47.34	1.0×10^{-14}	1.0×10^{-13}	10	6
Kirkfield	39.53	8.0×10^{-15}	8.0×10^{-14}	10	3
Cobokonk	7.97	4.0×10^{-12}	4.0×10^{-11}	1000	1
Gull River	53.39	7.0×10^{-13}	7.0×10^{-12}	1000	4
Shadow Lake	7.58	1.0×10^{-9}	1.0×10^{-8}	1000	1

Notes: * Sensitivity Case examines the effect of a factor of 10 increase in geosphere hydraulic conductivity. Section 7.2.1 and Table 7-3 provide further explanation. Data are from Gobien et al. (2013).

Properties of the engineered barrier system are shown in Table 7-18. Within the repository, excavation damaged zone (EDZ) properties are derived from the properties of the Cobourg limestone host rock. All repository tunnels have an inner EDZ with hydraulic conductivity 1000 times higher than the host rock horizontal hydraulic conductivity, and porosity twice that of the host rock. Outer EDZ is assigned hydraulic conductivities 100 times greater than the host rock, while porosity is set equal to the host rock.

An inner and outer EDZ were defined for the shafts as well, with inner EDZ having hydraulic conductivity 100 times greater than the vertical hydraulic conductivity and outer EDZ conductivity increased by a factor of 10 relative to the host rock vertical conductivity. Inner EDZ porosity is doubled compared to the host rock.

All other EDZ parameters are set equal to those of the host rock.

There are minor simplifications in the implementation; in particular, the inner and outer EDZ is specified only on the tops and bottoms of the access tunnels and placement rooms. However, the EDZ hydraulic conductivity is increased to match the transmissivity of the reference EDZ cross section to account for the missing EDZs at the sides of tunnels. Similarly, porosity of the EDZ is corrected to achieve the same effective cross sectional area for flow, and thus match flow velocities along the EDZ given the same hydraulic gradient. The scaling factors used depend on the type of tunnel (i.e., access, perimeter or placement) but values are on the order of two.

More details on the definition of EDZ properties can be found in Gobien et al. (2013).

Table 7-18: Engineered Barrier Hydraulic Conductivity

Property Identifier	Description	Hydraulic Conductivity (m/s)		
		Reference Case	Shaft Seal Failure* (Base Case)	Shaft Seal Failure* (Extreme Case)
Tunnel Dense Backfill	Used to backfill repository tunnels	1.0×10^{-10}	1.0×10^{-10}	1.0×10^{-10}
Tunnel Seal Bentonite (Compacted Bentonite)	Used for room seals	8.2×10^{-13}	8.2×10^{-13}	8.2×10^{-13}
Placement Room Bentonite (Homogenized Backfill)	100% bentonite, homogenized mixture of gap fill and compacted pedestals in placement rooms	5.3×10^{-12}	5.3×10^{-12}	5.3×10^{-12}
Concrete (LHHPC), degraded	LHHPC concrete used for room closure and shaft bulkheads	1.0×10^{-10}	1.0×10^{-9} (degradation of all shaft-seal materials)	1.0×10^{-7} (further degradation of all shaft-seal materials to the equivalent of fine silt or sand)
Shaft Bentonite/Sand	Primary Shaft Seal material, 70:30 bentonite to sand	1.6×10^{-11}		
Shaft Soil Backfill	Well compacted soil backfill	1.0×10^{-8}		
Shaft Asphalt	Additional shaft sealing material	1.0×10^{-12}		

Note: * See Table 7-4 for a description of these cases. Data are from Gobien et al. (2013)

Figure 7-11 shows the vertical hydraulic conductivity profile on a cross-section through the Site-Scale Model. The figure shows properties of the repository along Access Drift 1, and two of the three shafts (Vent and Service shaft).

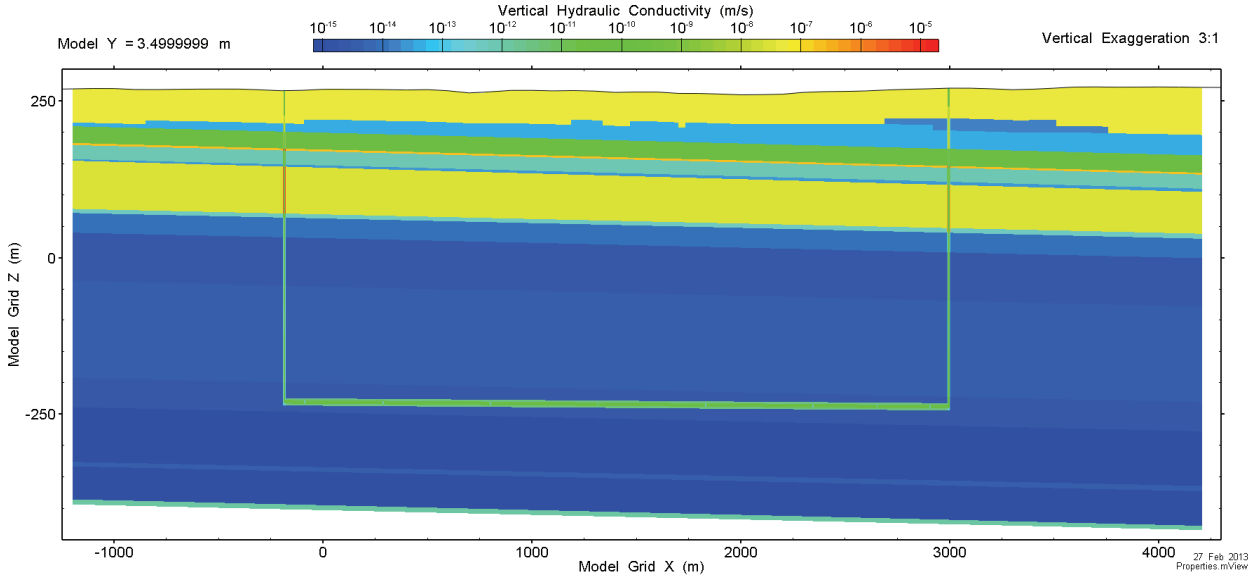

Figure 7-11: Site-Scale Model - Vertical Hydraulic Conductivity Profile

Transport properties include dispersivity, diffusivity, and sorption. Longitudinal dispersivity is set to 50 m for all materials, approximately 10% of the plume travel path length to discharge at the well, with transverse dispersivity specified as 5 m. Diffusivity and sorption values in the Site-Scale Model are shown in Table 7-14 and Table 7-15.

Figure 7-12 shows property assignments on a vertical cross-section through the entire domain while Figure 7-13 and Figure 7-14 illustrate property assignments on vertical cross-sections through a placement room seal and the main shaft. Figure 7-15 shows a plan section through part of the repository, showing a number of placement rooms, access tunnels, and associated seals, along with their material property assignments. The curved entrances to the rooms are simplified and represented as right-angle intersections.

Figure 7-16 shows a three-dimensional illustration of the property distribution, showing layered geology and the representation of the repository and shafts within the model.

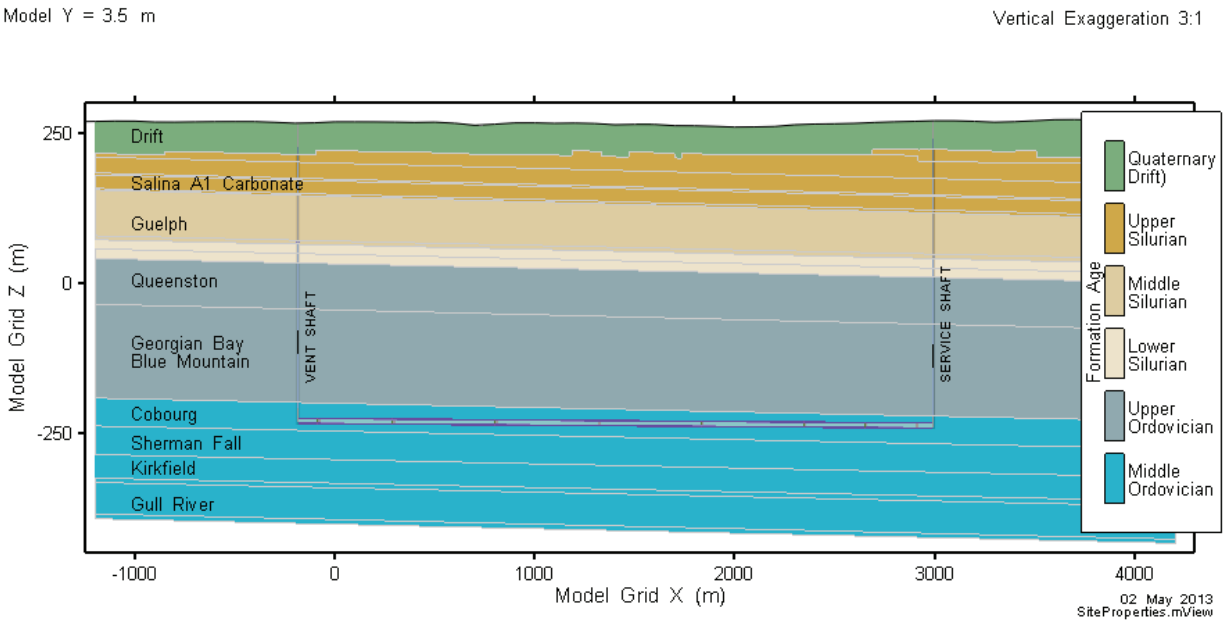

Figure 7-12: Site-Scale Model - Property Assignment on Vertical Cross-Section through Entire Model Domain

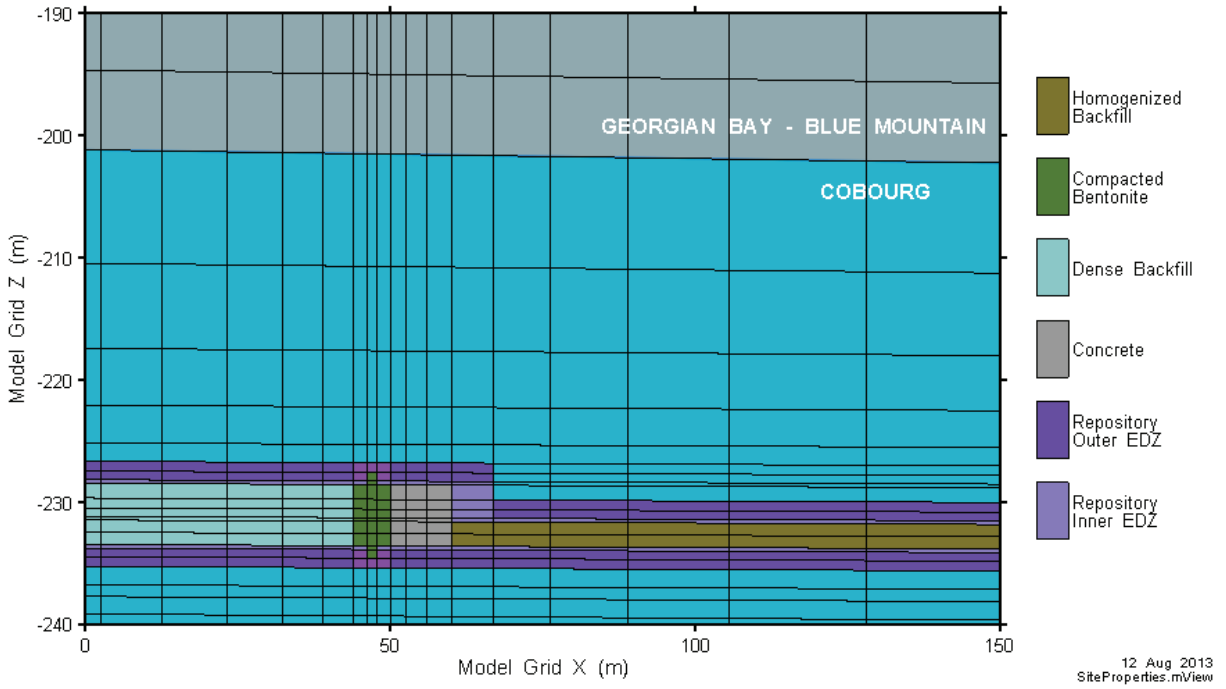

Note: 2:1 Vertical Exaggeration. The pink material around the seal is a combination of tunnel Seal Inner EDZ and outer EDZ

Figure 7-13: Site-Scale Model - Property Assignment on Vertical Cross-Section through Placement Room Seal

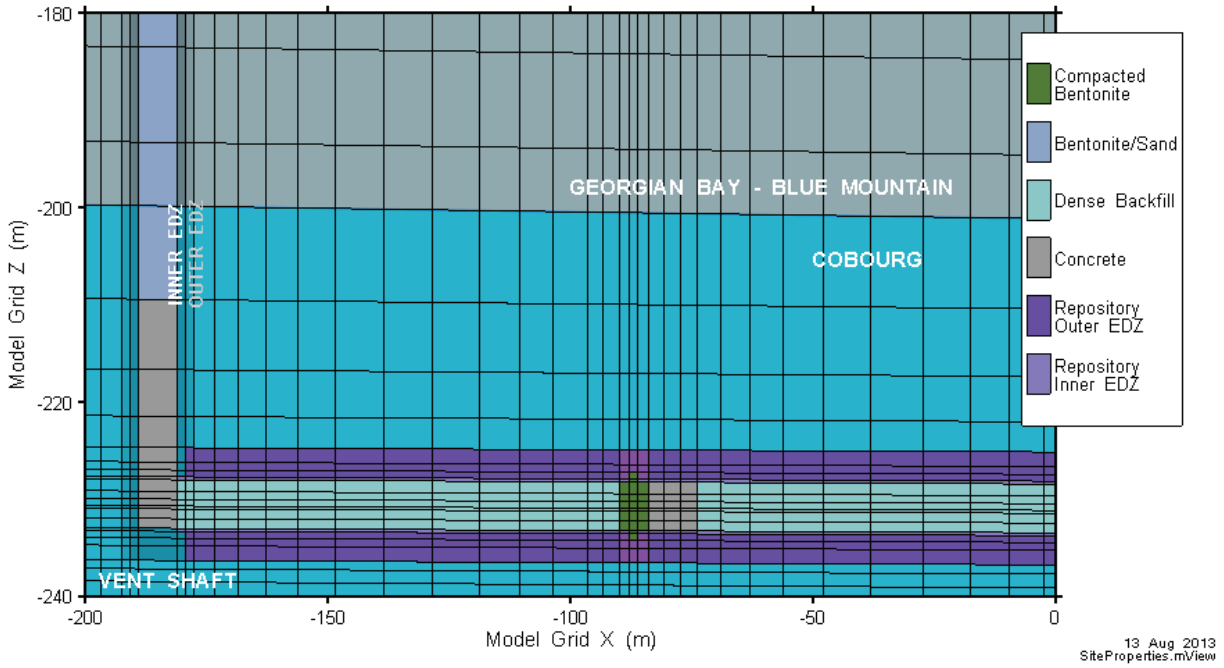

Note: 2:1 Vertical Exaggeration. The pink material around the seal is a combination of tunnel Seal Inner EDZ and outer EDZ

Figure 7-14: Site-Scale Model - Property Assignment on Vertical Cross-Section through Base of Vent Shaft

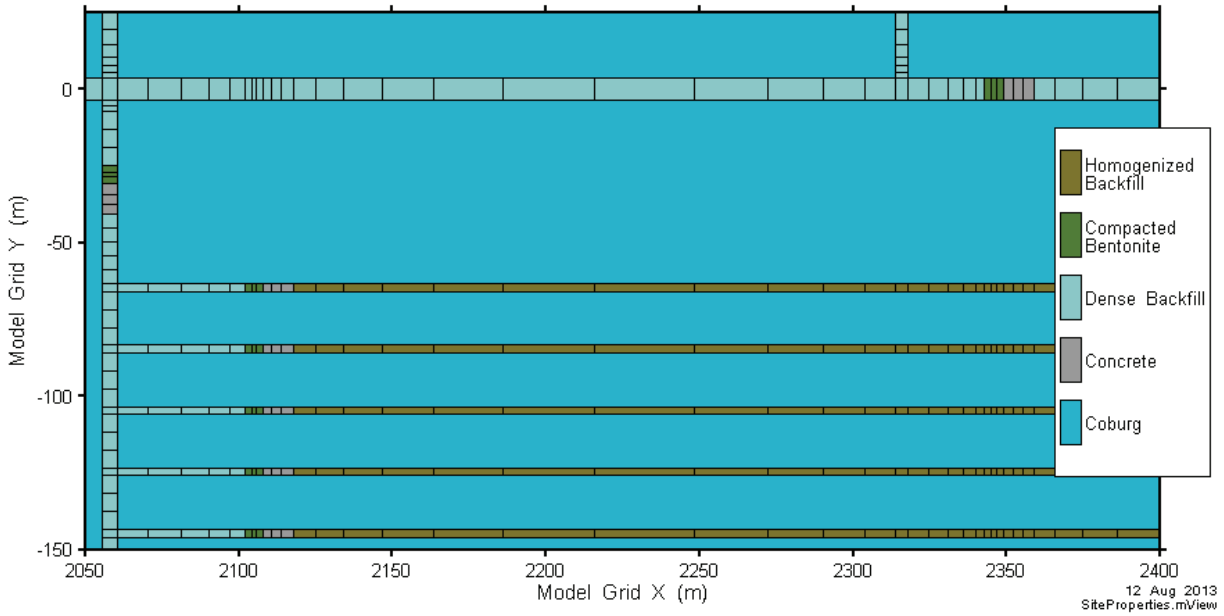

Figure 7-15: Site-Scale Model - Property Assignment on Plan View through Placement Rooms

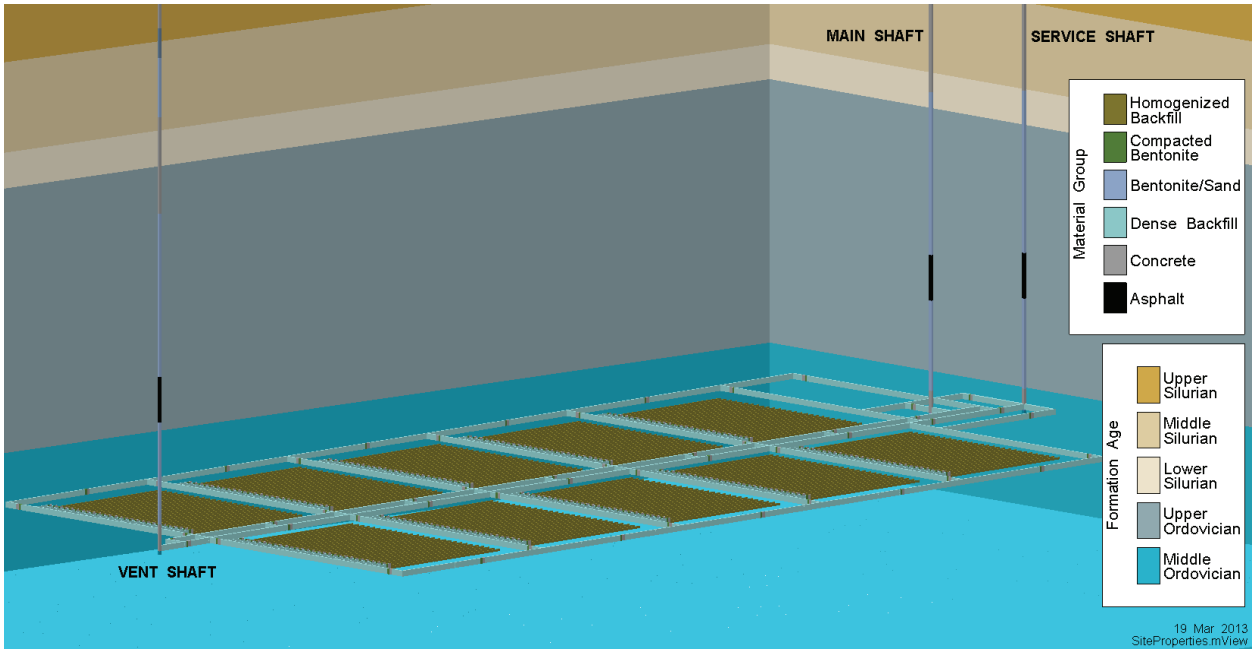

Figure 7-16: Site-Scale Model - Property Assignment in 3D View

Water Supply Well and Defective Containers

The water supply well is located based on results from simulations performed using the Reference Case hydraulic conductivities. The goal is to choose the most conservative location, largely based on the maximum rate of contaminant uptake at the well. At this hypothetical site, the very low hydraulic conductivities in the geosphere create a diffusion-dominated transport regime. In such a system, particle tracking does not provide useful information to locate the shortest transport pathway with the greatest mass transport rate. An alternative approach is to release a tracer from all locations across the repository footprint and examine the results to determine whether there are any variations in concentration at the base of the Guelph aquifer (i.e., the water supply aquifer for the well). The I-129 container release term was used as the tracer, and a release from all containers in the repository was simulated. The model was run without a pumping well.

Figure 7-17 shows the results of this simulation at ten million years. The repository floor is at an average elevation of approximately -237 mASL. The grey contours show the plume in the Fossil Hill formation, at an average depth of 55 mASL. This formation is directly below the Guelph formation, where the transport is still diffusion-dominated. The blue contours show the plume in the lowest layer of the Guelph (average elevation 66 mASL). Here, advection is the dominant transport process and the I-129 plume is swept down-gradient. Finally, the colours on the plot indicate the distance between the base of the Guelph and the top of the placement room outer EDZ, essentially the thickness of the diffusive barrier separating the repository from the Guelph aquifer. It is evident that where this barrier is thinnest, transport is fastest and the

concentrations in the plume, both in the Fossil Hill (diffusive) and Guelph (advective) portions of the plume, are highest.

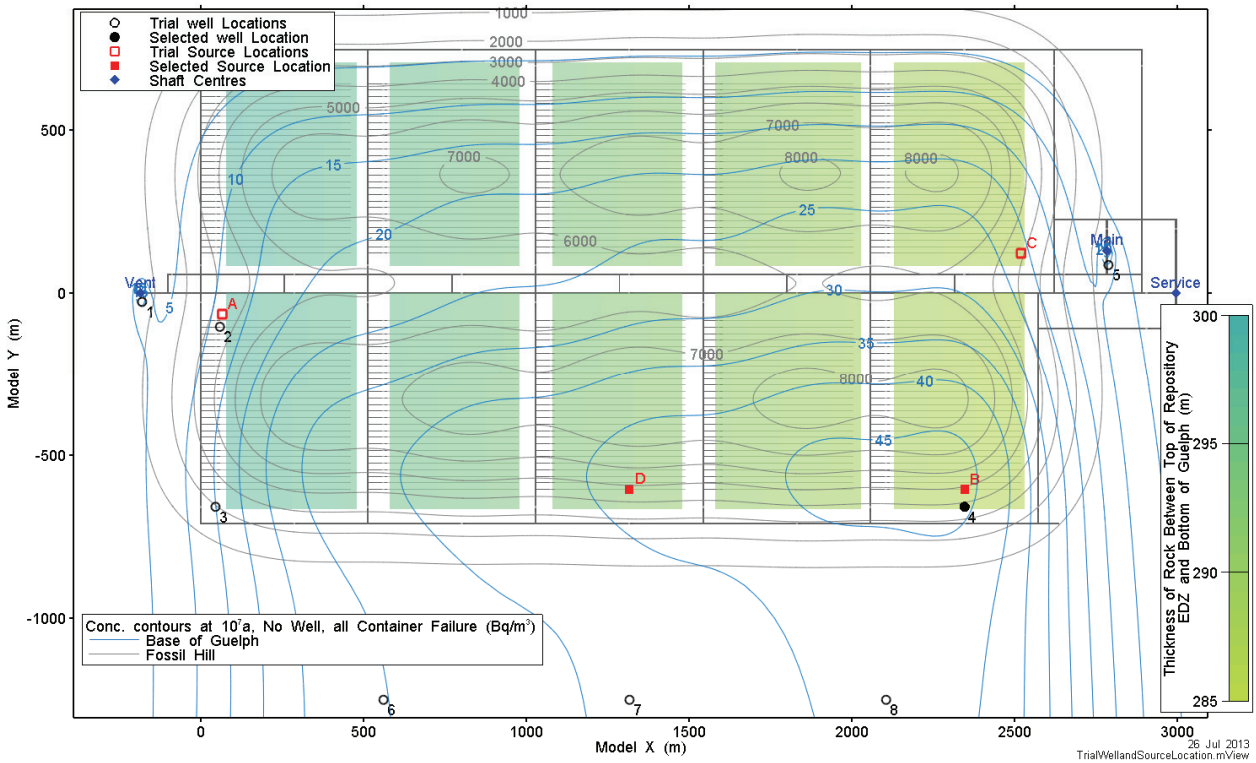

Figure 7-17: Site-Scale Model - Selecting Well Location

To discount the possibility that other factors, such as the more permeable shafts and EDZ, could outweigh the effect of the diffusive barrier thickness, a number of different well locations and source locations were also assessed. This was done in two stages. First, the model was run with releases from all containers with the well locations varied as shown in Table 7-19. Wells were placed in three downstream locations (Wells 6, 7, and 8 in Figure 7-17), and at the location of highest concentration at the base of the Guelph formation (Well 4 in Figure 7-17).

Table 7-19: Source and Well Locations, Release from All Containers

Well Location*	Description
4	Well near plume centre
6	Well downstream of repository footprint, closer to vent shaft side
7	Well downstream of repository footprint, closer to center
8	Well downstream of repository footprint, closer to main shaft side

Note: * For well locations refer to Figure 7-17

Maximum radionuclide concentration is relatively insensitive to the location of the well, as shown in Figure 7-18. Well 7 has a slightly higher maximum radionuclide transport rate, largely due to its higher plume capture rate.

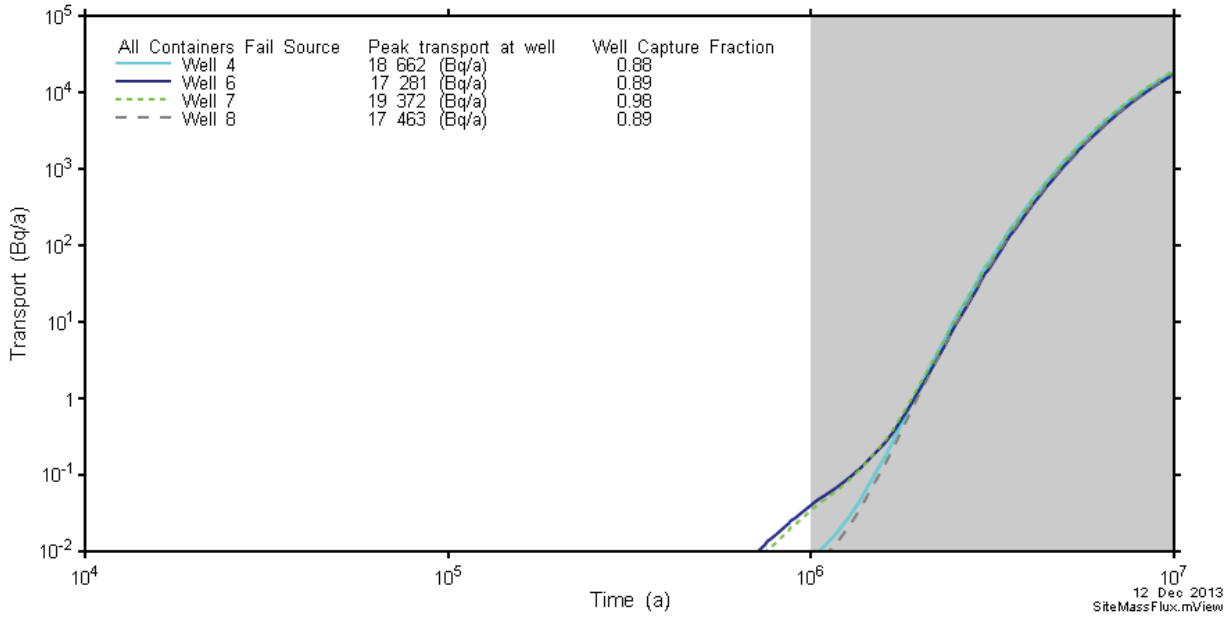

Figure 7-18: Site-Scale Model - Radionuclide Transport, Release from All Containers

To examine the possible influence of the shafts as a more rapid pathway for transport, the source term for three failed containers was used. The source release points and well locations were placed in various combinations in close proximity to the shafts in the location where the diffusive barrier is thinnest and in the location closest to Well 7, as shown in Figure 7-17 and described in Table 7-20.

Figure 7-19 shows that while there is relatively little variation in maximum transport rate, the combination of Source B and Well 4 yielded the maximum rate, while the second highest rate is for Source C and Well 5. This shows that the thickness of the diffusive barrier is the most important factor determining maximum contaminant transport to the well.

Table 7-20: Source and Well Locations, Release from Three Containers

Source Location*	Well Location*	Description
A	1	Source near the vent shaft, well directly adjacent to vent shaft.
A	2	Source near the vent shaft, well above the source.
A	3	Source near vent shaft, well downstream of source (in the Guelph).
B	4	Source near all container failure plume centre (see Figure 7-17), well above the source.
C	5	Source near the main shaft, well directly adjacent to the main shaft.
D	7	Source near centre of repository, well downstream of source.

Note: * For source and well locations refer to Figure 7-17

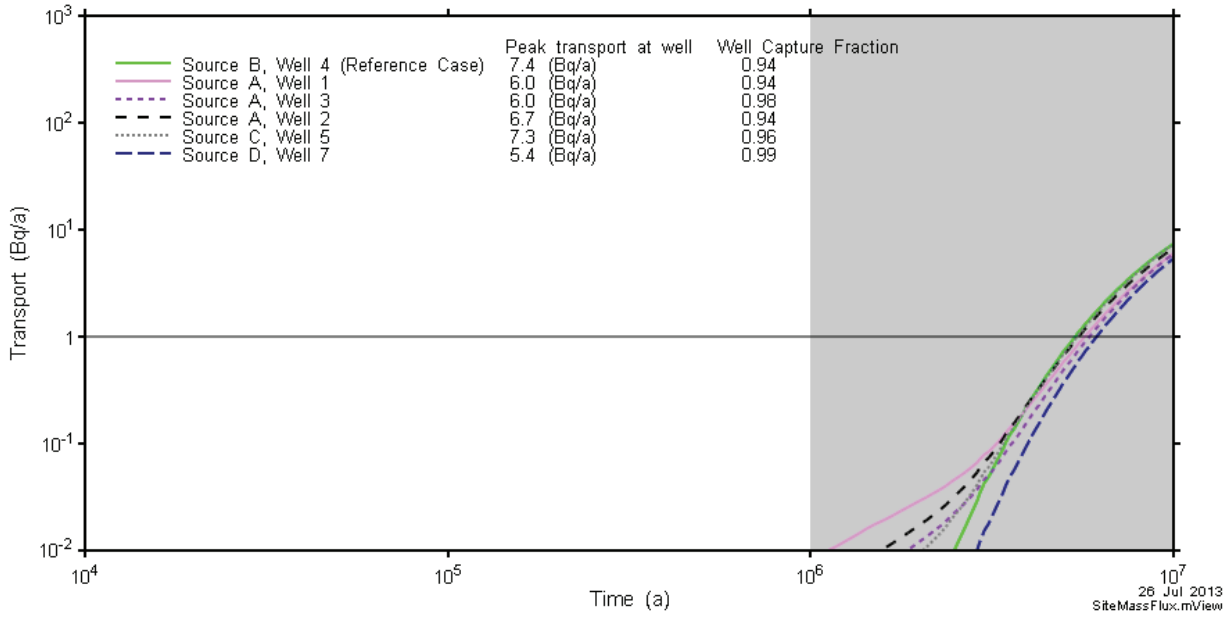

Figure 7-19: Site-Scale Model - Radionuclide Transport to Different Well Locations, Release from Three Containers

The relative homogeneity of the layered geology means that the rate of solute transport to the well is not very sensitive to the exact location of the source and well, although the two should be located relatively near each other on a horizontal projection to maximize well capture. Accordingly, the Reference Case water supply well was placed above the region where the diffusive barrier is thinnest, and the source term is placed in the centre of the nearest placement room (Source B and Well 4).

The well is represented as a 2D line element forming a segment, or edge, of a 3D element. Properties appropriate to a nominal 4” diameter well are assigned to the segment to specify the

hydraulic conductivity of the well. The lowest node on the segment is defined as the withdrawal node from which water is abstracted. The well location is shown on a cross sectional view in Figure 7-20.

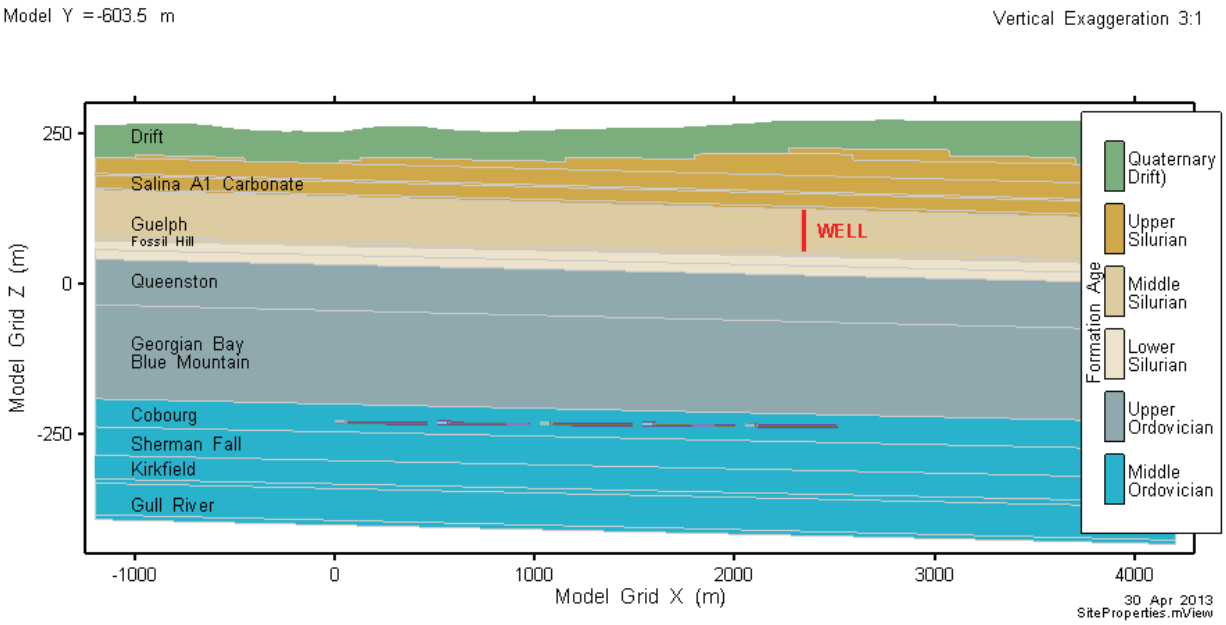

Figure 7-20: Site Scale Model – Well Location on Cross-Section

Hydraulic Head Boundary Conditions

Head boundary conditions for the Site-Scale Model were extracted from the head field calculated with the Regional Model described in Chapter 2. Boundary conditions remain unchanged for each well demand case, and are based on a flow field in which no pumping well is present. Head values for the Reference Case along the vertical model boundaries are shown in Figure 7-21.

Surface boundary conditions follow the surface topography and bottom boundary conditions (1500 mBGS) are set to zero flow; these are not illustrated in the figure.

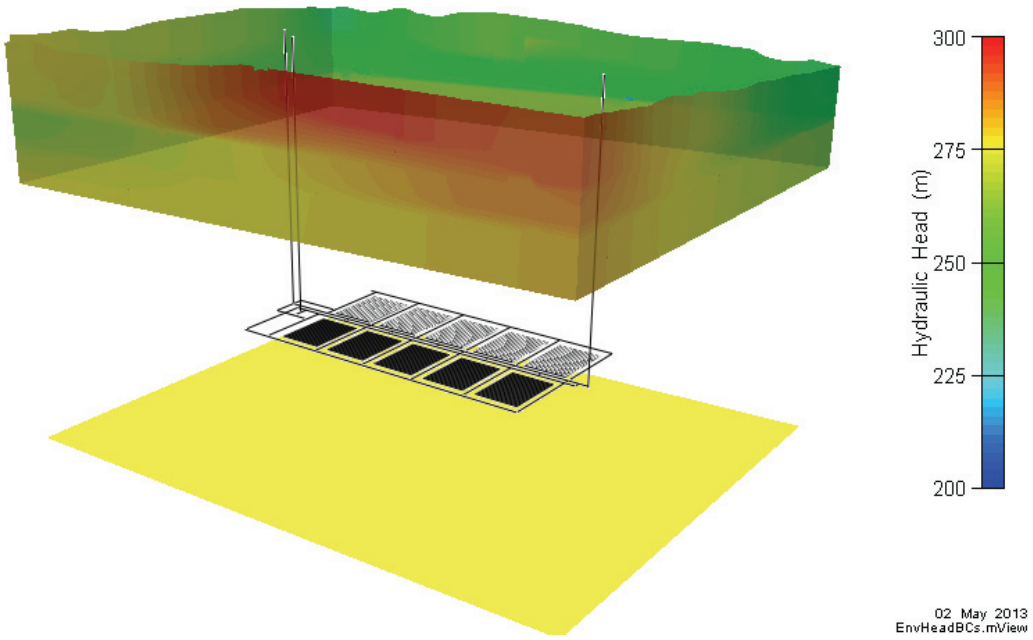

Note: Sides are no-flow boundaries

Figure 7-21: Site-Scale Model - Reference Case Head Boundaries, Sides and Bottom.

The hydraulic head was set by assuming constant head boundary conditions at the surface, with the water table following the surface topography. As the digital elevation model for the Site-Scale Model is more accurate than the coarser Regional Model, this leads to some differences between the heads in the two models.

For the vertical boundaries between the base of the unconsolidated drift and the base of the relatively permeable Guelph unit, constant head boundaries were set by interpolating heads directly from the Regional Model. In the permeable units (Guelph and above), the Regional Model predicts that the pore water is largely fresh within the Site-Scale Model domain, with a moderate increase in salinity down-dip in the Guelph. As a result, within the Site-Scale Model there is a good correspondence between flow directions and freshwater head in the Guelph without accounting for the slightly saline water in the deeper parts of the Guelph unit (see Figure 7-35 and Figure 7-36.

In the very low permeablility units below the Guelph, vertical boundaries were set as no-flow boundaries. This is a reasonable approximation of the Regional Scale Model, as within these units velocities are extremely low, and the flow direction is predominantly vertical.

Due to the low permeability of the Ordovician host rock and the resulting very low flow velocity (see Chapter 2, Figure 2-13), transport through these limestone and shale formations is

diffusion-dominated. For the lower boundary condition, the concept of environmental head was used to estimate a freshwater head that would provide a similar vertical driving force for flow in a steady-state freshwater model to the brine head derived from the density-driven Regional Model. A freshwater head of 275 m was found to approximate the brine head in the upper Precambrian predicted by the Regional Model at the one million year pseudo-equilibrium state. A scenario with a constant head boundary of 433 m was also run, and showed that due to the low permeability of the Ordovician host rock, the transport results are largely insensitive to the specified head at this boundary.

In summary, representative boundary conditions for the Site-Scale Model were achieved as follows:

- In the permeable (and largely fresh) units (Guelph and above), freshwater heads were extracted from the regional model and surface elevations are used to set constant head (Dirichlet) boundaries.
- In the units below the Guelph, no-flow (Neumann) boundaries were applied at the Site-Scale Model vertical boundaries, neglecting any horizontal flows across this boundary. This is reasonable given the very low permeability of these units and the predominantly vertical nature of the flow field.
- For the lower boundary, a constant head (Dirichlet) boundary was specified to approximate the regional model pseudo-equilibrium state and provide a similar vertical driving force.

7.5.3.2 Repository-Scale Model

This model encompasses a small section of the repository surrounding the source location and the adjacent geosphere. The model incorporates significant detail and individual containers are represented. The model is used to corroborate results of the Site-Scale Model, to provide radionuclide transport results for comparison with results of the SYVAC3-CC4 system model, and to provide a more complete understanding of repository component functions.

Radionuclide transport calculations are performed for I-129, Cs-135, U-234 and U-238. These radionuclides are typically the most important in terms of potential radiological impact or in representing a range of low-sorption to high-sorption species.

Domain Discretization and Property Assignment

The model is discretized over a domain of approximately 1410 m × 1170 m × 560 m in the X, Y, and Z directions, respectively. The domain incorporates a small number of placement rooms and a section of the perimeter access tunnel near the well. The model extends from the Shadow Lake formation to the top of the Guelph formation, and includes the water supply well. The model discretization is 239 nodes in the X direction, 702 nodes in the Y direction, and 105 node layers in the Z direction, for a total of 17.35 million elements.

The extent of the model is shown in Figure 7-22. Material properties are the same as those listed in Table 7-17 and Table 7-18.

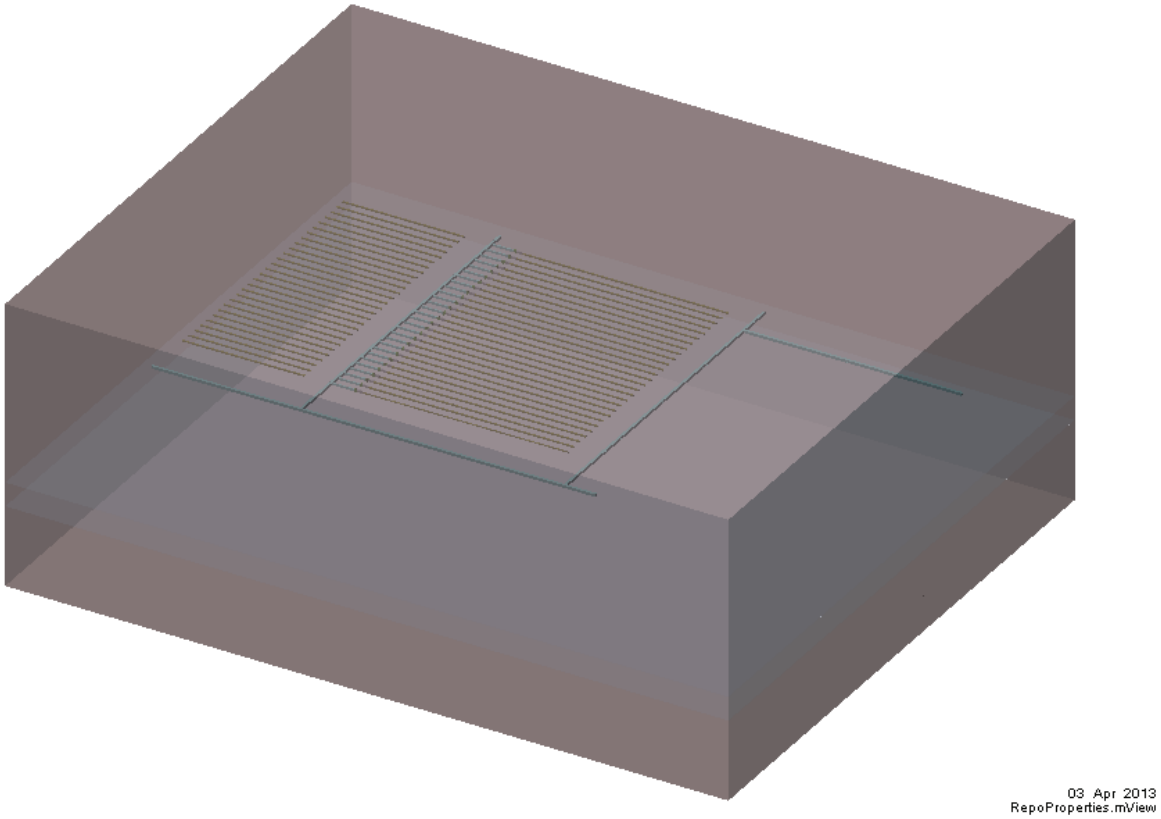

Figure 7-22: Repository-Scale Model - 3D Visualization of Domain Elements

The placement rooms and engineered barrier system are discretized at differing levels of detail. The room containing the radionuclide source is discretized at the highest level and contains representations of the containers in the room. The geometry includes a basic representation of the round room cross-section, and includes homogenized backfill surrounding the containers in the source room. All other placement rooms and access tunnels are square, as shown in Figure 7-23.

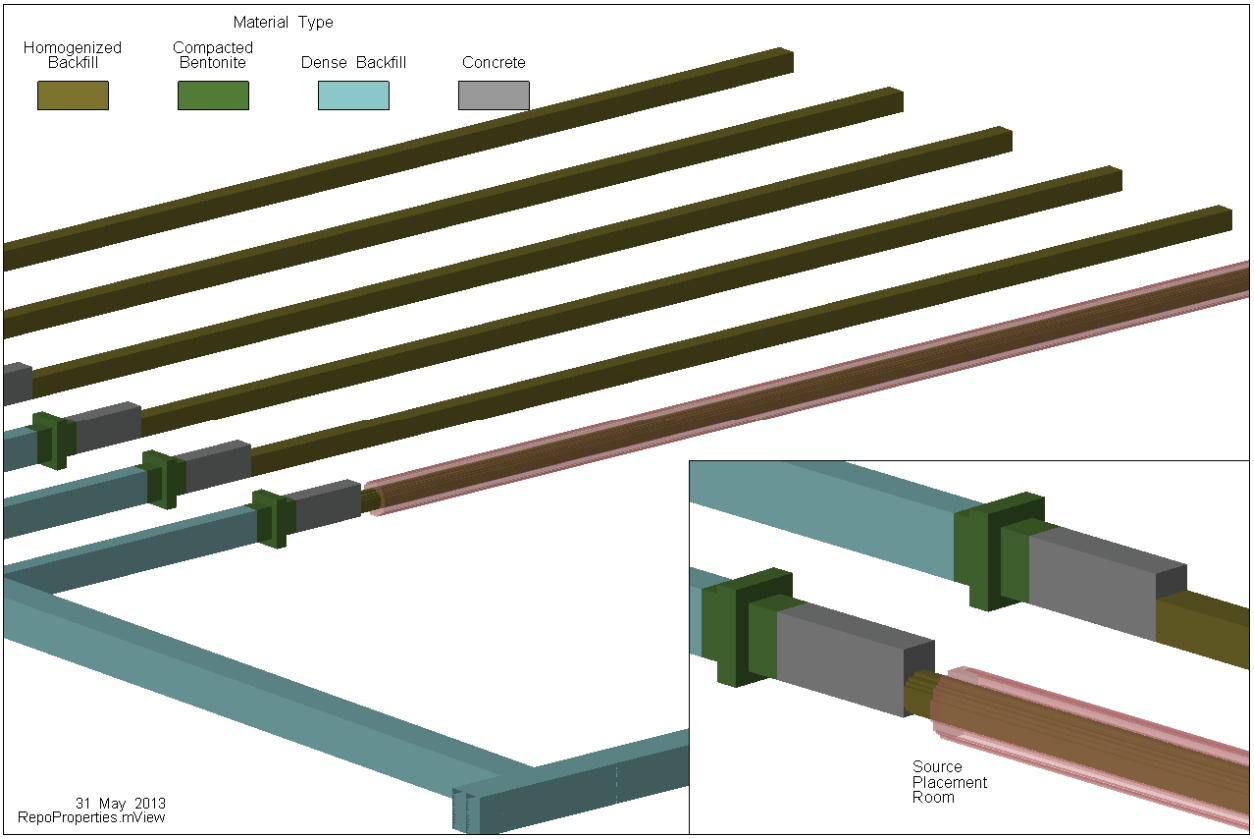

Figure 7-23: Repository-Scale Model - 3D View of Repository Room and Tunnel Seals

Figure 7-24 is a cross section through the model domain showing repository properties and geological setting at Y = 0 metres. The coordinate system is modified slightly from the Site-Scale Model, in that the X axis (Y = 0 m) is centred on the detailed placement room and the Y axis (X = 0 m) is shifted to the start of the placement room, as shown in Figure 7-25.

Figure 7-26 and Figure 7-27 show property assignments in vertical cross-sections along the placement room containing the containers with undetected defects (source room) and perpendicular through the room seal, respectively.

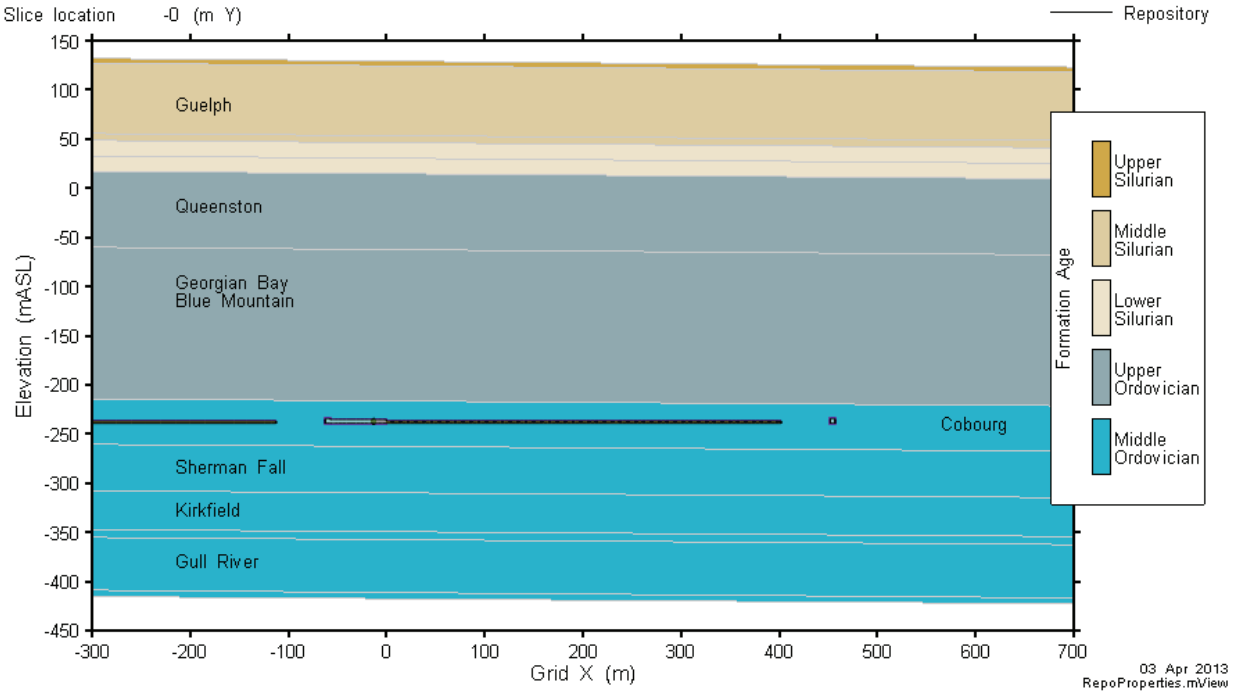

Figure 7-24: Repository-Scale Model - Section View of Repository and Geology

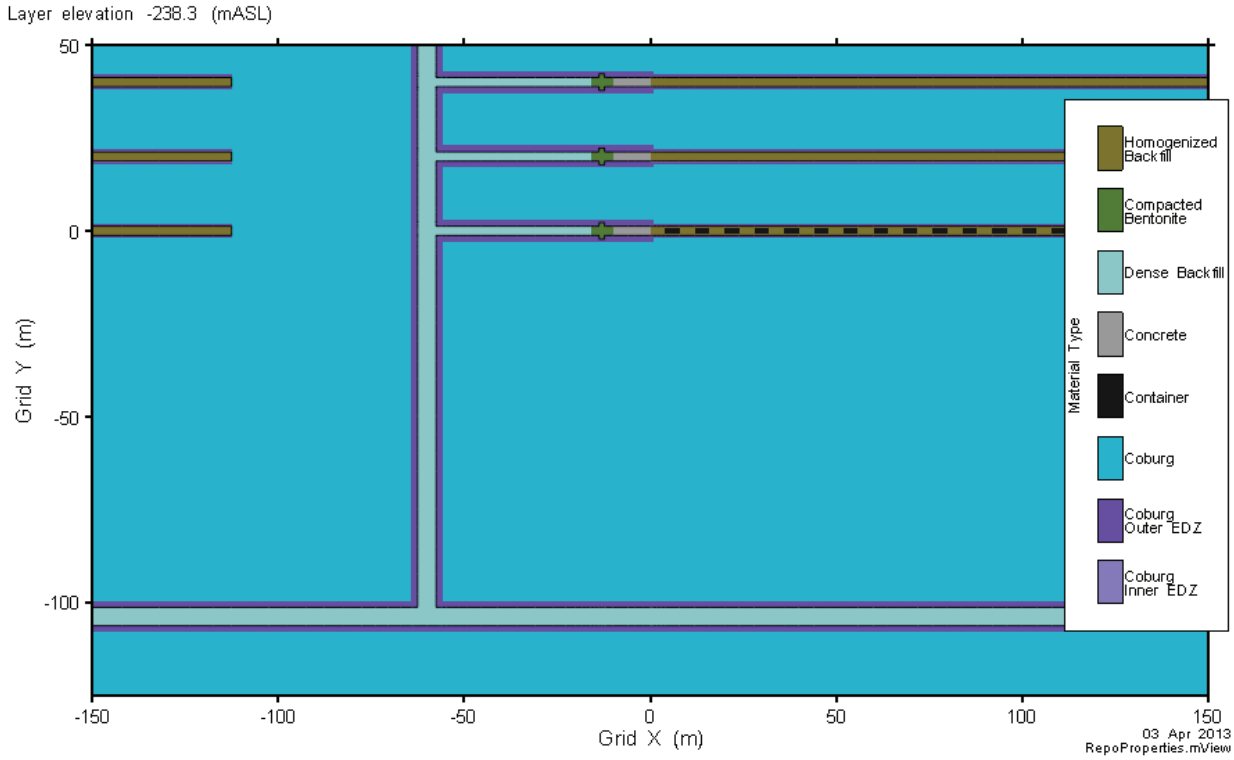

Figure 7-25: Repository-Scale Model - Plan View of Rooms and Tunnel

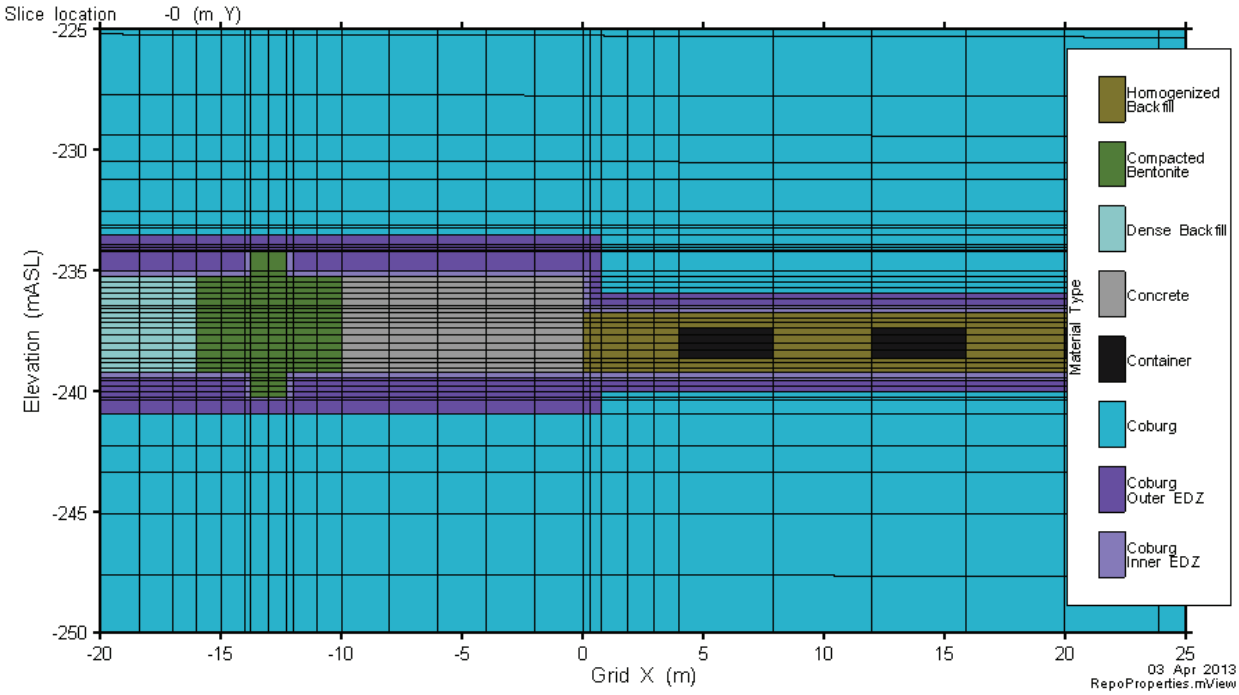

Figure 7-26: Repository-Scale Model - Vertical Slice along Placement Drift (Y = 0 m)

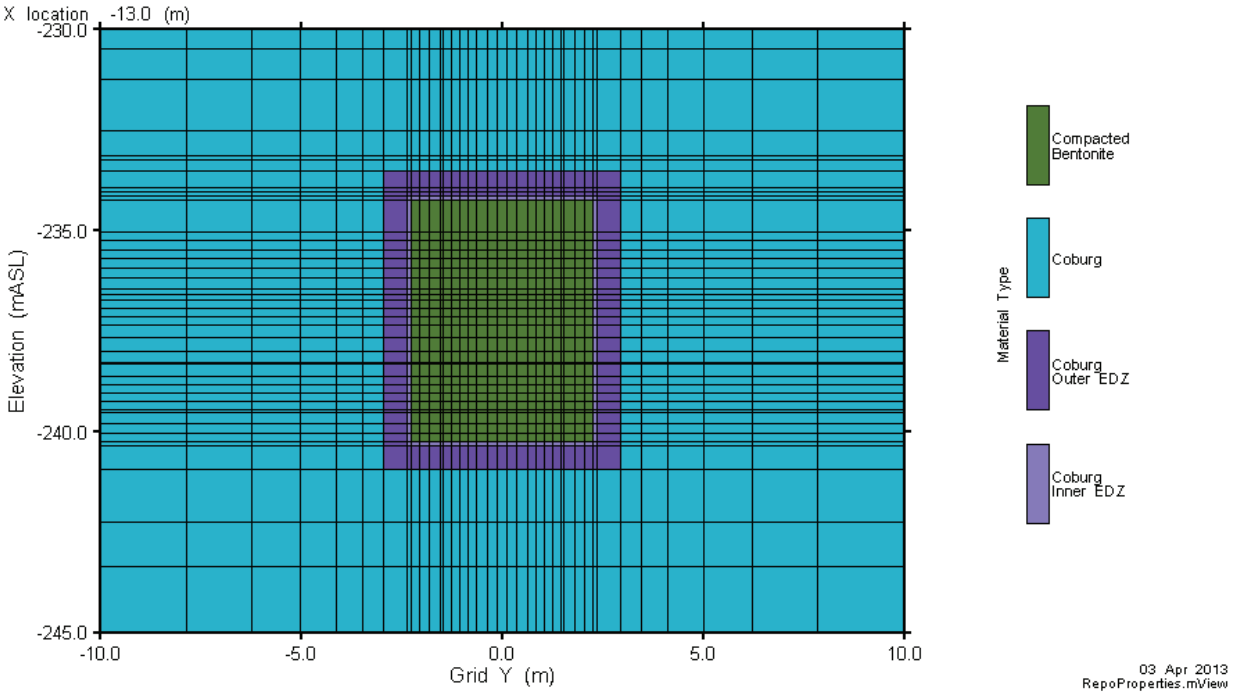

Figure 7-27: Repository-Scale Model - Vertical Slice through Placement Drift Room Seal (X = -13.0 m)

Figure 7-28 is a 3D cutaway showing the assignment of EBS and EDZ materials.

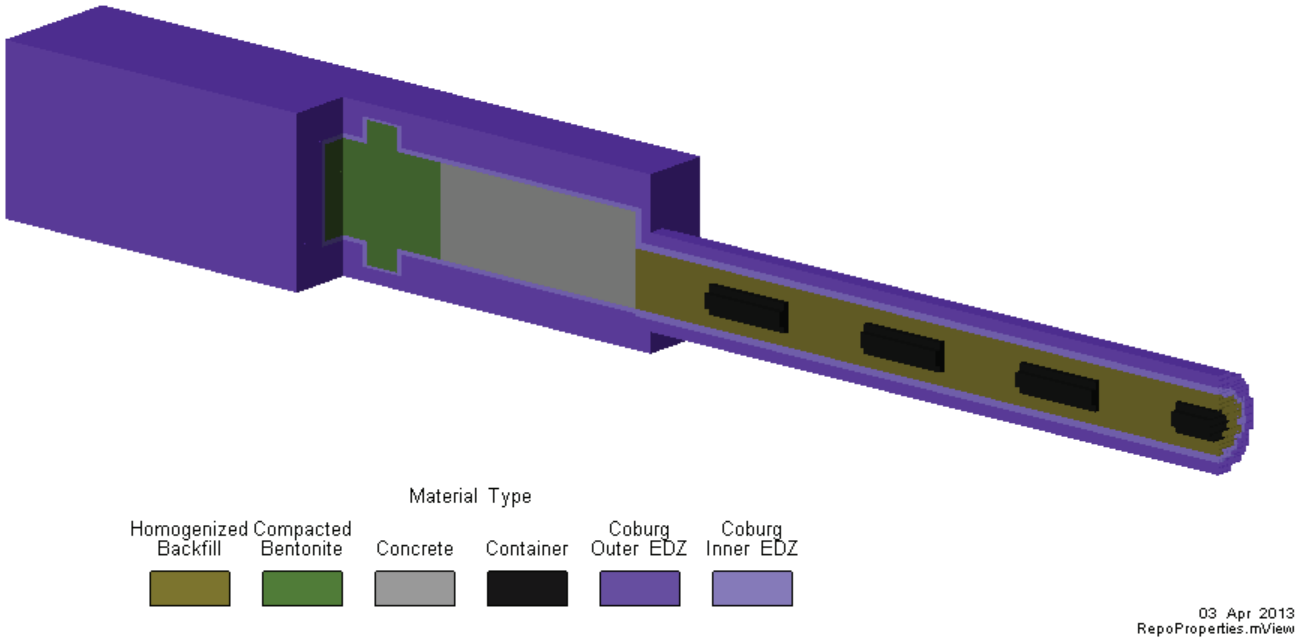

Figure 7-28: Repository-Scale Model - 3D View Showing Engineered Barrier System

Source term nodes are shown in Figure 7-29. Contaminants that escape the containers are applied over four nodes at the interface between the container[1] and the surrounding buffer material, at the container-lid weld to represent a small hole. Note that only one source node is visible in the figure.

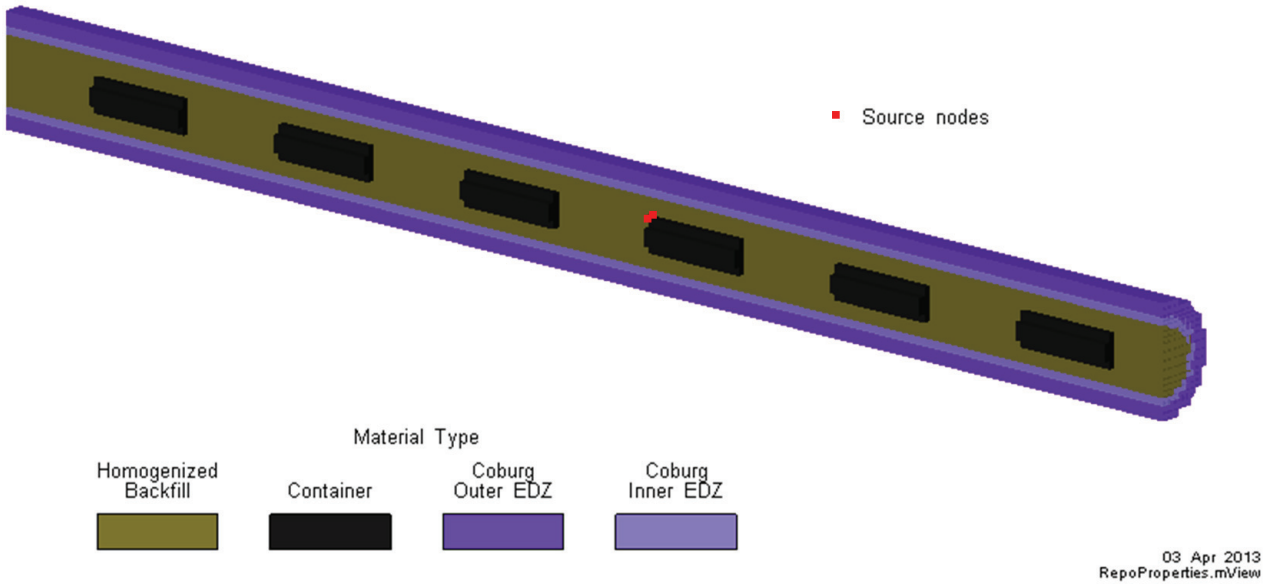

Figure 7-29: Repository-Scale Model - 3D View Showing Defective Container Source Nodes

[1] The Reference Case assumes three used fuel containers are placed in the repository with small undetected defects. Accordingly, mass transport simulations assume the release rate from the defective container is equivalent to the calculated release from three defective containers.

Hydraulic Head Boundary Conditions

Head boundary conditions are extracted from the Site-Scale Model and values are specified for all external model nodes.

Boundary conditions for the Reference Case are shown in Figure 7-30.

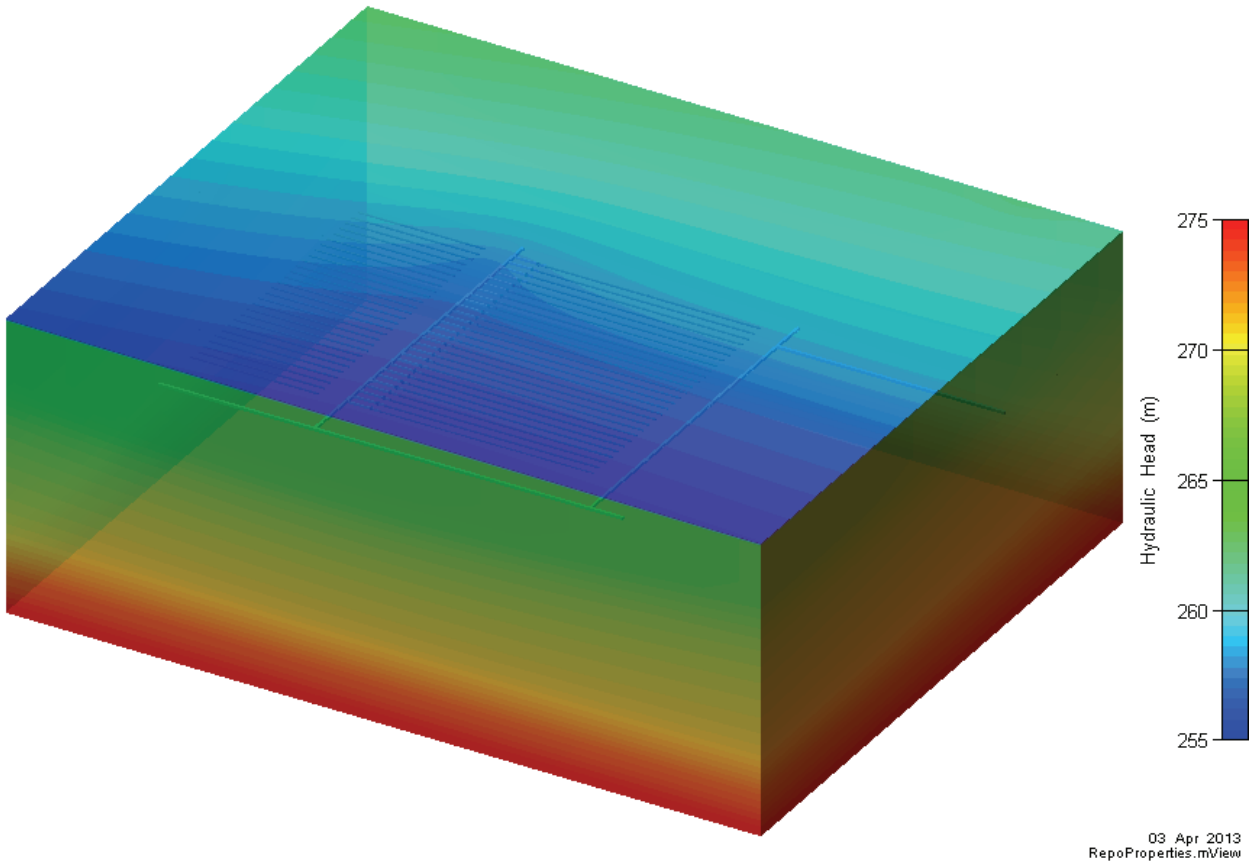

Figure 7-30: Repository-Scale Model - 3D View of Reference Case Head Boundary Conditions

7.5.3.3 Radionuclide Source Term

The FRAC3DVS-OPG code does not have a contaminant release model. Radionuclide release rates from the container[2] are therefore calculated with the SYVAC3-CC4 release model and imposed as a boundary condition at the source nodes, one of which is shown in Figure 7-29.

The radionuclide release rates used are shown in Figure 7-31. The same source term is used in both the Site-Scale and Repository-Scale Models.

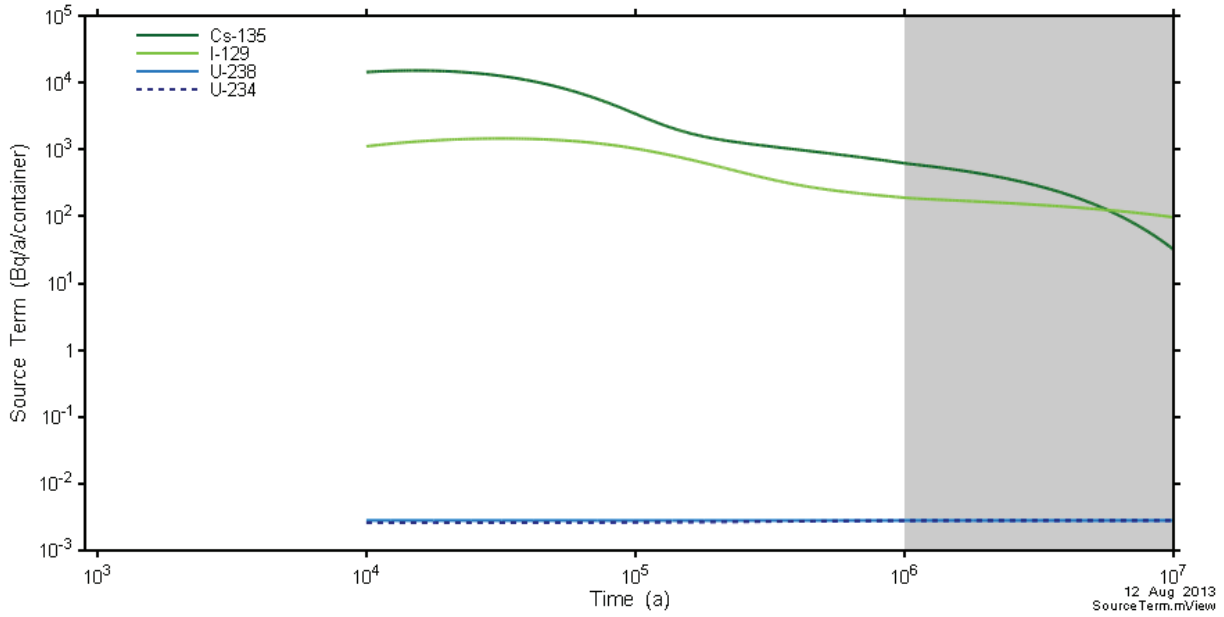

Figure 7-31: Radionuclide Release Rate per Container

7.5.4 System Model

The SYVAC3-CC4 system model combines an idealized geometric description of the repository and a simple geosphere transport model with more detailed representations of releases from the used fuel and radionuclide transport in the biosphere to compute the radiological consequences of releases to the environment.

The description provided here applies to the situation in which the climate, biosphere and geosphere are constant throughout the simulation. The groundwater flow field is also constant.

[2] The Reference Case assumes three used fuel containers are placed in the repository with small undetected defects. Accordingly, mass transport simulations assume the release rate from the defective container is equivalent to the calculated release from three defective containers.

7.5.4.1 Radionuclide Source Term

The reference waste form is a standard CANDU 37-element fuel bundle with a burnup of 220 MWh/kgU and an average fuel power during operation of 455 kW. Chapter 3 identifies the radionuclides of interest and their associated inventories.

Section 7.3.1 describes that radionuclides within the UO_2 fuel are released by two distinct mechanisms which operate on very different time scales. These mechanisms are referred to as "instant release" and "congruent dissolution".

Table 7-21 shows the instant release fractions for selected elements used in this study.

Table 7-21: Fuel Instant-release Fractions for Selected Elements

Radionuclide	Instant-Release Fraction (% of Inventory)
C	2.7
Cl	6
Cs, I, Po, Rn	4
Ra	2.5
Pd, Tc	1
Bi, Se	0.6
Ac, Am, Np, Pa, Pu, Sm, Th, U	0

Note: From Gobien et al. (2013)

Figure 7-32 presents fractional and cumulative information for congruent dissolution of the fuel.

The system model uses the instant release and congruent release together with solubility limits and information on the water volume inside the container to calculate radionuclide concentrations. Radionuclides thereafter escape the container and enter the surrounding low hydraulic conductivity buffer.

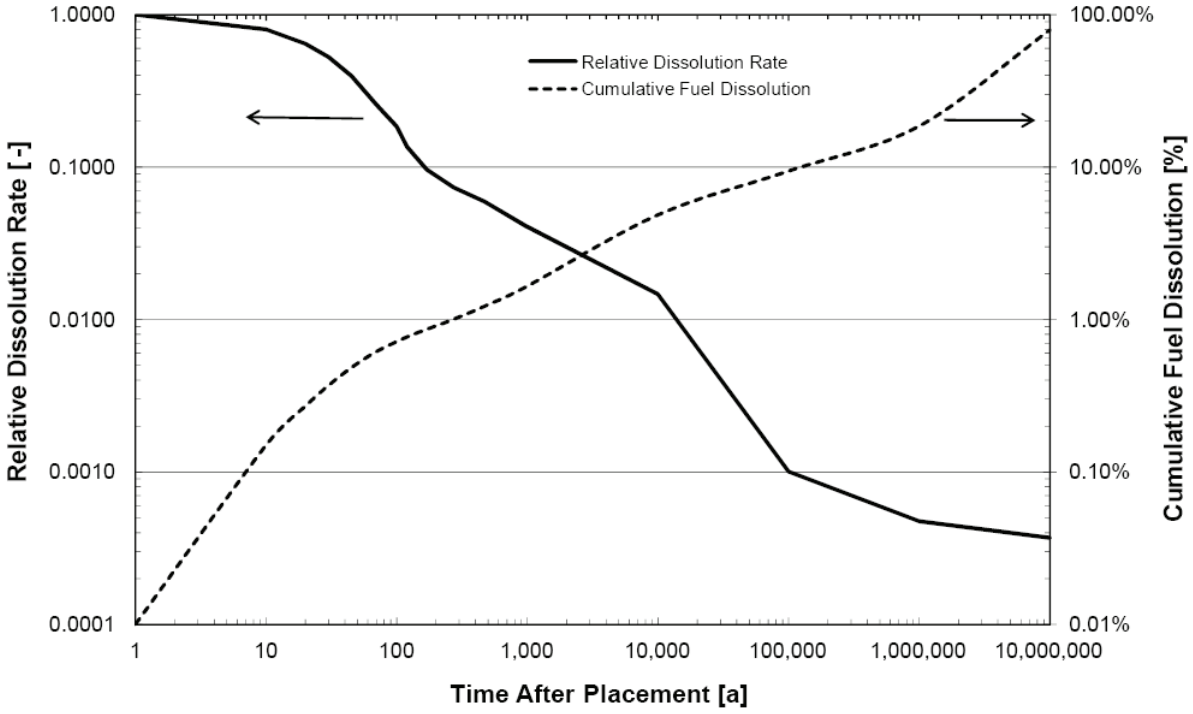

Notes: Relative Dissolution Rate is the ratio of the time-dependent fuel dissolution rate to the maximum fuel dissolution rate. The maximum dissolution rate is 3.12×10^{-3} [mol/m^2/a] where the area is the surface area of the fuel in contact with water. A contact area of 1570 m^2 per container is used in this study which assumes the fuel is highly fragmented. The maximum dissolution rate is therefore 4.9 mol/a.

Figure 7-32: Fuel Dissolution Rate

7.5.4.2 Repository Model

The repository model uses a series of concentric cylinders of varying thicknesses as shown in Figure 7-33 to approximate radionuclide transport through the buffer, backfill and excavation damaged zone. This simplification allows for the use of semi-analytical solutions which result in fast computation times suitable for use in probabilistic analyses.

Conceptually, the model represents one container within a placement room surrounded by concentric cylinders of buffer material, backfill material and EDZ. Because the conceptual repository in this study does not have placement room backfill, input data for the concentric

cylinders are specified such that only the buffer (63 cm thick) and placement room inner EDZ (30 cm thick) are represented. The outer EDZ is and its associated rock thickness is conservatively ignored. The length of the concentric cylinders is about 401 m, corresponding to the length of the placement room. A semi-infinite boundary condition that maintains continuity of concentration and continuity of flux is established at the outer boundary.

The radionuclide release from the defect is represented by a source that lies along the axis of the nested cylinder. The container is not physically represented.

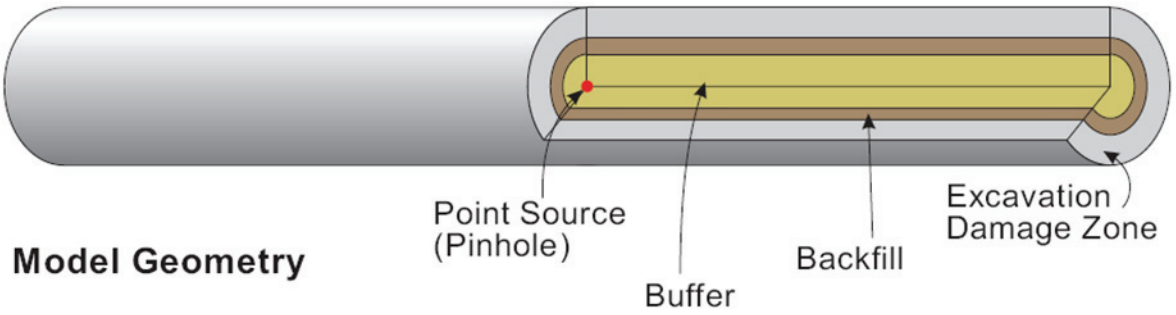

Note: the backfill thickness is 0 cm in the repository model used in this study.

Figure 7-33: SYVAC3-CC4 Repository Model

The repository model simulates the following processes:

- Container Failure – At a specified time some of the containers are assumed to fail. In the Normal Evolution Scenario failure occurs in the form of a small initial defect in the corrosion resistant copper shell allowing water to enter the container.

- Instant Release – A fraction of soluble fission products at the UO_2 fuel grain boundaries and cladding gap is instantaneously dissolved once the container is breeched and water comes into contact with the fuel. A fraction of the C-14 in the Zircaloy is also released instantaneously when water contacts the Zircaloy.

- Congruent Release – A slow long-term radionuclide release consistent with the long-term corrosion / dissolution of the ceramic fuel pellet and release of radionuclides trapped within the fuel matrix. Radionuclides are also released from the Zircaloy as it dissolves.

- Precipitation – The precipitation of elements whose concentration in the container exceeds the solubility of the element.

- Radioactive Decay and Ingrowth – Radioactive decay of radionuclides and progeny.

- Transport – The diffusive and advective transport of radionuclides through the engineered barrier system (including the defective container).

The failed container begins to fill with water as soon as the surrounding buffer is saturated. Buffer saturation is assumed to occur 10,000 years after the container is placed in the repository. The time for the container to fill with water is conservatively neglected so that a continuous water pathway between the container interior and the surrounding buffer is assumed to exist immediately at 10,000 years.

In the deterministic analyses, the three failed containers are conservatively assumed to be in the repository location with the shortest contaminant transport time to the well. In the probabilistic analysis, since each container has only two states (i.e., intact or failed), the failure rate is described by a binomial distribution with the probability of failure being approximately 1 in 5000 containers. The location, the time of failure, and the number of failed containers are random variables.

The radius of the container defect for the Reference Case of the Normal Evolution Scenario is 1 mm. An upper limit of 2 mm is applied in the probabilistic analysis since defects of this size and larger will be readily detectable during the container inspection process prior to placement.

7.5.4.3 Geosphere Model

The geosphere is represented as a network of 1D transport segments. Each 1D segment represents a path in which transport is primarily in one direction, with relatively uniform material properties. This network is defined to approximate the stratigraphy and the hydrological and geochemical features of the geosphere zones located between the repository and the surface biosphere. Transport in each segment is characterized using the 1D advection-diffusion equation, for which robust semi-analytical solutions are available.

The starting point for generation of the SYVAC3-CC4 geosphere network is a detailed steady-state groundwater flow field for the site computed using the FRAC3DVS-OPG code. However, because the hydraulic conductivity of the hypothetical geosphere is so low, radionuclide transport is effectively entirely diffusive and advective flow trajectories have not been used. Instead, a series of diffusive transport pathways have been independently defined and the geosphere model created through execution of the following steps:

- Sector Selection – The repository is divided into sectors. A sector is typically defined so that its properties are uniform. For example, it has the same waste form type and room length, and it connects to a portion of the groundwater flow field (when applicable) whose properties are approximately uniform for the entire sector. Different sectors typically have different properties, and often the properties of the surrounding geosphere are the delineating factor.

- Selection of Representative Pathways – A representative pathway for each sector is generally chosen to give the conservatively shortest travel time to the surface. In areas of low flow velocity, diffusion towards fractures (if present) may be the shortest travel path.

- Selection of Nodes along Pathways – Nodes are generally selected at material property boundaries so that the resulting segments have constant properties.

- Addition of Well and Near-surface Nodes – Additional nodes are required for the well - for example, upper and lower reference nodes define the range of positions for the well and drawdown nodes, which give a better representation of the drawdown cone in the vicinity of the well.

- Property Assignment – Data needed include the Cartesian coordinates of all the nodes, hydraulic heads and temperatures at the nodes, and hydraulic and chemical properties of the different geosphere zones.

- Well Model – The effects of the well drawdown on adjacent node heads is accounted for via an analytical well model within the aquifer, and by a site-specific well-effects model outside the aquifer.

Sector Selection

Since all containers contain the same used fuel waste form and the placement room design is common across the repository, the main distinction between the sectors is generally the influence of the surrounding groundwater flow field. However, for this study, with diffusion-dominated sedimentary rock, the key feature of the geosphere is the geologic layering. The pathways start in the placement rooms at the repository horizon and end at the Guelph formation. There is sufficient variation in the distance from the mid room vertical location and the top of the Cobourg layer over the 10 repository panels to warrant the use of five sectors to represent the repository. Panels A and B, C and D, E and F, G and H, and I and J, are numbered 1 through 5 respectively. Figure 4-14 shows the panel labelling scheme.

Table 7-22 shows the numbers of containers in each sector and their contributions to transport via the host rock and the shafts.

Table 7-22: Container Distribution by Repository Sector

Repository Sector	Number of Containers	Transport Fraction	
		Host Rock (%)	Shaft (%)
1	2555	100	$6.92\times10^{-5*}$
2	2556	100	0%
3	2556	100	0%
4	2556	100	0%
5	2555	100	$1.47\times10^{-4*}$

Note: *this is the ratio between the shaft footprint and the repository footprint. The Sector 1 value represents the area ratio for the ventilation shaft while the Sector 5 value represents the area ratio for the combined main and access shafts.

Selection of Representative Pathways

For each sector, a representative transport pathway is selected to approximate the transport segment leading to the surface discharge point(s). These pathways may converge and combine on the way to the surface, or conversely may diverge and lead to different discharge points, depending on conditions such as the well demand rate.

In this study, the representative pathways are straight lines directly up to the Guelph aquifer because the geosphere is diffusion-dominated. This results in five pathways leading away from the five sectors of the repository to the top of the Cobourg layer. From the top of the Cobourg layer, a single pathway is used through the next four layers to the bottom of the Guelph layer. The transport pathway to the Guelph layer is vertical and eventually discharges to the Well with a capture fraction of 93.7% (Section 7.5.3.1). In parallel to this single pathway, another vertical pathway representing the shaft is also included. Note that no credit is taken for contaminant transport into the deeper geosphere below the repository.

Although a Lake is not present in the biosphere, a small Lake discharge is included in the model since the code assumes there is an Aquatic Discharge somewhere. The Lake is sufficiently far down-aquifer of the well that no additional dose to the critical group occurs. In practice, doses to people exposed to these radionuclides would be less than those associated with the critical group due to the smaller radionuclide fraction entering the Lake and the much greater dilution.

Selection of Nodes along Pathways

Nodes are defined at material property boundaries and at some intermediate points. Pathways are merged where appropriate, and divergence nodes are located where the fraction of the flow is re-directed to a shaft.

Addition of Well, Overburden and Sediment, and Other Features

Four additional nodes are associated with the well. A well discharge node is located at the ground surface immediately above the well aquifer node. The fraction of the contaminant plume entering the Guelph layer captured by the well as a function of well demand is determined using the FRAC3DVS-OPG code, as discussed in Section 7.5.3.1.

For proper operation of the code, the Lake is assumed to have both a terrestrial discharge node and an aquatic discharge node. The aquatic and terrestrial discharges have an overburden and associated sediment / soil node for a total of 4 additional nodes.

With these additional 8 nodes, the complete network consists of 41 nodes. The network and its connectivity are shown schematically in Figure 7-34.

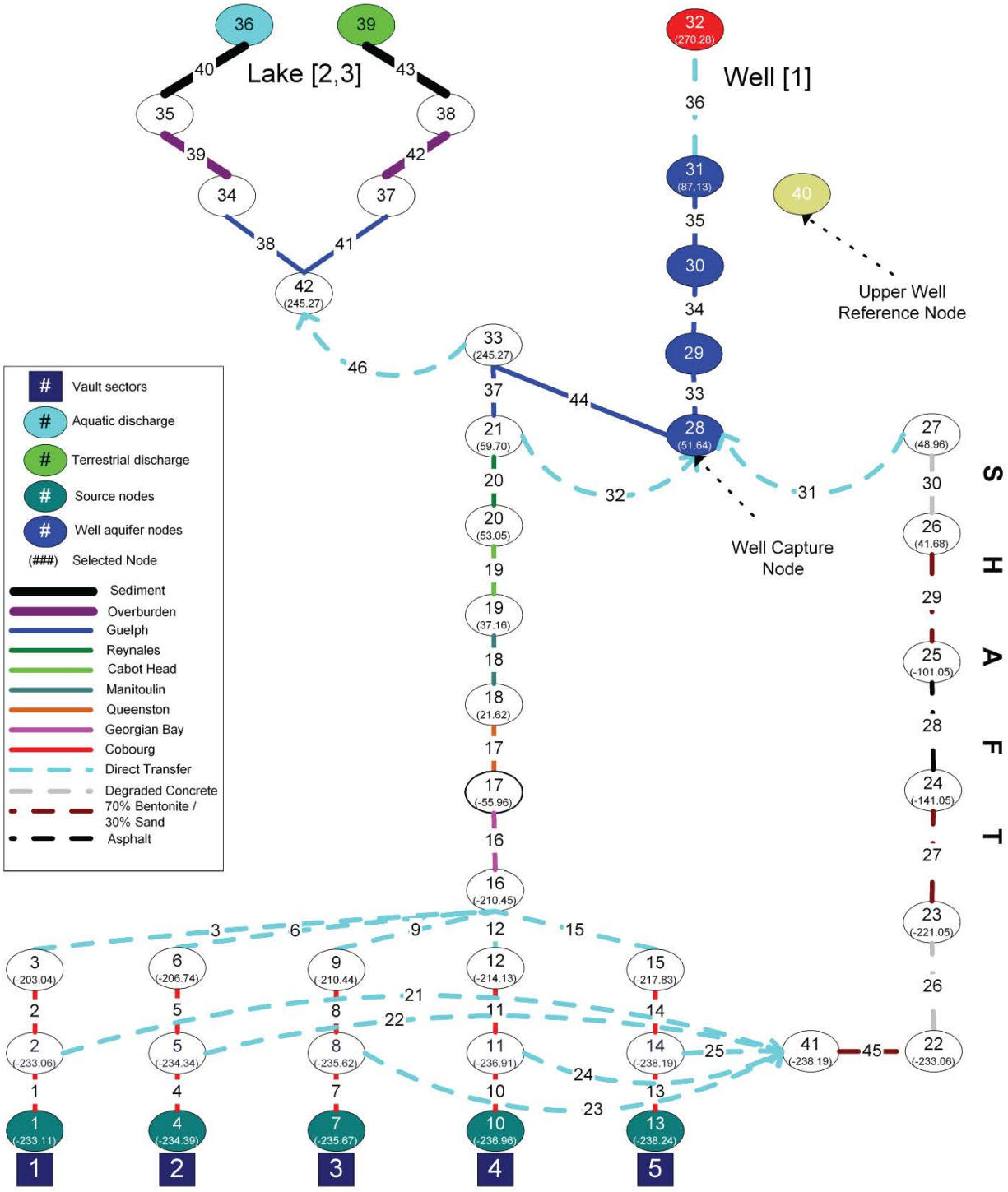

Notes: Only nodes (ellipses) with a particular function are colour coded. The line segments, representing the 1D transport pathways, are colour coded (see legend) to indicate the geosphere zone through which they pass.

Figure 7-34: SYVAC3-CC4 Transport Network Showing Connectivity

Well Model

The well must be located in a permeable zone capable of supplying significant water. This permeable zone is referred to as an “aquifer”. In the current study, the aquifer is located in the permeable, slightly sub-horizontal Guelph formation. This is a conservatively deep groundwater well, at 219 m.

SYVAC3-CC4 uses an analytical solution to provide the hydraulic head drawdown at the nodes and the capture envelope for the groundwater flowing in the aquifer. The analytical solution is based on a constant head boundary condition at the discharge end of a non-leaky aquifer (where “non-leaky” means there is little inflow from the surrounding rock). The well model allows the assessment of well demands other than the Reference Case value, which is useful in assessing alternative lifestyles or other critical groups, and in probabilistic calculations.

Property Assignment

Once the network is defined, physical and chemical properties are assigned to the various rock, overburden, and sediment nodes and segments.

Values for the hydraulic heads at each node location are obtained from the FRAC3DVS-OPG results. Values for transport parameters such as porosity and permeability and sorption are supplied for each network segment. The model accounts for both advective and diffusive transport processes.

Table 7-23 shows times corresponding to the transport peaks calculated using the SYVAC3-CC4 geosphere model for I-129 transport through the various rock layers at the reference well demand of 1,307 m^3/a. These results show that the transport through the shales is very slow, around 20 million years. This can be compared with Figure 7-41 that shows Mean Life Expectancies of a similar range.

Table 7-23: I-129 Transport from the Repository to Surface

Layer	Time of Maximum Release from Layer [a]	Time of 0.1% of Maximum Release from Layer [a]
Geosphere Pathway		
Cobourg	205,000	25,000
Georgian Bay	15,200,000	1,190,000
Queenston	18,500,000	2,290,000
Manitoulin	19,100,000	2,590,000
Cabot Head	19,600,000	2,780,000
Reynales/Fossil Hill	20,000,000	3,010,000
Shaft Pathway (0.015 % of release from Sector 5 only)		
Shaft Bentonite/Sand	685,000	72,000
Concrete (LHHPC)	691,000	74,000
Shaft Bentonite/Sand	1,400,000	118,000
Shaft Asphalt	2,810,000	264,000
Shaft Bentonite/Sand	5,600,000	410,000
Concrete (LHHPC)	5,900,000	418,000
Combined Geosphere and Shaft Pathway Flow into Well		
Well	20,000,000	2,423,000

7.5.4.4 Biosphere Model

The biosphere model represents a hypothetical but plausible Southern Ontario site.

The topography of the watershed area near the repository is relatively flat as shown in Figure 7-8. The local biosphere is assumed to have the characteristics of a temperate climate region of Southern Ontario and its properties are assumed constant during the simulation period. The normal present-day variation of climate and other biosphere parameters are included via the use of probabilistically sampled parameter values.

Key elements of the model are discussed below. A detailed description of the input data used in the model is available in Gobien et al. (2013).

Surface Water Submodel

Surface waters are not modelled in this study. As explained in Section 7.5.4.3, any radionuclides not directed to the well would remain in the Guelph aquifer, be diluted and travel to regions outside the boundary of the model.

Soil Submodel

The soil submodel calculates the concentration of contaminants in the surface (rooting or cultivated) soil layer. This layer is assumed to be well-mixed due to, for example, plowing in an agricultural field or bioturbation. Two soil models are considered, one for upland soil and one for shallow soil. The upland soil model describes a typical soil layer, with the water table a reasonable distance below the surface soil layer. In the shallow soil model, the water table extends into the surface soil layer on a regular and extended basis (as in the case of marsh or swamp land). The distinction between these two soil types is important in determining how readily contaminated groundwater can reach the surface. In the upland soil model, it must be transported by processes such as capillary action while in the shallow soil model groundwater is discharged directly into the surface soil.

Areas of surface soils have specific designations including use as a vegetable garden, a forage field, and a woodlot. Some of the parameters describing the transport pathways in the soil model are dependent on the type of field (i.e., irrigation rate).

The transport processes considered in the soil submodel are:

- Irrigation – contaminated water from the well (or surface water if present) is added to the soil.
- Groundwater Discharge – direct discharge from a contaminated groundwater water source below the surface soil (shallow soil only).
- Capillary Rise – upwelling of contaminated groundwater from the water table (upland soil only).
- Leaching – contaminants in surface soil migrate to deeper soil layers as water percolates through the soil layer.
- Runoff – precipitation runoff from the watershed area entering the water body.
- Root Uptake – uptake of contaminants by plants and trees.
- Suspension and Volatilization – loss from the soil to the atmosphere due to soil resuspension (wind erosion) and volatilization.
- Deposition – deposition of contaminants from the atmosphere onto surface soils.

Some of the physical characteristics of the soil at the hypothetical site are described in Table 7-24 (Gobien et al. 2013). These reflect the values in CSA (2008) where available.

Table 7-24: Soil Properties

Parameter	Reference Case Value	Comment
Soil types	Clay type	Distribution of soil types: 10% sand, 40% organic, 40% clay, and 10% loam. Soil properties (e.g., sorption coefficient) depend on soil type.
Active surface soil depth	0.2 m	This is the active or root zone layer for which radionuclide concentrations in the soil are determined.
Soil Depth to water table	1.5 m	Normal PDF, 1.5 m mean, 0.5 m standard deviation, and bounds of 0.01 to 2.5 m.
Minimum soil depth to water table for upland soil model	0.5 m	This is the minimum depth-to-water-table at which the upland soil model is used. For smaller depths, a shallow soil model is used that allows for flooding of the surface soil by contaminated groundwater.
Upland soil leach rate fraction	0.55	Fraction of net precipitation (precipitation + irrigation - evapotranspiration) that infiltrates into soil. The remainder runs off along the surface. Uniform PDF from 0.1 to 1.

Note: Data taken from Gobien et al. (2013).

Atmosphere Submodel

The atmosphere submodel calculates radionuclide concentrations in air due to the following transport processes:

- Suspension and Volatilization – contamination of the air from particulate or gaseous releases from surface water (if present) and soil.
- Dispersion – reduction in the concentration of contaminants in the air by having them disperse over a larger area.
- Fire – release of contamination into the air from fires assumed to occur on-site. This includes fuel fires used by the critical group as well as natural fires such as a forest fire.

A list of parameters important to the concentration of airborne contaminants is given in Table 7-25 (Gobien et al. 2013). When calculating the concentrations in the atmosphere, all contaminants are conservatively assumed to be located within a couple of metres above the land surface.

Table 7-25: Climate and Atmosphere Parameters

Parameter	Reference Case Value*	Comment
Annual total precipitation	0.84 m/a	Normal PDF, with a standard deviation of 0.15 m/a and bounds of 0.39 and 1.68 m/a.
Annual average runoff	0.19 m/a	This is the balance between total precipitation and evapotranspiration, and includes surface runoff as well as infiltration into the water table.
Average wind speed	2.36 m/s	Normal PDF with mean of 2.36 m/s (8.5 km/h), standard deviation of 0.64 m/s, and bounds of 0.44 and 6 m/s.
Dry deposition velocity	0.006 m/s	Constant
Atmospheric dust load	3.2×10^{-8} $kg_{drysoil}/m^3_{air}$	Lognormal PDF with geometric mean calculated from suspended particulate matter concentrations in Ont, NB, Que and Sask during years 1996 to 2002. Geometric standard deviation (GSD) of 1.7 with bounds of 7.0×10^{-9} and 7.5×10^{-8} $kg_{drysoil}/m^3$air.
Atmospheric aerosol load	2.9×10^{-10} m^3_{water}/m^3_{air}	Lognormal PDF with geometric mean of 2.9×10^{-10} m^3_{water}/m^3_{air}, and GSD of 1.41. Based on estimate for sea salt aerosol over oceans.
Washout Ratio	630 000	CSA (2008) washout ratio for deposition to plants for all elements other than noble gases and iodine. This value is conservative for iodine. CSA (2008) recommends 200 000 for elemental iodine and 8400 for organic iodine.

Note: Data taken from Gobien et al. (2013).

Dose Calculations

The dose model uses the concentrations of radionuclides in the various biosphere compartments to calculate the annual dose to a member of the critical group.

To ensure that dose rates are not underestimated, conservative assumptions are made concerning the characteristics of the critical group. Specifically, it is assumed that the members of the critical group spend all their lives in the local biosphere and obtain all their food, water, fuel and building materials from the local biosphere. The water source for the critical group is a well that intercepts the radionuclide plume. The food includes plants grown in a garden, domesticated animals and fish. All plant and animal biota used as food are subject to contamination from surface water, soil and air. This lifestyle is consistent with but more self-sufficient than current habits and leads to an overestimate of the impact. Because of these characteristics, the hypothetical member of the critical group is referred to as a Self-Sufficient Farmer. The Self-Sufficient Farmer has been found in previous studies to be a good indicator of risk for a range of plausible lifestyles (Garisto et al. 2005).

Some critical group lifestyle characteristics are shown in Table 7-26.

Table 7-26: Human Lifestyle Data

Parameter	Reference Case Value	Comment
People per household	3	Piece-wise uniform PDF from 1 to 12 people.
Domestic water demand per person	110 m^3/a	Lognormal PDF with geometric mean 110 m^3/a, geometric standard deviation of 2 and bounds of 40 and 240 m^3/a.
Total energy needs per person	18744 kJ/d	Fixed value, set conservatively high at 90th percentile value.
Man's air inhalation rate	8400 m^3/a	95th percentile
Man's water ingestion rate	840 L/a	90th percentile
Man's meat ingestion rate*	103 g/d	Median intake for male adult. Defined as lognormal PDF with geometric mean equal to median and geometric standard deviation equal to 1.65. For a total energy intake of 18744kJ/d, this intake is prorated to 249 g/d.
Man's milk ingestion rate*	283 g/d	Median intake for male adult. Defined as lognormal PDF with geometric mean equal to median and geometric standard deviation equal to 1.35. For a total energy intake of 18744kJ/d, this intake is prorated to 685 g/d.
Man's plant ingestion rate*	796 g/d	Median intake for male adult. Defined as lognormal PDF with geometric mean equal to median and geometric standard deviation equal to 1.65. For a total energy intake of 18744 kJ/d, this intake is prorated to 1928 g/d.
Man's poultry ingestion rate*	53 g/d	Median intake for male adult. Defined as lognormal PDF with geometric mean equal to median and geometric standard deviation equal to 1.65. For a total energy intake of 18744 kJ/d, this intake is prorated to 128 g/d.
Man's fish ingestion rate*	7.9 g/d	Median intake for male adult. Defined as lognormal PDF with geometric mean equal to median and geometric standard deviation equal to 4.48. For a total energy intake of 18744 kJ/d, this intake is prorated to 19 g/d.
Soil ingestion rate	0.12 kg/a	95th percentile of incidental soil ingestion rate.
Annual energy consumption per household	$1.2x10^5$ MJ/a	Normal PDF with mean of 1.2×10^5 MJ/a, standard deviation of 8×10^3 MJ/a and bounds of 10^5 MJ/ and 1.3×10^5 MJ/a.
Building occupancy factor	0.8	Fixed value
Building air infiltration rate	0.35 /hr	Fixed value, minimum recommendation for tightly-sealed house.

Notes: Data taken from Gobien et al. (2013). * Based on a total energy intake of about 7750 kJ/d.

7.6 Results of Radionuclide and Chemical Hazard Screening Analysis

This section presents the results of the RSM screening analysis performed to identify the potentially significant radionuclides and potentially significant chemically hazardous elements. The methodology used is described in Section 7.5.2.

Table 7-27 lists the radionuclides and hazardous elements that emerged from the screening assessment. Results are shown for each case simulated, with radionuclides listed in order of their dose contribution and hazardous elements listed in alphabetical order.

The results indicate the most important potentially significant radionuclides are I-129, Cs-135, Pd-107 and Cl-36. Actinides only appear in simulation cases with no sorption or no solubility limits. The parents and progeny of the screened in radionuclides are also included in the simulations to ensure that ingrowth is accounted for.

For the potentially significant chemically hazardous elements, the “No Sorption” case has the highest number of contributors (due to the conservative nature of this case) while elements associated with the other cases are Ag, Be, Cr, Hg, Mo and Sm. It should be noted that the amount of some the chemical elements of interest (e.g., Pb, Te and Ag) increase with time due to radioactive decay of parent nuclides. Consequently, these parent nuclides are also included in the simulations of the potentially chemically hazardous elements carried out with system model.

Table 7-27: Summary of Screened in Radionuclides and Chemically Hazardous Elements for Each Case Considered

Case	Radionuclide	Chemically Hazardous Element
Base Case*	I-129, Cs-135, Cl-36, Pd-107, Se-79, Sm-147	Ag, Be[1], Mo, Sm
No Sorption	Ra-225, Th-229, Th-230, Po-210, Pb-210, Ac-225, Th-234, Pa-231, Ra-228, Ra-226, Ac-227, Ra-223, Np-237, U-233, Pa-233, U-234, U-238, U-236, Ra-224, I-129, Th-232, Pu-242, Th-227, Th-228, Cs-135	Ag, Al, Ba, Be[1], Cd[2], Ce, Co, Cr[2], Eu, Hg, La, Mo, Nd, P, Pb, Pr, Se, Sm, Te, U, Y, Zr[2]
High Solubility	I-129, Cs-135, Ra-228, Cl-36, Pd-107, Ra-224, Se-79, Th-232, Tc-99, Th-228	Ag, Be[1], Cr[1], Mo, Sm
High Instant Release Fraction	I-129, Cs-135, Cl-36, Ra-228, Pd-107, Se-79, Ra-224, Tc-99, Sm-147	Ag, Be[1], Hg, Mo, Sm
10x Diffusion	Th-230, Po-210, Ra-226, Cl-36, I-129, Ra-228, Cs-135, Tc-99, Se-79, Th-234, Ra-224, Pb-210, Rn-222	Ag[2], Al, Be[1], Bi, Co, Cr[2], Hg, Mo, Ni, Sb[2], Se, Sm, U, V[2]

Notes:
*The Base Case corresponds to the All Containers Fail Scenario (see Table 7-11) with all parameter values set at their median values
[1] From Zircaloy only, [2] From Fuel and Zircaloy

Table 7-28 shows the set of potentially significant radionuclides and Table 7-29 shows the set of potentially significant chemically hazardous elements. Items in red are items identified directly in the screening (i.e., Table 7-27) while items in black are added to include in-growth contributions.

Table 7-28: List of Potentially Significant Radionuclides

Radionuclides	
Single Nuclides	I-129, Cl-36, Cs-135, Pd-107, Se-79, Sm-147, Tc-99
Chain	
Neptunium Series	Am-241 → Np-237 = Pa-233 → U-233 → Th-229 = Ra-225 = Ac-225
Uranium Series	Pu-242 → U-238 = Th-234 → U-234 → Th-230 → Ra-226 = Rn-222 = Pb-210 = Bi-210 = Po-210
Actinium Series	Pu-239 → U-235 = Th-231 → Pa-231 = Ac-227 = Th-227 = Ra-223
Thorium Series	Pu-240 → U-236 → Th-232 = Ra-228 = Th-228 = Ra-224

Note: '=' means the radionuclides are assumed to be in secular equilibrium with their parent

Table 7-29: List of Potentially Significant Chemically Hazardous Elements

Chemically Hazardous Elements	
Fuel	
Elements	Al, Cd, Ce, Co, Cr, Hg, La, Mo, Nd, Ni, P, Pr, Sb, Se, Sm, V, Y
Chain	
Neptunium Series	Am-241 → Np-237 = Pa-233 → U-233 → Th-229 = Ra-225 = Ac-225 → Bi-ST
Uranium Series	Pu-242 → U-238 = Th-234 → U-234 → Th-230 → Ra-226 = Rn-222 = Pb-210 = Bi-210 = Po-210 → Pb-ST
Actinium Series	Pu-239 → U-235 = Th-231 → Pa-231 = Ac-227 = Th-227 = Ra-223 → Pb-ST
Thorium Series	Pu-240 → U-236 → Th-232 = Ra-228 = Th-228 = Ra-224 → Pb-ST
Misc	Sn-126 → →Te Sr-90→ →Zr Cs-135→Ba Cs-137→Ba Pd 107 → Ag Sm-151 → Eu
Zircaloy	
Elements	Be, Cr, Cd, Sb, V
Chain	
Misc	Pd-107→Ag Sr-90→ →Zr

Note: '=' means the radionuclides are assumed to be in secular equilibrium with their parent

7.7 Results of Detailed 3D Groundwater Flow and Transport Analysis

This section presents results of the detailed FRAC3DVS-OPG groundwater flow and radionuclide transport analysis performed for the Reference Case of the Normal Evolution Scenario and for those sensitivity cases with the potential to affect the groundwater flow field. The sensitivity cases examined are:

- Geosphere hydraulic conductivities increased by a factor of 10 times the Reference Case values;
- Hydraulic conductivity of the EDZ increased by a factor of 10;
- Overpressure in the Shadow Lake formation (i.e., a constant head boundary at the bottom of model domain);
- 100 m of surface erosion;
- Increased spatial resolution (assessed by comparing Site-Scale and Repository-Scale results); and
- Increase and decrease in the number of time steps.

A further description of the cases is provided in Section 7.2.

A detailed description of the models used to generate the results is provided in Section 7.5.

Radionuclide transport is calculated for I-129, Cs-135, U-234 and U-238. These radionuclides are typically the most important in terms of potential radiological impact and / or represent a range of low-sorption to high-sorption species.

Figures in this section show advective[3] velocity vectors only in locations where velocities are greater than 10^{-4} m/a. Transport is diffusion-dominated at lower velocities.

7.7.1 Site-Scale Model

The Site-Scale Model domain includes the repository and a section of the surrounding geosphere that encompasses the repository influenced flow domain. The model is used to determine:

- the container location with the fastest contaminant transport to the well;
- Reference Case and sensitivity case radionuclide transport to the well and surface environment; and
- boundary conditions for the Repository-Scale Model.

A simplified representation of the repository and engineered barrier system is included at this scale of resolution; however, individual containers are not modelled.

[3] Advective velocity is the Darcy velocity divided by the material porosity.

The sensitivity simulations examine the effects of:

- geosphere hydraulic conductivities increased by a factor of 10;
- hydraulic conductivity of the EDZ increased by a factor of 10;
- overpressure in the Shadow Lake formation; and
- increased spatial resolution and increase / decrease in the number of time steps.

A discussion of the anticipated effects of 100 m erosion is included.

The Site-Scale model is also used in the assessment of the Shaft Seal Failure Disruptive Scenario.

7.7.1.1 Flow Results

7.7.1.1.1 Reference Case – No Well

Figure 7-35 and Figure 7-36 compare hydraulic head and Darcy velocity results in the Guelph aquifer with similar results from the Regional Model described in Chapter 2 to verify correct implementation of the boundary conditions. In these simulations the well demand was set to zero in the Site-Scale model to allow direct comparison.

The results show continuity of heads at the Site-Scale Model boundary and close correspondence within the model domain. Flow directions and velocities are also very similar between the two models. Minor differences are seen at the boundaries, largely due to the influence of the different surface Digital Elevation Models used to define the top surface hydraulic head boundary. These differences do not influence flow within the Guelph layer to a significant degree.

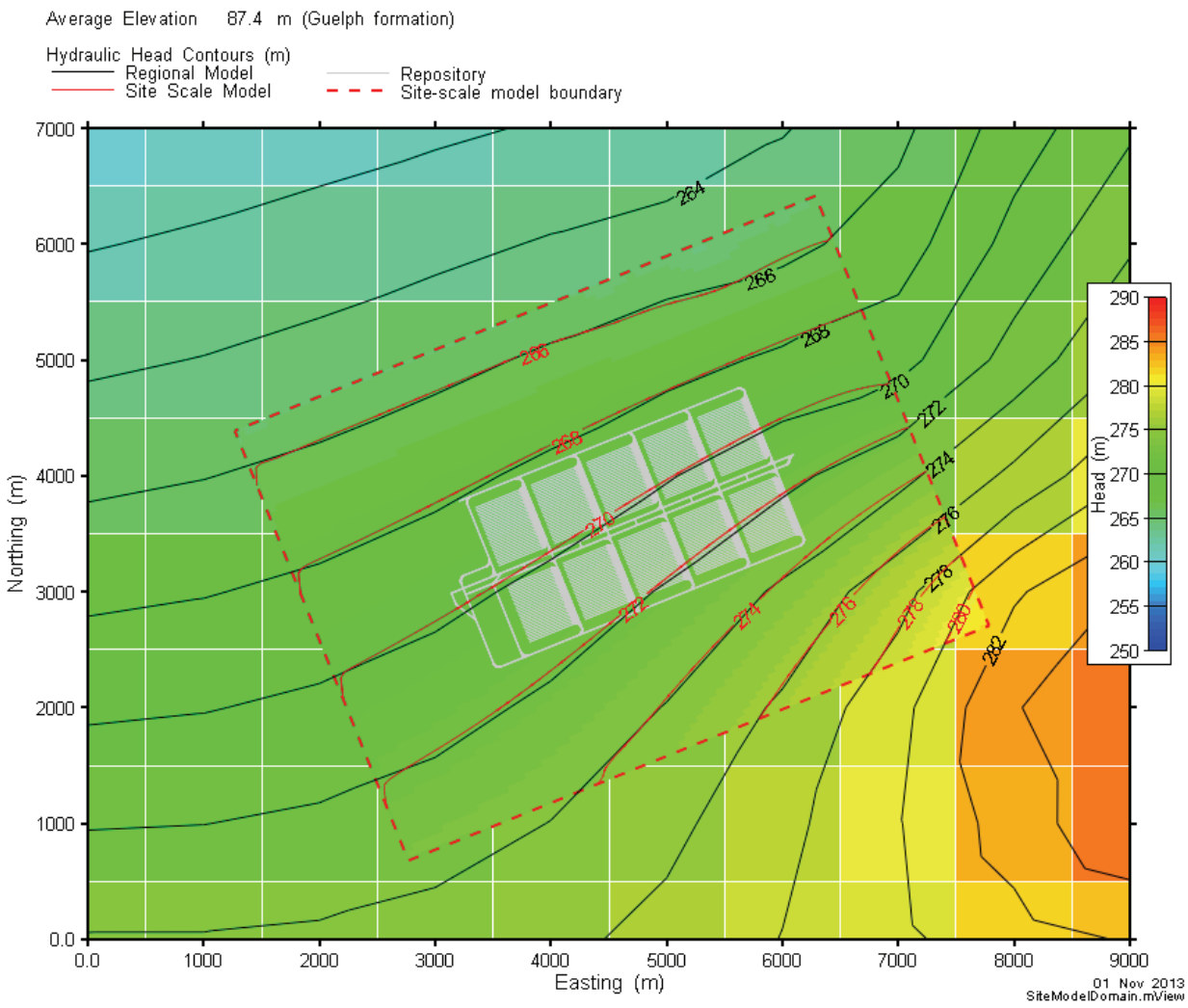

Figure 7-35: Site-Scale Model - Comparison of Hydraulic Heads with Regional Model at Guelph Formation Elevation (87 mASL)

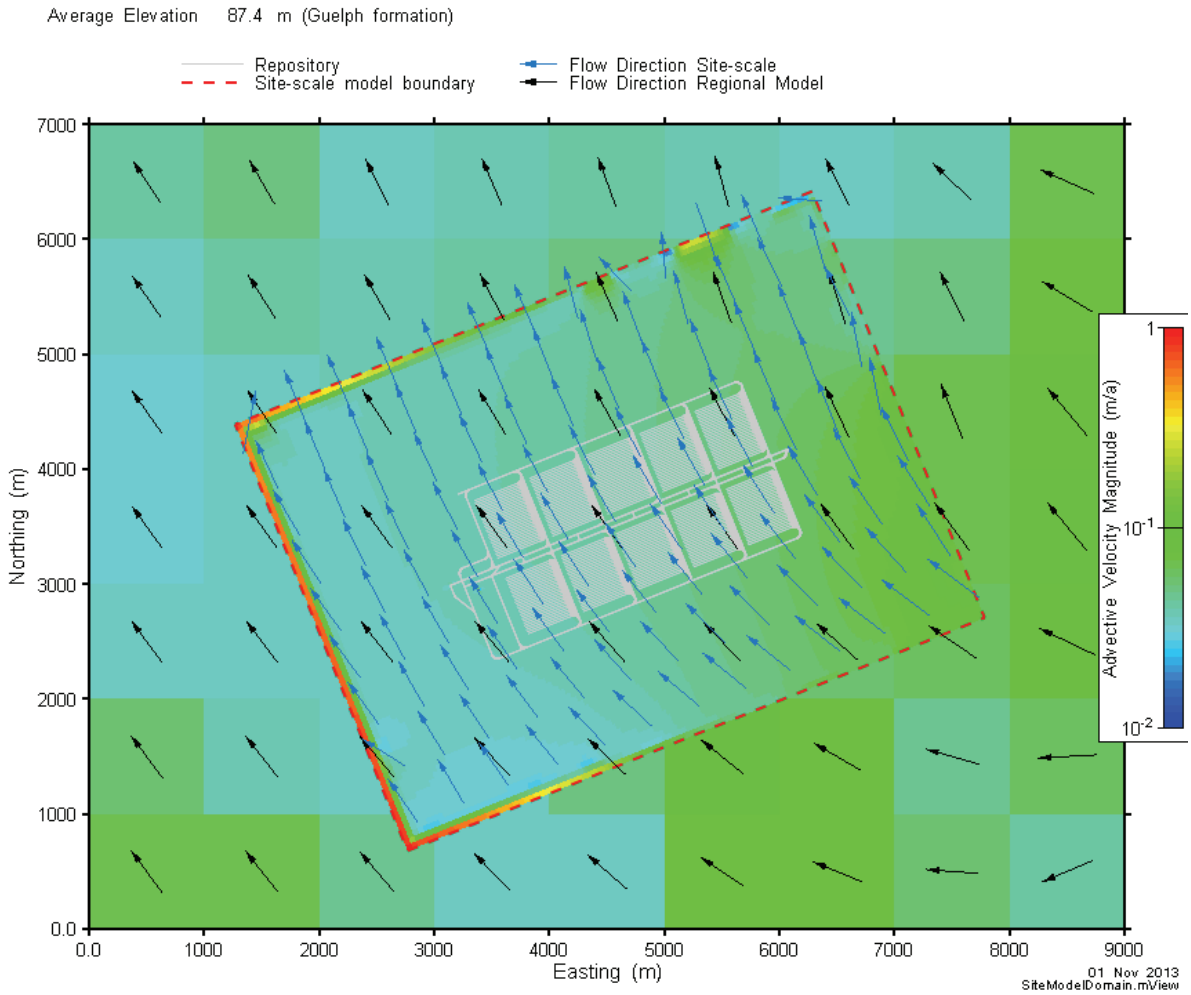

Note: minor differences occur due to the influence of a higher resolution Digital Elevation Model

Figure 7-36: Site-Scale Model - Comparison of Velocities in the Guelph Formation with Regional Model

Figure 7-37 shows a similar comparison of Darcy velocity magnitudes between the Regional and Site-Scale Models. The figure illustrates that repository features have no significant effect on the flow system (since the repository is not included in the Regional Model). The higher hydraulic conductivities of the repository EBS and EDZ cause higher velocity within the repository and shafts; however, even these velocities are very low – transport is clearly diffusion-dominant even in these features.

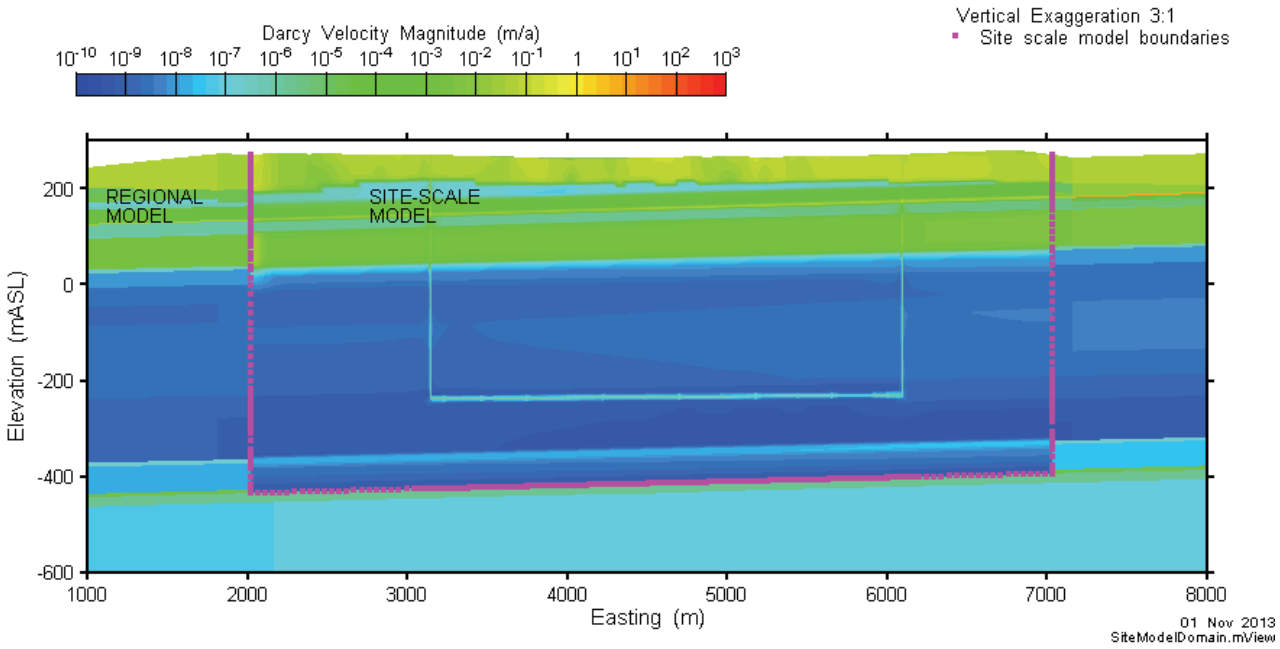

Figure 7-37: Site-Scale Model - Comparison of Velocities at a Vertical Cross-Section along Access Tunnel 1

Figure 7-38 shows the Mean Life Expectancy (MLE), taking both advective and diffusive processes into account. In this context, “Life Expectancy” is the time for a contaminant at any subsurface location to discharge to the biosphere. Since transport disperses the species through the geosphere, life expectancy is represented by a probability density function, obtained by solving for transport at each nodal upstream point. The Mean Life Expectancy represents the average time for a contaminant at any subsurface location to discharge to the biosphere.

In the Site-Scale model, MLEs are defined by the time taken for a contaminant to reach a model boundary and then exit the model. Contaminants can only exit through boundaries defined by fixed hydraulic heads, not through no-flow boundaries. Accordingly, MLEs for the Site-Scale model illustrate the time for contaminants to reach the surface or the sides of the model above the Guelph – the sides of the model below the Guelph are defined as no-flow.

The figure shows the majority of the repository is situated in rock in which the MLEs are 10^8 to 10^9 years. The relatively minor effect of the repository and shafts on the MLE is also evident.

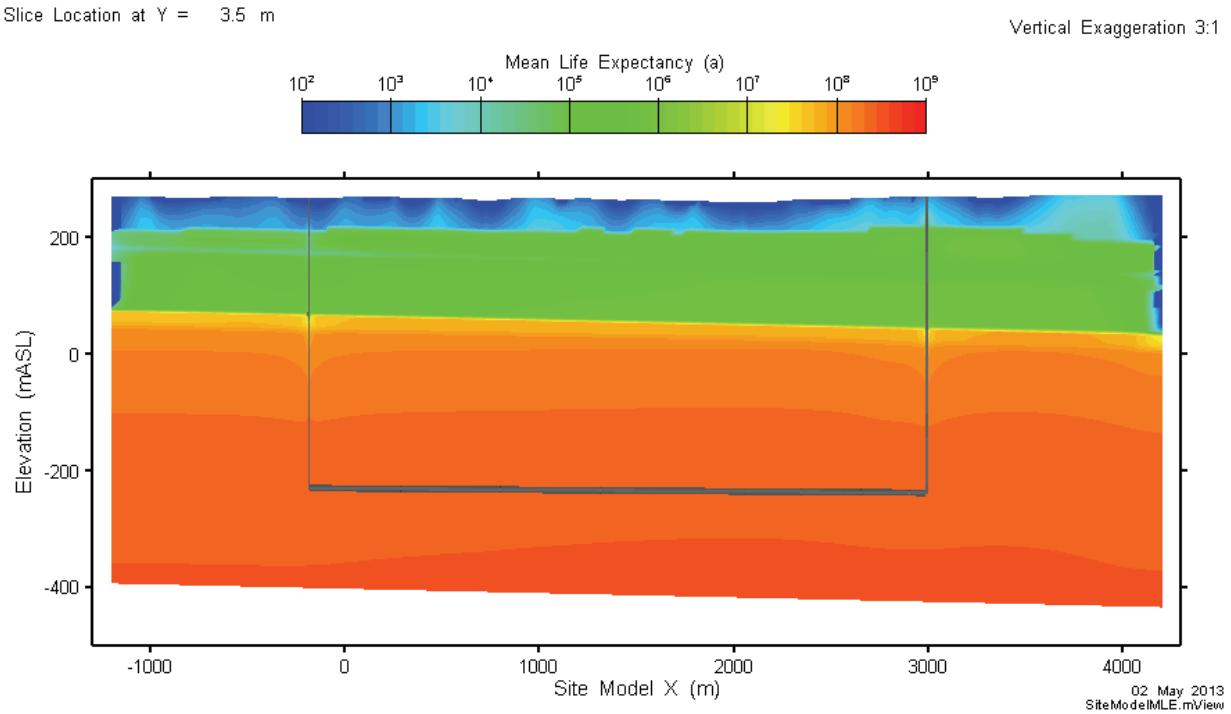

Note: The shafts and repository are shown to provide orientation.

Figure 7-38: Site-Scale Model - Mean Life Expectancy

7.7.1.1.2 Reference Case

Figure 7-39 and Figure 7-40 show the results of flow modelling on two cross sections (an XZ and a YZ section) and two plan sections at different elevations (repository depth and bottom of the Guelph aquifer) with well demand set to 1307 m^3/a.

Figure 7-39 displays the hydraulic head distribution. The cross sections were chosen to intersect the pumping well in the Guelph layer, and do not intersect the shafts. There is a small upward vertical hydraulic head gradient from the bottom of the model towards the Guelph and parts of the model surface. The two cross sections and the Guelph plan section clearly show the influence of the water supply well.

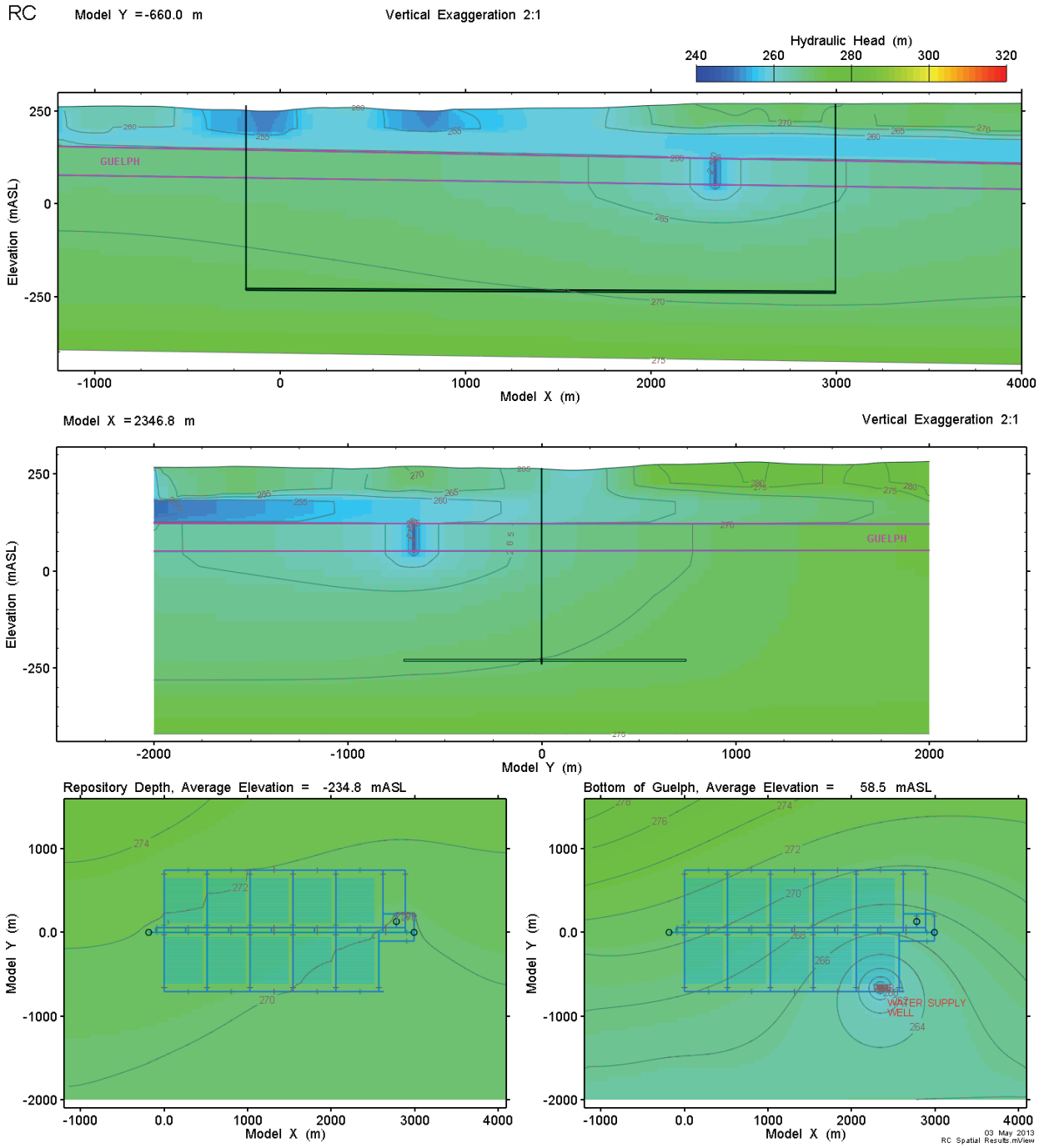

Note: The shafts and repository are shown to provide orientation.

Figure 7-39: Site-Scale Model - Reference Case Hydraulic Head Distribution

Figure 7-40 shows advective velocities on the same set of sections, with the exception of the XZ section which has been moved to show velocities along the main tunnel and in two shafts. It is clear that velocities in the deep system are extremely low. Even where shafts and tunnels are

present the velocity remains very low. Due to the low relief of the terrain and the higher conductivity of the Guelph unit there is very little hydraulic gradient between the shafts. Velocity arrows are only shown where velocity exceeds 10^{-4} m/a, below which the system is diffusion-dominated. Once again, the plan section through the Guelph shows the area influenced by the water supply well.

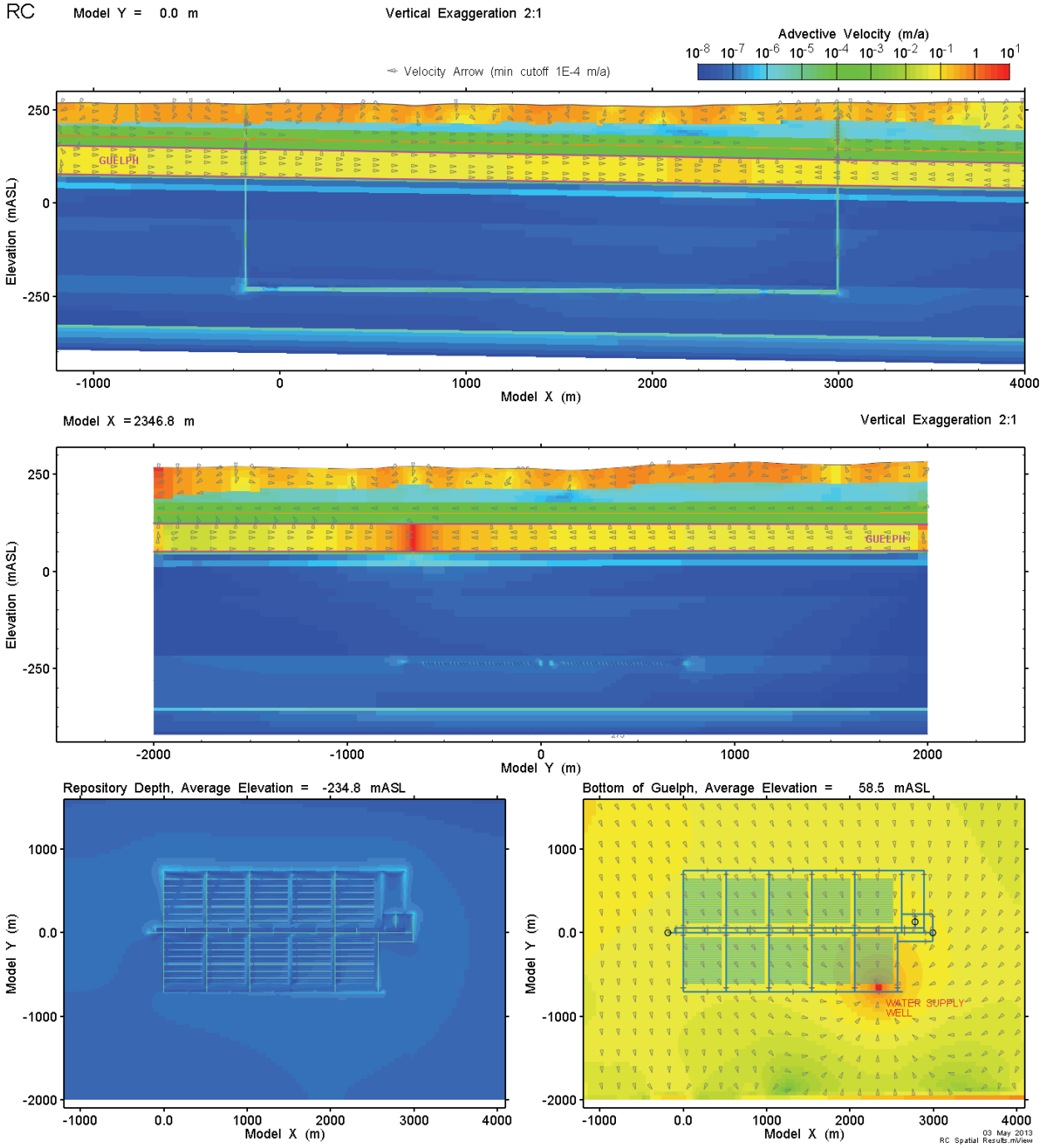

Figure 7-40: Site-Scale Model - Reference Case Advective Velocity Distribution

Figure 7-41 and Figure 7-42 show mean life expectancy on two cross sections. As was the case with no pumping well, mean life expectancy in the repository is very long.

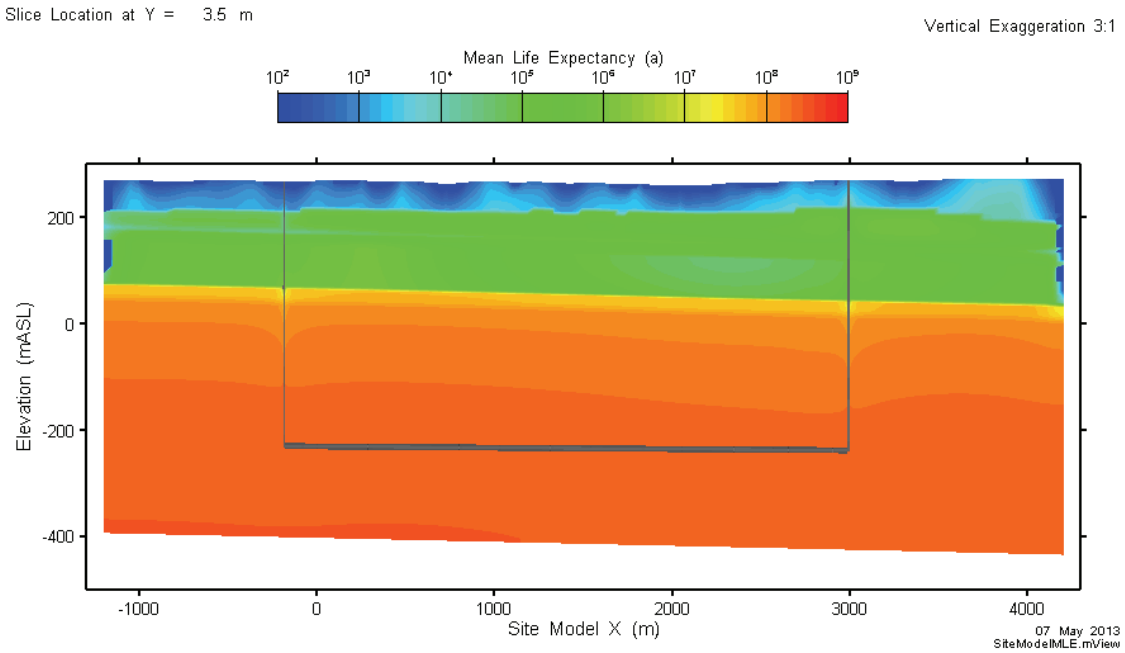

Note: The shafts and repository are shown to provide orientation.

Figure 7-41: Site-Scale Model - Mean Life Expectancy at Repository Centre

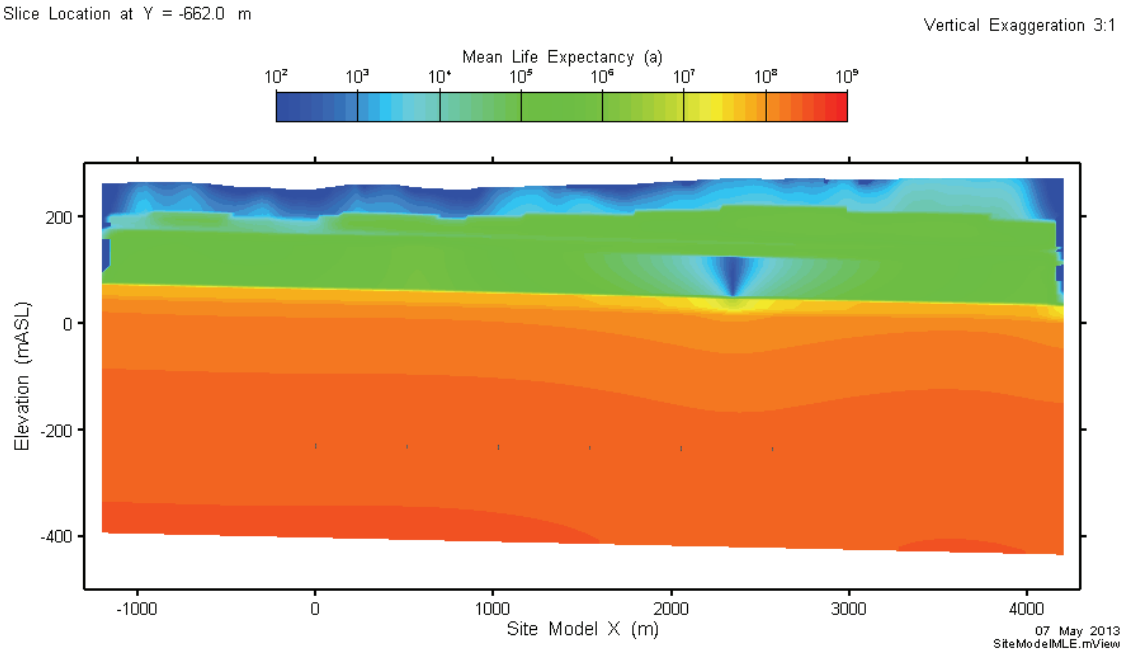

Figure 7-42: Site-Scale Model - Mean Life Expectancy at Water Supply Well

7.7.1.2 Radionuclide Transport Results

Radionuclide transport modelling has been performed for I-129, Cs-135, U-234 and U-238. The FRAC3DVS-OPG model calculates both advective and diffusive transport.

Radionuclide fluxes out of the defective containers, determined from the SYVAC-CC4 model, are applied as a boundary condition equally over two nodes located at the vertical midpoint of the placement room at the location of the three defective containers[4]. The defective containers are located approximately midway through the room closest to the water supply well, in the corner of the repository where the geological barrier is thinnest.

Figures are shown with shading at times greater than one million years to emphasize that results at these times are illustrative and included only to indicate model behaviour.

7.7.1.2.1 Location of the Well and Defective Containers

The choice of well location is based on earlier modelling (Section 7.5.3.1) in which seven different well locations were assessed in terms of the flux of contaminants captured by each well, while simulating a release from all containers in the repository. Some of the well locations were near the sealed shafts, while others were located downstream of the plume in the Guelph aquifer. This analysis found the maximum contaminant transport is to a well located slightly downstream (in the Guelph) of the repository sector for which the rock separating the Guelph from the repository (essentially, the diffusive barrier thickness) is thinnest.

7.7.1.2.2 Reference Case

Figure 7-43 and Figure 7-44 illustrate the time dependent behaviour of the I-129 plume on two cross sections (an XZ and a YZ section) and two plan sections at different elevations (repository depth and bottom of the Guelph aquifer). The contour plots are on a logarithmic scale. The outer concentration contour, 1 Bq/m^3, corresponds to an effective I-129 drinking water dose of about 0.1 μSv/a based on the Table 7-26 water consumption rate of 0.84 m^3/a per person.

The round shape of the plume indicates that transport is diffusion-dominated. Higher diffusivity, particularly in the dense backfill blocks does cause some preferential transport along tunnels in the repository, evident in the repository-depth plan sections.

[4] Although applied at two nodes, the source term represents a simultaneous failure of three containers.

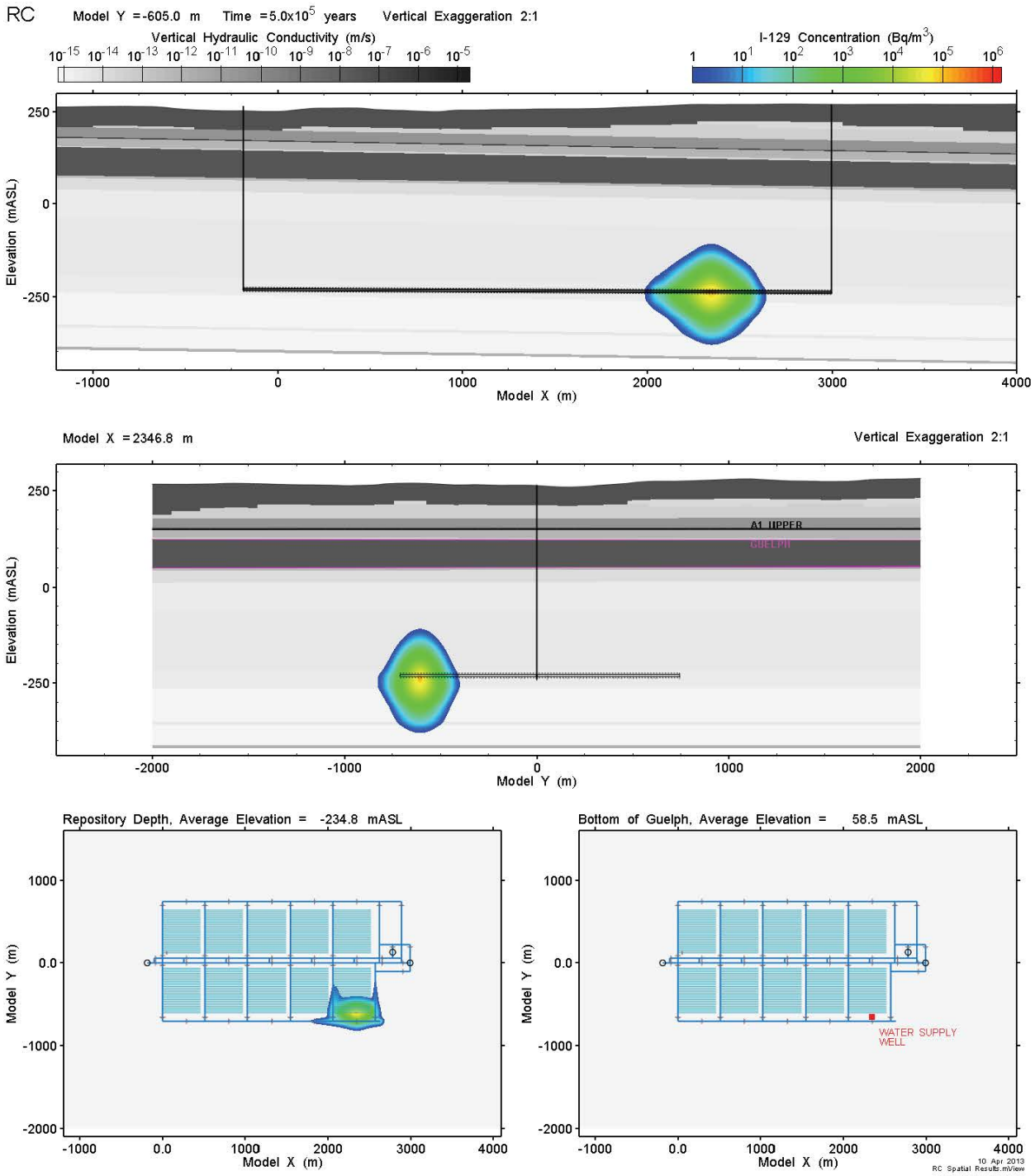

Note: The shafts and repository are shown to provide orientation.

Figure 7-43: Site-Scale Model - Reference Case I-129 Concentration at 500,000 Years

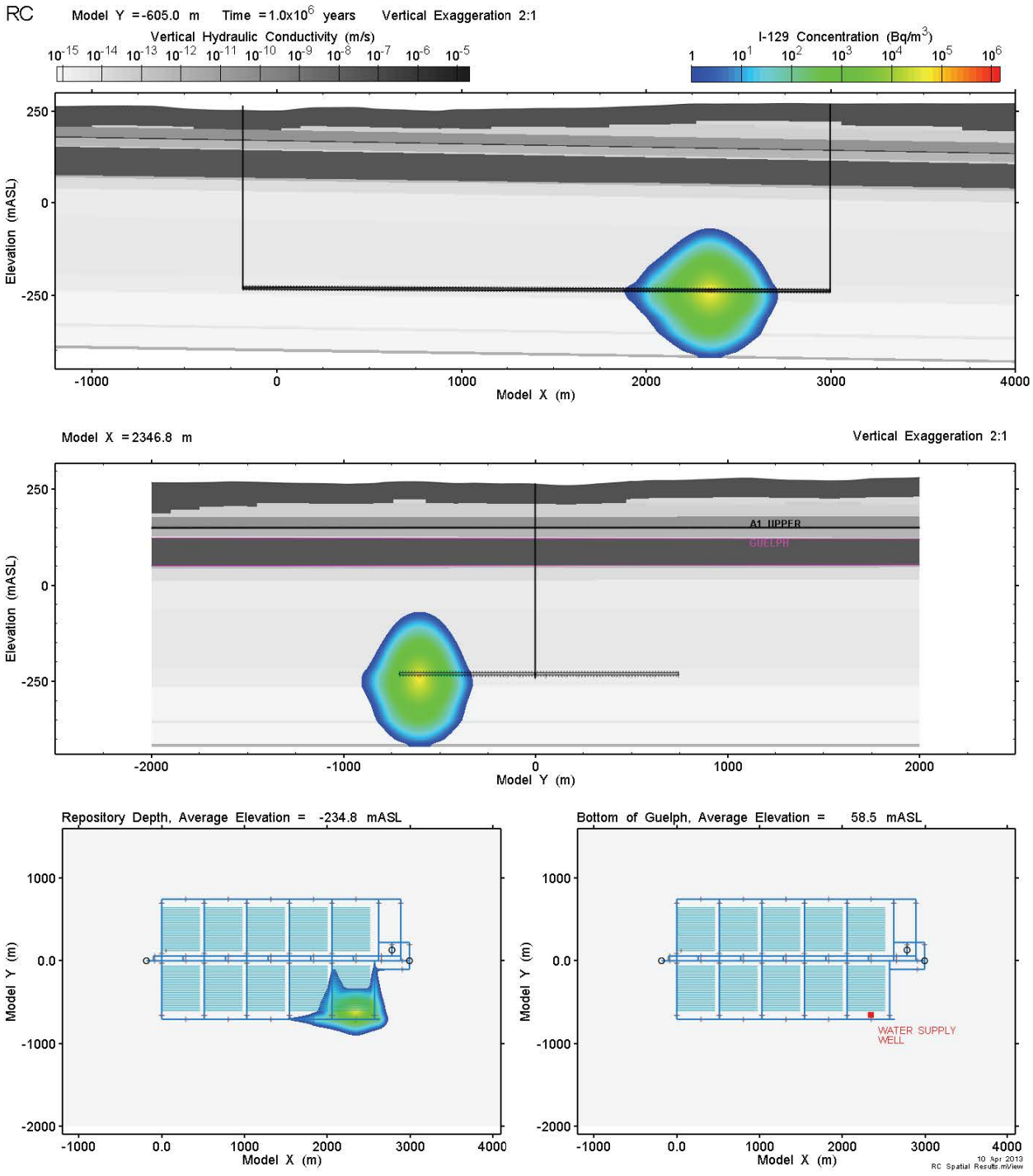

Note: The shafts and repository are shown to provide orientation.

Figure 7-44: Site-Scale Model - Reference Case I-129 Concentration at One Million Years

Figure 7-45 shows the Cs-135 concentration distribution on a vertical cross section at 1 million years. Compared to I-129, transport of Cs-135 is greatly reduced by sorption of cesium on rock and EBS materials. The asymmetrical shape of the plume is caused by much higher sorption coefficients in the Georgian Bay, Blue Mountain, and Queenston shale above the repository compared to those in the predominantly limestone Cobourg, Sherman Fall, and Kirkfield units (see Table 7-15).

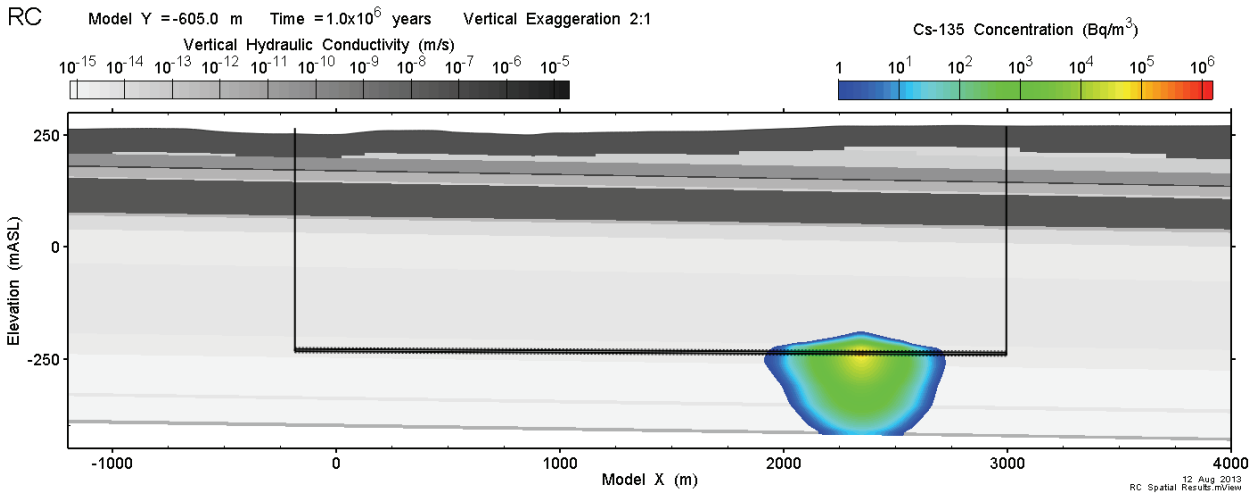

Note: The shafts and repository are shown to provide orientation.

Figure 7-45: Site-Scale Model - Reference Case Cs-135 Concentration at One Million Years

The U-234 and U-238 concentration distributions at 1 million years are not resolvable on the scales used in these figures. Sorption coefficients for uranium (see Table 7-15) are much higher than those for cesium, and this has a clear impact on the movement and concentration of uranium.

Figure 7-46 presents radionuclide transport rates to the well for all simulated nuclides. The results show that there is essentially no release to the well over the one million year baseline period.

Beyond that time, I-129 would start to be seen, while the sorbing species Cs-135, U-234, and U-238 do not reach the well in significant amounts due to retention and decay in the engineered barrier system and geosphere near the repository. The time of peak concentration for I-129 at the well is outside the 1 million year time frame of interest, and also outside the 10 million year period that is shown to illustrate model behaviour.

The maximum I-129 transport rate over the 10 million year period is 7.4 Bq/a.

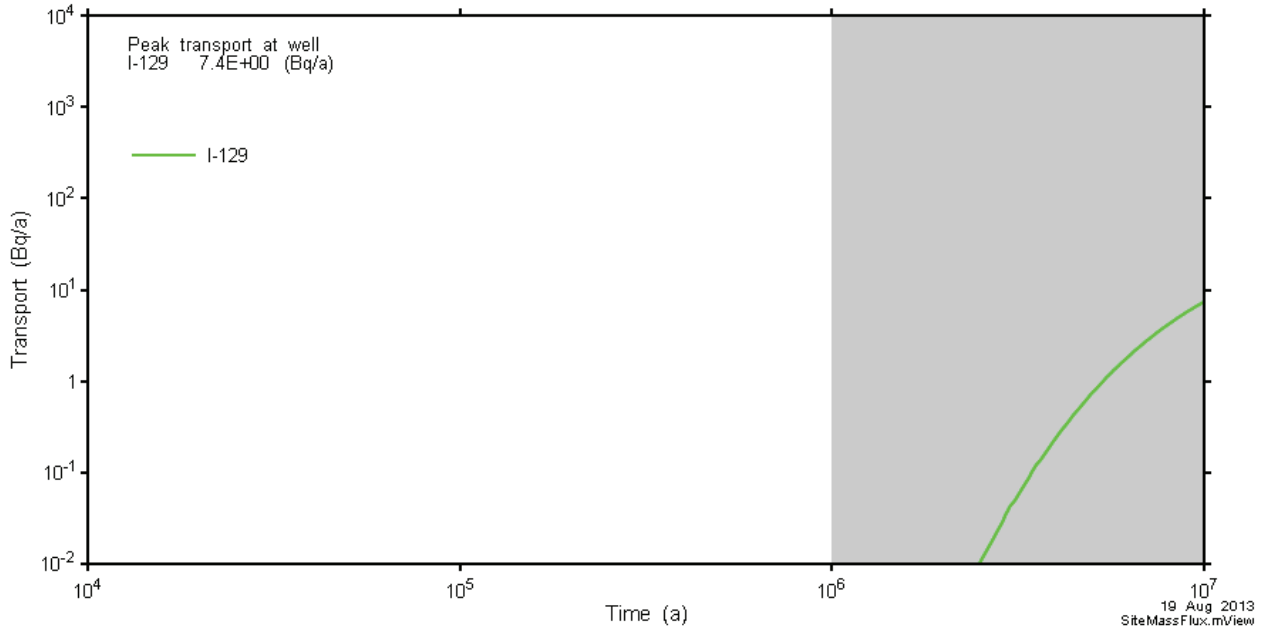

Note: Cs-135, U-234 and U-238 are off-scale low

Figure 7-46: Site-Scale Model - Reference Case Radionuclide Transport to Well

7.7.1.2.3 Sensitivity to a Factor of 10 Increase in Geosphere Hydraulic Conductivity

This section examines the effect of increasing geosphere hydraulic conductivities by a factor of 10. Table 7-17 shows the values used.

Figure 7-47 and Figure 7-48 show I-129 plume development over time is very similar to the Reference Case. The round shape of the plume indicates that transport is diffusion-dominated with no apparent effect of the upward vertical flow gradient on the shape of the plume. As before, higher diffusivity causes some preferential transport along tunnels in the repository, evident in the repository depth plan sections. Results for uranium and cesium are not shown, as they are also similar to the Reference Case results discussed in the previous section.

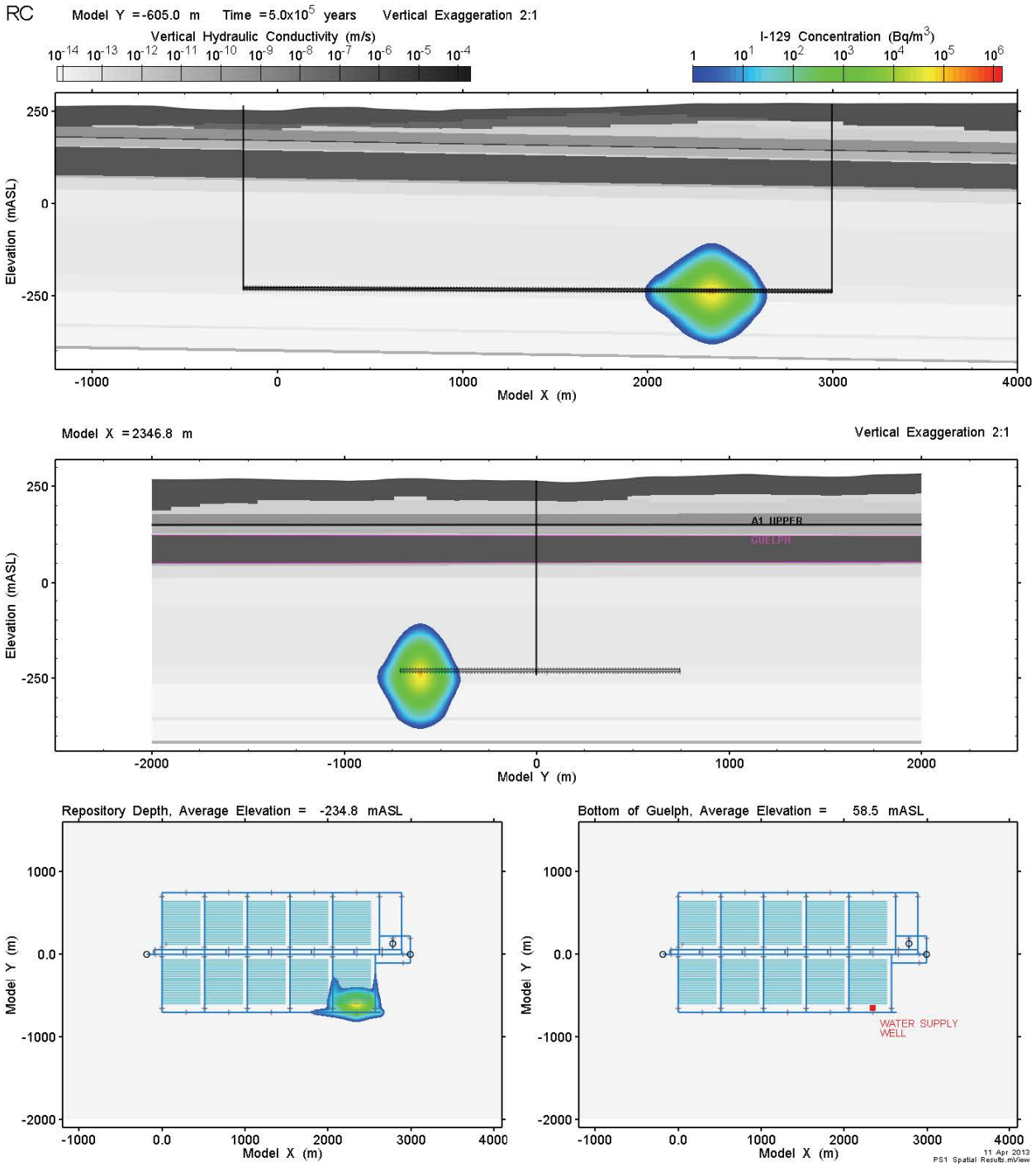

Figure 7-47: Site-Scale Model - Geosphere Hydraulic Conductivity Increased by a Factor of 10: I-129 Concentration at 500,000 Years

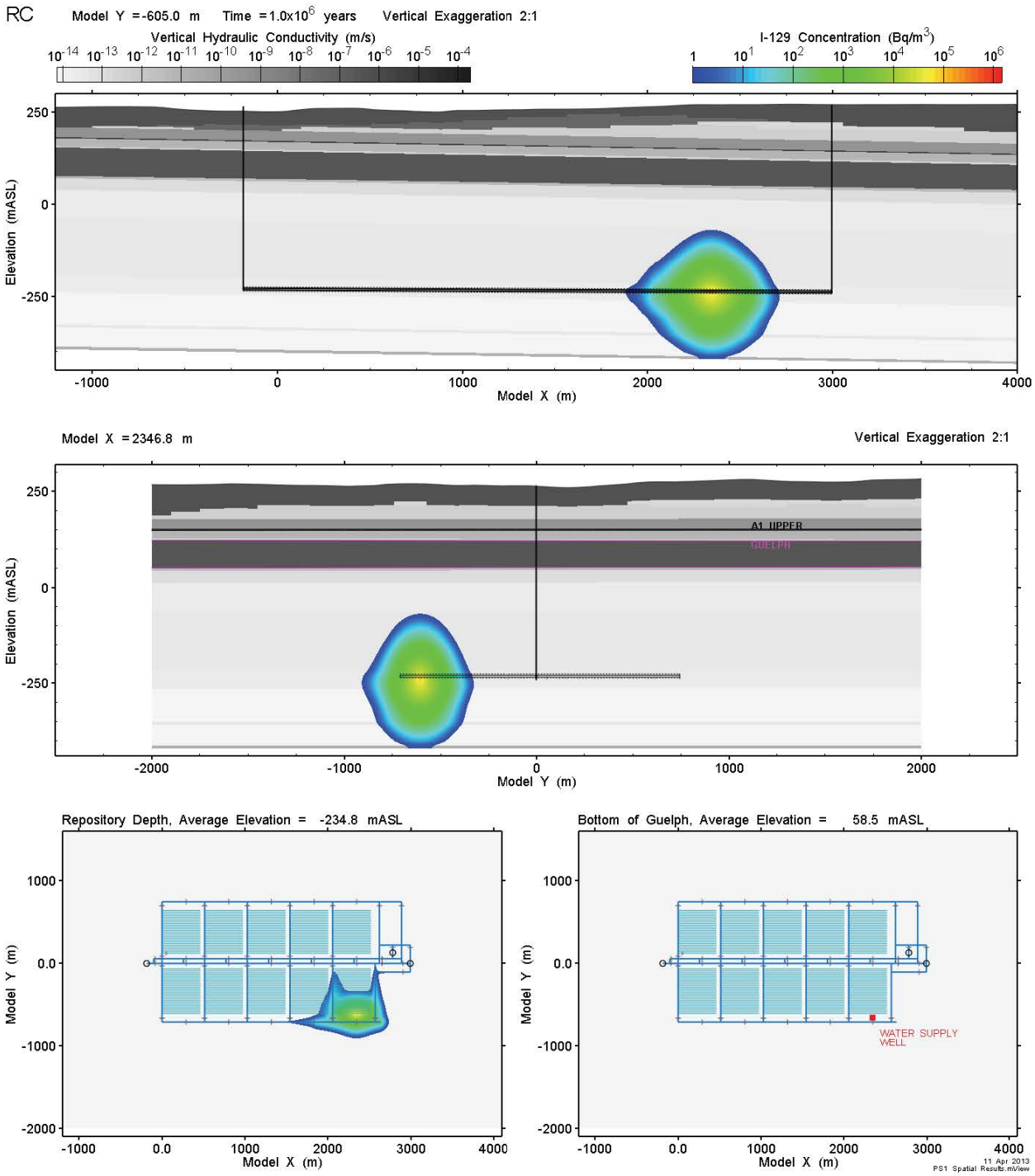

Figure 7-48: Site-Scale Model - Geosphere Hydraulic Conductivity Increased by a Factor of 10: I-129 Concentration at One Million Years

Figure 7-49 shows the radionuclide transport rates to the well for I-129 together with the Reference Case results.

The I-129 transport rate reaches a maximum value of 6.2 Bq/a at 10 million years. This is lower than the Reference Case value of 7.4 Bq/a due to the higher hydraulic conductivity of the Guelph unit. This higher conductivity reduces the capture zone of the well, allowing a larger proportion of the plume to bypass the well and cross the model boundary. The radionuclide arrival time is only very slightly earlier, again indicating that the transport of radionuclides from the repository remains diffusion-dominated.

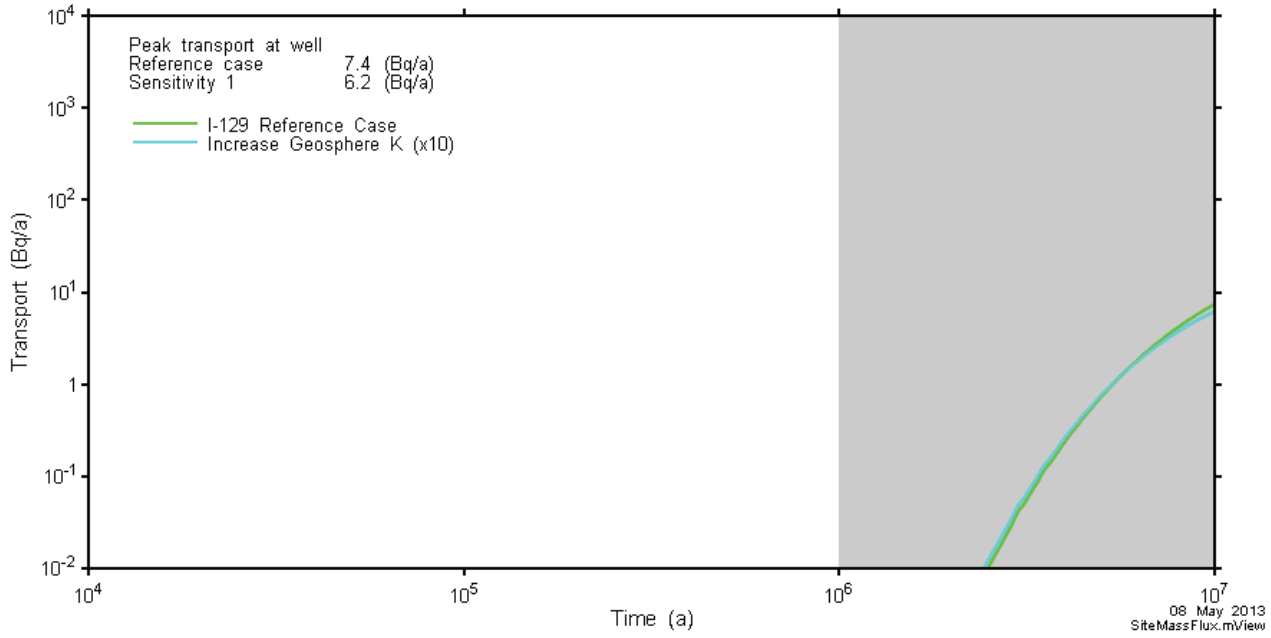

Figure 7-49: Site-Scale Model - Hydraulic Conductivity Increase by a Factor of 10: Radionuclide Transport to Well

7.7.1.2.4 Sensitivity to 100 m of Surface Erosion

This section examines the effect of 100 m of surface erosion caused by repeated glaciations occurring over the one million year period of interest.

FRAC3DVS-OPG simulations have not been performed for this case. With 100 m of erosion, the top of the Guelph formation would be about 40 m below grade (rather than 140 m below grade), but still capped with the very low permeability units of the Salina formation. Even if these units become more permeable due to their nearer surface exposure, the overall system would remain diffusion-dominant, with radioactivity reaching the Guelph on the same time-scale and proceeding from there to the well and biosphere with the same capture rate.

No significant changes to the rate of radionuclide release to the biosphere would therefore result.

7.7.1.2.5 Sensitivity to Spatial Resolution and Time Step Size

This section examines the effect of increasing the spatial resolution and decreasing the time step size on the Reference Case results.

Spatial Resolution

The potential impact of changing spatial resolution has been assessed by comparing results obtained from the Site-Scale Model and the Repository-Scale Model. The Repository-Scale Model has a more highly resolved grid, with a node density increase of more than 10 times.

Figure 7-50 shows a comparison of head contours between the two models. There is very good correspondence, indicating that the resolution of the Site-Scale Model is sufficient to adequately model the flow field.

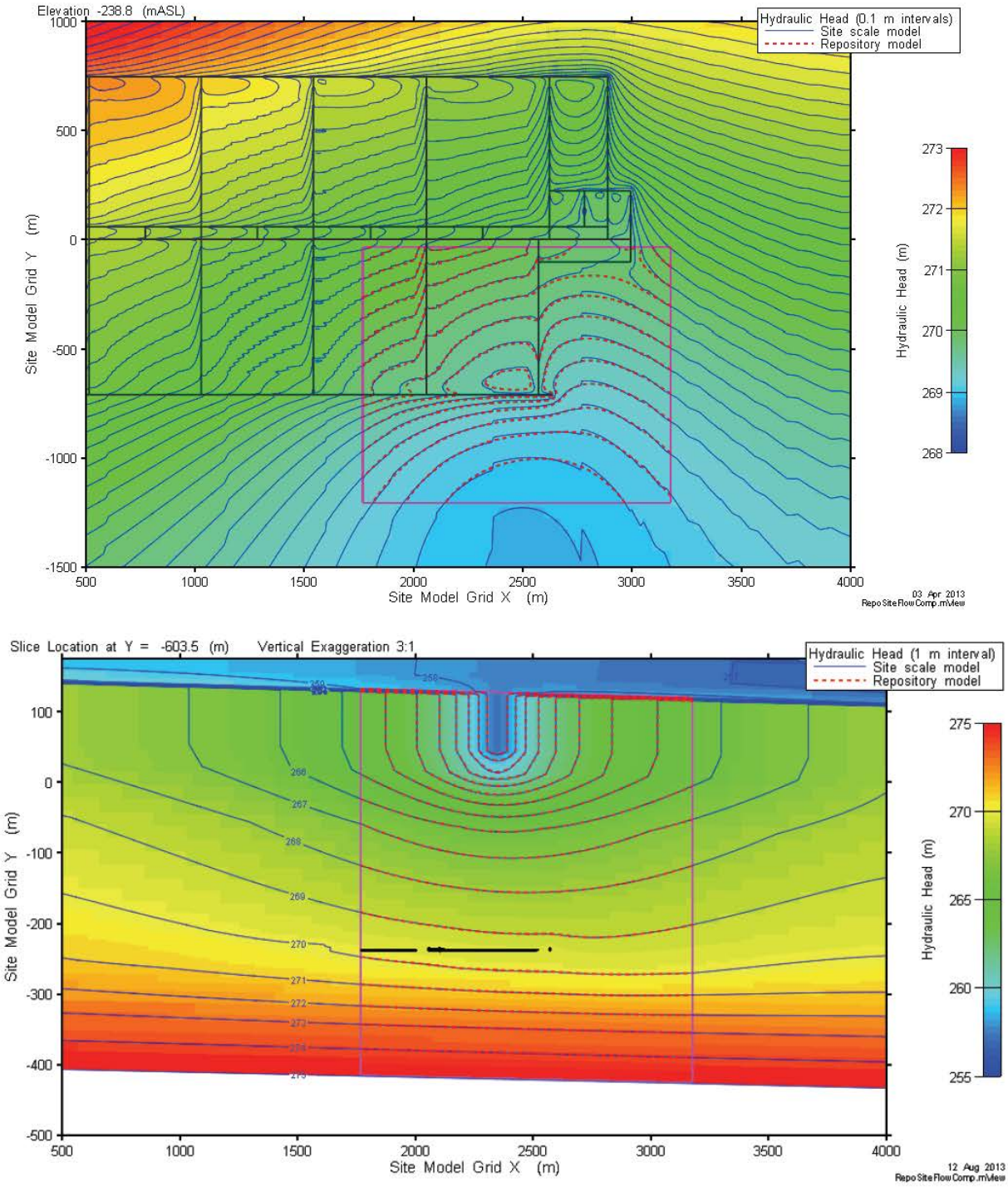

Figure 7-50: Site-Scale Model - Spatial Convergence Sensitivity Comparison of Head Contours

Figure 7-51 compares results for the I-129 plume at 1 million years. The figure shows only minor differences in concentration contours, with the largest variations occurring where differences in tunnel representation (especially the EDZ representation) have a minor influence on solute transport. The lower resolution grid slightly increases diffusive flux in the formations above the repository.

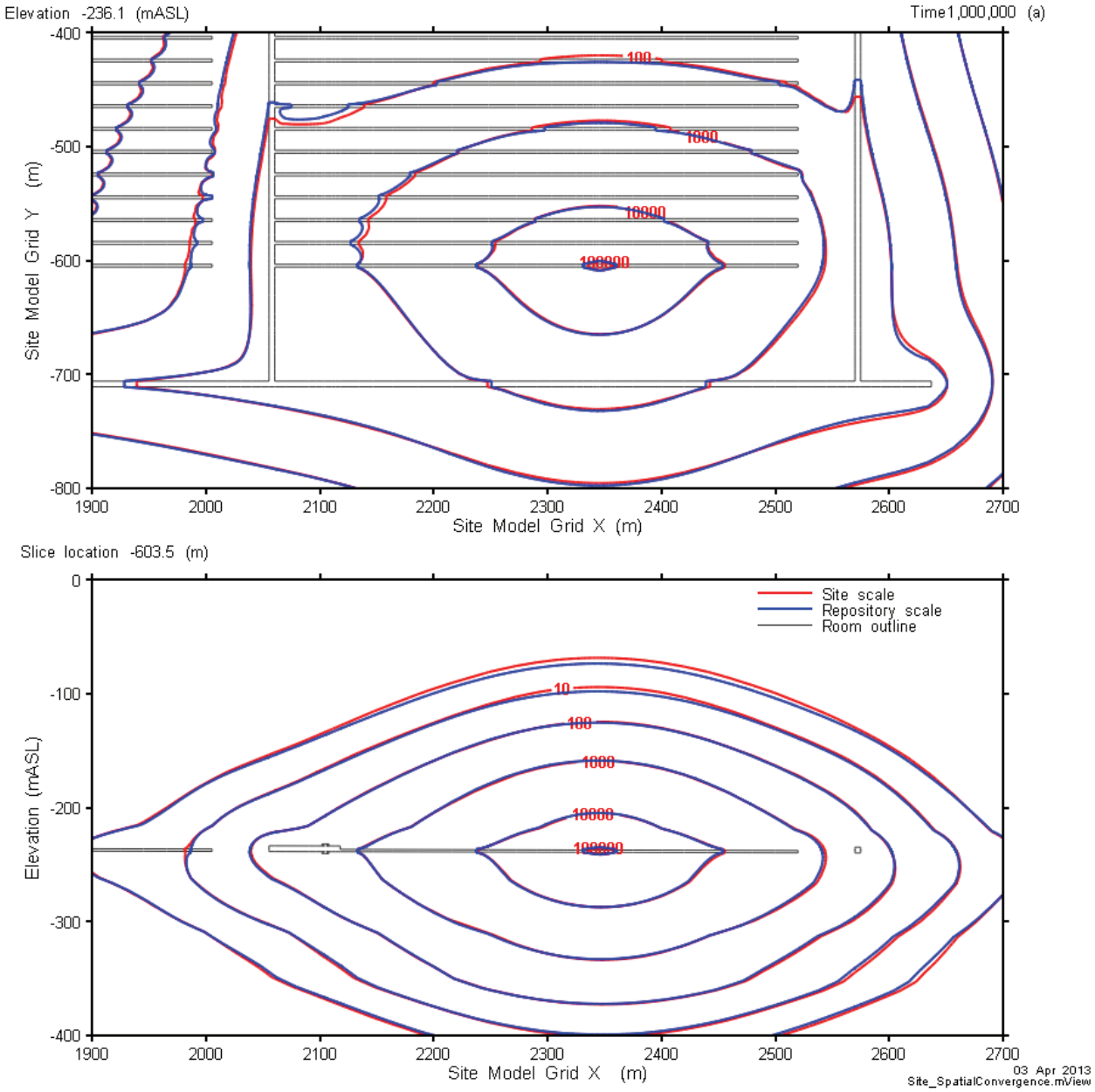

Figure 7-51: Site-Scale Model - Spatial Convergence Sensitivity I-129 Plume

Figure 7-52 compares results for I-129 transport across two planar surfaces (i.e., the top of the Cobourg and Georgian Bay formations) as well as transport to the well. Results compare very well, and the minor differences are not significant in the context of the postclosure safety assessment.

It is therefore concluded that the spatial discretization in the Site-Scale Model is appropriate.

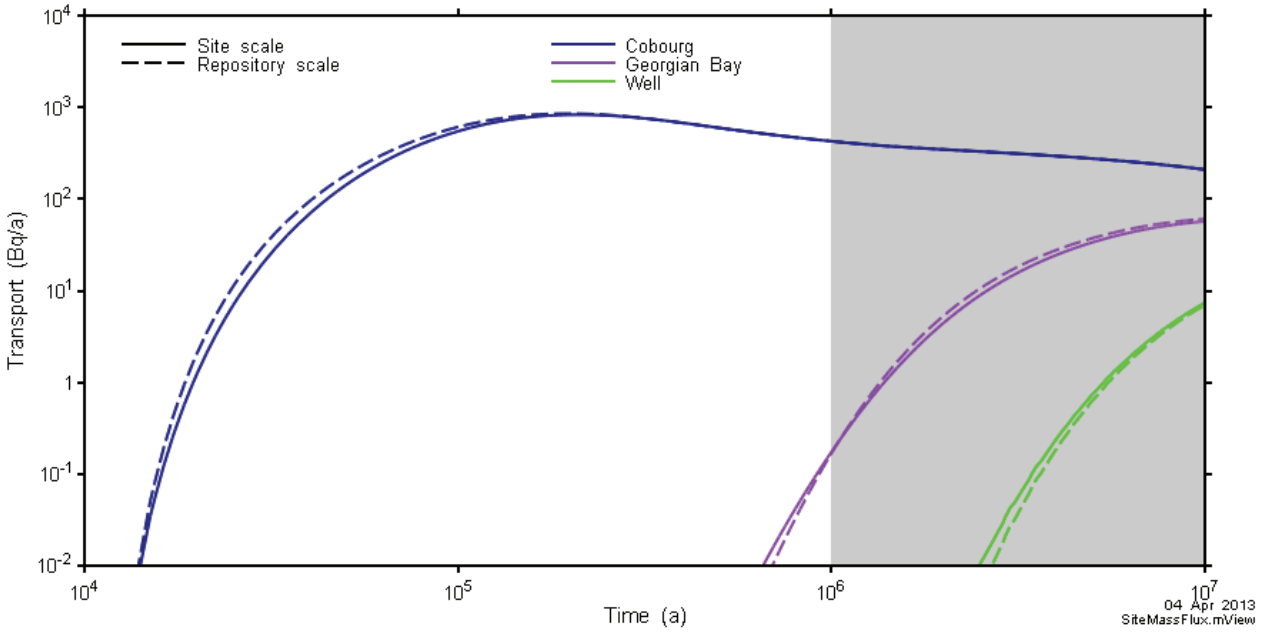

Figure 7-52: Site-Scale Model - Spatial Convergence Sensitivity, I-129 Transport

Temporal Resolution

To determine the effect of time step size, control parameters were modified in the Reference Case Site-Scale Model. These changes result in a factor of two decrease in the number of time steps in one simulation and a factor of three increase in another.

Figure 7-53 shows that these changes have essentially no effect on the I-129 transport rate to the well.

It is therefore concluded that the temporal discretization in the Site-Scale Model is appropriate.

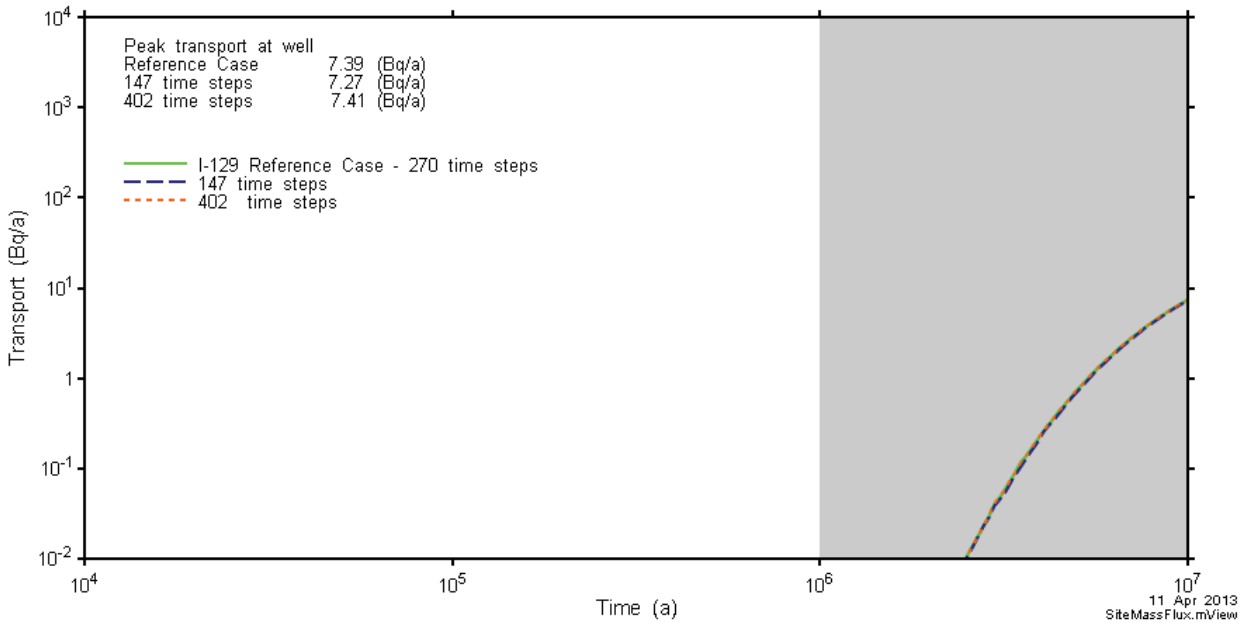

Figure 7-53: Site-Scale Model - Time Step Convergence Sensitivity: I-129 Transport to the Well

7.7.1.2.6 Other Sensitivity Cases

This section presents results for the sensitivity cases listed in Table 7-30.

Results for the Shaft Seal Failure Disruptive Scenario are also presented here for ease of comparison.

Table 7-30: Site-Scale Transport Sensitivity Cases

Sensitivity Case	Description
EDZ High	Reference Case EDZ permeabilities increased by a factor of 10.
Shaft Seal Failure*	The hydraulic conductivities of all shaft seal materials are set to $1x10^{-9}$ m/s and to 1.0×10^{-7} m/s in a subsequent simulation. Results are shown for the latter case. The locations of the defective container and the well are the same as in the Reference Case.
Overpressure in the Shadow Lake Formation	The constant head boundary at the base of the model domain is increased from 275 m to 433 m.

Note: * Disruptive Scenario

Figure 7-54 shows summary results for I-129 transport to the well for all cases. Included for comparison are results for the Reference Case.

The results show there is very little effect on either radionuclide arrival times at the well or on radionuclide transport rates. Increasing the EDZ (the “EDZ High” case) or the shaft permeability

(the “Shaft Seal Failure” case) results in no perceptible difference in transport. Increasing the constant pressure boundary at the base of the model domain from 275 m to 433 m (the “Increased Overpressure” case) increases the vertical hydraulic gradient by approximately a factor of 10. This leads to a slightly earlier plume arrival and slightly higher transport to the well.

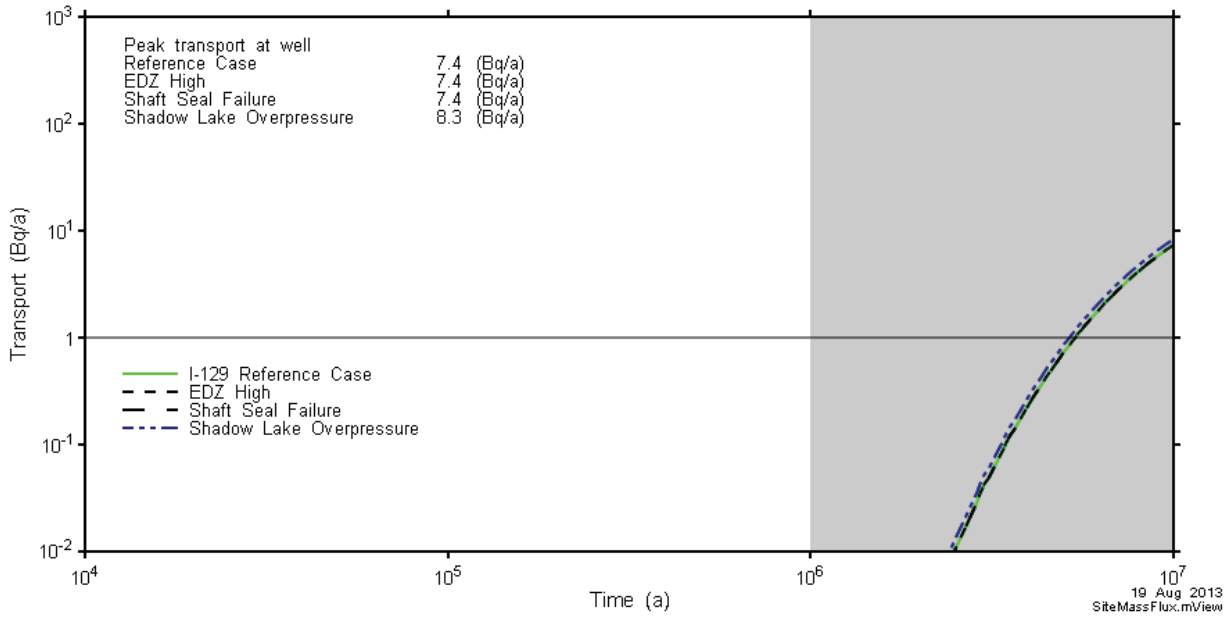

Figure 7-54: Site-Scale Model - I-129 Transport in Sensitivity Cases

7.7.1.2.7 Effect of Barriers on Radionuclide Transport

This section provides information on the effect of the various barriers on radionuclide transport for the Reference Case.

Figure 7-55 through Figure 7-57 show the transport rate for I-129 (a non-sorbing fission product), Cs-135 (an intermediate-sorbing fission product), and U-238 (a highly sorbing actinide). Each figure shows:

- The release rate from the defective containers. As noted in Section 7.5.3.3, the release rates are determined using the SYVAC3-CC4 release model and specified as input to the FRAC3DVS-OPG simulation. The release rates are the same as those shown in Figure 7-31.
- The release rate from the repository. This corresponds to transport through the pink-hued surface in Figure 7-61.
- The release rate through the top of the Cobourg and Georgian Bay formations.
- The release rate to the well and all surface locations.

The figures show the retarding effects of the various barriers on the transport of the different radionuclides.

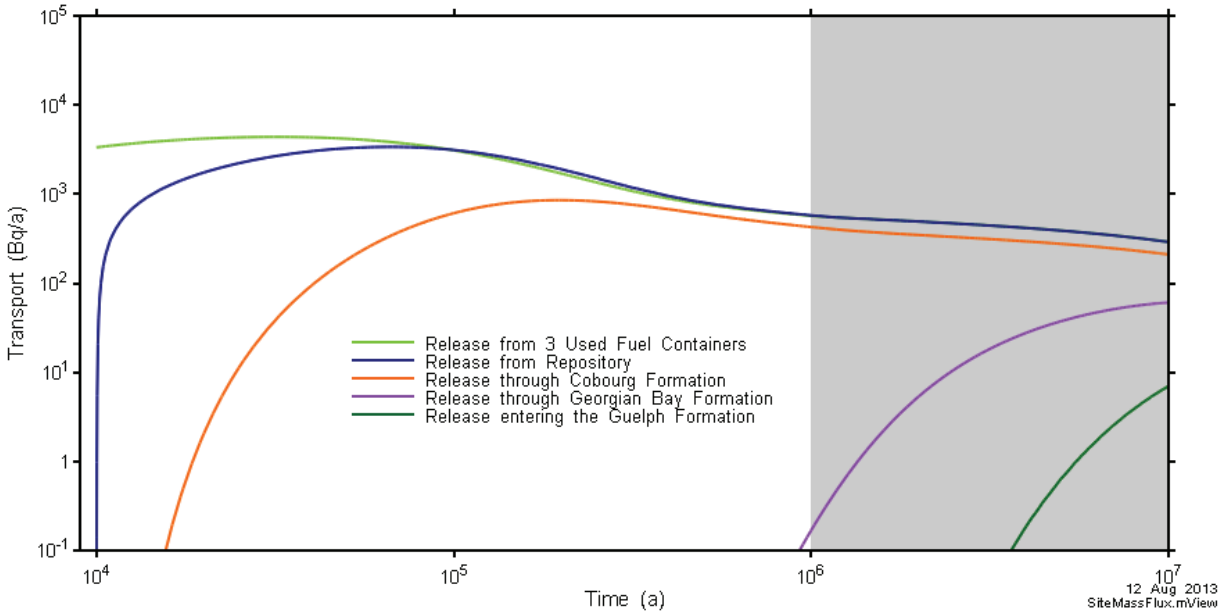

Figure 7-55: FRAC3DVS-OPG - I-129 Transport through Barriers and Selected Geosphere Formations

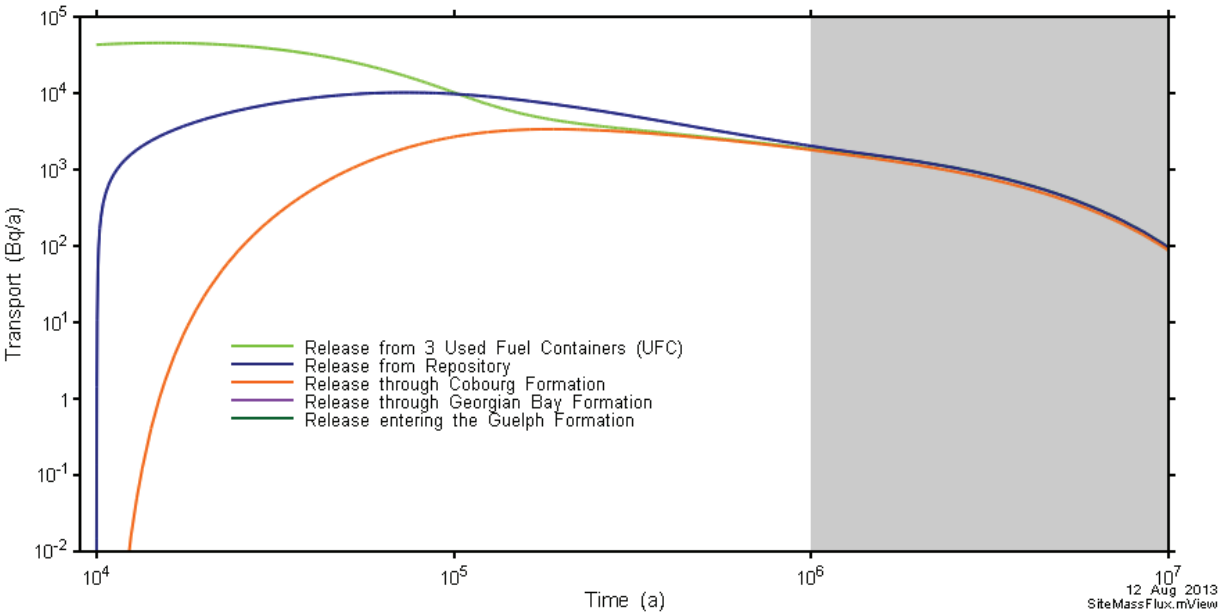

Note: Releases through the Georgian Bay formation and to the Geosphere are off-scale low

Figure 7-56: FRAC3DVS-OPG - Cs-135 Transport through Barriers and Selected Geosphere Formations

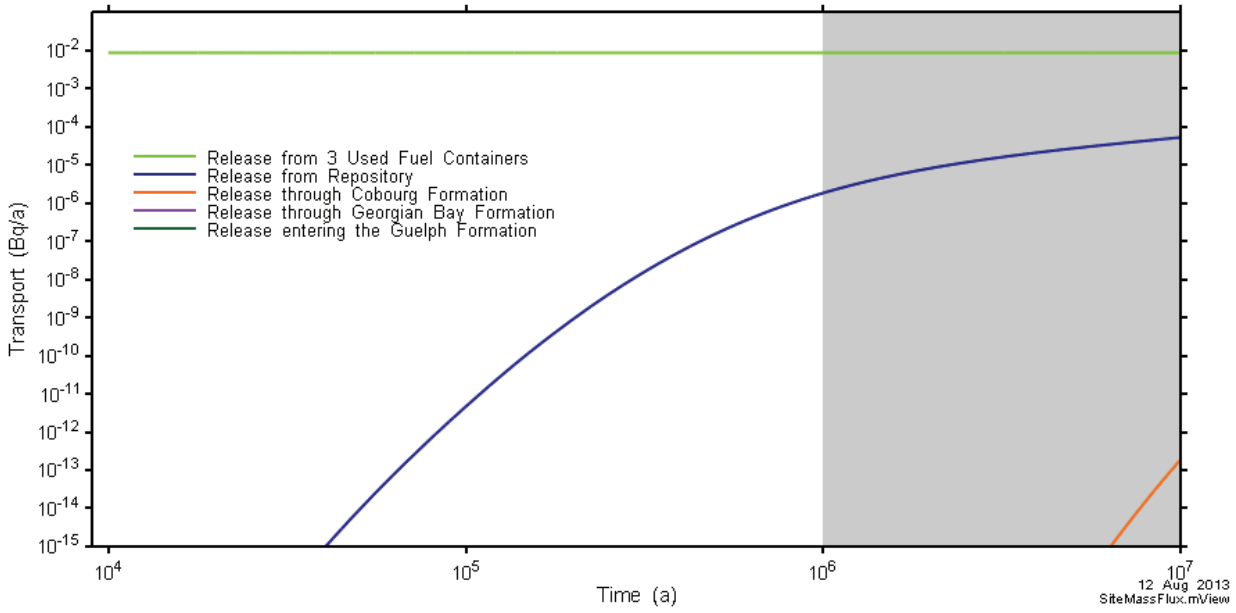

Note: Releases through the Georgian Bay formation and to the Geosphere are off-scale low

Figure 7-57: FRAC3DVS-OPG - U-238 Transport through Barriers and Selected Geosphere formations

In Figure 7-56, releases through the Georgian Bay formation and from the geosphere are off-scale low as a consequence of cesium sorption in Ordovician shales.

In Figure 7-57 releases of U-238 through the top of the Cobourg formation are very low due to sorption on bentonite and Cobourg limestone.

The figures also show that for non-sorbing or moderately sorbing species in a diffusion-dominated system, the bentonite surrounding the containers provides a relatively minor barrier to radionuclide transport. For such species, the geosphere (in this case the Ordovician shales) acts as the primary barrier isolating the radioactive waste from the environment.

7.7.2 Repository-Scale Model

The Repository-Scale Model represents a small section of the repository surrounding the defective containers and the adjacent geosphere. The model incorporates a high level of detail and individual containers are represented at the source location.

Reference Case simulations are performed to corroborate results of the Site-Scale Model and to provide a more complete understanding of repository component functions.

7.7.2.1 Flow Results

7.7.2.1.1 Reference Case

Figure 7-58 and Figure 7-59 show hydraulic head and advective velocities on a plan section through the placement room at the elevation of the repository tunnels. The isolation of the placement rooms and the low velocities throughout the repository are evident in the figures.

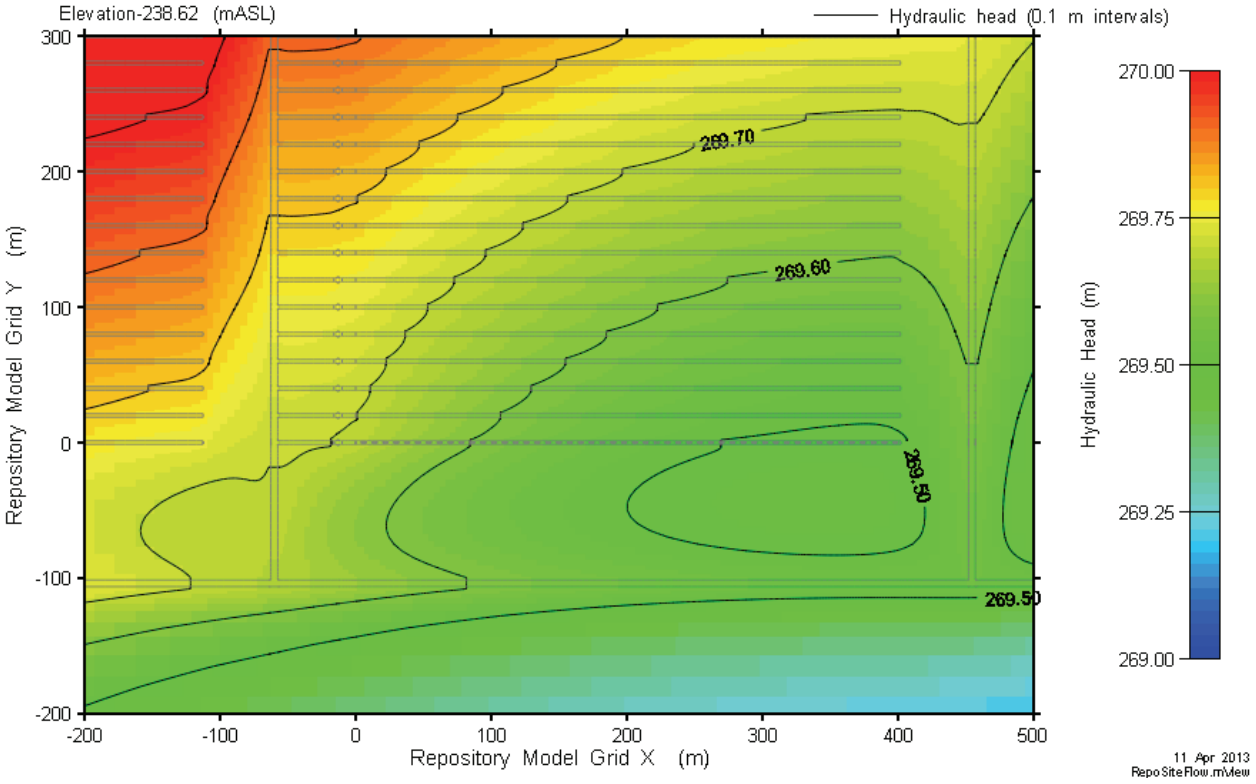

Figure 7-58: Repository-Scale Model - Head at Tunnel Elevation

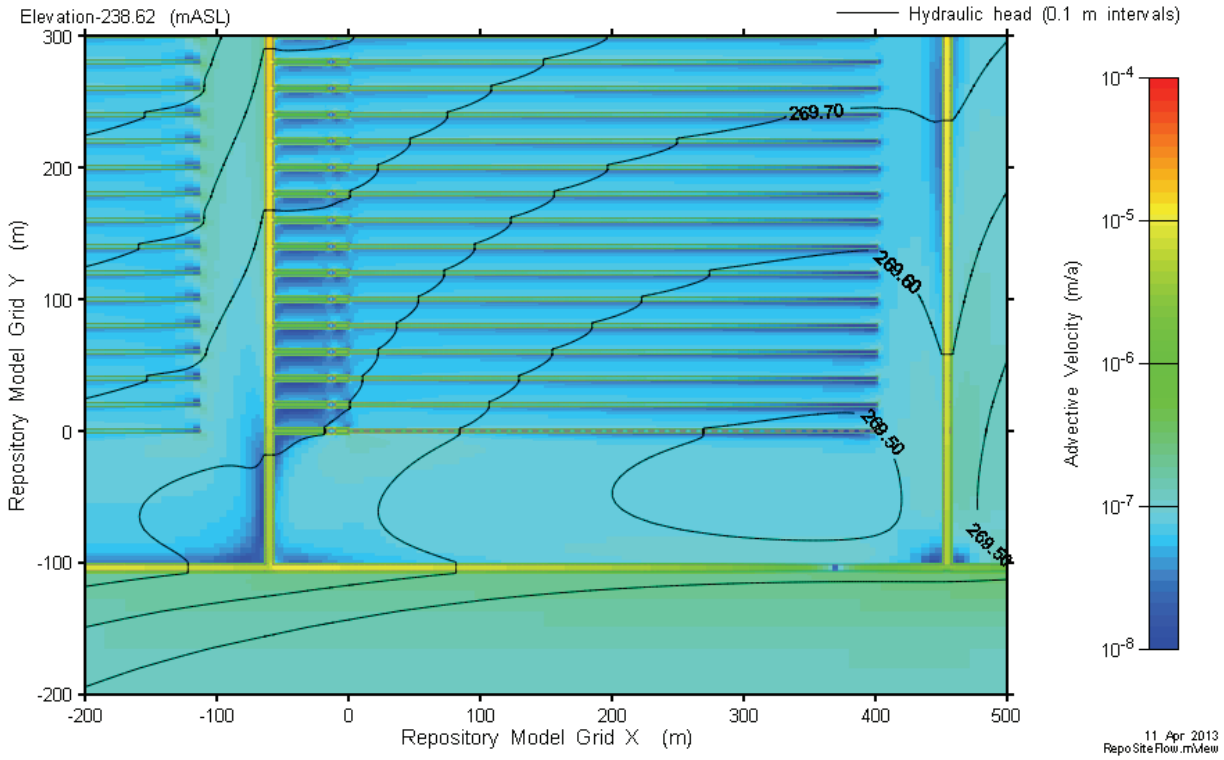

Figure 7-59: Repository-Scale Model - Advective Velocities at Tunnel Elevation

Figure 7-60 shows advective velocities in a 3D view through the EBS and EDZ materials. The highest velocities are in the inner EDZ and in the thin section of inner EDZ around the seal EDZ intercept. The maximum velocities in this plot are below 10^{-4} m/a. At such low velocities, diffusive transport will dominate over advective transport, as the Site-Scale Model results in the previous section indicate.

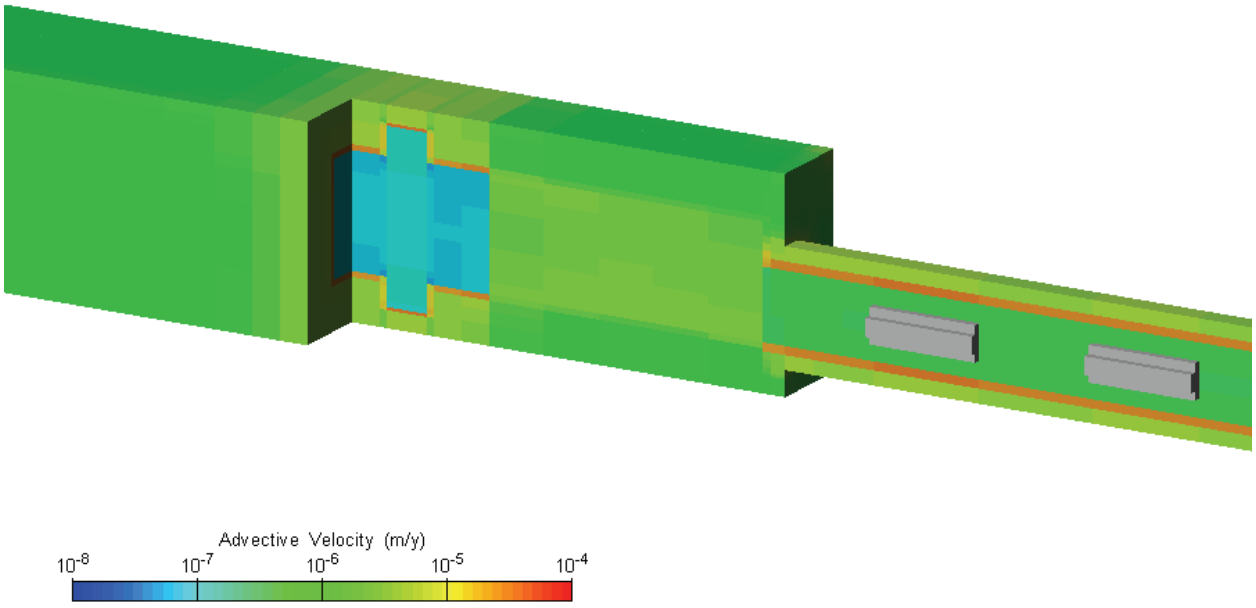

Figure 7-60: Repository-Scale Model - 3D View of Advective Velocity Magnitudes

7.7.2.2 Radionuclide Transport Results

Radionuclide transport modelling is performed for I-129, Cs-135, U-234 and U-238.

Although the source term is from three defective containers, the release is applied to a single container for modelling simplicity. The results are indistinguishable from adjacent container releases at significant distances from the source.

To provide data for later verification of the SYVAC3-CC4 model (Section 7.8.1), radionuclide transport from the used fuel container into the placement room and geosphere (i.e., out of the buffer) is computed over a volume surrounding the defective container as shown in Figure 7-61.

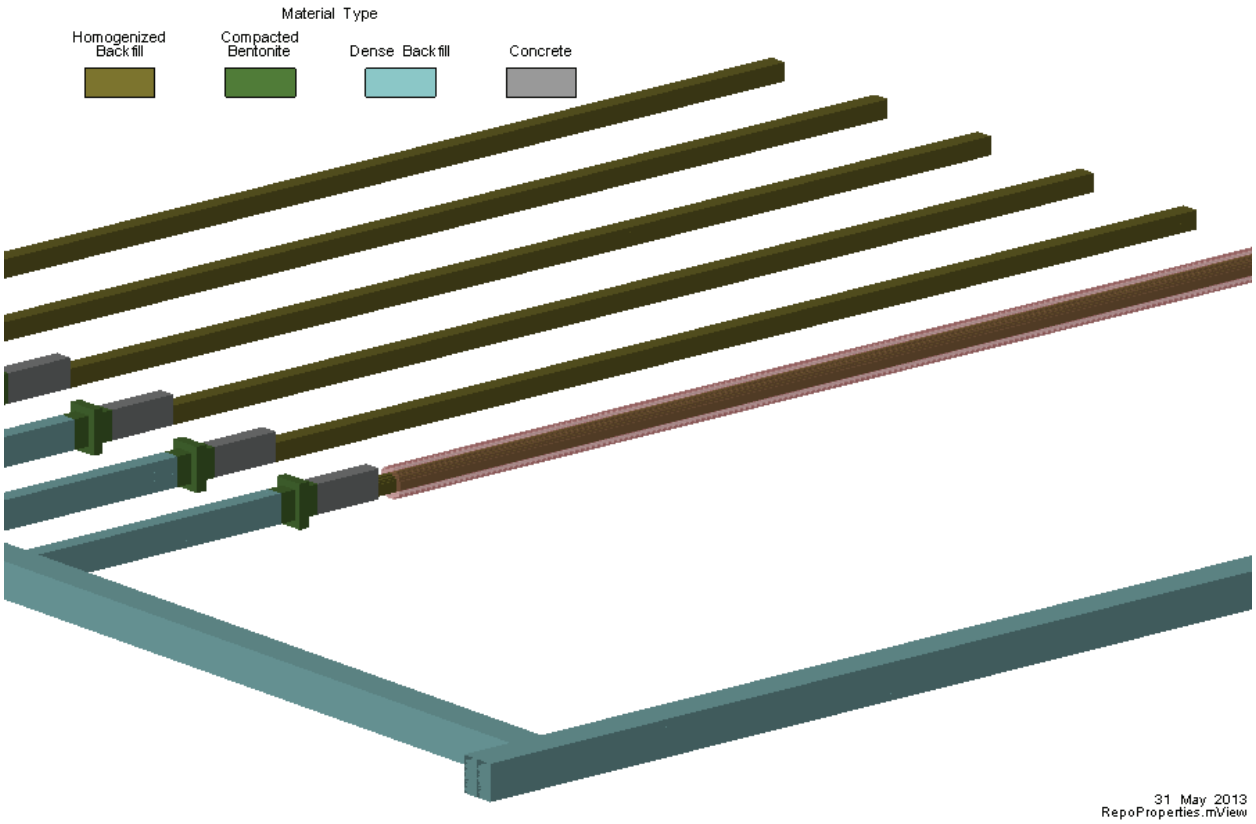

Notes: the pink-hued surface is set at the boundary between the EDZ and the intact rock surrounding the placement room. The surface extends the full length of the room to include all 50 containers.

Figure 7-61: Repository-Scale Model - Control Surface for Calculation of Radionuclide Releases from Repository

7.7.2.2.1 Reference Case

This section presents detailed results for I-129, U-238 and Cs-135. The three selected radionuclides are representative of the behaviours for non-sorbing, highly sorbing and intermediate-sorbing species.

Figure 7-62 through Figure 7-64 illustrate the time dependent behaviour of the I-129 plume along the repository level and on a vertical slice through the placement room. Contours of equivalent results from the Site-Scale Model are overlaid for comparison. The results show similar core concentration profiles with slightly lower I-129 concentrations at the plume margins, likely due to the more detailed discretization.

This comparison provides confidence in the Site-Scale results.

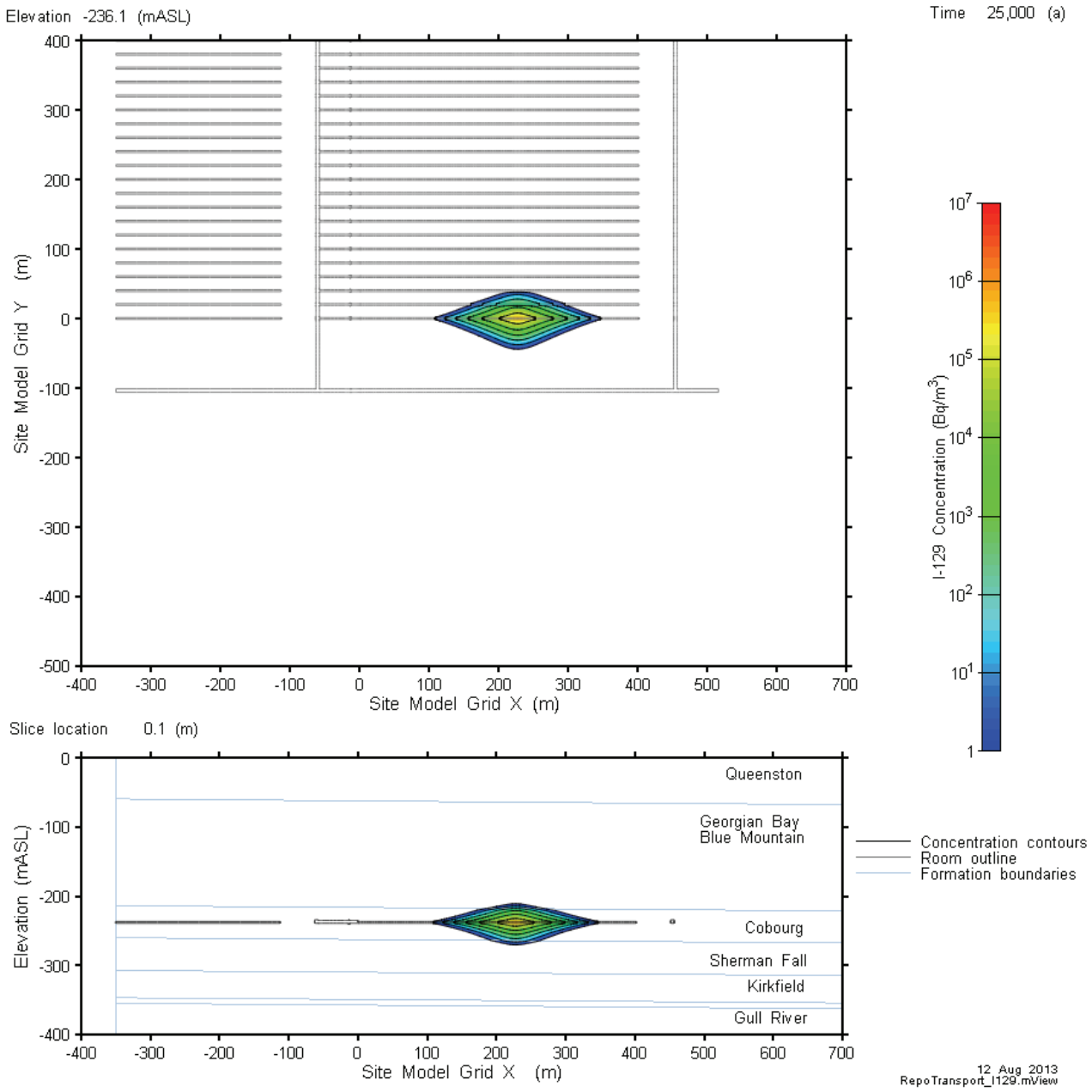

Figure 7-62: Repository-Scale Model - I-129 Concentrations at 25,000 Years

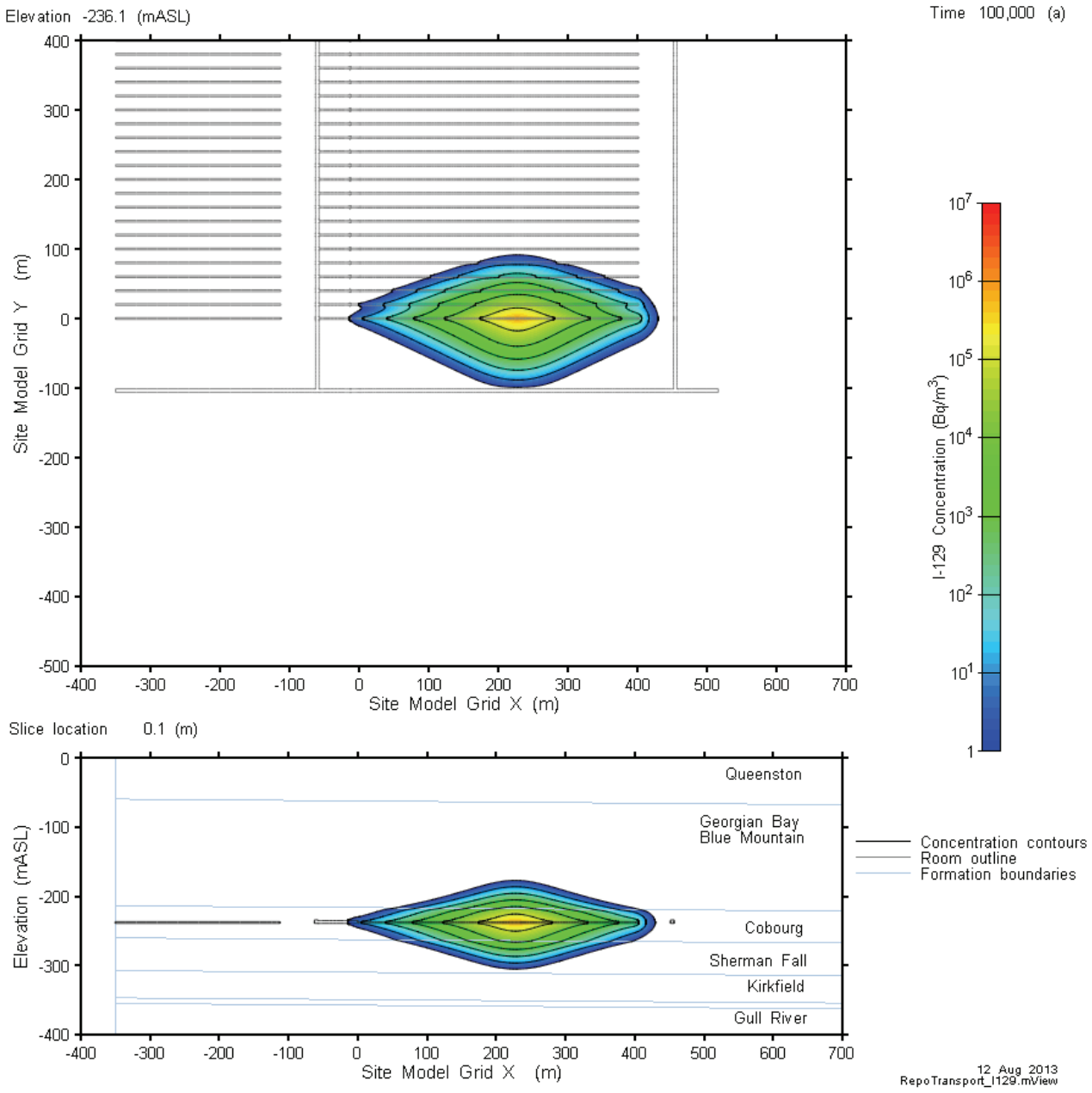

Figure 7-63: Repository-Scale Model - I-129 Concentrations at 100,000 Years

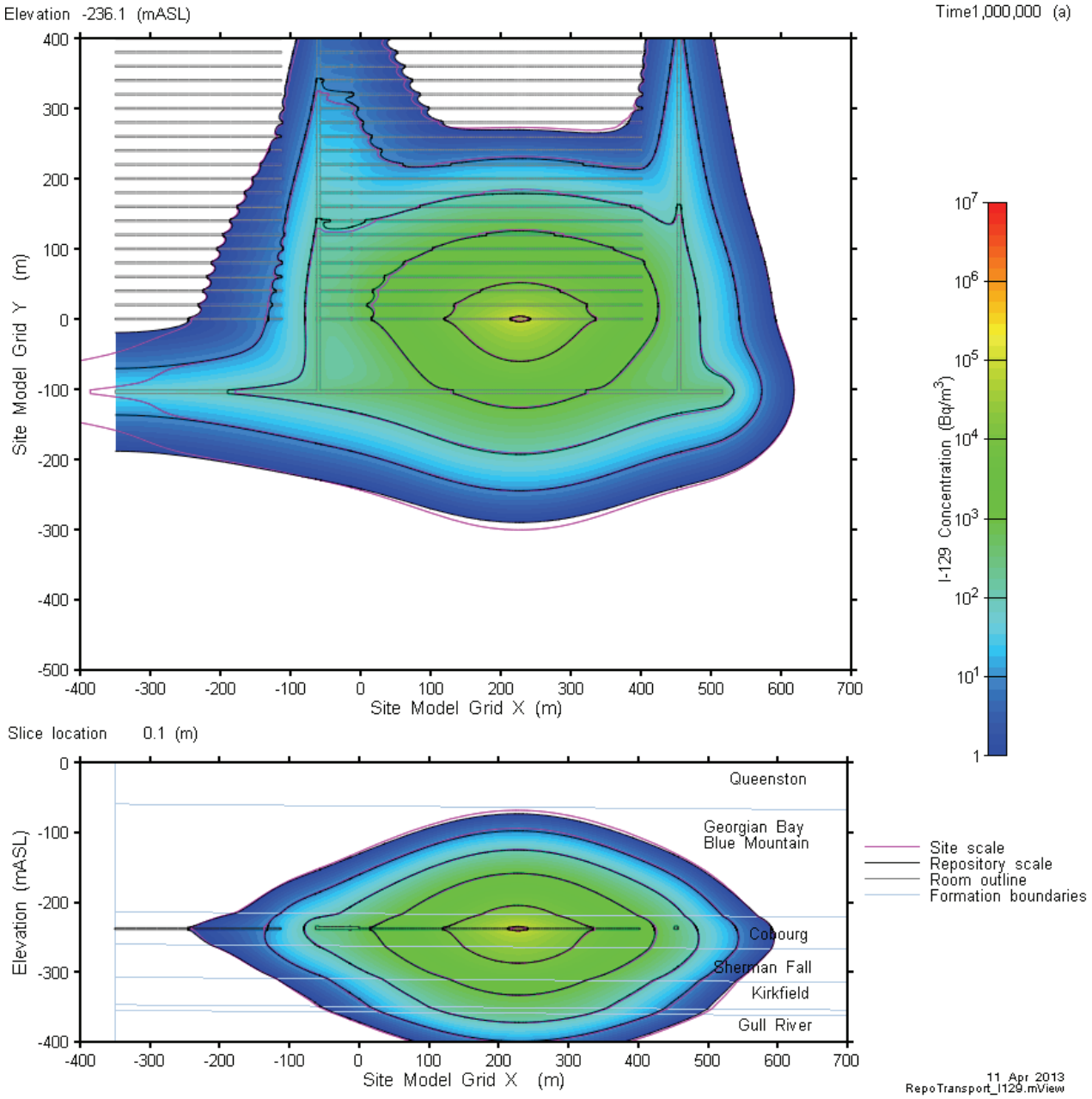

Figure 7-64: Repository-Scale Model - I-129 Concentrations at One Million Years

Unlike I-129, U-238 is strongly sorbed onto sealing materials and the host rock. Consequently, transport of U-238 is limited to a very small domain immediately surrounding the defective container. Figure 7-65 shows sectional views through the release plane and adjacent buffer at one million years.

The contour plots are on a logarithmic scale. The 0.001 Bq/m^3 concentration contour corresponds to an effective U-238 drinking water dose of about 0.00003 µSv/a based on the Table 7-26 water consumption rate of 0.84 m^3/a per person.

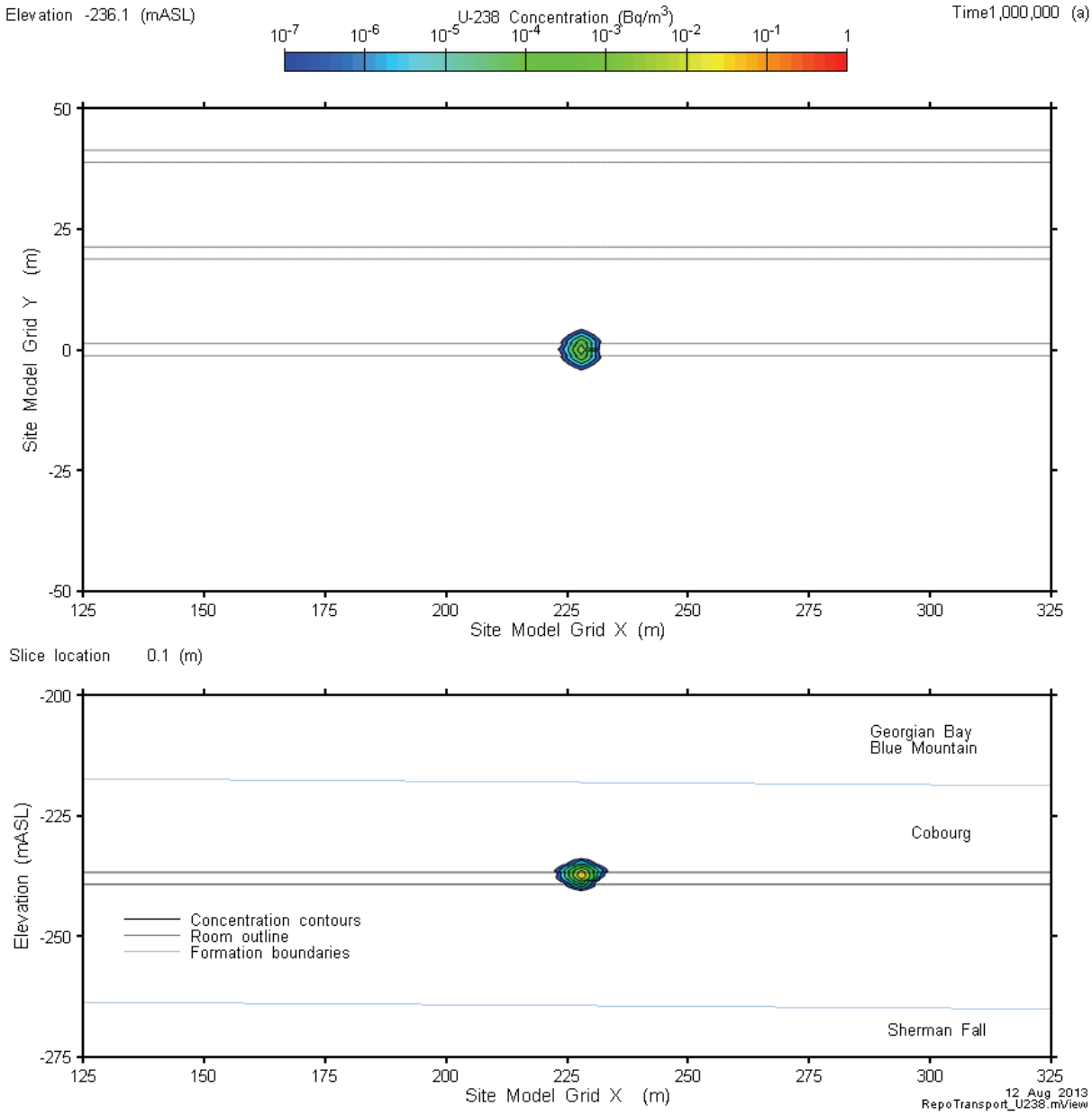

Figure 7-65: Repository-Scale Model - U-238 Concentration at One Million Years

Figure 7-66 and Figure 7-67 show the Cs-135 plume at 100,000 years and one million years. Cs-135 is less strongly sorbed than U-238 but is still subject to retardation. The results show transport is largely confined to the vicinity of the placement room and that the room seal is effective in limiting transport towards the access tunnels. As previously noted, the non-spherical

shape of the Cs-135 plume is due to the fact that cesium is sorbed more strongly by the geosphere layers above the repository than those below the repository.

The 100 Bq/m^3 contour line corresponds to a Cs-135 drinking water dose of about 0.02 µSv/a based on the Table 7-26 water consumption rate of 0.84 m^3/a per person.

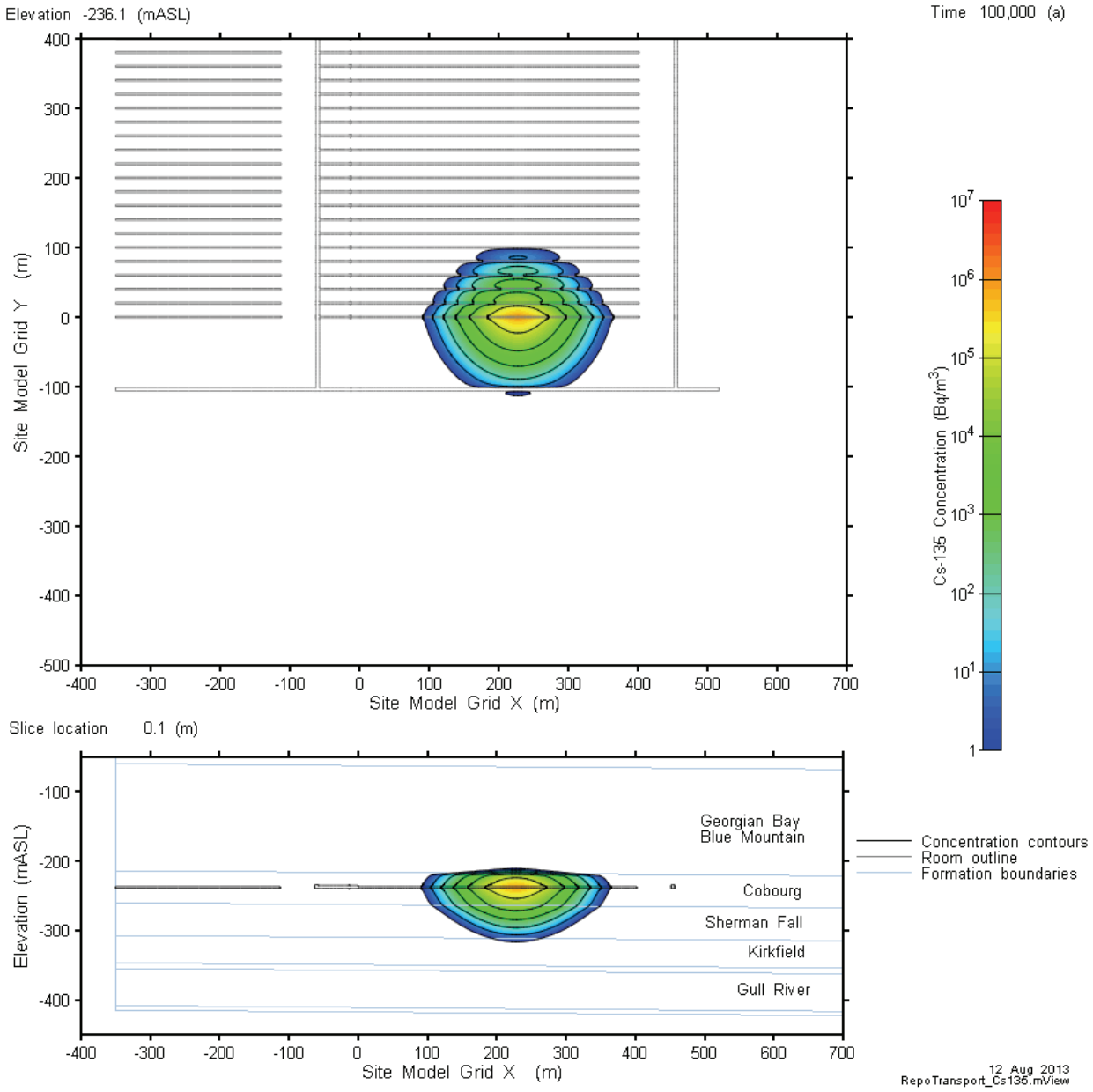

Figure 7-66: Repository-Scale Model - Cs-135 Concentrations at 100,000 Years

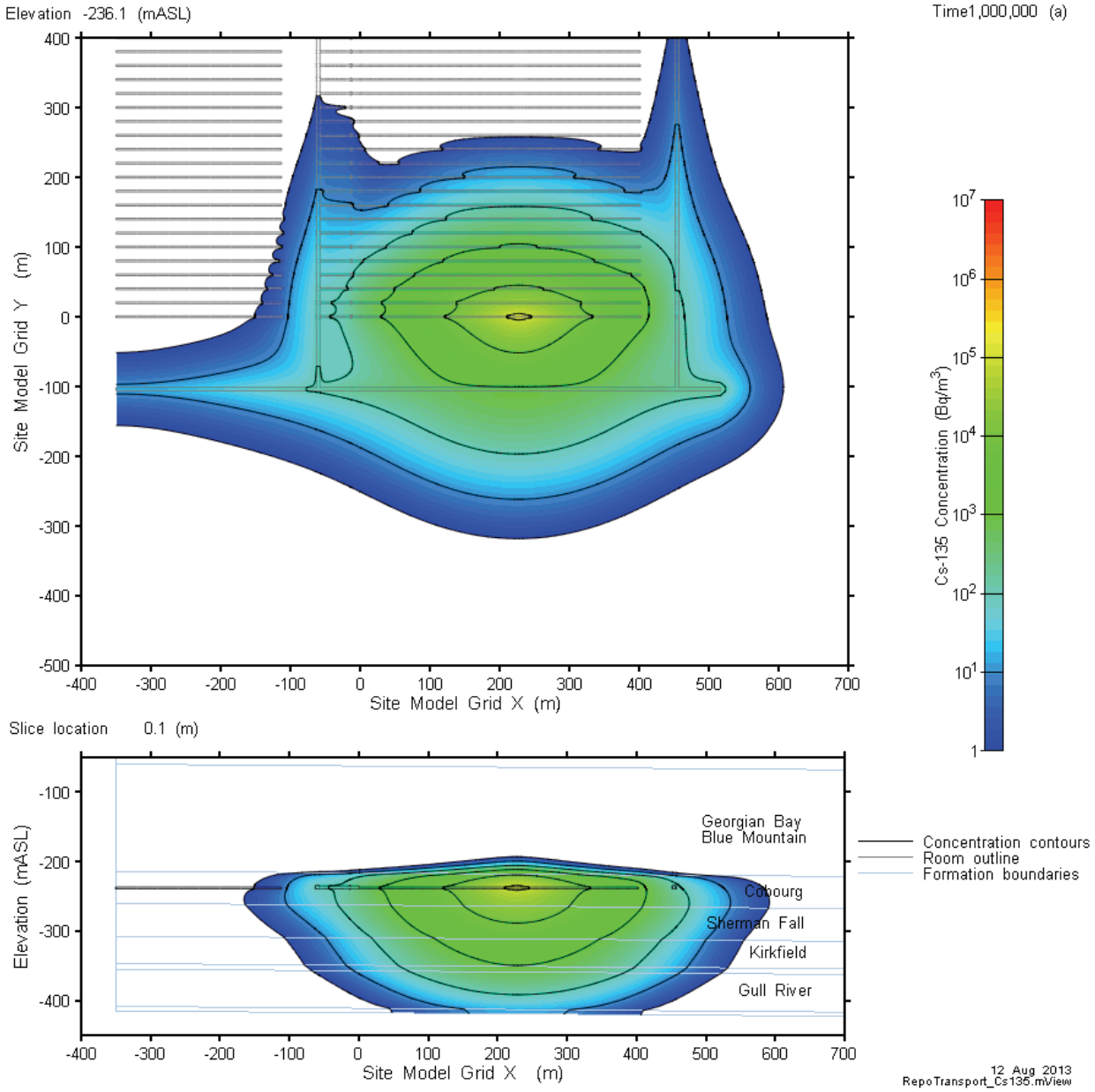

Figure 7-67: Repository-Scale Model - Cs-135 Concentrations at One Million Years

Figure 7-68 shows summary results for all radionuclides considered. This figure shows the transfer rates out of the boundary volume surrounding the placement room shown in Figure 7-61.

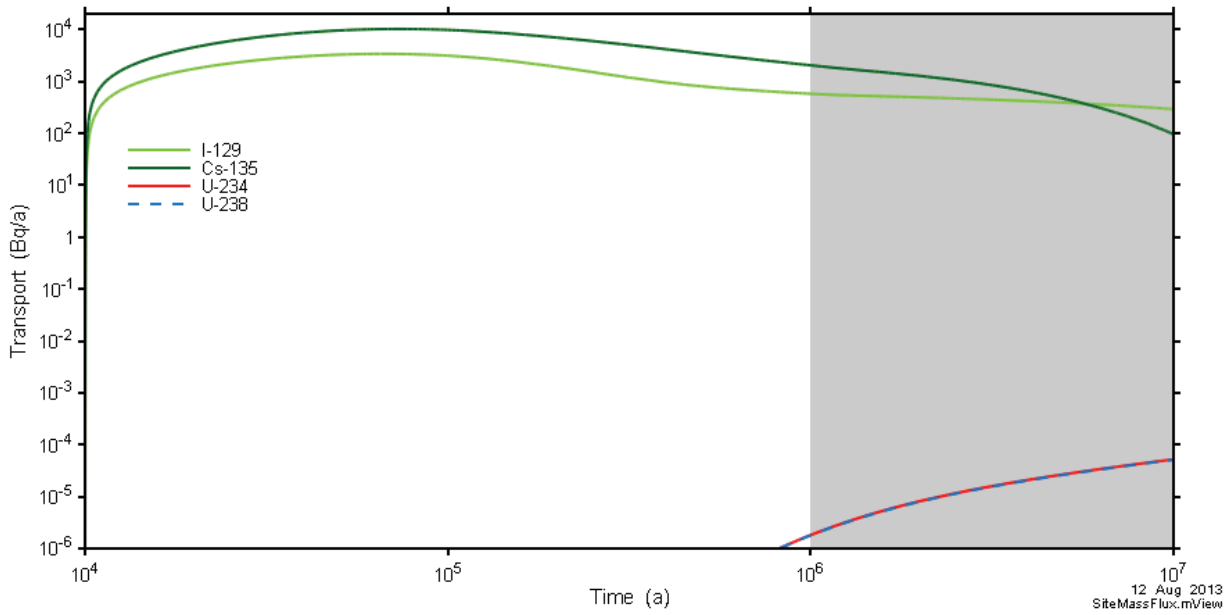

Figure 7-68: Repository-Scale Model - Transport Rates out of the Placement Room for I-129, Cs-135, U-234 and U-238

7.8 Results of System Modelling

The SYVAC3-CC4 system model combines an idealized geometric description of the repository and a simple geosphere transport model with representations of releases from the used fuel and container, and radionuclide transport in the biosphere to determine the radiological consequences of releases to the environment.

This section presents the results of deterministic and probabilistic analysis of the Reference Case and a set of related sensitivity cases.

The deterministic sensitivity cases are:

- Fuel dissolution rate increased by a factor of 10;
- Instant release fractions set to 0.10 for all radionuclides;
- Container defect area increased by a factor of 10;
- No solubility limits in the container;
- No sorption in the EBS;
- No sorption in the geosphere;
- Low sorption in the geosphere with coincident high solubility limits in the container; and
- Geosphere diffusivity increased by a factor of 10.

For ease of presentation, the sensitivity cases are separated into those that represent a degraded physical barrier and those that represent a degraded chemical barrier.

Probabilistic simulations examine the effect of simultaneous variation of all probabilistically defined parameters.

Deterministic and probabilistic simulations are also performed for complementary indicators.

A detailed description of these cases is provided in Section 7.2.1.

Figures in this section are shown with shading at times greater than one million years to emphasize that these results are illustrative and included only to indicate maximum impacts. Shading for dose rates below 10^{-9} Sv/a indicates these values are negligible and are included to indicate trends.

7.8.1 Transport Model Verification

To provide confidence in the SYVAC3-CC4 model, transport results for I-129, Cs-135, U-234 and U-238 are compared with similar results obtained from the detailed FRAC3DVS-OPG 3D simulations.

Near-Field Transport Comparison

Transport from the container to the geosphere for the Reference Case is shown in Figure 7-69 and Figure 7-70. For FRAC3DVS-OPG the transport is across the surface of the pink hued cylinder in Figure 7-61 while for SYVAC3-CC4 the transport is across the outer surface of the grey cylinder in Figure 7-33. In both cases, the surface represents the excavation damaged zone / rock boundary around a placement room.

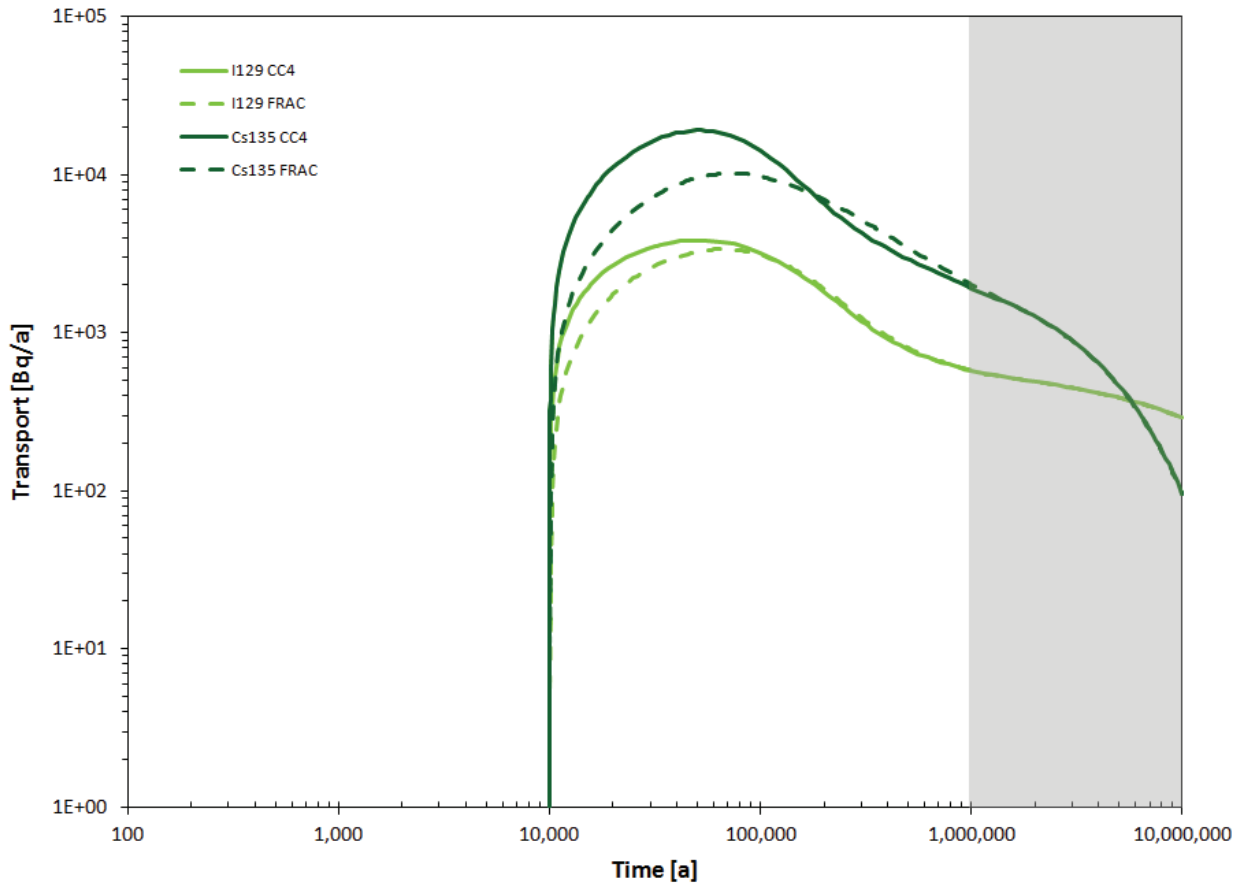

Figure 7-69: Comparison of SYVAC3-CC4 and FRAC3DVS-OPG Transport of I-129 and Cs-135 to the Geosphere

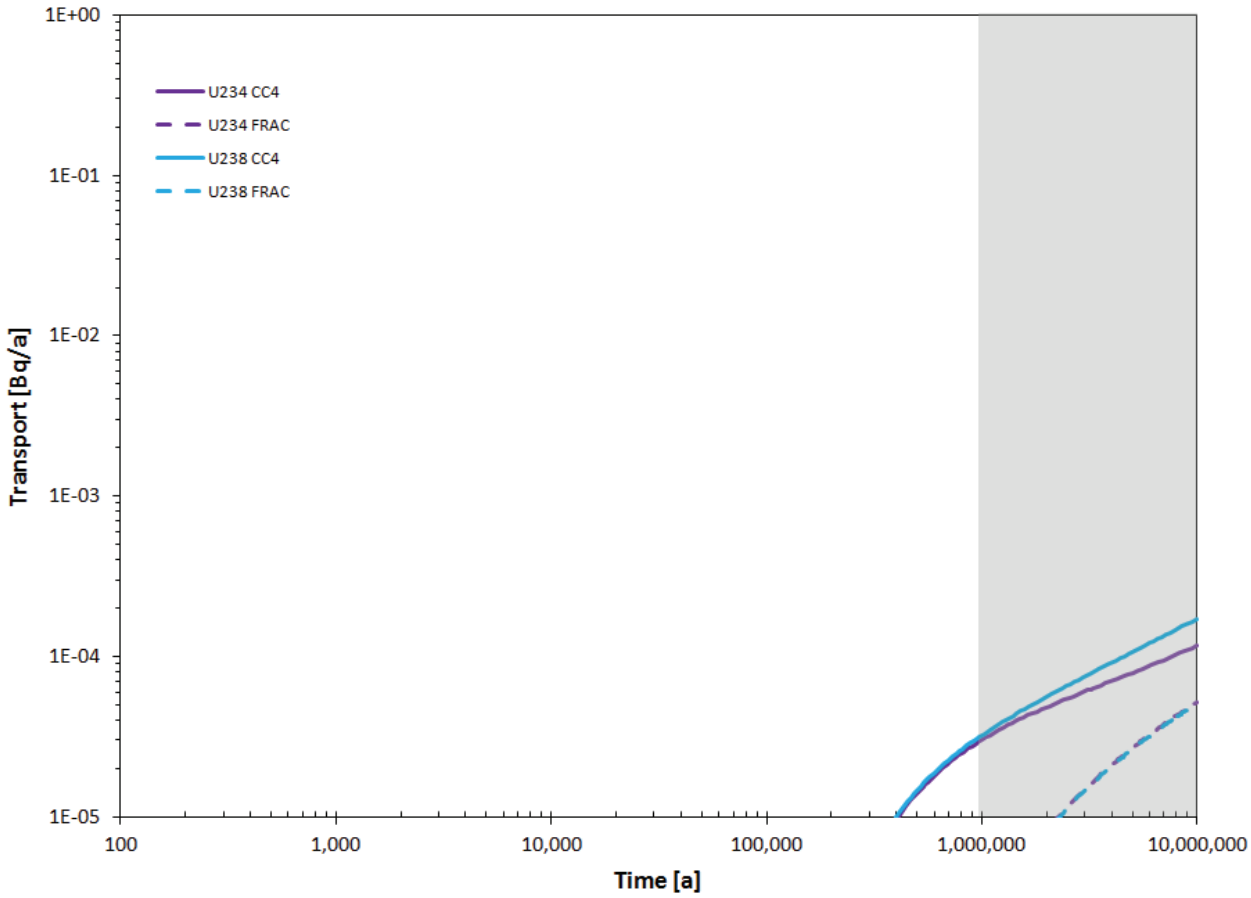

Note: FRAC3DVS-OPG-calculated transport of U-234 and U-238 overlap

Figure 7-70: Comparison of SYVAC3-CC4 and FRAC3DVS-OPG Transport of U-234 and U-238 to the Geosphere

Results for the maximum values and their associated time occurrences are shown in Table 7-31. The agreement is very close for the non-sorbing and weakly sorbing radionuclides I-129 and Cs-135. The peak rates for the strongly sorbing U-234 and U-238 are not reached during the simulation period in either model. The greater differences for sorbing radionuclides occur because the buffer in the SYVAC3-CC4 model (Figure 7-33) is represented as a cylinder whereas in reality it is an annulus. Even though the buffer thickness is maintained, the cylinder representation has less material volume and less sorbing surface area.

Table 7-31: Comparison of Maximum Transport Rates to the Geosphere

Nuclide	Highest Transport Rate in 10 million years (Bq/a)			Time of Highest Value (a)		
	SYVAC3-CC4	FRAC3DVS-OPG	Ratio[1]	SYVAC3-CC4	FRAC3DVS-OPG	Ratio[1]
I-129	3.86×10^{3}	3.38×10^{3}	1.14	4.98×10^{4}	6.75×10^{4}	0.74
Cs-135	1.91×10^{4}	1.02×10^{4}	1.87	5.26×10^{4}	7.27×10^{4}	0.72
U-234	1.16×10^{-4}	5.21×10^{-5}	2.23	1×10^{7}	1×10^{7}	1.0
U-238	1.72×10^{-4}	5.12×10^{-5}	3.35	1×10^{7}	1×10^{7}	1.0

Note: [1] Ratio is the SYVAC3-CC4 value divided by the FRAC3DVS-OPG value.

Geosphere Transport Comparison

The transport of I-129 and Cs-135 through the geosphere for the Reference Case is shown in Figure 7-71, with Table 7-32 summarizing the highest transport rates in the 10 million year time frame. The figure also compares the transport of I-129 at various sedimentary layers including the Cobourg and Georgian Bay formations.

For U-238 and U-234, the release rates are effectively zero in both models due to the highly sorbing nature of these radionuclides.

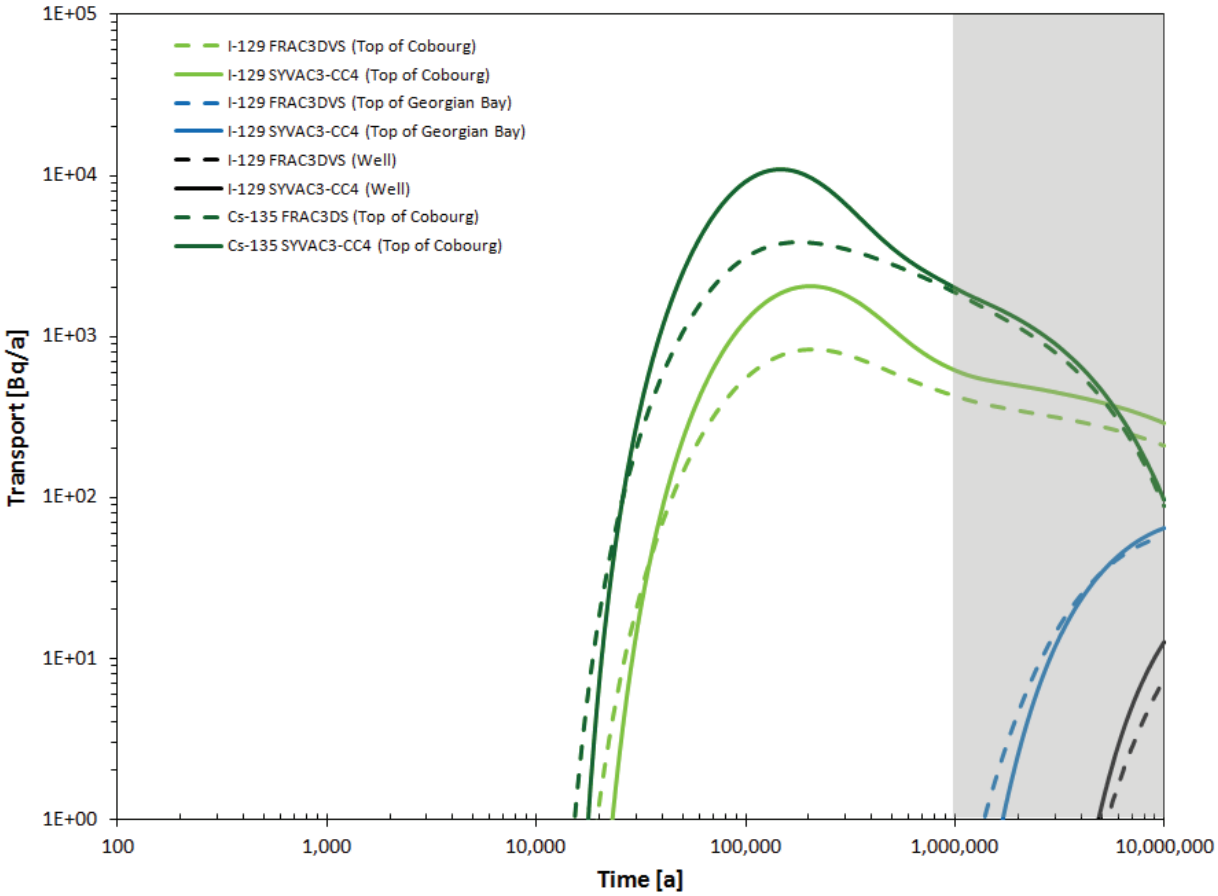

Note: Cs-135 transport through the top of the Georgian Bay layer and to the Well is off-scale low

Figure 7-71: Comparison of SYVAC3-CC4 and FRAC3DVS-OPG Transport of I-129 and Cs-135

Table 7-32: Comparison of Maximum Transport Rates to the Surface

Nuclide	Layer	Highest Transport Rate (Bq/a)			Time of Highest Transport (a)		
		SYVAC3-CC4	FRAC3DVS-OPG	Ratio[1]	SYVAC3-CC4	FRAC3DVS-OPG	Ratio[1]
I-129	Cobourg	2.06×10^{3}	8.29×10^{2}	2.48	2.05×10^{5}	2.10×10^{5}	0.98
	Georgian Bay	6.45×10^{1}	5.69×10^{1}	1.13	1×10^{7}	1×10^{7}	1.0
	Well	1.28×10^{1}	7.39×10^{0}	1.73	1×10^{7}	1×10^{7}	1.0
Cs-135	Cobourg	1.09×10^{4}	3.82×10^{3}	2.86	1.49×10^{5}	1.75×10^{5}	0.85

Note: [1] Ratio is the SYVAC3-CC4 value divided by the FRAC3DVS-OPG value.

The above comparisons indicate the SYVAC3-CC4 maximum transport rates are greater than those arising from the FRAC3DVS-OPG model while their associated time of occurrences are earlier. This implies that the SYVAC3-CC4 near-field and far-field models provide a conservative representation of radionuclide transport for key radionuclides as compared to FRAC3DVS-OPG.

7.8.2 Deterministic Analysis

Due to the very low hydraulic conductivity of the host rock and the dominance of diffusive transport, the dose rates arising in the one million year period of interest are below the 10^{-9} Sv/a threshold value for almost all cases. The peak dose rate is also not reached in this time frame.

To provide a basis for comparing cases, results are therefore quoted for a 10 million year period; however, even with this extension the peak dose rate for many cases is not reached.

To put the quoted results into context, results obtained for the sensitivity case with geosphere diffusivities increased by a factor of 10 can be used. These results, illustrated in Figure 7-77 in Section 7.8.2.2, indicate that a peak dose rate of 2.6×10^{-8} Sv/a is reached at 5.6×10^{6} years. This shows that the long-term doses are expected to remain extremely low, even in cases where the peak dose rate is not reached in the 10 million year simulation time.

7.8.2.1 Reference Case

Figure 7-72 shows the total dose rate for the Reference Case. This is the sum of the individual contributions from all radionuclides of potential interest and their progeny (Section 7.6).

The maximum dose rate is 2.0×10^{-9} Sv/a occurring at 1.0×10^{7} years. The peak dose rate is not reached within this simulation period. This dose rate maximum is well below the average natural background dose rate and the 3×10^{-4} Sv/a interim dose acceptance criterion established in Section 7.1 for the radiological protection of persons.

Figure 7-73 shows the individual contributions to the total dose rate from the most significant radionuclides. I-129 is the dominant dose rate contributor, followed to a much lesser extent by Pd-107 and Sm-147. This is because I-129 has a sizeable initial inventory, a non-zero instant release fraction, a very long half-life, is non-sorbing in the buffer, backfill and geosphere and

has a radiological impact on humans. The shape of the curve is defined by the release of radionuclides into the Guelph layer from both the shaft and the rock layers. The shaft releases are low and appear first. The rock layer releases are greater and appear later. When the two are summed together, this results in the shape of the curve shown in Figure 7-72.

Pd-107 and Sm-147 are not usually identified as dose contributors in used fuel repository assessments, but show here at very low levels as they are long-lived and, in the absence of data, have been assumed to have no sorption and no solubility limits. Other fission products and actinides either decay away, or are released very slowly as the fuel dissolves and are thereafter sorbed in the engineered barriers and geosphere.

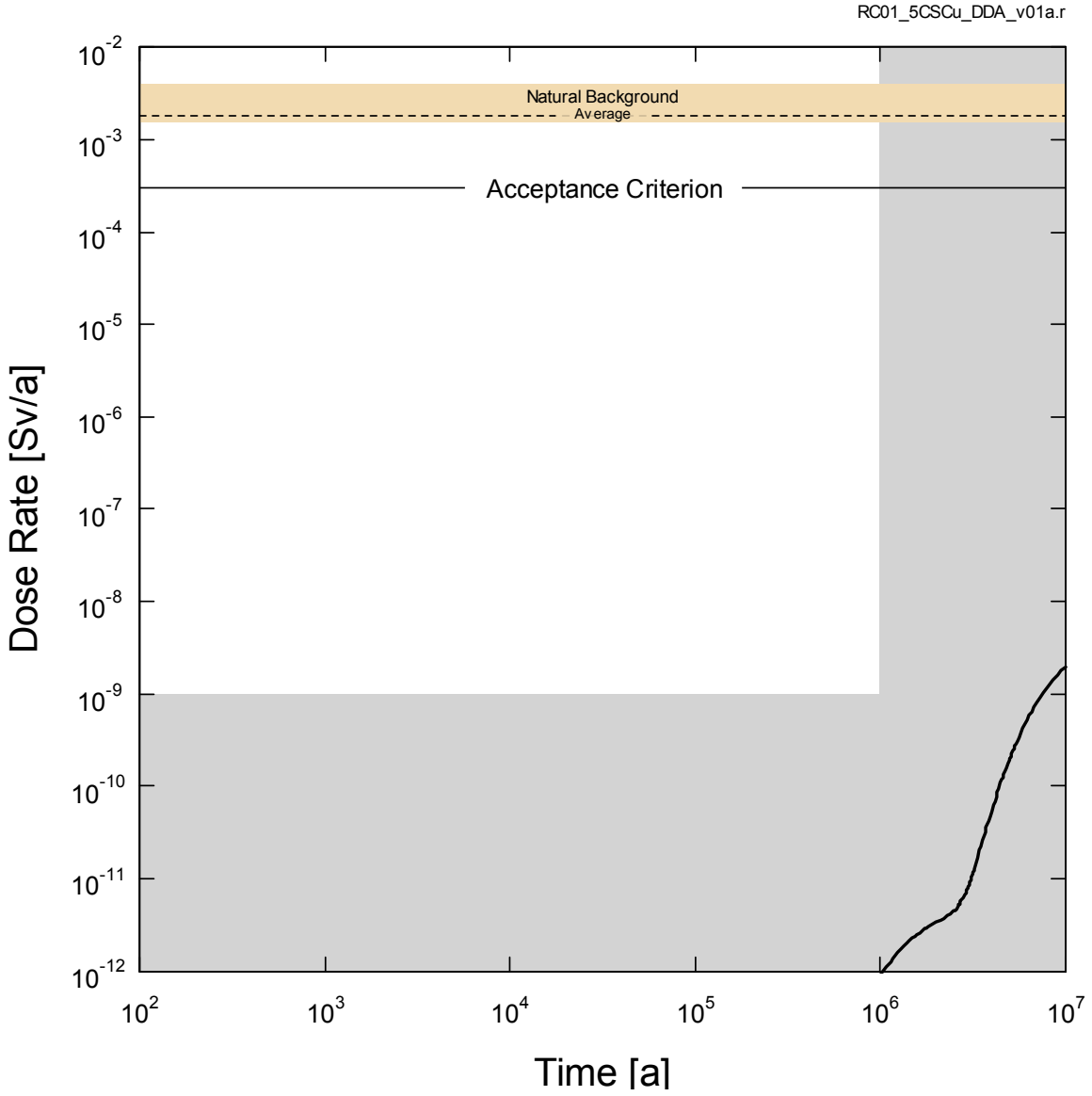

Figure 7-72: SYVAC3-CC4 - Reference Case Total Dose Rate

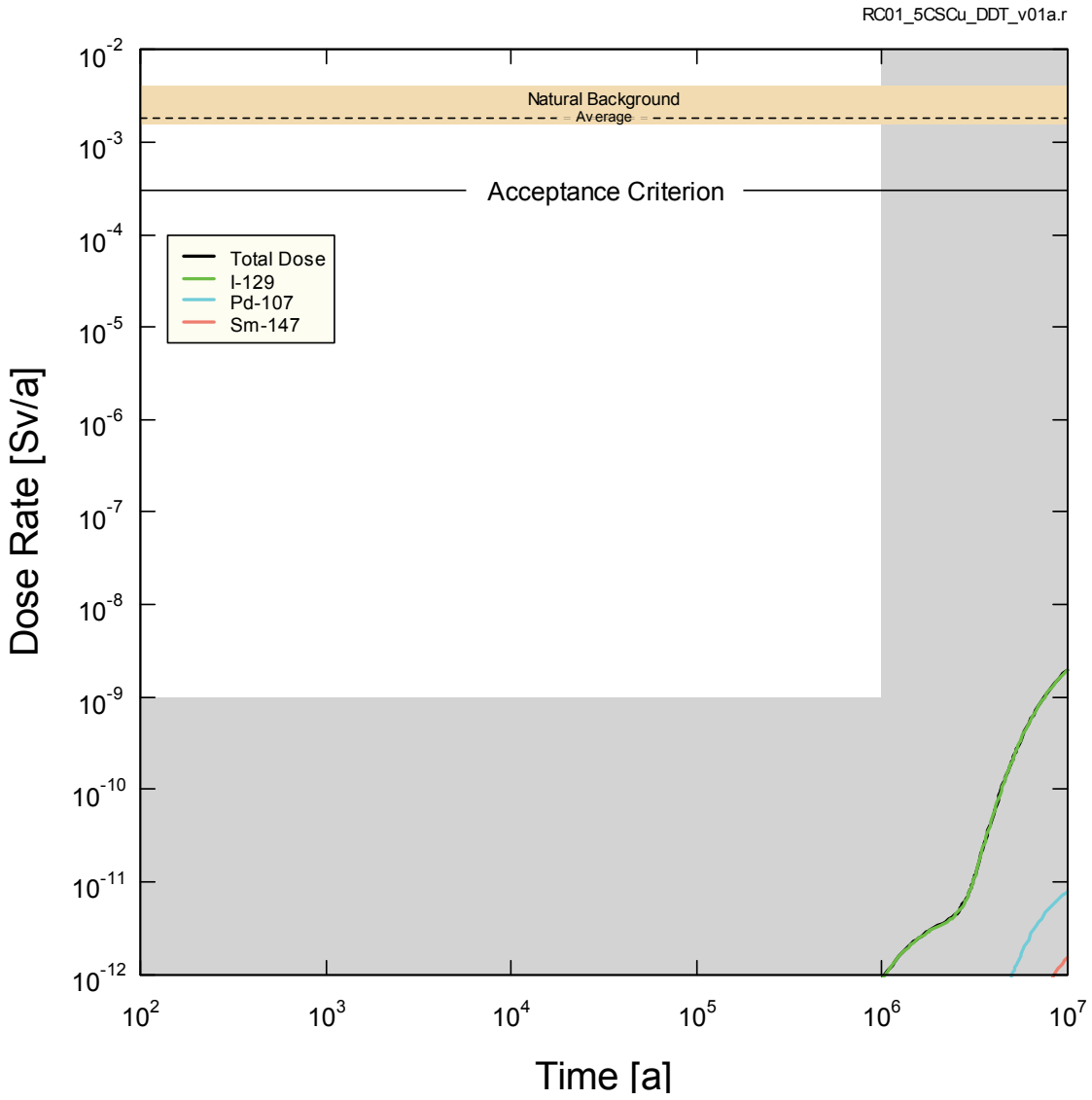

Figure 7-73: SYVAC3-CC4 - Reference Case Individual Radionuclide Dose Rates

Table 7-33 shows the dose pathways for each of the main dose contributors in Figure 7-73. These data are tabulated for times corresponding to the maximum individual radionuclide contributions.

Table 7-33: Radionuclide Dose Pathways for the Reference Case

Element	Internal Dose [Sv/a]	Primary Pathway(s)	%	External Dose [Sv/a]	Primary Pathway(s)	%
I-129	2.0×10^{-9}	Food Ingestion Water Ingestion	54 46	6.4×10^{-14}	Groundshine Water Immersion	86 13
Pd-107	7.9×10^{-12}	Food Ingestion Water Ingestion	90 8	0	None	0
Sm-147	1.6×10^{-12}	Food Ingestion Air Inhalation	57 34	0	None	0

7.8.2.2 Sensitivity to a Degraded Physical Barrier

The following sensitivity cases investigate the effect of a degraded physical barrier on the Reference Case results:

- Fuel dissolution rate increased by a factor of 10;
- Container defect area increased by a factor of 10;
- Instant release fractions set to 10% for all radionuclides; and
- Geosphere diffusivities increased by a factor of 10.

Figure 7-74 shows the individual contributions to the total dose rate from the most significant radionuclides for the sensitivity case with the fuel dissolution rate increased by a factor of 10. For this case, all fuel in the container dissolves within one million years whereas in the Reference Case only about 22% of the fuel dissolves in this time frame (see Figure 7-32).

As in the Reference Case, I-129, Pd-107 and Sm-147 are the most significant dose contributors. The maximum total dose rate occurs at 1.0×10^{7} years and reaches a value of 5.9×10^{-9} Sv/a or about 3 times that of the Reference Case. The maximum dose does not increase by a factor of 10 because the instant release fraction for I-129 also affects its dose rate and this parameter is independent of the fuel dissolution rate.

Actinide dose rates are zero because they are strongly sorbed in the buffer and geosphere and do not reach the biosphere during the simulation time.

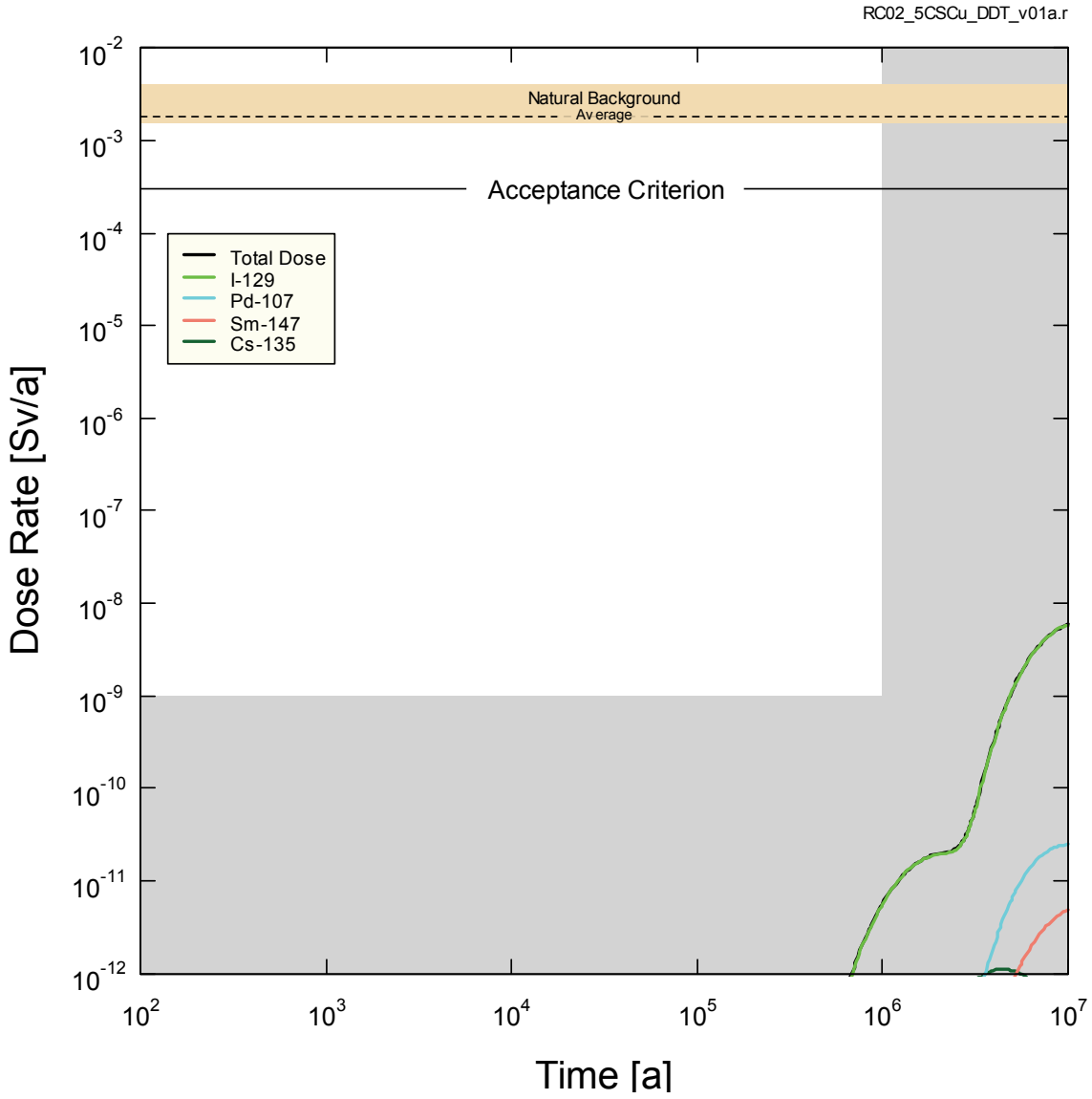

Figure 7-74: SYVAC3-CC4 - Sensitivity to a Factor of 10 Increase in Fuel Dissolution Rate

Figure 7-75 shows the individual contributions to the total dose rate from the most significant radionuclides for the sensitivity case with the defect area in the three defective containers increased by a factor of 10.

As in the Reference Case, I-129 is the main dose contributor. The maximum total dose rate occurs at 1.0×10^{7} years and reaches a value of 2.0×10^{-9} Sv/a or about the same as the Reference Case. The I-129 maximum dose rate is largely unaffected by the defect size because the release of I-129 is buffer-limited rather than defect size-limited.

The actinide dose rates are zero because they are strongly sorbed in the buffer and geosphere and do not reach the biosphere during the simulation time.

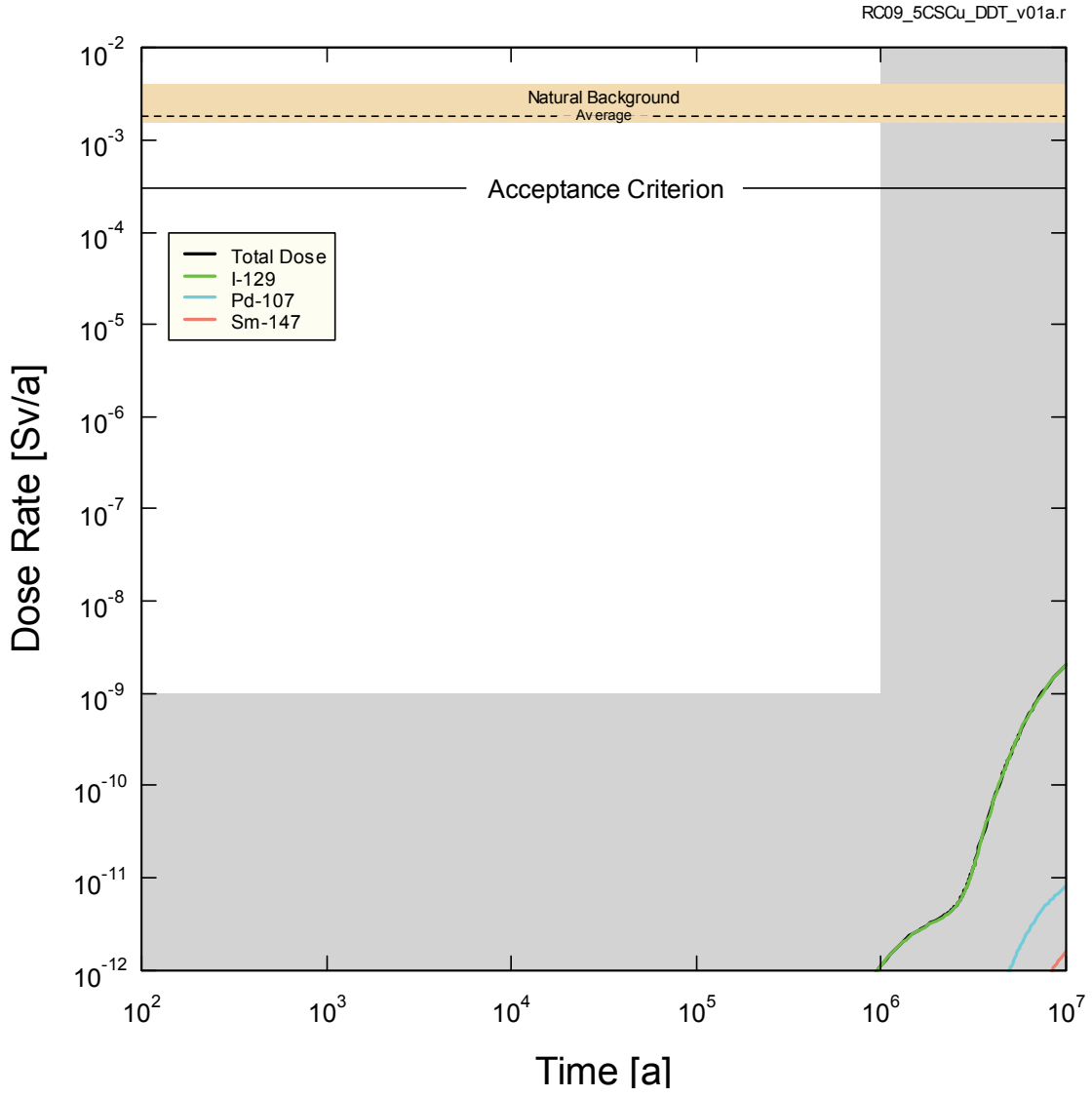

Figure 7-75: SYVAC3-CC4 - Sensitivity to a Factor of 10 Increase in Container Defect Area

Figure 7-76 shows the individual contributions to the total dose rate from the most significant radionuclides for the sensitivity case with the instant release fractions set to 10%.

As in the Reference Case, I-129 is the main dose contributor. The maximum total dose rate occurs at 1.0×10^{7} years and reaches a value of 2.2×10^{-9} Sv/a or about 1.1 times that of the Reference Case. The increase is smaller than the increase in instant release fraction because of spreading of the plume as it rises to the surface.

The actinide dose rates are zero because they are strongly sorbed in the buffer and geosphere and do not reach the biosphere during the simulation time.

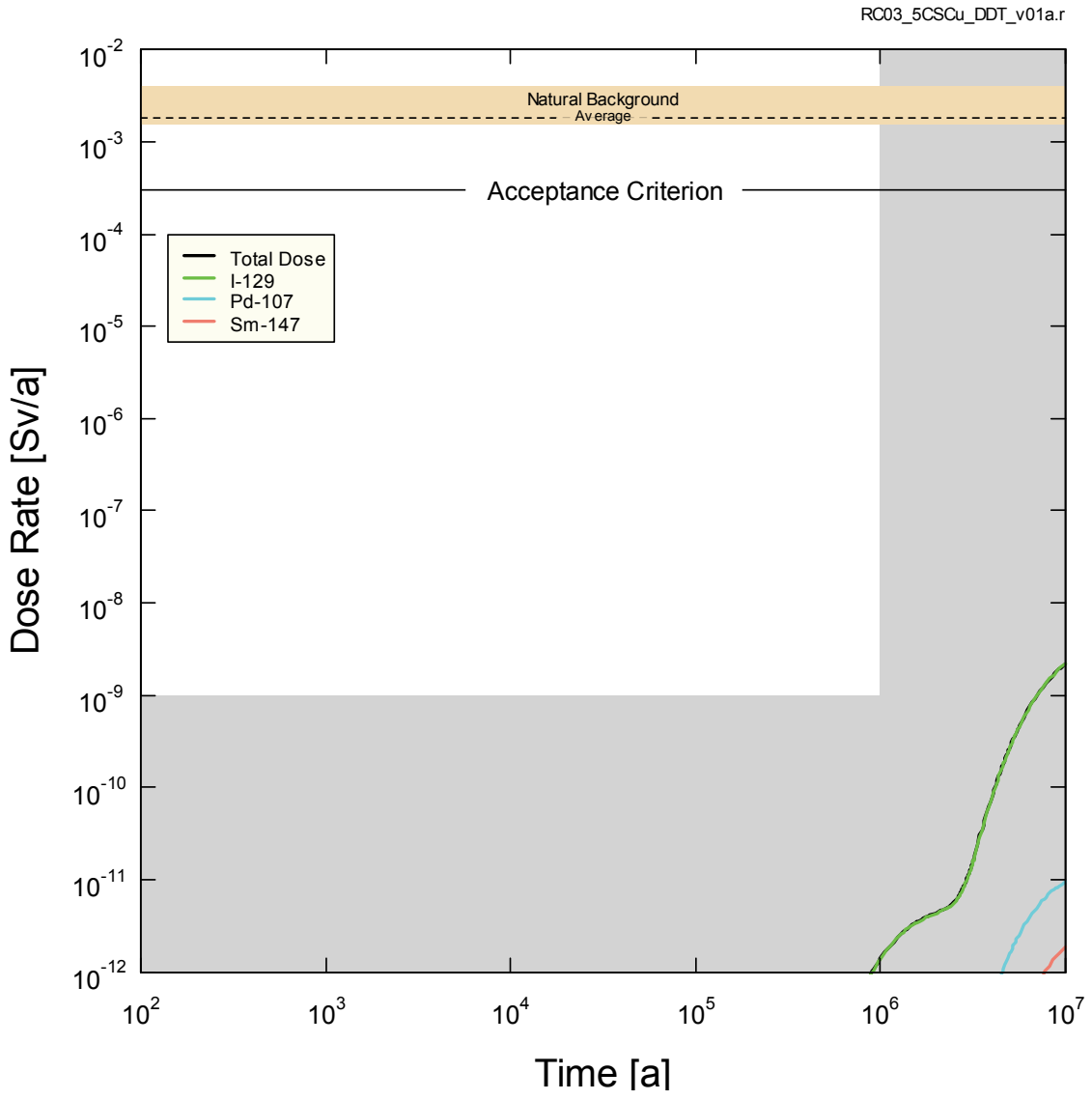

Figure 7-76: SYVAC3-CC4 - Sensitivity to All Instant Release Fractions Set to 10 Percent

Figure 7-77 shows the individual contributions to the total dose rate for the most significant radionuclides for the sensitivity case with geosphere diffusivity increased by a factor of 10.

As in the Reference Case, the highest dose contributor is I-129. Since the geosphere diffusivities are higher, I-129 reaches its peak dose rate within the 10 million year simulation time frame. The peak total dose rate occurs at 5.6×10^{6} years and reaches a value of 2.6×10^{-8} Sv/a. This is about 13-fold higher than for the Reference Case; however, as in the Reference Case, the peak total dose rate is still well below the average natural background dose rate and the 3×10^{-4} Sv/a interim dose acceptance criterion established in Section 7.1 for the radiological protection of persons.

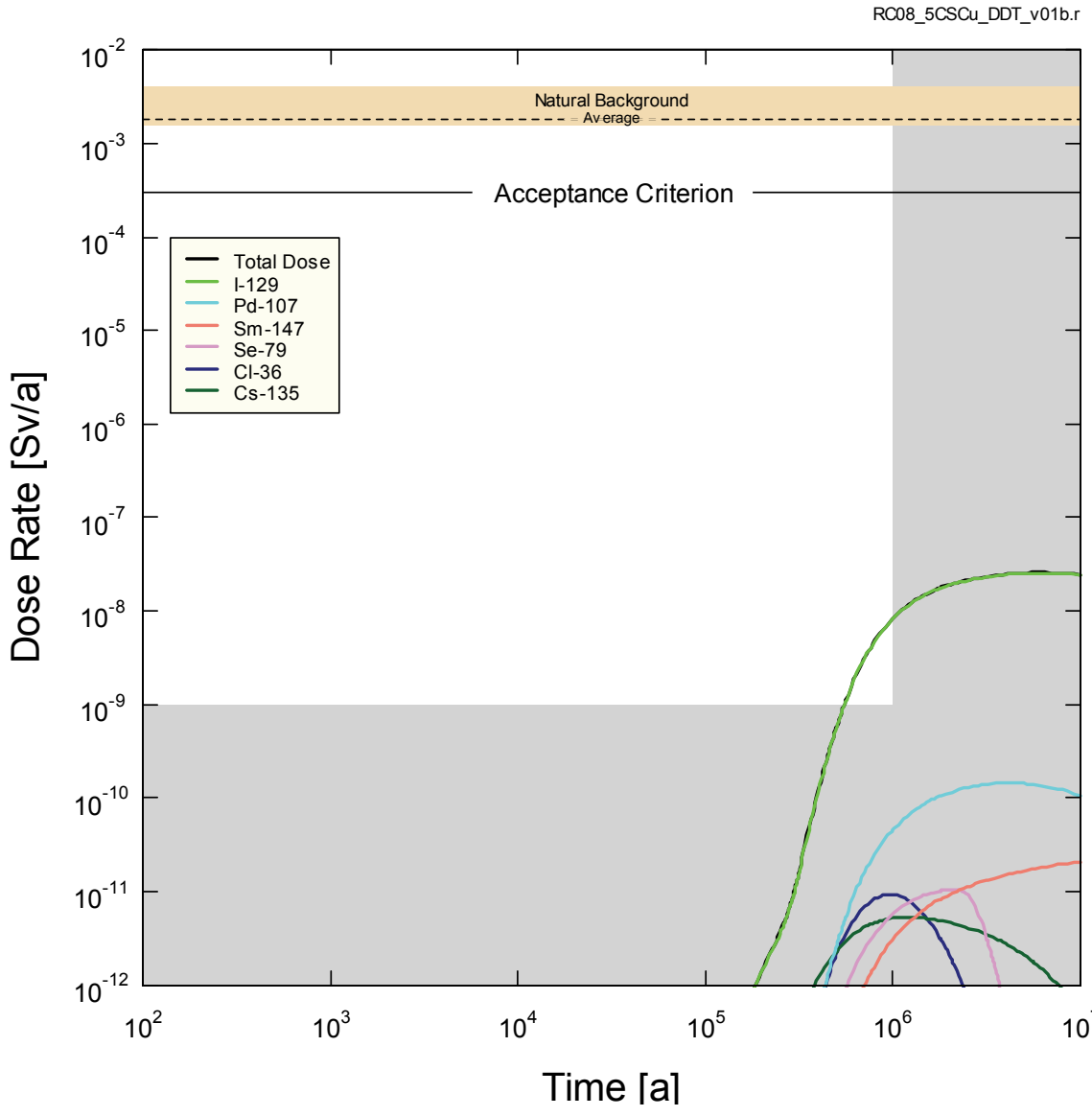

Figure 7-77: SYVAC3-CC4 - Sensitivity to a Factor of 10 Increase in Geosphere Diffusivity

Figure 7-78 summarizes the total dose rates for the Reference Case and all four degraded physical barrier cases. Table 7-34 provides results in numerical form. All results are many orders of magnitude below the interim dose acceptance criterion. The peak dose rate is not reached in the one million year period of interest except for the high geosphere diffusivity sensitivity case.

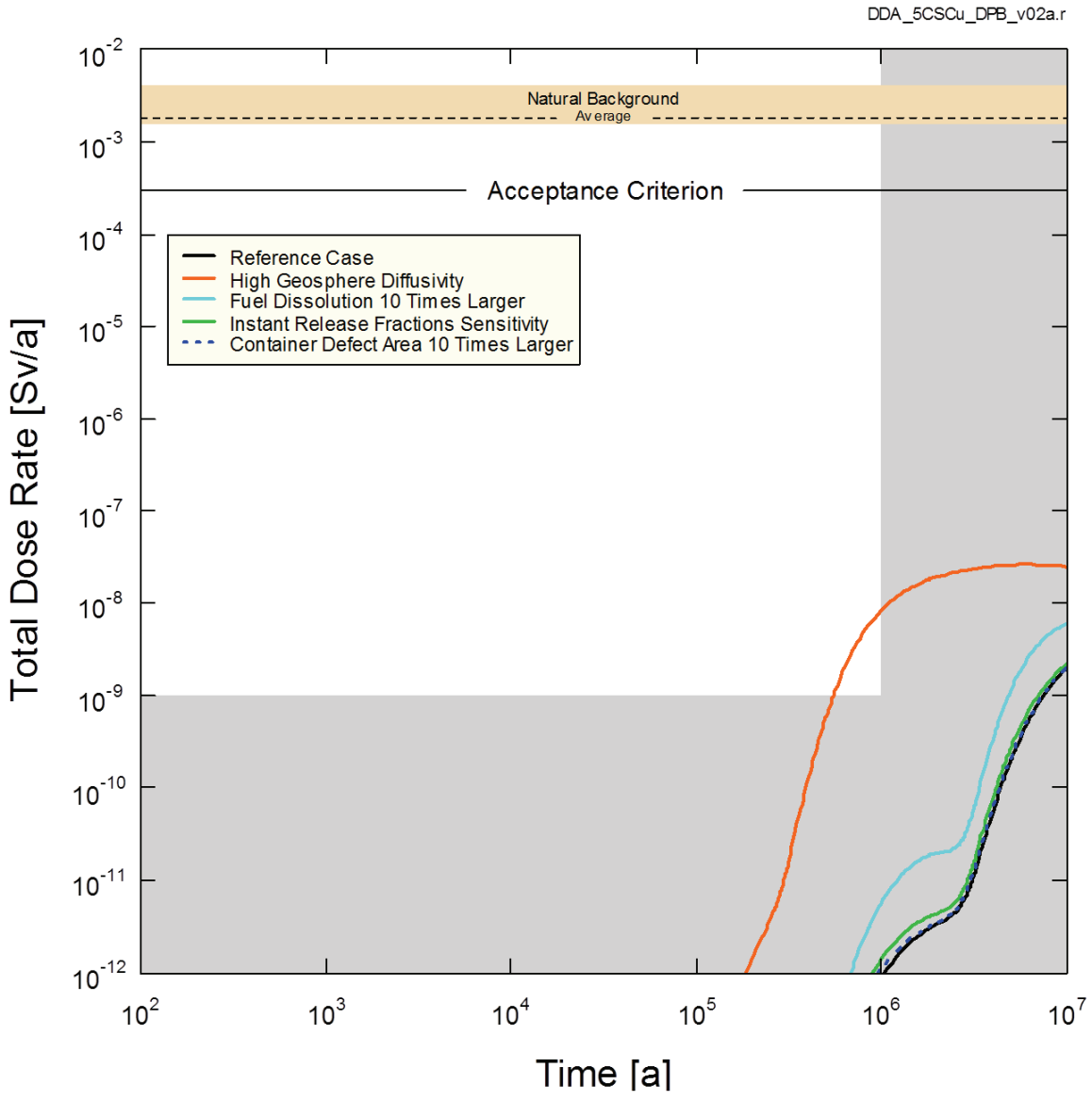

Figure 7-78: SYVAC3-CC4 - Result Summary for Defective Physical Barrier Sensitivity Cases

Table 7-34: Result Summary for Defective Physical Barrier Sensitivity Cases

Case	Maximum Dose Rate (Sv/a)	Ratio to Reference Case	Time of Maximum Dose Rate* (a)
Reference Case	***2.0×10^{-9}***	**-**	***1.0×10^{7}***
Fuel Dissolution Rate 10 times Higher	5.9×10^{-9}	3.0	1.0×10^{7}
Container Defect Area 10 times Higher	2.0×10^{-9}	1.0	1.0×10^{7}
Instant Release Fraction Sensitivity	2.2×10^{-9}	1.1	1.0×10^{7}
Geosphere Diffusivity Increased by a Factor of 10	2.6×10^{-8}	13	5.6×10^{6}

Note: * The peak dose rate will be greater than the maximum dose rate if the maximum is not obtained within the 10 million year simulation time.

7.8.2.3 Sensitivity to a Degraded Chemical Barrier

The following sensitivity cases investigate the effect of a degraded chemical barrier on the Reference Case results:

- No sorption in the geosphere;
- No solubility limits in the container;
- No sorption in the EBS; and
- Low sorption in the geosphere with coincident high solubility limits in the container.

Figure 7-79 shows the individual contributions to the total dose rate from the most significant radionuclides (i.e., those accounting for 99% of the total dose) for the sensitivity case with no sorption in the geosphere.

The maximum total dose rate occurs at 1×10^{7} years and reaches a value of 3.3×10^{-9} Sv/a or 1.7 times higher than the Reference Case.

The dominant dose contributors are Cs-135 and I-129; however, at longer times there are also contributions from U-238 and U-235 progeny. Since there is no sorption in the geosphere, the long-lived U-238 and U-235 are able to reach the surface biosphere, where they decay to form their progeny.

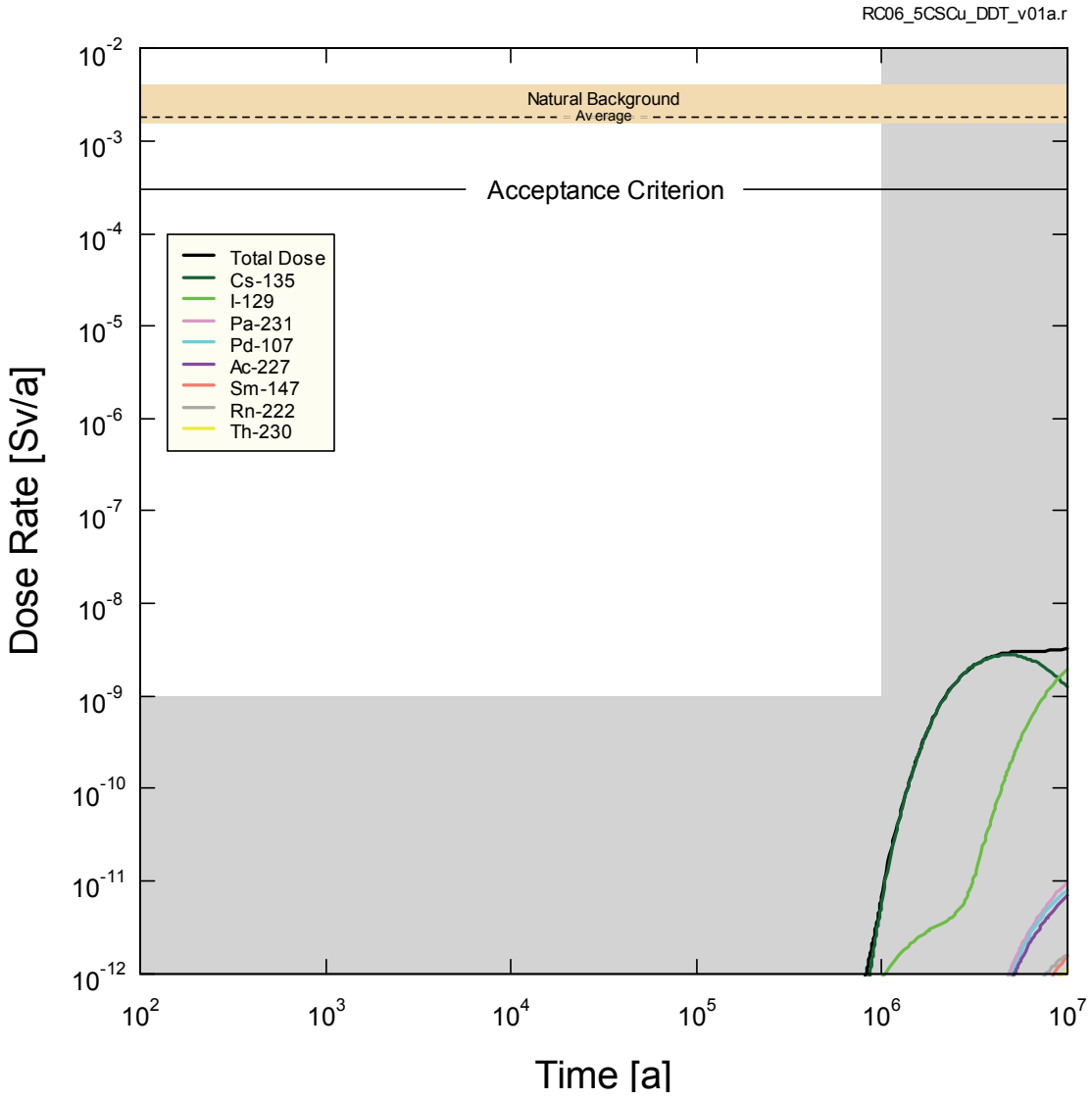

Figure 7-79: SYVAC3-CC4 - Sensitivity to No Sorption in the Geosphere

Figure 7-80 shows the individual contributions to the total dose rate for the most significant radionuclides for the sensitivity case with no radionuclide solubility limits.

As in the Reference Case, I-129 is the main dose contributor. The maximum total dose rate occurs at the same time as in the Reference Case and reaches the same value of 2.0×10^{-9} Sv/a. There is low sensitivity to solubility because I-129 is not solubility limited and because the actinides (which are solubility limited) continue to be strongly sorbed in the geosphere and do not reach the biosphere in the time period of interest.

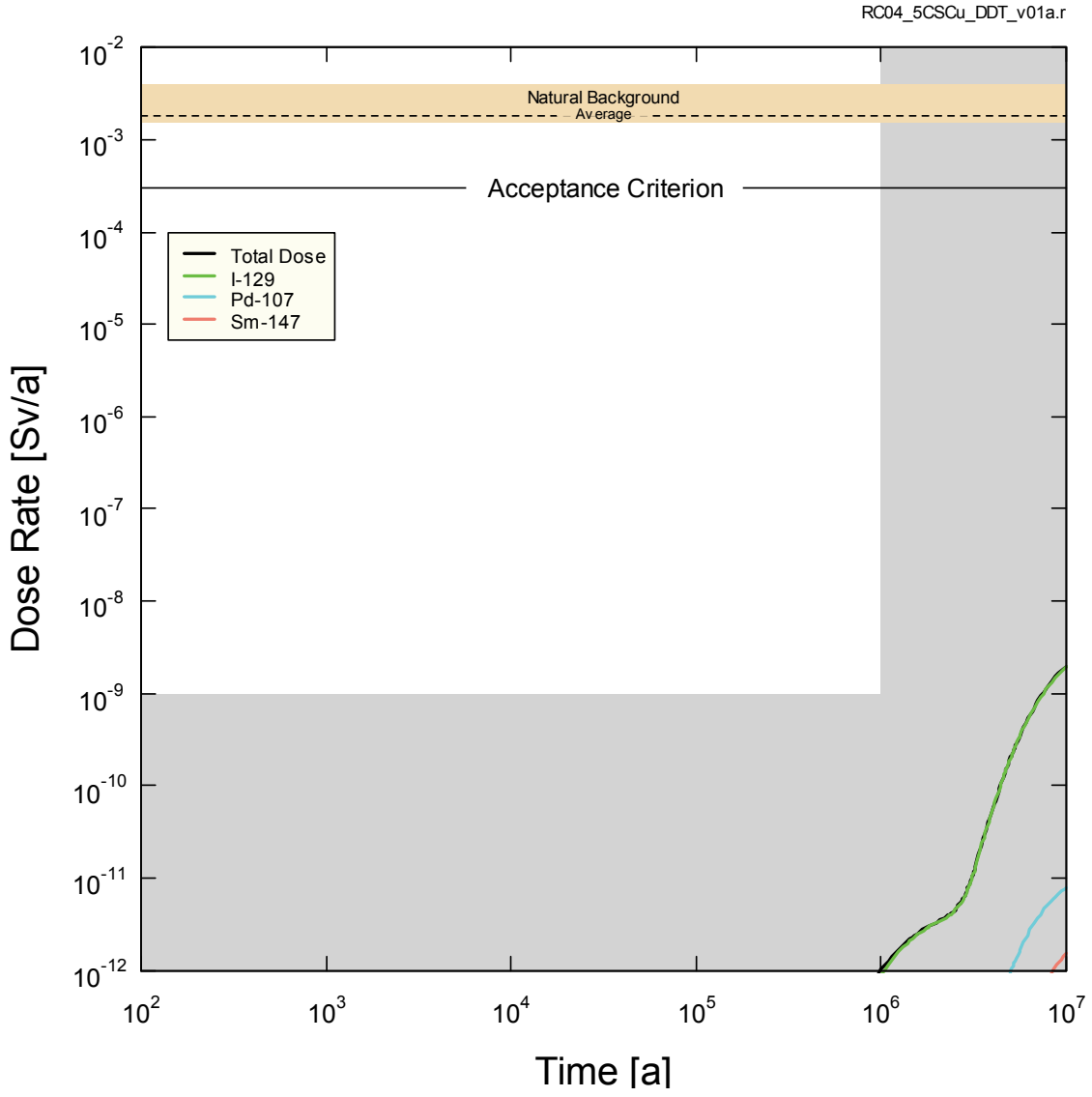

Figure 7-80: SYVAC3-CC4 - Sensitivity to No Solubility Limits

Figure 7-81 shows the individual contributions to the total dose rate for the most significant radionuclides for the sensitivity case with no sorption in the EBS.

The maximum total dose rate occurs at 1.0×10^{7} years and reaches a value of 6.7×10^{-9} Sv/a or about 3.4 times higher than the Reference Case. Unlike the Reference Case, the main dose contributor is Ac-227 followed by I-129 and several other actinides. Since there is no sorption in the near field (where they are normally sorbed), the long-lived U-238 and U-235 are able to migrate via the shafts to the surface biosphere, where they decay to form their progeny radionuclides.

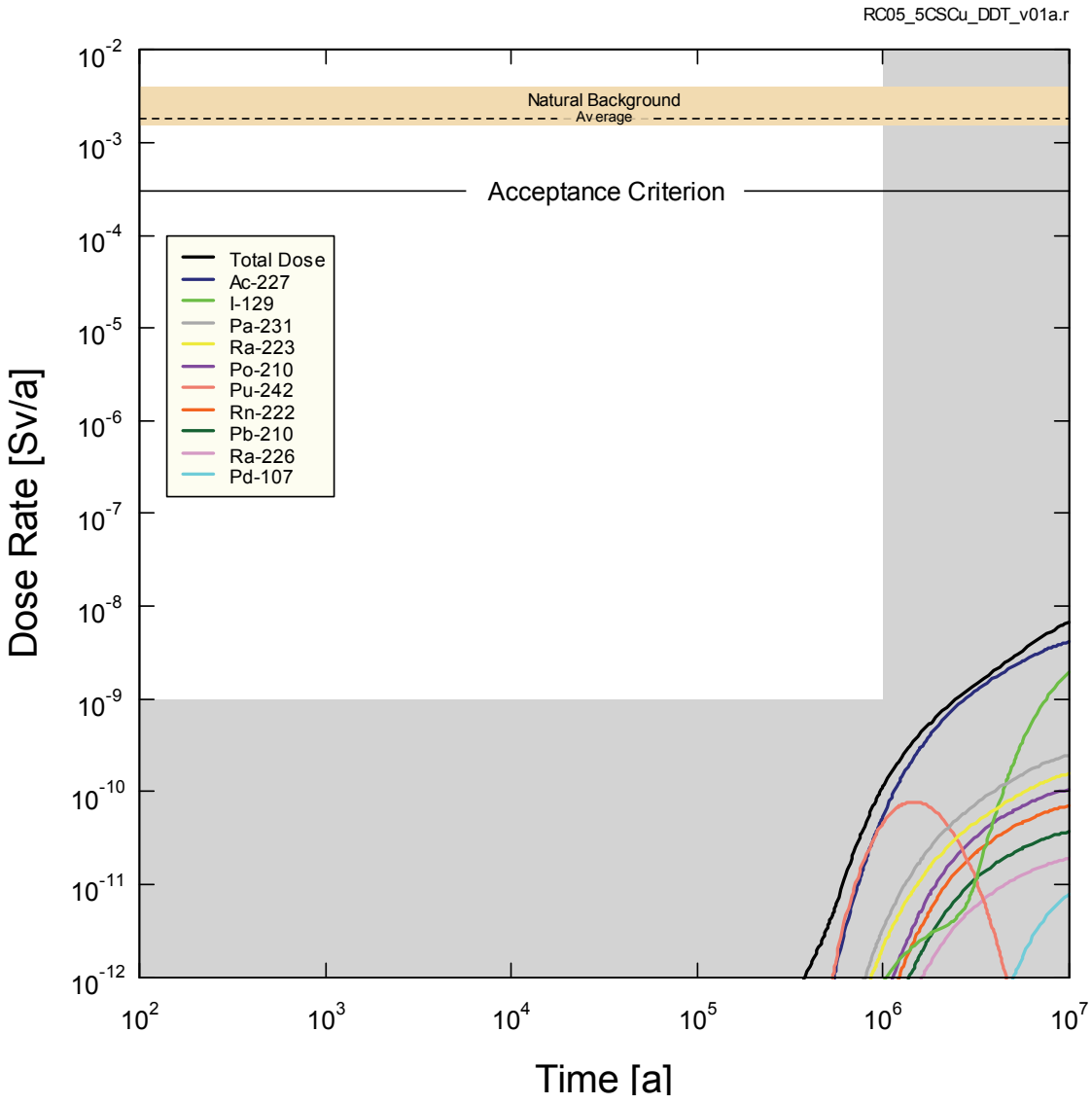

Figure 7-81: SYVAC3-CC4 - Sensitivity to No Sorption in the EBS

Figure 7-82 shows the individual contributions to the total dose rate for the most significant radionuclides for the sensitivity case with low sorption in the geosphere and coincident high radionuclide solubility limits (where "low" and "high" mean 1st percentile and 99th percentile, respectively, of their sampling ranges).

As in the Reference Case, the highest dose contributor is I-129. The maximum total dose rate occurs at the same time as in the Reference case ($1x10^7$ years) and reaches a value of 2.0×10^{-9} Sv/a or the same as in the Reference Case. Actinides (which are solubility limited) continue to be sorbed in the buffer and geosphere.

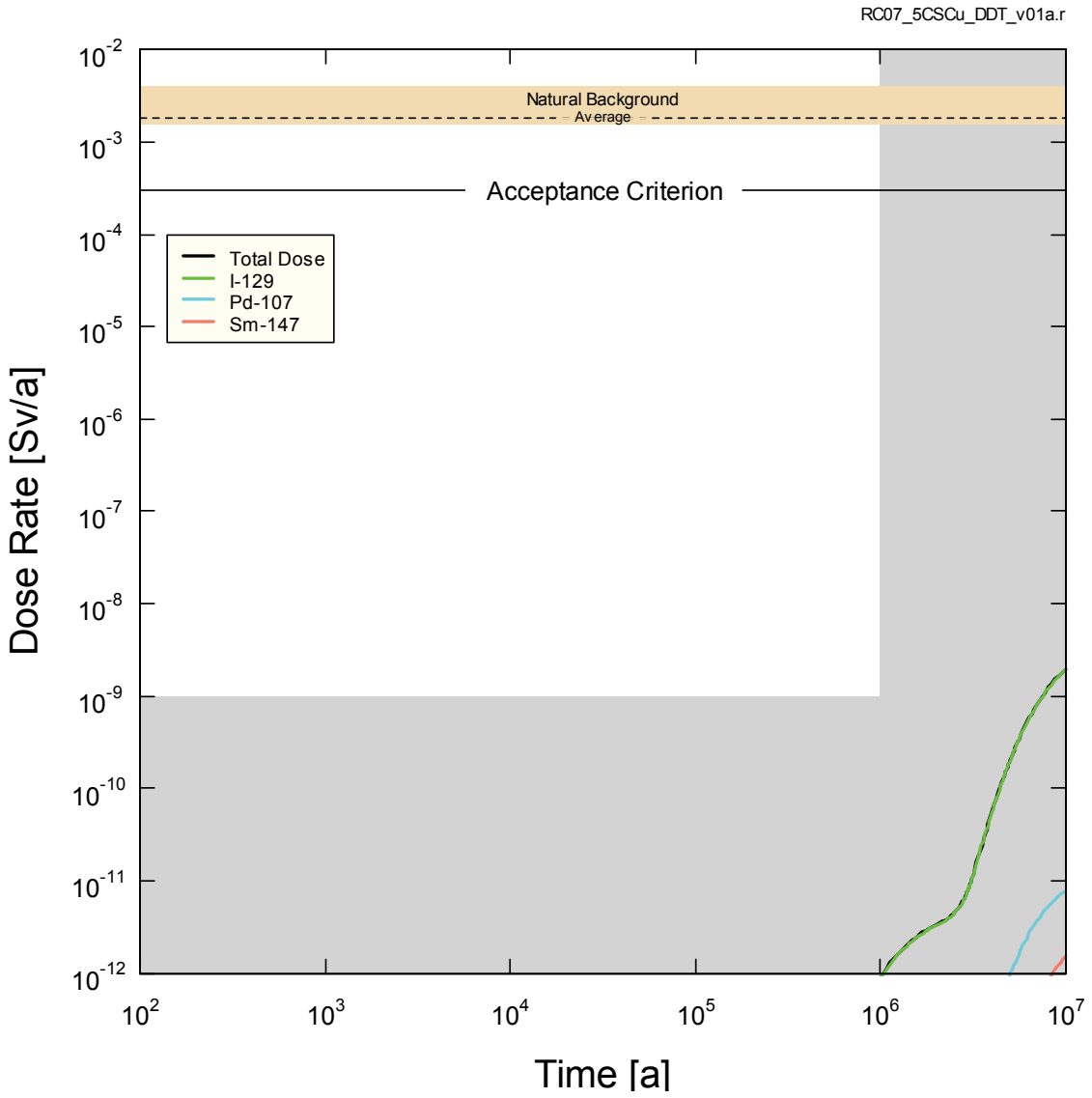

Figure 7-82: SYVAC3-CC4 - Sensitivity to Low Sorption in the Geosphere with Coincident High Solubility Limits

Figure 7-83 shows the total dose rates for the Reference Case and all four degraded chemical barrier cases. Table 7-35 provides the results in numerical form. All results are orders of magnitude below the interim dose acceptance criterion. The peak dose rate is not reached in the one million year period of interest.

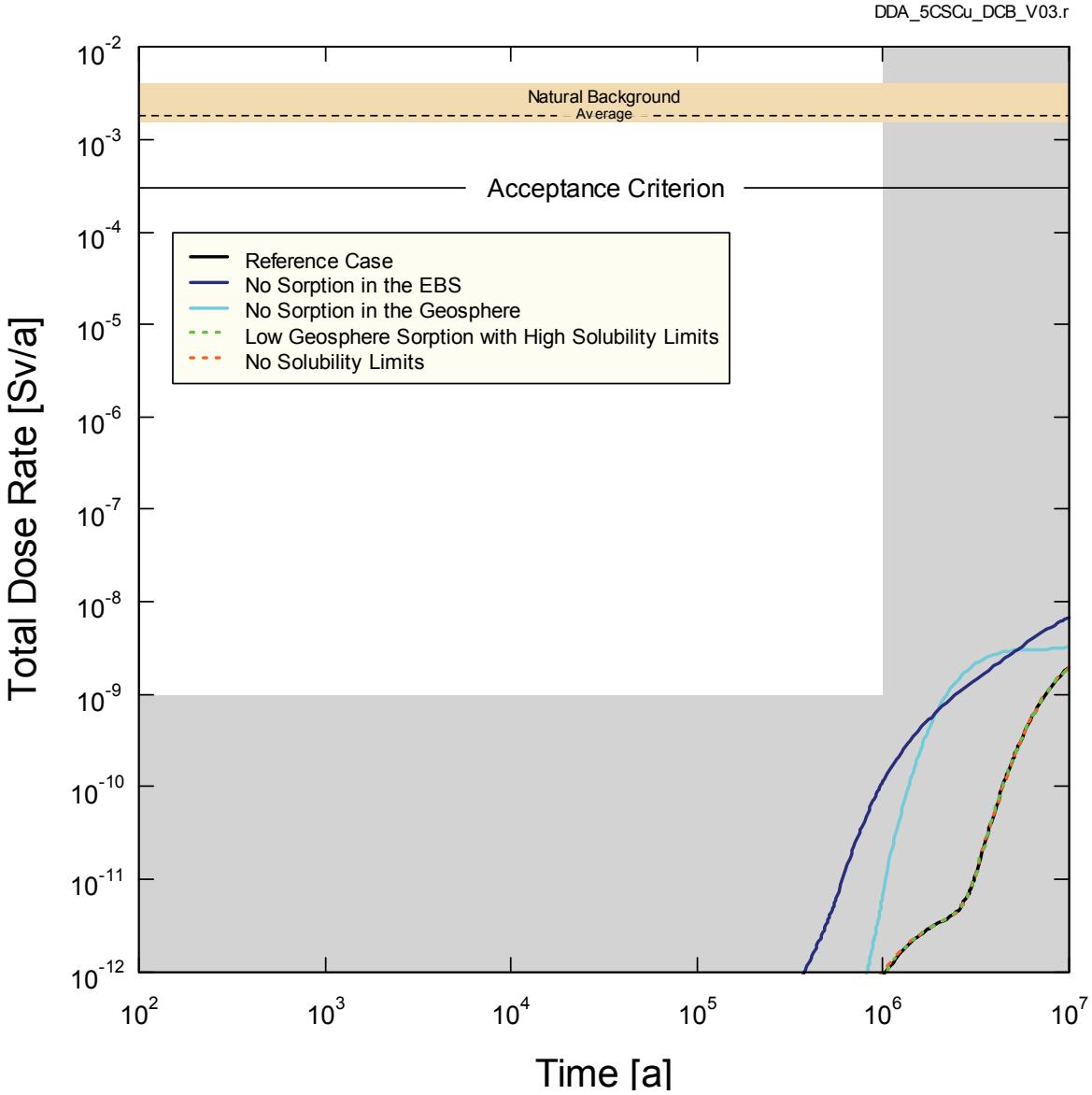

Figure 7-83: SYVAC3-CC4 - Summary for Defective Chemical Barrier Sensitivity Cases

Table 7-35: Result Summary for Defective Chemical Barrier Sensitivity Cases

Case	Maximum Dose Rate (Sv/a)	Ratio to Reference Case	Time of Maximum Dose Rate* (a)
Reference Case	$\boldsymbol{2.0x10^{-9}}$	**-**	$\boldsymbol{1.0x10^{7}}$
No Sorption in the Geosphere	$3.3x10^{-9}$	1.7	$1.0x10^{7}$
No Solubility Limits	$2.0x10^{-9}$	1.0	$1.0x10^{7}$
No Sorption in EBS	$6.7x10^{-9}$	3.4	$1.0x10^{7}$
Low Sorption in the Geosphere With Coincident High Radionuclide Solubility Limits	$2.0x10^{-9}$	1.0	$1.0x10^{7}$

Note: * The peak dose rate will be greater than the maximum dose rate if the maximum is not obtained within the 10 million year simulation time.

7.8.3 Probabilistic Analysis

In the previous sections, deterministic analyses are performed for a Reference Case and a series of sensitivity studies that examine the effect of degraded physical and chemical barriers.

Many of the modelling parameters are uncertain or have a natural degree of variability, and are therefore more generally characterized by a range or distribution of values. Simultaneous accounting of these uncertainties is achieved by using the SYVAC3-CC4 system model in probabilistic mode.

Probabilistic mode uses a Monte Carlo random sampling strategy that considers the full range of possible parameter values. The results presented here draw from 120,000 simulations in which parameter values are sampled randomly from their probability density functions. Each of these thousands of simulations produces a unique estimate of impact that is used to collectively generate a distribution that reflects the underlying uncertainty. An important caveat is that parameter values that could affect groundwater flow are not varied in these simulations. Groundwater flow effects are very limited in this geosphere because transport is diffusion dominant.

Geosphere diffusivities are varied according to a loguniform distribution with upper and lower bounds set to 10 and 0.1 times the median value.

A selection of biosphere parameters represented by probability distributions is provided in Table 7-24 through Table 7-26. A detailed description of the probability distributions for all parameters is provided in Gobien et al. (2013).

Number of Defective Containers

The number of defective containers is described by a binomial distribution that is characterized by the number of containers in the repository and the probability of a container with an initial penetrating defect escaping detection. Uncertainty in the container failure probability is

accounted for by expressing the failure probability per container as a lognormal probability density function with a geometric mean of 2×10^{-4}, a geometric standard deviation of 2, and bounds of 10^{-4} and 10^{-3}. The best-estimate failure probability is 2×10^{-4} per container. The locations of defective containers are randomly assigned within the repository in each simulation.

Figure 7-84 shows the as-sampled distribution of container failures.

From Monte Carlo sampling of the probability distribution, the most probable number of defective containers, or *mode* of the distribution, is 2 (i.e., the peak in the profile), while the average or *mean* value is 2.6. The maximum number in any one simulation is 12, and in 60% of the simulations there is at least one defective container in Sector 5. Defective containers in Sector 5 produce the highest dose rates to the critical group.

There are 9259 simulations (about 8% of the total) with zero defective containers.

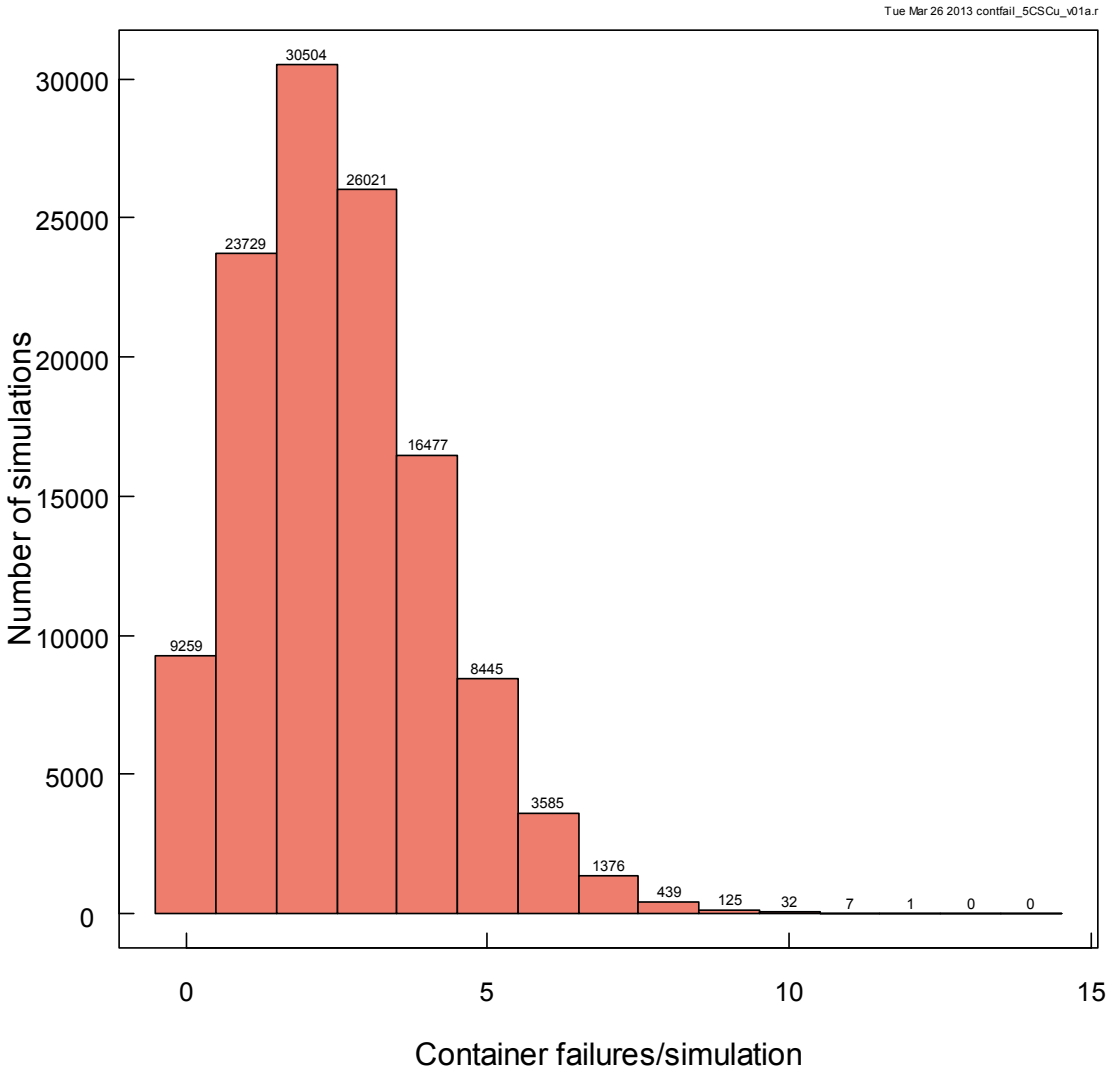

Figure 7-84: SYVAC3-CC4 - Distribution of Container Failures for 120,000 Simulations

Dose Rates

Figure 7-85 shows the distribution of the maximum total dose rate over a 10 million year simulation period to a member of the critical group for simulations with at least one defective container. The maximum total dose rate is the maximum, at any time during a simulation, of the sum of the individual dose rates for all radionuclides. The average dose rate, representing the arithmetic average of the maximum total dose rates over all simulations, is also shown.

The median maximum total dose rate is 1.5×10^{-9} Sv/a while the average maximum dose rate is 1.6×10^{-8} Sv/a. The average dose rate is greater than the median dose rate because of the asymmetrical shape of the distribution. These values can be compared against the maximum dose rate for the Reference Case of 2.0×10^{-9} Sv/a.

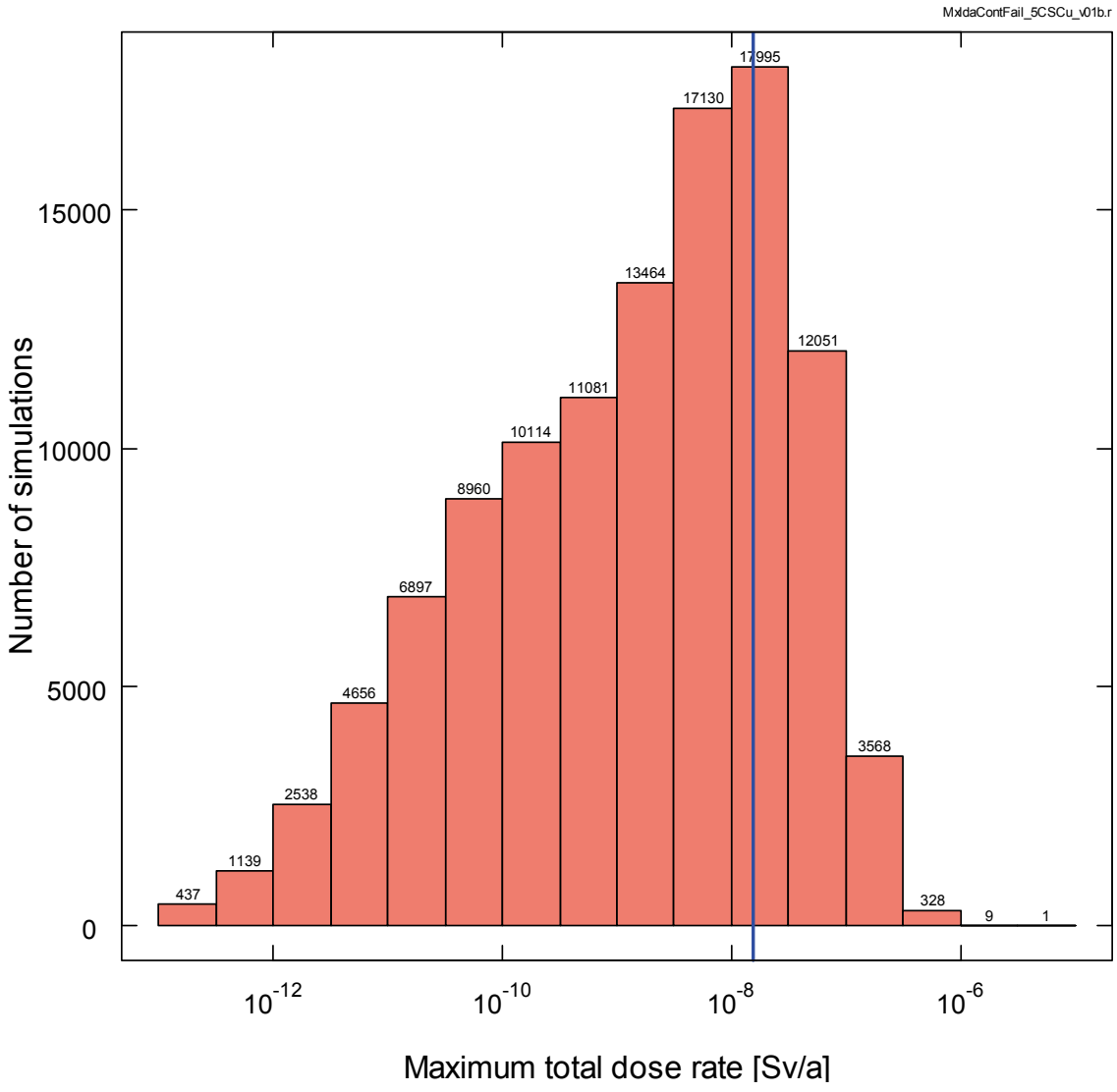

Note: the blue line represents the average value of 1.6×10^{-8} Sv/a

Figure 7-85: SYVAC3-CC4 - Distribution of the Maximum Dose Rate for Simulations with at Least One Defective Container

Statistical information concerning the distribution is summarized in Table 7-36. This table shows that the 95% confidence bound is symmetric around the average value. The median value and the average value differ by approximately a factor of 10, indicating that the average maximum dose is influenced by a number of higher-consequence simulations (i.e., the distribution of results is somewhat skewed). The simulations causing the results to be skewed have been reviewed and are discussed later in this section; however, none were found to result in dose rates very close to the interim dose acceptance criterion of 3.0×10^{-4} Sv/a.

Table 7-36: Statistical Information Concerning the Distribution of the Peak Dose Rate

Statistic	Value	Bootstrap 95% Confidence Bounds[1]	
		Lower Bound	Upper Bound
Average (Sv/a)	$1.55\text{x}10^{-8}$	$1.52\text{x}10^{-8}$	$1.57\text{x}10^{-8}$
95th Percentile (Sv/a)	$7.46\text{x}10^{-8}$	$7.35\text{x}10^{-8}$	$7.57\text{x}10^{-8}$
99th Percentile (Sv/a)	$1.82\text{x}10^{-7}$	$1.78\text{x}10^{-7}$	$1.88\text{x}10^{-7}$
Probability the peak dose rate exceeds $3.0\text{x}10^{-4}$ Sv/a [2]	0%	0%	0%
Median (Sv/a)	$1.52\text{x}10^{-9}$	$1.47\text{x}10^{-9}$	$1.57\text{x}10^{-9}$

Notes:

[1] Based on 10,000 replicates of the dataset obtained using the bootstrap methodology. The confidence intervals are calculated using the bootstrap method (with replacement). Since the distribution of peak dose rates is skewed, the bootstrap BC_a methodology described by DiCiccio and Efron (1996) is used.

[2] Interim dose acceptance criterion.

The average and median maximum dose rates for the individual radionuclides for all simulations are shown in Table 7-37. As in the Reference Case, I-129 is the dominant dose contributor.

Table 7-37: Average and Median Maximum Dose Rates for Individual Radionuclides

Radionuclide*	Average (Sv/a)	Median (Sv/a)
I-129	$1.50\text{x}10^{-8}$	$1.00\text{x}10^{-9}$
Pd-107	$4.49\text{x}10^{-10}$	$4.10\text{x}10^{-12}$
Sm-147	$8.68\text{x}10^{-11}$	$1.10\text{x}10^{-12}$
Cl-36	$4.10\text{x}10^{-11}$	-
Cs-135	$2.19\text{x}10^{-11}$	-
Se-79	$1.08\text{x}10^{-11}$	-
Tc-99	$6.93\text{x}10^{-13}$	-

Note: * A cutoff of 10^{-14} Sv/a is used.

Figure 7-86 shows the average dose rate as a function of time together with its 95% confidence intervals. The intervals are calculated using Chebychev's inequality (Guttman and Wilks 1965). Note that the Chebychev inequality gives upper bounds for the confidence intervals. The narrowness of the 95% confidence band indicates high statistical confidence.

The peak average dose occurs at 5.6×10^6 years.

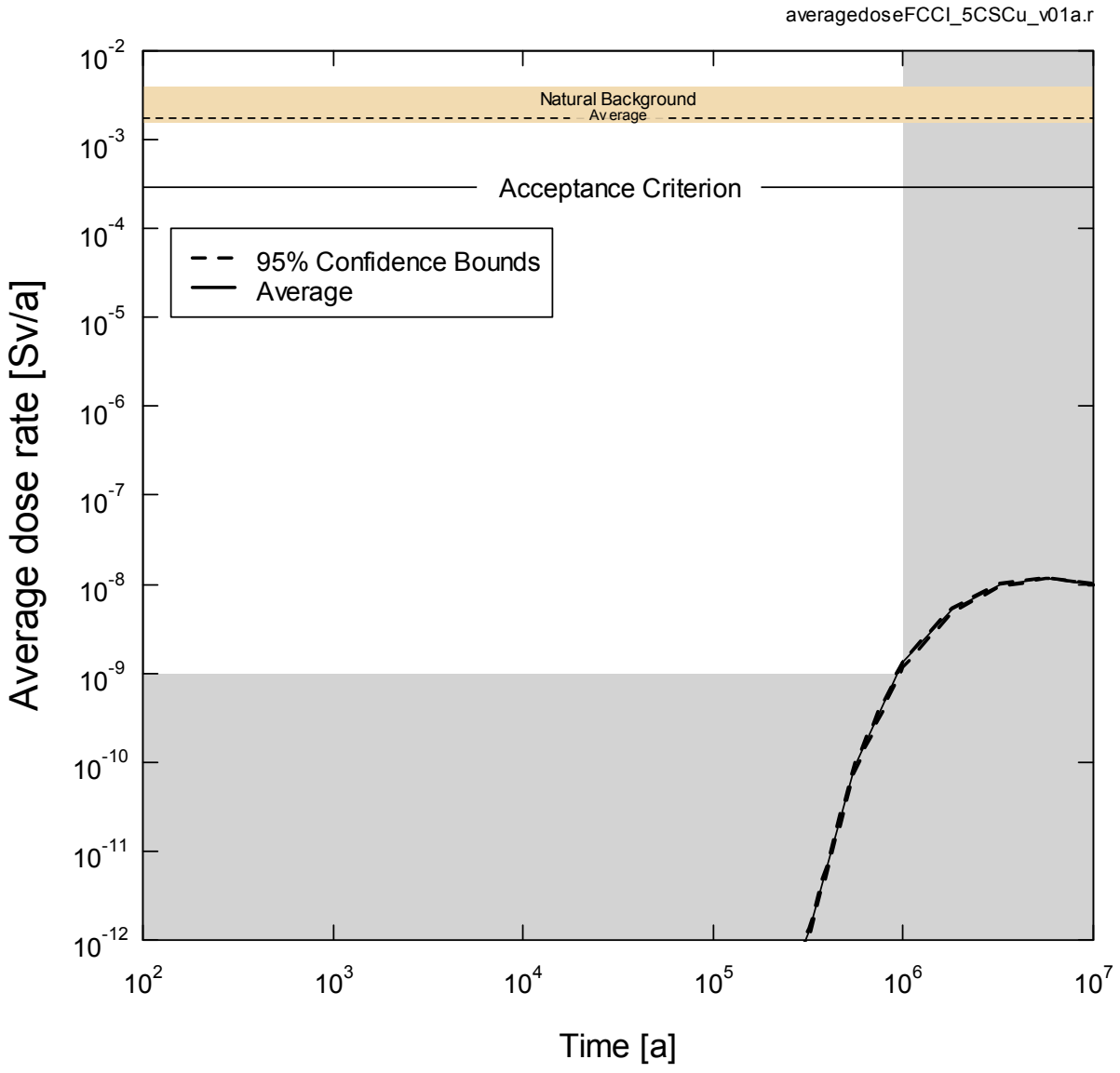

Figure 7-86: SYVAC3-CC4 - Average Dose Rate With 95% Confidence Bounds

Figure 7-87 shows the distribution of dose rates from all 120,000 simulations illustrating the 25, 50, 67, 90 and 99th percentile bands. These curves are all well below the interim dose

acceptance criterion of 3.0×10^{-4} Sv/a established in Section 7.1.1 for the radiological protection of persons.

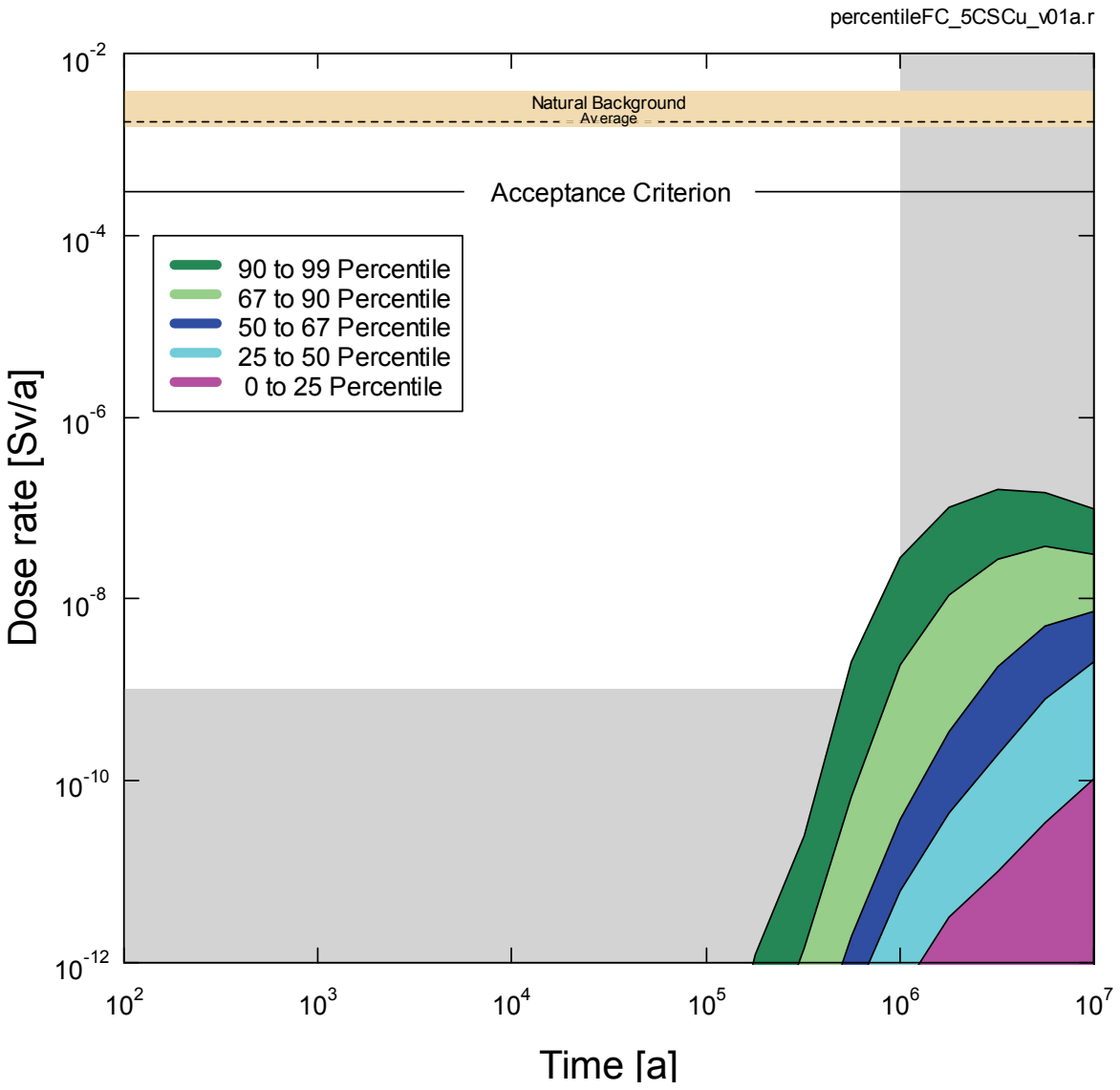

Figure 7-87: SYVAC3-CC4 - Dose Rate Percentile Bands

Maximum Value Simulations

Regulatory document G-320 (CNSC 2006) specifies that if the range of assessment results from probabilistic simulations indicates that acceptance criteria are exceeded, then it should be demonstrated that those results do not represent unreasonable risk to the environment or to the health and safety of persons, taking into account the conservatism built into the assessment and the likelihood of the circumstances leading to the results.

As per this guidance, all simulations were reviewed to identify runs that result in dose rates either very close to or above the interim dose acceptance criterion of 3.0×10^{-4} Sv/a. No such cases were identified.

7.9 Disruptive Scenarios

Disruptive Scenarios postulate the occurrence of unlikely events leading to possible penetration of barriers and abnormal loss of containment. Chapter 6 describes how the Disruptive Scenarios are identified and concludes that the following are relevant to the hypothetical site and conceptual repository design:

- Inadvertent Human Intrusion;
- Shaft Seal Failure;
- Abandoned Repository;
- Poorly Sealed Borehole;
- Undetected Fault;
- Severe Erosion;
- All Containers Fail; and
- Container Failure.

As noted in Section 7.2, a limited scope of work has been adopted in this study to reflect the level of effort required to meet the study objectives. The Abandoned Repository Scenario, the Poorly Sealed Borehole Scenario, the Undetected Fault Scenario, the Severe Erosion Scenario, the Container Failure Scenario and the variant case of the Human Intrusion Scenario in which the intrusion borehole is assumed to remain open are not within the scope of work.

Analysis results and dose consequences for the remaining Scenarios are discussed below.

7.9.1 Inadvertent Human Intrusion

The Inadvertent Human Intrusion Scenario considers the same evolution of the repository system as for the Normal Evolution Scenario with the only difference being the occurrence of human intrusion some time after institutional control of the site is no longer effective. In this scenario, an exploratory borehole is drilled through the geosphere and into the repository. The drill bit is assumed to intersect a used fuel container.

In an exploratory borehole, the investigators will most likely collect samples or conduct measurements at the repository level, which will readily identify any significant residual radioactivity (e.g., gamma logging is a standard borehole measurement). The investigators would then likely initiate appropriate precautions to prevent further exposure, including ensuring that any surface-released materials were appropriately disposed and that the borehole was sealed. Under normal drilling circumstances, there would be little impact.

Nevertheless, the Inadvertent Human Intrusion Scenario assumes:

- Interception of the repository is not recognized and therefore no safety restrictions are imposed; and
- The drill site is not managed according to current standards, and material from the borehole is released onto the surface.

As per Section 7.2.2, the scope of this study does not include the variant case in which the borehole is poorly sealed thereby resulting in a long-term pathway for contaminants to escape the repository. Such a case has been considered in SKB (2010a), and this work shows the consequences are orders of magnitude less than the SKB acute exposure dose rate for the human intrusion scenario. Although not calculated here, a similar conclusion is expected because there is little driving force to transport contaminated material up the (narrow) borehole, and any such release would be further diluted in the groundwater flowing in the upper geosphere aquifers.

7.9.1.1 Description

Figure 7-88 presents an event tree defining the possible outcomes associated with drilling in a repository location.

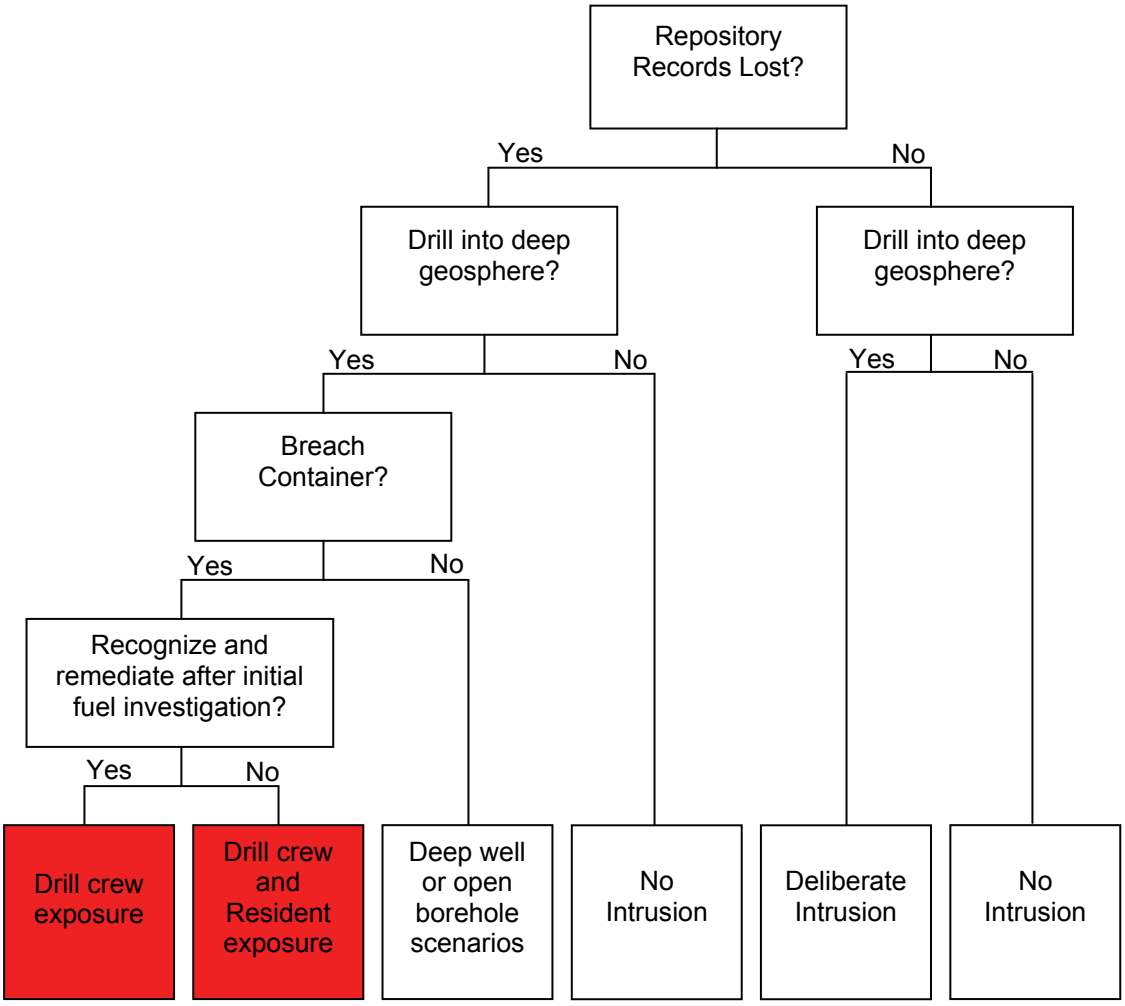

Figure 7-88: General Sequence of Events for Inadvertent Human Intrusion

Of interest to this discussion is the outcome in which:

- The repository records are lost;
- There is drilling into the deep geosphere; and
- The drilling breaches a used fuel container such that used fuel is inadvertently brought to the surface.

This then leads to potential exposure of the following two groups:

- The drill crew, exposed to contaminated drill slurry spread on the surface around the drill rig and to a core section containing used fuel; and
- A resident at the site, exposed by living nearby and growing food on soil contaminated by drill slurry[5].

To provide context, Table 7-38 presents a summary of the exposure groups considered in recent national and international inadvertent human intrusion safety assessments.

Table 7-38: Human Intrusion Pathways Considered in Recent Safety Assessments

Assessment	Scenario / Exposure Cases Considered
Gierszewski et al. 2004 (Canada)	Drill crew Core examination technician Construction worker on contaminated soil from drilling slurry Resident on contaminated soil from drilling slurry *
SKB 2011 (Sweden)	Drill crew * Resident on contaminated soil from slurry growing a garden or exposed from irrigation and drinking from well using open borehole into waste
JNC 2000 (Japan)	Excavation workers (exposed externally to core sample and internally by inhalation)
DOE 2008 (USA)	Reasonable Maximally Exposed Individual (Resident) exposed as a result of direct pathway to the groundwater created by the borehole.
Nagra 2002 (Switzerland)	Resident exposed as result of open borehole into waste creating pathway for waste to reach aquifer

Note: * Represents most limiting exposure case.

Intrusion Likelihood

Regulatory document G-320 (CNSC 2006) recognizes that inadvertent human intrusion events could result in dose rates that exceed the regulatory limit and it states that reasonable efforts

[5] Note that current drilling standards would not permit drill slurry to be left at the drill site, but is conservatively assumed here.

should be made to limit the probability of such high consequence scenarios. The following repository characteristics have been adopted to minimize the likelihood of this event:

- A deep location;
- Site selection based on an absence of groundwater resources at repository depth that could be used for drinking or agricultural purposes;
- Site selection based on an absence of economically exploitable natural resources; and
- The use of records and markers to preserve institutional memory to the extent practicable.

7.9.1.2 Model and Assumptions

Computer Code

The radiological consequences are determined using HIMv2.0 (Medri 2012), a human intrusion computer model developed using the AMBER v5.5 platform.

Screening calculations were initially done to identify the potentially radiologically significant radionuclides; consequently, 74 radionuclides are tracked in HIMv2.0. Short-lived radionuclides are included through the dose coefficients of their parents. Doses are obtained using inhalation, ingestion, groundshine and external dose coefficients.

A detailed description of the parameters and equations used in HIMv2.0 is available in Medri (2012).

Exposure Scenarios

The HIMv2.0 model determines the dose consequences to both exposure groups from the pathways illustrated in Figure 7-89. It models the acute dose to the drill crew at the time the material is brought to the surface and the annual chronic dose to residents who are assumed to live nearby and grow crops on the site after the intrusion has occurred.

In the Drill Crew exposure case, waste is brought to surface in the form of drill core and drill mud / slurry. Normal practice is for drill slurry to be contained at the site and ultimately be disposed of according to regulatory requirements. In this analysis, the drill slurry is conservatively assumed to be spilled around the drill rig without containment. The contaminated slurry would become mixed with surface material, as well as with subsequent drilled material. The waste is assumed to be uniformly mixed through a small near-surface volume of soil around the rig. The drill crew member handles the core sample containing used fuel for a short period of time, leading to an external exposure. This exposure is modelled using a point source approximation. The drill crew member is also exposed to the waste through groundshine, inhalation of contaminated dust and ingestion of contaminated soil from the mixed volume of near-surface material. The drill crew member is assumed not to wear a mask.

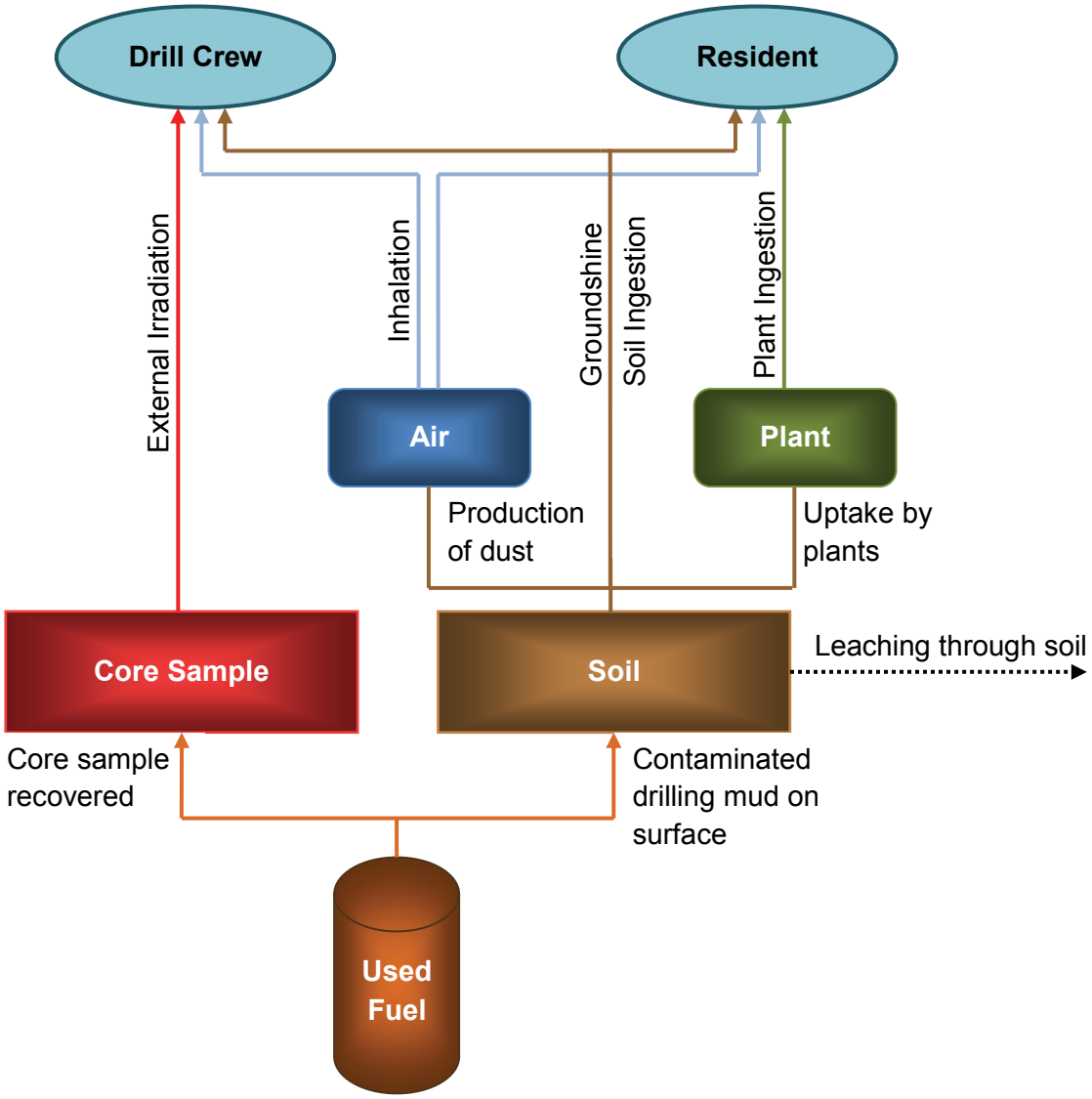

Figure 7-89: Inadvertent Human Intrusion - General Conceptual Model

In the Resident exposure case, the waste brought up with the drill slurry and deposited on the surface around the drill rig is assumed to remain in place without remediation. It remains on the surface, subject only to radioactive decay and leaching. Leaching is caused by precipitation that percolates downwards into the deeper soil. The resident lives around the contaminated site some time after the original intrusion, and grows some food on the contaminated soil. The resident is exposed to the contaminants through groundshine, dust inhalation and through ingestion of contaminated plants and soil. The area contaminated by drilling fluid would be small but have high contaminant concentrations, and therefore an allowance is made for the fraction of time that the resident is exposed to the contaminated site on an annual basis.

As a conservative estimate, the Resident case assumes that the exposure occurs in the first year after intrusion, before leaching has any significant effect on contaminant levels in the soil.

Key Assumptions and Parameters

Key assumptions are:

- Institutional control is maintained for a minimum of 300 years after closure, at which point intrusion becomes possible;
- Decay and ingrowth calculations start at the time of placement, at which point the used fuel is 30 years old;
- There is a minimum period of 70 years of extended monitoring and 25 years of decommissioning and closure following placement, which means the fuel is 425 years old (i.e., 30 + 70 + 25 +300) at the earliest time of intrusion. This is conservative in that the fuel will likely be older at a real site; and
- The drill intercepts a container in the repository and brings used fuel debris to the surface, either mixed with the drill slurry or as a section of intact drill core.

Table 7-39 lists parameters common to the intrusion cases and Table 7-40 lists the main exposure specific parameters used in HIMv2.0. Source references for these values can be found in Medri (2012).

Table 7-39: Common Parameters for Human Intrusion Scenario

Parameter	Value
Fraction of used fuel per container that is damaged by borehole	0.04
Mass of used fuel in a container (kg)	8650
Net infiltration rate of water through soil (m/a)	0.325
Human air inhalation rate (m^3/a)	8400
Soil type	Clay
Soil density (kg/m^3)	1400
Soil water content (m^3/m^3)	0.3
Instant release fractions (selected radionuclides)	Table 7-21

Table 7-40: Exposure Specific Parameters for Human Intrusion Scenario

Parameter	Drill Crew	Resident
Slurry area (m^2)	30	80
Activity duration	168 hrs (14 days, 12 hr shifts) 1 hr (core handling)	10% of the time (year-round)
Dust loading in air (kg_{soil}/m^3)	1.0×10^{-7}	3.2×10^{-8}
Plant ingestion (kg/a)	-	291
Soil ingestion	4.62×10^{-3} kg	0.12 kg/a
Contaminated food fraction (%)	-	10
Thickness of contaminated soil (m)	0.2	0.2
Fraction of U intercepted brought to surface as core	0.4	-
Fraction of U intercepted brought to surface as slurry	0.3	0.3

7.9.1.3 Results

Dose Impact

Figure 7-90 shows the acute dose to the Drill Crew and chronic annual dose to the Resident as a function of time after closure.

The exposure scenarios are stylized. They include all credible exposure pathways such that the overall dose estimate is credible, but not necessarily accurate.

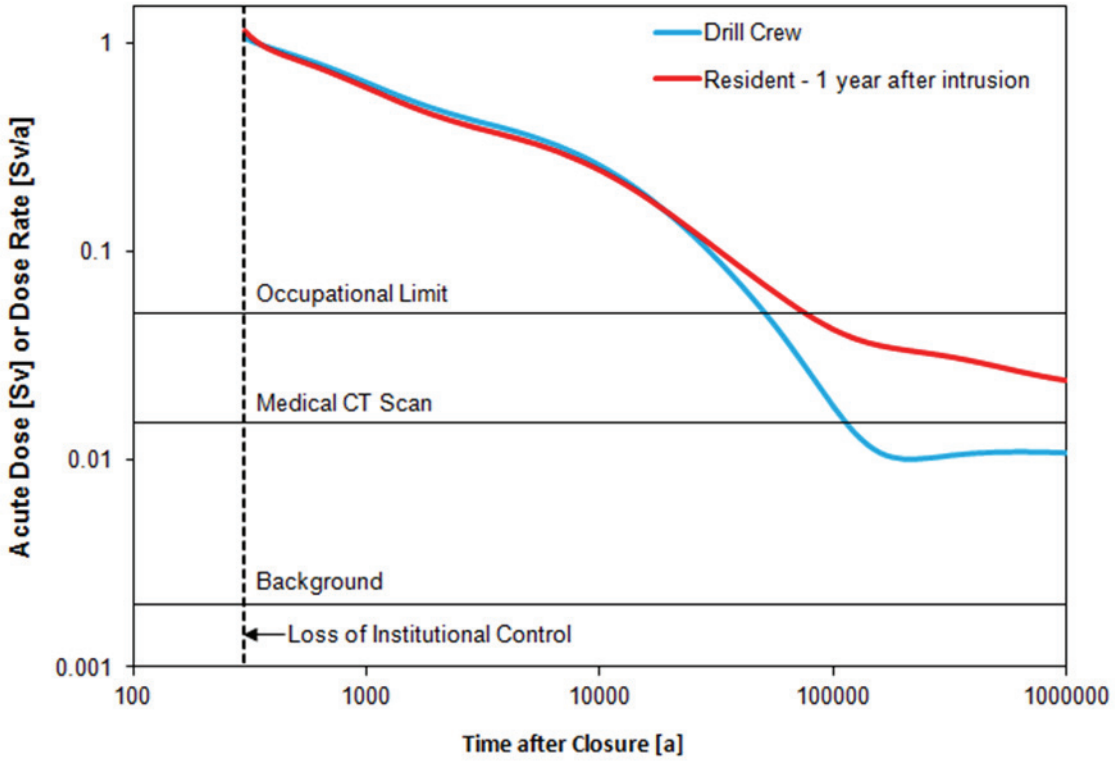

Note: The drill crew receives a one-time (acute) dose, while the resident receives a (chronic) dose rate

Figure 7-90: Inadvertent Human Intrusion - Exposure as a Function of Intrusion Time without Leaching

The results show:

- The maximum one-time dose to the Drill Crew is 1.06 Sv;
- The maximum annual chronic dose to the Resident in the first year after intrusion is 1.14 Sv;
- Doses decrease as a function of the assumed time of intrusion due to radioactive decay.

Figure 7-91 and Figure 7-92 show the breakdown of exposure pathways for the Drill Crew and the Resident.

The dose for both groups tends to be dominated by Am-241 for the first 300 to 1000 years, by Pu-240 and Pu-239 from 10^3 to 10^5 years, and by the U-238 decay chain radionuclides for longer times. This is in contrast to the Normal Evolution Scenario in which actinides are slow to dissolve, sorb strongly in the repository and geosphere, and generally do not reach the surface.

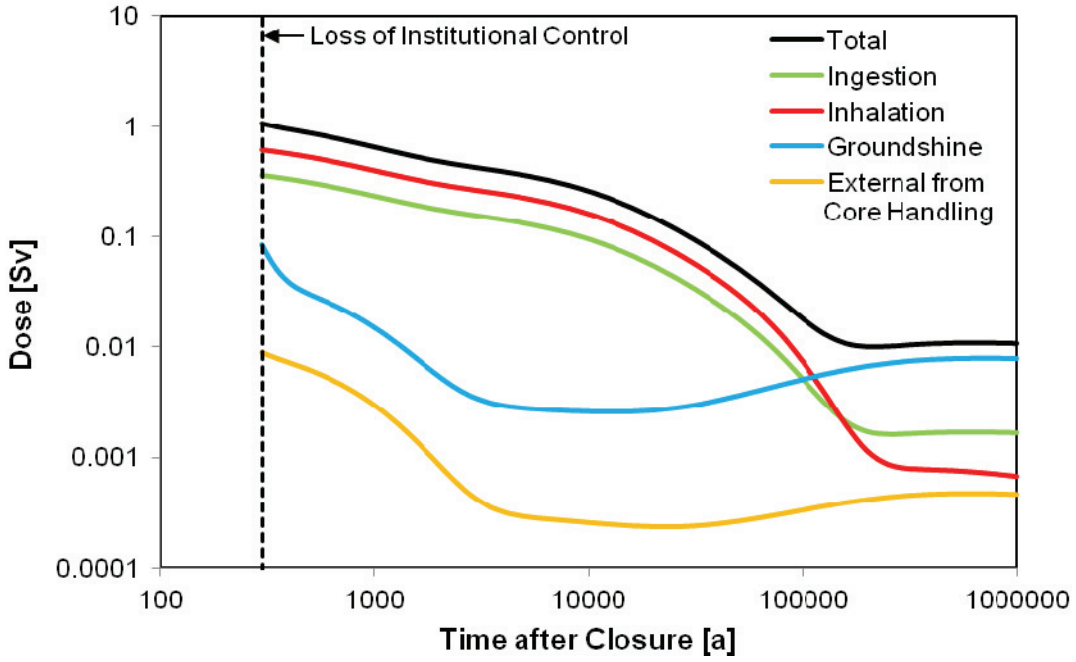

Note: Drill crew receives a one-time (acute) dose

Figure 7-91: Inadvertent Human Intrusion - Exposure Pathway Doses for Drill Crew

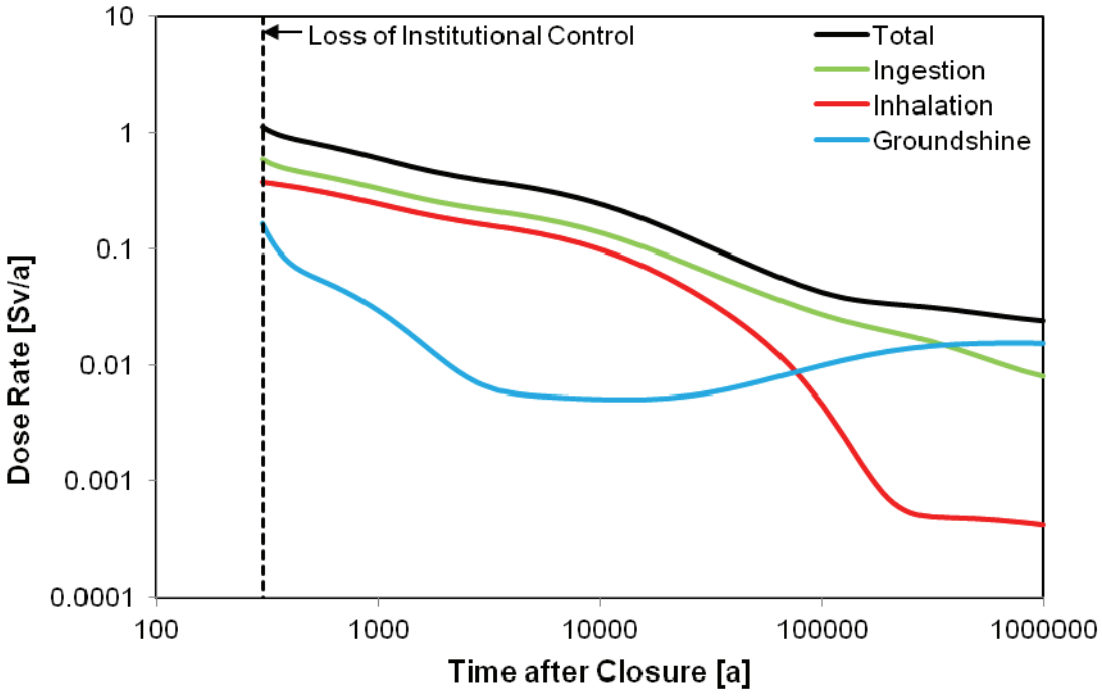

Note: Resident receives a chronic dose rate

Figure 7-92: Inadvertent Human Intrusion - Exposure Pathway Dose Rates for Resident

For the Resident, the exposure could potentially occur any time after the used fuel is deposited on the surface, assuming the site is not remediated in the interim. Figure 7-93 shows the dose to the Resident as a function of arrival time at the site, assuming the intrusion occurs at the earliest possible time after closure (i.e., 300 years). The results show that leaching can cause a substantial reduction in dose at later times.

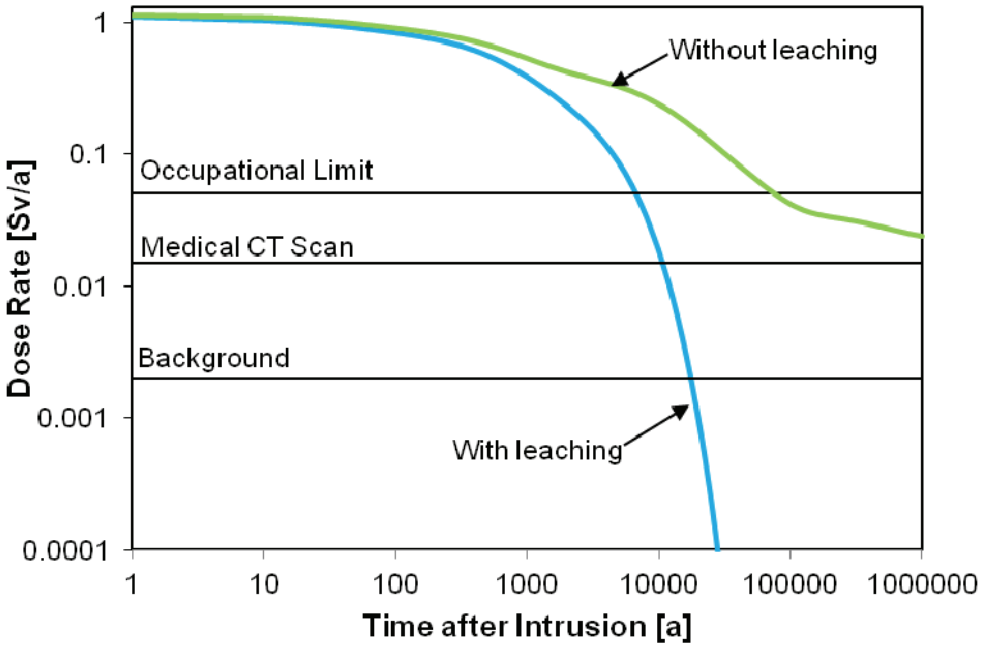

Figure 7-93: Dose Rate to Resident as a Function of Arrival Times Assuming Intrusion Occurs 300 Years after Closure

The results shown for the Resident dose in Figure 7-90 and Figure 7-92 conservatively assume all Rn-222 stays in the soil. In reality, because Rn-222 is a gas, much of it is likely to escape the soil and be dispersed in the atmosphere. Figure 7-94 shows the effect on the Resident dose of removing the groundshine contribution of Rn-222 and its short-lived daughters (i.e., Po-218, Pb-214, Bi-214 and Po-214) is significant at long times. The contribution from Pb-210 (a longer-lived daughter) is still included because Pb-210 formed underground would not quickly decay away when it reaches the surface.

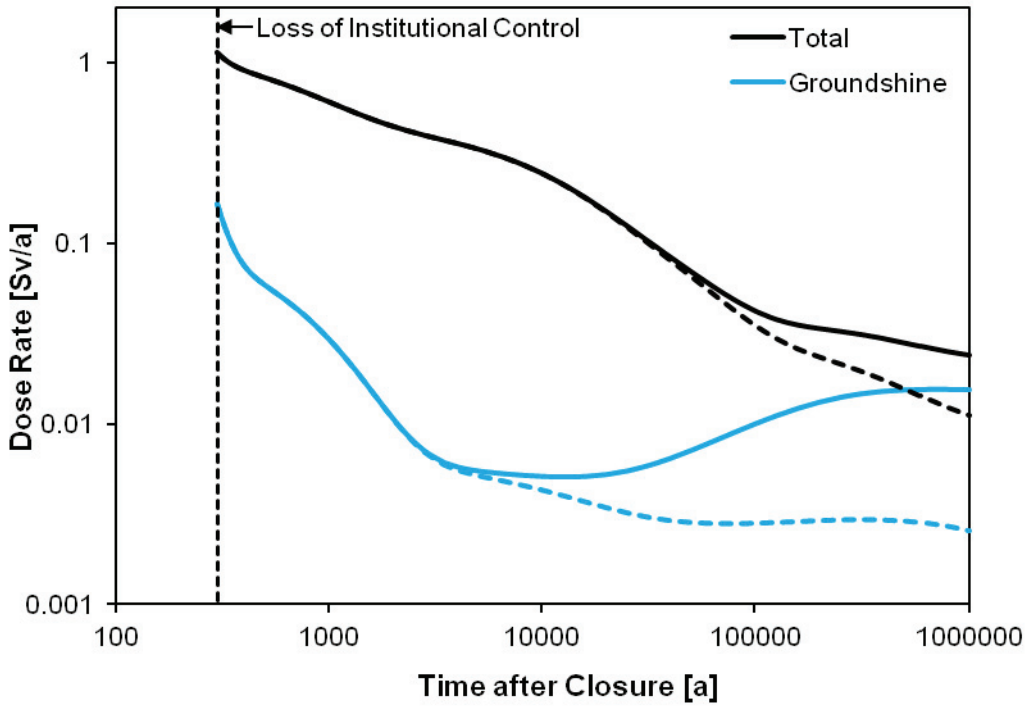

Note: Dotted lines show the dose rates without Rn-222 and its short-lived daughters

Figure 7-94: Effect of Rn-222 and Short-Lived Daughters in Groundshine Pathway on Resident Exposure

Annual Risk

To provide context for the dose rates, the annual risk to the most exposed individual can be estimated.

The annual risk to the Resident (R_R), which is the most exposed group, is determined via:

$$R_R = \Upsilon \cdot H \cdot P \qquad (7\text{-}3)$$

where: Υ is the probability coefficient for stochastic effects per Sv or 0.057 according to ICRP (2007);

H is the highest dose in the time period of concern; and

P is the intrusion frequency.

While the intrusion frequency could be estimated by assigning numerical values to each of the events in Figure 7-88, in practice these values are to a large extent non-quantifiable. Consequently, a more simplistic approach is adopted to illustrate the frequency with which an intrusion event may occur. This approach considers only the frequency of drilling.

Specifically, given that the area around the repository has no significant mineral resources, a deep drilling frequency to resurvey or update the geological information of about once every 100 years is estimated. Assuming this surveys an area of 10 km × 10 km, this is a drilling frequency of $10^{-10}/m^2a$. Since the repository consists of 275 rooms, with each room having a projected area of 1030 m^2, the frequency of inadvertent human intrusion into a room can be estimated as $2.8 \times 10^{-5}/a$. If only the container area is used, the intrusion frequency is estimated as $6.1 \times 10^{-6}/a$.

With Υ = 0.057/Sv, H = 1.14 Sv and P = $2.8 \times 10^{-5}/a$, the annual risk to the Resident from an inadvertent human intrusion event is $1.8 \times 10^{-6}/a$. This is below the risk target of $10^{-5}/a$ for disruptive scenarios identified in Section 7.1.1.

The intrusion probability does not take into account the beneficial effect of institutional memory. Institutional memory could decrease with time, but at earlier times when high doses are more likely, ongoing institutional memory would significantly reduce the intrusion probability (and the risk) of such an event.

The repository might also be detected through surface geophysical measurements, but not recognized as a used fuel facility. In this case exploration drilling would specifically aim for the repository and the intrusion probability could be higher than the above random drilling frequency. But since the drilling program would be specifically designed to explore the anomaly, it is also more likely that the repository would be recognized before or shortly after the repository level was reached and the consequences would therefore be less than those estimated above.

At long times, the cumulative probability of intrusion increases, but the consequences also decrease until eventually they are similar to those for inadvertent intrusion into a uranium ore body.

7.9.2 All Containers Fail

The long-lived used fuel containers are an important feature of the multi-barrier concept. The reference copper containers are anticipated to last for a period of time in excess of one million years, based on the copper corrosion barrier, sturdy mechanical design, and favourable site attributes. Nevertheless, the All Containers Fail Scenario considers the hypothetical case in which all the containers fail.

Since the containers are durable and there is no identified mechanism to fail all containers, the base case considers failure at 60,000 years. This corresponds, for example, to the earliest possible timeframe for an ice sheet to cover the site, and it is possible that some unanticipated effect of the ice sheet might cause failure.

The sensitivity to earlier failure times is examined in a sensitivity case in which all containers are assumed to fail at 10,000 years.

7.9.2.1 Model and Assumptions

The dose assessment is performed using the same SYVAC3-CC4 model described in Section 7.5.4. All model parameters are identical to those in the Reference Case of the Normal Evolution Scenario except that:

- All 12,778 containers fail simultaneously;
- The radionuclide release model takes no credit for the presence of the container. As such, the release of radionuclides from the slowly dissolving fuel to the near field is limited only by the buffer properties; and
- The potential presence of a few containers with small initial defects is not included. This modelling simplification does not affect the peak dose rate.

The behaviour of hydrogen gas generated through corrosion of the internal steel container is discussed in Chapter 8.

7.9.2.2 Results

<u>All Containers Fail at 60,000 Years</u>

Figure 7-95 shows the dose rate for the base case in which all containers fail at 60,000 years. Also included for comparison is the dose rate for the Reference Case. The maximum dose rate is 7.5×10^{-6} Sv/a, occurring at 1.0×10^{7} years. While the maximum is about 3750 times that of the Reference Case, it remains a factor of 133 below the interim dose acceptance criterion of 1×10^{-3} Sv/a.

Although not shown in the figure, the simulation has been extended to allow for calculation of an illustrative peak value. The result shows a value of 1.62×10^{-5} Sv/a is reached at 2.1×10^{7} years.

The discussion in Chapter 8 indicates that no adverse dose consequences are anticipated due to gas generation and migration.

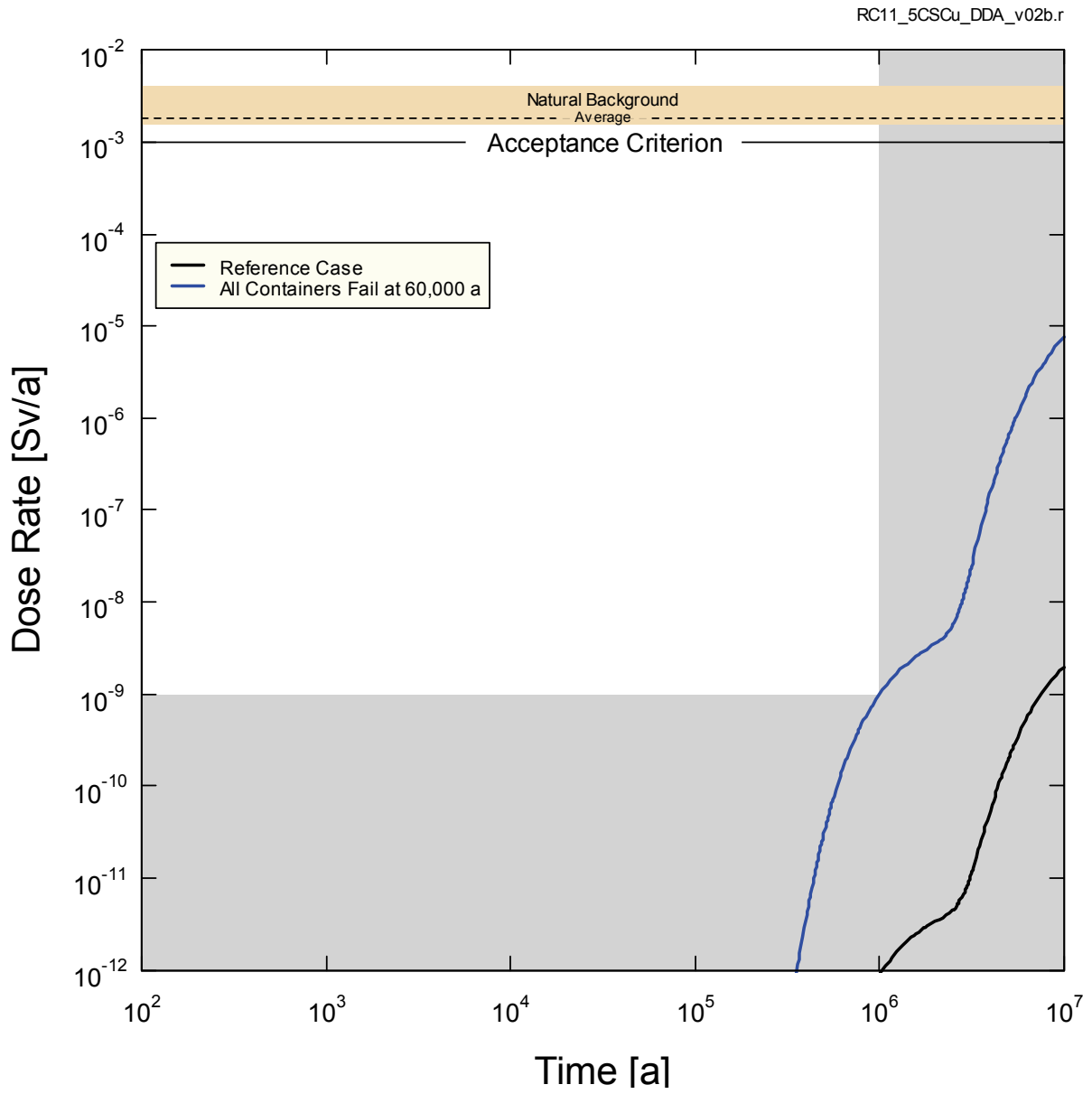

Figure 7-95: All Containers Fail at 60,000 Years - Dose Rate

Figure 7-96 shows the dose contributions from the most significant radionuclides. As in the Reference Case, I-129 is the dominant contributor.

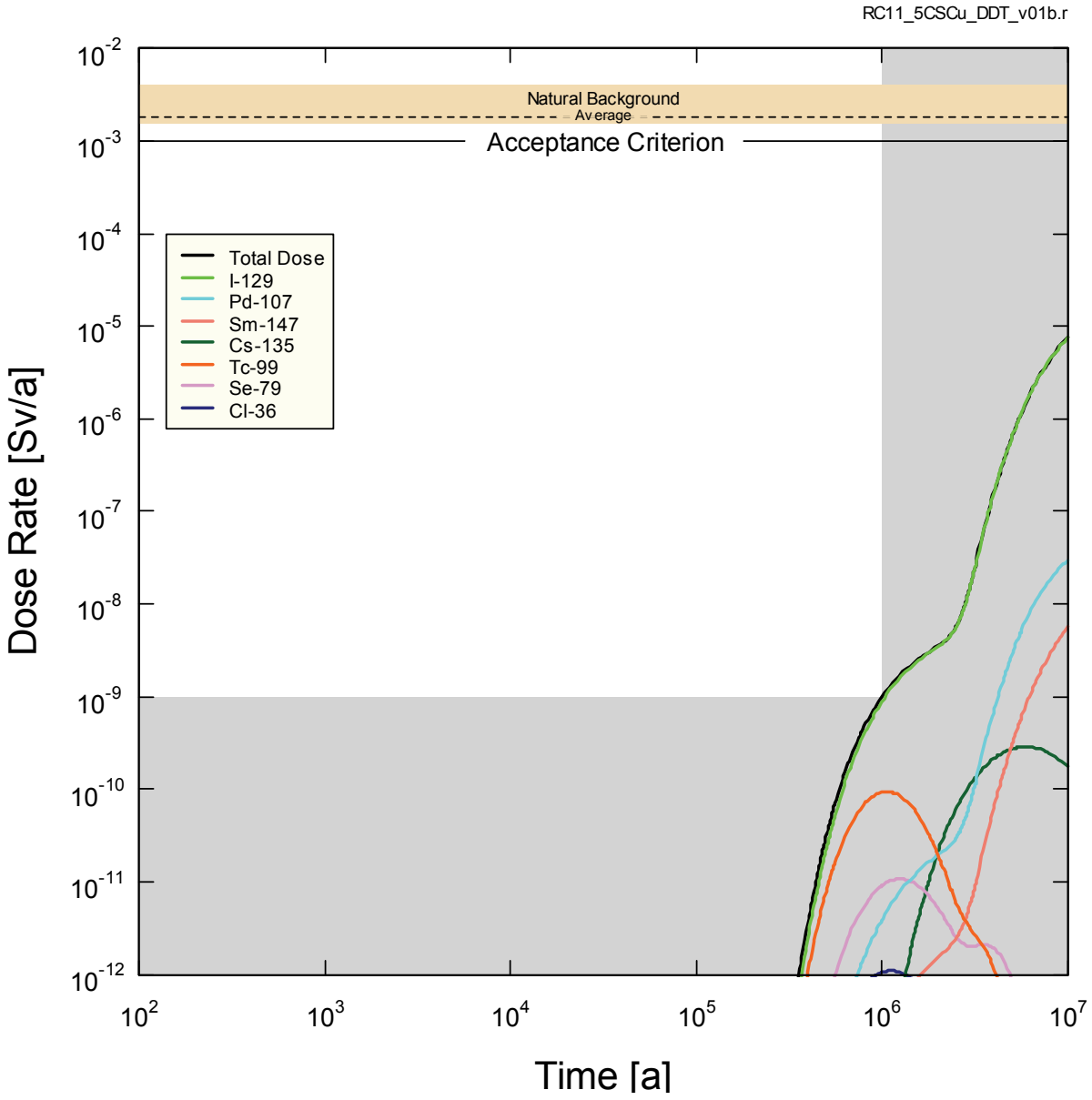

Figure 7-96: All Containers Fail at 60,000 Years – Contributing Radionuclides

All Containers Fail at 10,000 Years

Figure 7-97 compares the dose rate for the sensitivity case in which all containers fail at 10,000 years with results for the base case in which all containers fail at 60,000 years. The results are not substantially different, with a maximum dose rate of 8.4×10^{-6} Sv/a (or 1.1 times the base case value) occurring at 1.0×10^{7} years. The increase in dose rate occurs as a result of less time being available for radioactive decay.

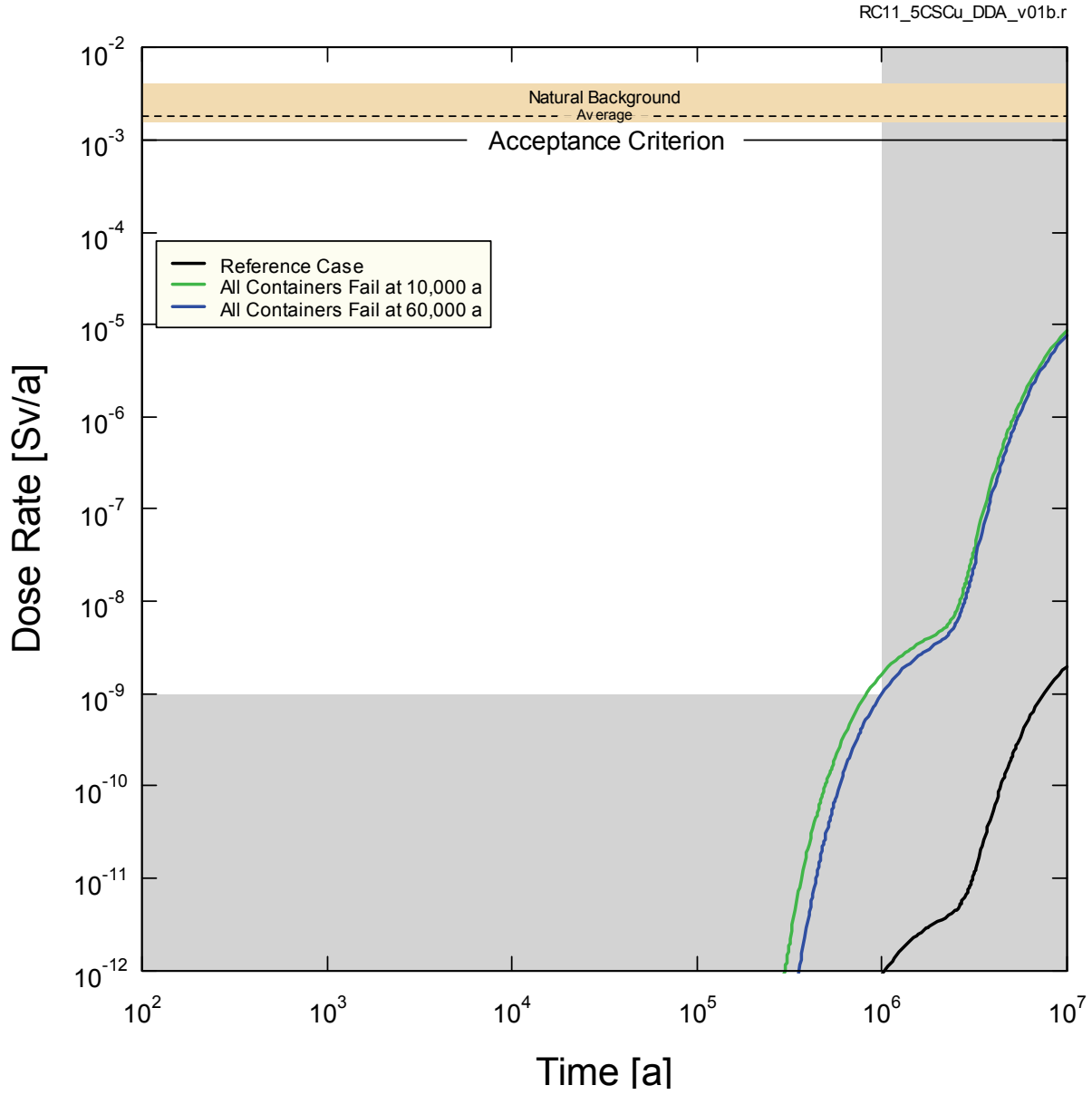

Figure 7-97: Sensitivity - All Containers Fail at 10,000 Years - Dose Rate

7.9.3 Shaft Seal Failure

The repository shafts represent a potentially important pathway for contaminant release and therefore the repository design includes specific measures to provide good shaft seals.

The Normal Evolution Scenario considers the likely behaviour of the shaft seals and the repository / shaft excavation damaged zones. The Shaft Seal Failure Scenario considers the same evolution of the repository system and the same exposure pathways as in the Reference Case of the Normal Evolution Scenario except that there is rapid and extensive degradation of

the shaft seals. For conservatism, it is assumed that this degradation occurs at the time of repository closure.

7.9.3.1 Model and Assumptions

Analysis of the Shaft Seal Failure Scenario is performed using the FRAC3DVS-OPG model described in Section 7.5.3. This model is used in lieu of the SYVAC3-CC4 system model because the groundwater flow field in the repository and near-field geosphere could be affected by degradation of the shaft seals.

All model parameters are the same as in the Reference Case, except that the hydraulic conductivities of all shaft seal materials are set to high values. Two simulations have been performed:

- Base Case: the hydraulic conductivities are set to 1.0×10^{-9} m/s; and
- Extreme Case: the hydraulic conductivities are set to 1.0×10^{-7} m/s.

The locations of the defective containers and the well have not been changed. This implies that the analysis may not result in the most conservative consequence and therefore the results should be considered illustrative only. For a real candidate site, these locations would be varied to ensure the most conservative locations are selected.

7.9.3.2 Results

The results for I-129 transport to the well are reported together with other FRAC3DVS-OPG sensitivity studies in Figure 7-54 in Section 7.7.1.2.6. Only the Extreme Case results are shown.

The results show no perceptible difference from the Reference Case. This is due to a combination of the distance to the shaft, the direction of groundwater flow, the low hydraulic conductivity of the host rock and the effectiveness of the other intact seals.

7.10 The Anticipated Effects of Glaciation on the Normal Evolution Scenario

During past glacial cycles, much of Canada has been covered by kilometre-thick ice sheets. The main factors that initiated these cycles (i.e., solar insolation variation due to Earth orbital dynamics and the location and size of the continents) are still present. Current levels of greenhouse gases in the atmosphere may delay the onset of the next glaciation (Berger and Loutre 2002); however, glacial cycles are expected to reassert themselves in the long run.

The scenario identification discussion in Chapter 6 identifies glaciation as an important external factor influencing the behaviour of the Normal Evolution Scenario. Because the dose assessment is performed for a constant temperate climate, the presence of glacial cycles represents a perturbation that has not been accounted for. The purpose of this section is to discuss the likely effects of glaciation on the calculated dose rates.

The discussion is partially based on results of the regional glaciation modelling study described in Chapter 2. Highlights of this are summarized below.

7.10.1 Regional Glaciation Modelling Summary

To explore the possible effects of glaciation, a representative future glacial cycle was generated using the University of Toronto Glacial System Model (GSM) (Peltier 2011). Of the eight ensembles of paleoclimate simulations for the last 120,000 years, nn9930 (warm-based) and nn9921 (cold-based) were selected for further modelling. Scenario nn9921 has more frequent glacial cycles, and longer glacial and permafrost presence than does nn9930. Three outputs (ice-sheet thickness, lake depth and permafrost depth) are applied as the transient boundary conditions in the regional paleohydrogeologic modelling studies.

A set of eleven sub-regional scale simulations has been defined to explore the potential effects of glaciation on the hypothetical study site. Of these, one simulation is for a reference scenario using actual parameter values while the remaining simulations are sensitivity cases using perturbed parameter values. The sensitivity cases examine the significance of surface hydraulic boundary conditions and the characterization of hydro-mechanical coupling. Due to the relative large size of the grid, repository features are not incorporated.

Results indicate that the glacial loading process tends to generate downward groundwater flow while the unloading process tends to induce an upward hydraulic gradient. The sensitivity analyses show that the change in hydraulic gradient is strongly associated with the hydro-mechanical coupling process. Even though vertical groundwater velocities increase during glacial periods, Peclet number results (Figure 2-29 to Figure 2-32) show that molecular diffusion remains the dominant mechanism for contaminant transport at the repository level throughout the entire 120,000 year glacial cycle.

Tracer simulations, representing the recharge of fresh water, show that boundary conditions have a substantial influence on the vertical tracer concentration profiles in the shallow and intermediate system (Figure 2-24). The simulations also show that tracer penetration is greatly retarded by the low permeability Cabot Head, Manitoulin and Queenston layers, so that oxygenated glacial meltwater does not percolate through the bottom of the Queenston formation (~320 mBGS) in any of the eleven cases examined.

The absence of meltwater penetration is also indirectly supported by the simulated TDS concentration results shown in Figure 2-36. TDS concentration increases sharply in the low permeability Manitoulin and Queenston formations and then remains at a high level (> 200 g/L) below the Queenston layer. Field data collected at the Bruce site (i.e., a site with similar characteristics to the hypothetical study site) (NWMO 2011) show similar trends. It is therefore expected that the deep groundwater regime would not be diluted by fresh recharge during a glacial cycle.

Permafrost forms prior to advance of the ice sheet. Due to its extremely low permeability, permafrost is viewed as beneficial in terms of contaminant transport, because it tends to inhibit the downward penetration of fresh recharge and the upward migration of contaminants. As shown in Figure 2-2 and Figure 2-3, the cold-based scenario nn9921 has a longer permafrost presence and a slightly greater permafrost extent in comparison to the warm-based scenario nn9930. The vertical permafrost extent in both scenarios does not reach a depth of 70 mBGS, which is more than 400 m above the proposed repository level (500 mBGS).

7.10.2 Applicability to the Dose Assessment

Section 7.2.1 notes that a constant temperate climate is assumed in the Normal Evolution Scenario. This section discusses the anticipated effects of glaciation on dose calculations performed using this assumption. Consideration is given to the effects of glaciation on the integrity of the used fuel containers, on contaminant transport and on human behaviour.

Integrity of the Used Fuel Containers:

As the ice sheet moves over the repository site, vertical stress will increase and the groundwater pressure will rise due to the hydro-mechanical coupling effect. If a unity loading coefficient is assumed, the water pressure at repository level could increase by about 27 MPa for a 3 km thick ice sheet. Chapter 4 describes that the used fuel containers are designed to withstand this additional load.

The Chapter 2 glaciation studies summarized above in Section 7.10.1 indicate that oxygenated fresh water does not percolate through the low permeability formations to the repository level. Dissolved oxygen is also likely to be consumed by organics and other reducing materials within the shallow groundwater regime. Conditions at repository level are therefore expected to remain anaerobic and reducing such that no change in the copper corrosion rate would occur.

The glaciation studies also show that the maximum vertical extent of permafrost does not reach to a depth greater than 70 mBGS. This implies that the temperature at the repository level (500 mBGS) will likely remain above 0°C so freeze-thaw induced failures are also not a concern.

It is therefore concluded that container integrity is not adversely affected during a glacial cycle.

Contaminant Transport:

The advancing and retreating ice sheets both erode and deposit rock and till, and glacial erosion could progressively remove a fraction of the rock overlying the repository. The Normal Evolution Scenario, defined in Section 7.2.1, assumes a small amount (tens of metres) of surface erosion occurs in the first one million years, with 100 metres (Hallet 2011) adopted as a sensitivity case.

With 100 m of erosion, the top of the Guelph formation would be about 40 m below grade rather than 140 m below grade, but still capped with very low permeability units of the Salina formation. Even if these units become more permeable due to their nearer surface exposure, the overall system enclosing the repository would remain diffusion-dominant because hundreds of metres of low permeability rock would still be present above the repository. Contaminants would still reach the Guelph formation on the same time-scale and proceed from there to the well and biosphere with the same capture rate as in the Reference Case simulation. Erosion is therefore not expected to adversely affect contaminant release in the one million year time period of interest.

The Chapter 2 glaciation studies also indicate that molecular diffusion remains the dominant transport mechanism at repository level throughout the entire 120,000 year glacial cycle. The rate of contaminant migration to the shallow groundwater system is therefore not expected to be

significantly adversely affected by the loading / unloading effects of glaciation on the deep groundwater system.

Tracer and TDS simulation results support this expectation. The vertical tracer profile shows that no freshwater recharge reaches the bottom of the Queenston formation at 120,000 years and that the TDS concentration remains high (> 200 g/L) at depths greater than 250 mBGS. The presence of high salinity brine at the Bruce site further indicates that there has been essentially no interaction with freshwater recharge during the last several glacial cycles.

It is therefore concluded that contaminant transport rates are not expected to be significantly different during a glacial cycle.

Human Behaviour:

Biosphere changes associated with glaciation will have a significant effect on human behaviour. The future climate would range between a temperate state, a permafrost state and an ice sheet state, with various intermediate states and possibly proglacial lakes forming at a variety of locations. Farming would not be possible for lengthy periods.

The adoption of different critical groups and different dose pathways to account for human behaviour during the changing climate states would result in dose predictions different from those presented here. However, given that the contaminant transport rates are largely unaffected by glaciation, doses to people and non-human biota are expected to remain very low.

Garisto et al. (2010) illustrates how the effect of different climate states could be modelled. Although this analysis is performed for a repository constructed in the crystalline rock of the Canadian Shield, the analysis methods and techniques are transferrable to a sedimentary rock environment.

Summary:

Because container integrity is not challenged and because the contaminant transport rate is expected to remain extremely low, the assumption of a constant temperate climate in the dose assessment for this study is deemed reasonable. While detailed transient modelling of contaminant transport could result in changes to the dose predictions, the consequences of these changes are expected to be relatively minor given the large margins available to the interim dose acceptance criteria.

Note that for a real site, an in-depth site-specific analysis of erosion and contaminant transport would be conducted. Garisto et al. (2010) provides an example of how this could be done.

7.11 Other Considerations

This section presents results for complementary indicators for radiological assessment, results for the radiological protection of the environment, and results for the protection of persons and the environment from hazardous substances.

The effects of gas generation and migration are described in Chapter 8.

7.11.1 Complementary Indicators for the Radiological Assessment

An “indicator” is a characteristic or consequence of a repository which can be used to indicate the overall safety or performance of the system. The most widely used indicator is the peak radiological dose rate, which is calculated from the characteristics of the waste and repository, the properties of the geosphere and biosphere, and the characteristics of the critical group.

The relevance of the calculated dose rates as indicators of potential exposure tends to decrease with time, in part because of uncertainties in the models used to calculate them. In particular, assumptions concerning the biosphere (e.g., climate), human lifestyles (i.e., critical group characteristics) and water flows in the near-surface environment become increasingly uncertain. The purpose of complementary long-term indicators is to supplement the dose rate indicator using system characteristics that are much less sensitive to such assumptions.

The types of complementary indicators considered here address:

- Radionuclide concentrations in the biosphere; and
- Radionuclide transport to the biosphere.

Indicators of the first type avoid assumptions about biosphere pathways but make assumptions about flow rates in surface water bodies (i.e., dilution rates). Indicators of the second type avoid assumptions about surface water flows. Concentration type indicators are more useful on medium timeframes (about 10^4 to 10^5 years), while transport type indicators are more useful for very long timeframes (> 10^5 years) when there is more uncertainty about surface conditions.

The specific complementary indicators considered were selected based on the recommendations of the SPIN project (Becker et al. 2002). The indicators are:

- Radiotoxicity concentration in a water body, for medium time scales; and
- Radiotoxicity transport from the geosphere, for longer time scales.

Radiotoxicity concentration (in Sv/m^3) is the sum over all radionuclides of the activity concentrations in the water body (in Bq/m^3) multiplied by the corresponding radionuclide ingestion dose coefficient. Radiotoxicity transport from the geosphere (in Sv/a) is similarly defined.

Although these complementary indicators are expressed in units of Sv/m^3 or Sv/a, they do not represent a dose; rather, they are radiotoxicity-weighted concentration or transport indicators.

7.11.1.1 Reference Indicator Values

To make use of indicators, reference values are required for comparison purposes.

<u>Radiotoxicity Concentration in a Water Body:</u>

A reference value for the radiotoxicity concentration in a water body has been derived using information on present-day natural background radionuclide concentrations in Canadian surface waters. Table 7-41 shows these concentrations for a variety of radionuclides. Data

representative of Canadian surface waters are taken from Sheppard and Sanipelli (2011a) while Southern Ontario data are taken from a subset of samples in Sheppard and Sanipelli (2011b).

Table 7-41: Background Concentration of Radionuclides in Surface Waters

Surface Water Concentration [Bq/L]					Ingestion DCF [Sv/Bq]	Radiotoxicity [Sv/m^3]
Radionuclide	Canadian		Southern Ontario			
H-3	3.2×10^{0}		3.7×10^{0}		1.8×10^{-11}	5.8×10^{-8}
Cl-36	5.1×10^{-6}		2.0×10^{-6}		9.3×10^{-10}	4.7×10^{-12}
K-40	3.3×10^{-2}		3.4×10^{-2}	a	6.2×10^{-9}	2.0×10^{-7}
Rb-87	2.6×10^{-4}		1.1×10^{-3}	b	1.5×10^{-9}	3.9×10^{-10}
I-129	1.0×10^{-7}		8.7×10^{-8}		1.1×10^{-7}	1.1×10^{-11}
Bi-210	6.4×10^{-3}	c	2.0×10^{-2}	c	1.3×10^{-9}	8.3×10^{-9}
Pb-210	6.4×10^{-3}		2.0×10^{-2}		6.9×10^{-7}	4.4×10^{-6}
Po-210	7.1×10^{-3}		2.0×10^{-2}	c	1.2×10^{-6}	8.5×10^{-6}
Rn-222	2.7×10^{-3}	d	5.8×10^{-3}	d	2.5×10^{-10}	6.8×10^{-10}
Ra-223	2.0×10^{-7}	f	4.8×10^{-7}	f	1.0×10^{-7}	2.0×10^{-11}
Ra-224	7.8×10^{-3}	h	6.3×10^{-3}	h	7.1×10^{-8}	5.6×10^{-7}
Ra-226	2.7×10^{-3}		5.8×10^{-3}		2.8×10^{-7}	7.6×10^{-7}
Ac-227	2.0×10^{-7}	f	4.8×10^{-7}	f	1.1×10^{-6}	2.2×10^{-10}
Th-227	2.0×10^{-7}	f	4.8×10^{-7}	f	8.8×10^{-9}	1.8×10^{-12}
Ra-228	2.9×10^{-4}		3.1×10^{-4}	g	6.9×10^{-7}	2.0×10^{-7}
Th-228	9.6×10^{-4}		3.1×10^{-4}	g	7.2×10^{-8}	6.9×10^{-8}
Th-230	1.9×10^{-3}		5.1×10^{-3}	e	2.1×10^{-7}	4.0×10^{-7}
Pa-231	2.0×10^{-7}	f	4.8×10^{-7}	f	7.1×10^{-7}	1.4×10^{-10}
Th-231	1.5×10^{-7}		4.8×10^{-7}	f	3.4×10^{-10}	5.1×10^{-14}
Th-232	3.9×10^{-4}		3.1×10^{-4}		2.3×10^{-7}	9.0×10^{-8}
Th-234	3.3×10^{-3}	e	5.1×10^{-3}	e	3.4×10^{-9}	1.1×10^{-8}
U-234	7.3×10^{-3}		5.1×10^{-3}	e	4.9×10^{-8}	3.6×10^{-7}
U-235	9.3×10^{-5}		2.4×10^{-4}		4.7×10^{-8}	4.4×10^{-9}
U-238	3.3×10^{-3}		5.1×10^{-3}		4.5×10^{-8}	1.5×10^{-7}
					Total	1.6×10^{-5}

Notes:

(-) Indicates no data for that species
(a) Estimated using stable K concentration
(b) Estimated using stable Rb concentration
(c) Assumed to be in secular equilibrium with Pb-210
(d) Assumed to be in secular equilibrium with Ra-226
(e) Assumed to be in secular equilibrium with U-238
(f) Values are 500 times lower than for U-235 in water, as recommended by Amiro (1992, 1993)
(g) Assumed to be in secular equilibrium with Th-232
(h) Values are 20 times higher than for Th-232 in water, as recommended by Amiro (1992, 1993)

Sheppard and Sanipelli (2011a) suggest that the background concentration of radioactive species in surface water remains fairly homogeneous across Canada. Data extracted specifically for Southern Ontario appears to verify this with most radionuclide concentrations within a factor of two of the Canadian values. The largest difference is for Rb-87, with the Canadian value 4.5 times lower than the Southern Ontario value. However, given the limited number of samples for the Southern Ontario data and the error associated with measuring concentrations around the detection limit, it is likely that the variations between the Canadian values and the Southern Ontario values are within the variability of the measurements. Consequently, Canadian surface water data have been selected as representative of the surface waters applicable to this hypothetical site.

Radiotoxicity concentration is determined by multiplying the surface water concentrations by the appropriate ingestion dose conversion factor (Gobien and Garisto 2012). The results are shown in the rightmost column of Table 7-41, with the total value of 1.6×10^{-5} Sv/m^3 indicated at the bottom. For comparison, use of data specific to Southern Ontario only results in a higher radiotoxicity concentration of 4.2×10^{-5} Sv/m^3. Thus, the selected reference value is conservative when used as a comparative baseline.

Dose impacts associated with these natural background levels are not likely of concern so it follows that any dose impacts from the repository that are small in comparison are also not likely of concern.

Radiotoxicity Transport from the Geosphere:

Natural transport processes carry small amounts of natural radioactivity from within the geosphere to the biosphere. The most important process for the sedimentary rock site in the hypothetical geosphere is erosion. Surface erosion rates are primarily due to wind and surface water runoff; however, the likely source of significant long-term erosion is glaciation. Surface soil erosion rates can vary significantly (0.5-1.5 kg dw/m^2/a, CSA 2008) depending on the soil type, corresponding to about 0.0005 m/a (assuming a soil density of 2000 kg/m^3); however, soil is also naturally replenished. A realistic but conservative estimate of glacial erosion of 100 m over 1 million years is given in Hallet (2011), which implies an average erosion rate of 0.0001 m/a.

The natural radioactivity transport from the geosphere is estimated using the elemental composition of surface soils and shallow rocks. The primary source of Canadian surface rock concentrations is Sheppard and Sanipelli (2011a); however, Southern Ontario data from Sheppard and Sanipelli (2011b) and elemental data from shallow rock layers from rock cores drilled in the Michigan basin (Wigston and Jackson 2010a, 2010b; Jackson and Murphy 2011) have also been used.

Table 7-42 shows the natural concentration of the various radionuclides from Canadian sites, Southern Ontario sites and borehole data from the upper 100 m of the Michigan Basin. These data show limited variability for most species. Similar to the surface water data discussed above, the relatively small number of samples for Southern Ontario and the borehole data suggest that differences between the datasets may be within the natural variability of the measurements. Consequently, the more robust Canada wide dataset from Sheppard and Sanipelli (2011a) is selected as representative of the natural concentrations applicable to this hypothetical site.

The resulting radiotoxicity is shown in the rightmost column of Table 7-42 and is determined by multiplying the Canadian data in by the ingestion dose conversion factor. The total radiotoxicity is 1.2×10^{-4} Sv/kg.

Table 7-42: Background Concentration of Radionuclides in Surface Soils and Rocks

Soil/Rock Concentration [Bq/kg]							Radiotoxicity [Sv/kg]
Radionuclide	Canadian		Southern Ontario		Borehole		
H-3	0.04		-		-		7.2×10^{-13}
Cl-36	2.0×10^{-4}		-		-		1.9×10^{-13}
K-40	430		-		118	a	2.7×10^{-6}
Rb-87	25		-		17	b	3.8×10^{-8}
I-129	1.40×10^{-4}		3.4×10^{-4}		-		1.5×10^{-11}
Bi-210	49	c	77	c	16	e	6.4×10^{-8}
Pb-210	49		77		16	e	3.4×10^{-5}
Po-210	40		77	c	16	e	4.8×10^{-5}
Rn-222	29	d	30	d	16	e	7.2×10^{-9}
Ra-223	1	f	3.7	f	0.73	f	1.0×10^{-7}
Ra-224	22	g	16	g	8.3	g	1.6×10^{-6}
Ra-226	29		30		16	e	8.1×10^{-6}
Ac-227	1	f	0.83	f	0.73	f	1.1×10^{-6}
Th-227	1	f	0.83	f	0.73	f	8.8×10^{-9}
Ra-228	22	g	147		8.3	g	1.5×10^{-5}
Th-228	22	g	20		8.3	g	1.6×10^{-6}
Th-230	19		17	e	16	e	4.0×10^{-6}
Pa-231	1	f	0.83	f	0.73	f	7.1×10^{-7}
Th-231	1	f	0.83	f	0.73	f	3.4×10^{-10}
Th-232	22		16		8.3		5.1×10^{-6}
Th-234	23	e	17	e	16	e	7.8×10^{-8}
U-234	21		17	e	16	e	1.0×10^{-6}
U-235	1		0.83		0.73		4.7×10^{-8}
U-238	23		17		16		1.0×10^{-6}
					Total		1.2×10^{-4}

Notes:

(-) Indicates no data for that species
(a) Estimated using stable K concentration
(b) Estimated using stable Rb concentration
(c) Assumed to be in secular equilibrium with Pb-210
(d) Assumed to be in secular equilibrium with Ra-226
(e) Assumed to be in secular equilibrium with U-238
(f) Assumed to be in secular equilibrium with U-235
(g) Assumed to be in secular equilibrium with Th-232

Repeating the calculation using Southern Ontario data and borehole data results in total radiotoxicity values of 2.7×10^{-4} Sv/kg and 5×10^{-5} Sv/kg, respectively.

For the assumed erosion rate of 0.0001 m/a, the radiotoxicity transport over the 6 km^2 repository footprint is 200 Sv/a (assuming an average rock density of 2750 kg/m^3). For comparison, the resulting radiotoxicity transport computed using the Southern Ontario data and the borehole data are 400 Sv/a and 80 Sv/a respectively.

Reference Values:

Table 7-43 summarizes the reference values for the dose rate indicator and the complementary long-term indicators developed for use in this study. The reference values proposed in the EC SPIN project (Becker et al. 2002) are also shown for comparison.

Table 7-43: Reference Values for Indicators

Indicator	Reference Value	
	Current Study	SPIN
Dose rate (Sv/a)	3×10^{-4}	1×10^{-4} to 3×10^{-4}
Radiotoxicity concentration in surface water (Sv/m^3)	1.6×10^{-5}	2×10^{-5}
Radiotoxicity transport from the geosphere (Sv/a)	200	60

7.11.1.2 Results for Complementary Indicators

The portion of the hypothetical geosphere described in Chapter 2 that is modelled with the FRAC3DVS-OPG code in Section 7.5.3 does not contain any surface water bodies that receive contaminants within the modelled domain. The 'radiotoxicity concentration in a waterbody' indicator has therefore not been calculated. For a real site, water bodies would likely be nearby and this indicator would be assessed.

The radionuclide transport to the biosphere for the individual radionuclides is used to calculate the radiotoxicity transport indicator.

Figure 7-98 shows the radiotoxicity transport indicator for the Reference Case together with the dose rate indicator. The indicators have the same general shape because they both depend on radionuclide transport to the biosphere. The figure shows very large margins to the associated criteria for both indictors.

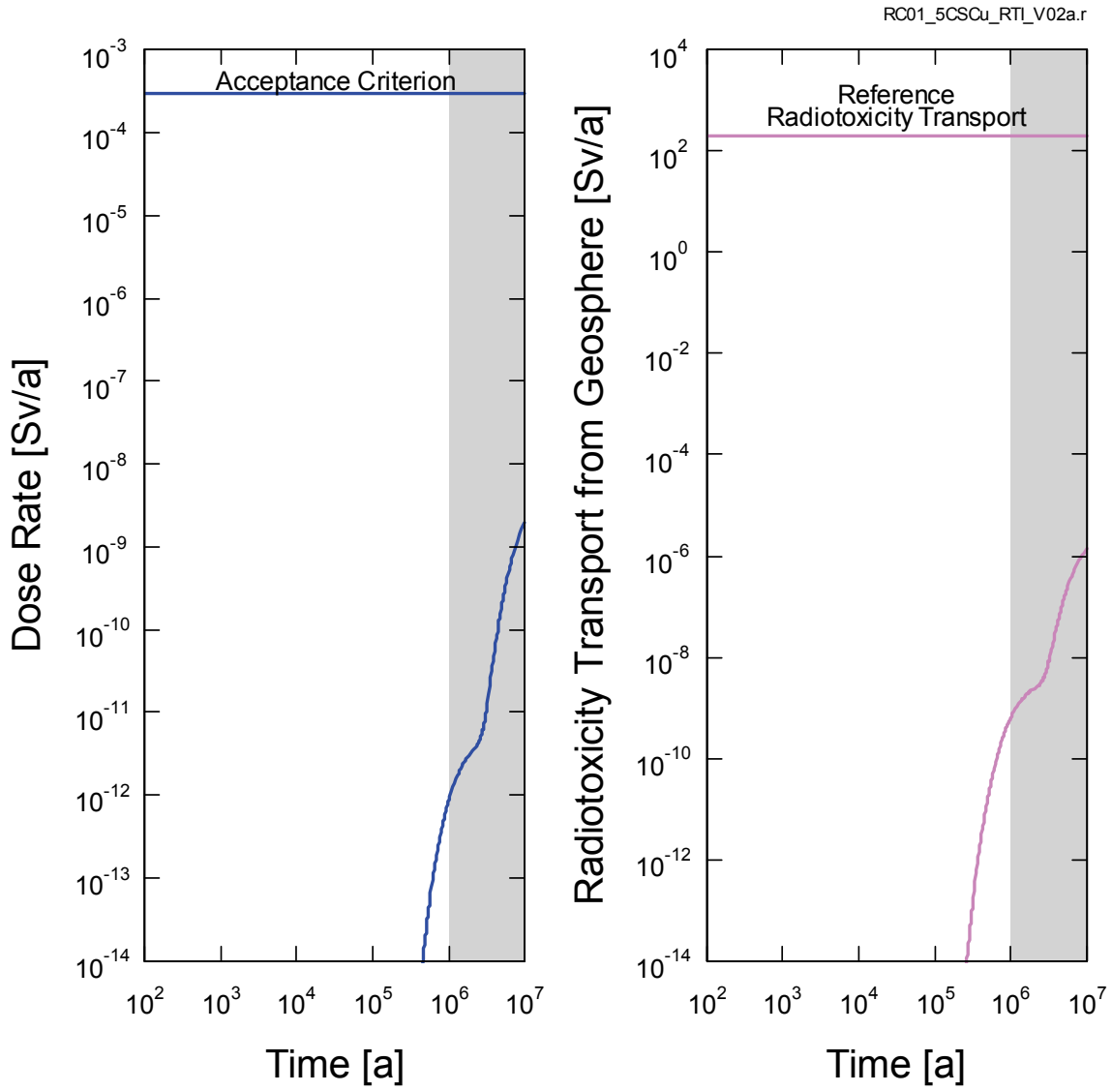

Figure 7-98: SYVAC3-CC4 – Reference Case Results for Complementary Indicators

Figure 7-99 shows the calculated distribution of the radiotoxicity transport indicator over the 120,000 probabilistic simulations. The average radiotoxicity transport to the biosphere is 5.8×10^{-6} Sv/a and the maximum transport to the biosphere is 1.8×10^{-4} Sv/a. These are orders of magnitude below the indicator reference value of 200 Sv/a.

Since the indicator is well below the acceptance / reference value, additional confidence is provided that at long times (i.e., when the dose rate is more uncertain) the impacts of the repository are likely to be very small.

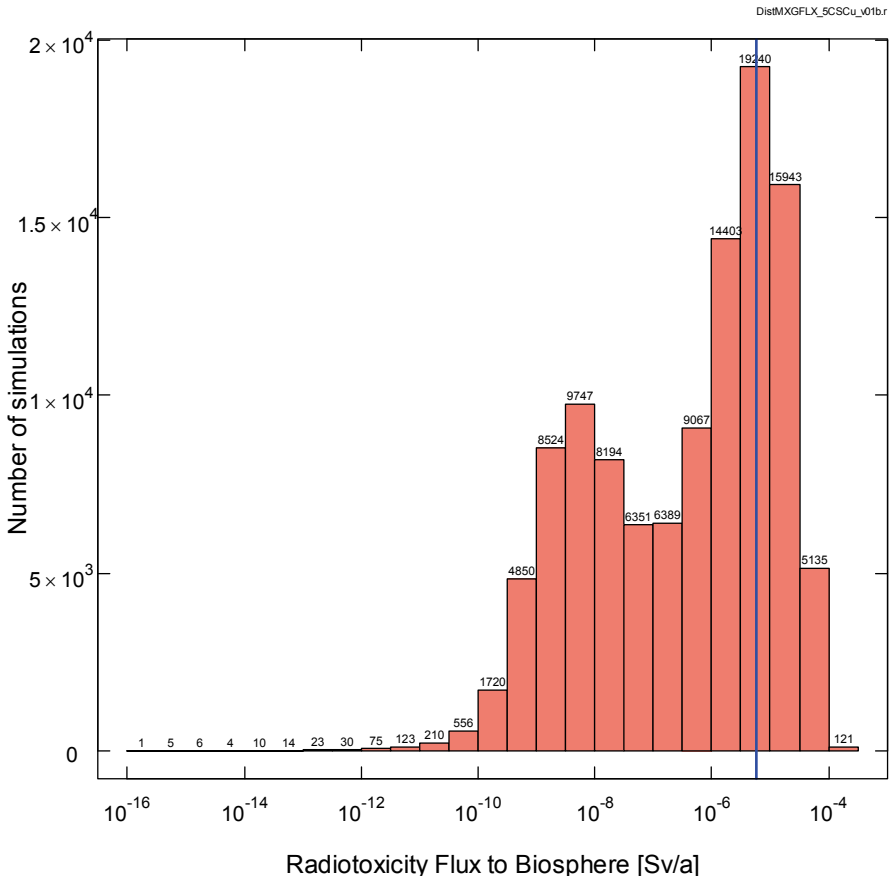

Note: The vertical blue line indicates the average value.

Figure 7-99: SYVAC3-CC4 – Radiotoxicity Transport Complementary Indicator

7.11.2 Radiological Protection of the Environment

The results presented in Section 7.7 through Section 7.9 address the potential radiological impact on persons. This section addresses the potential radiological impact on the environment.

The approach taken is to compare results obtained for the Reference Case of the Normal Evolution Scenario and its associated High Geosphere Diffusivity sensitivity case, and the All Containers Fail Disruptive Scenario against the interim acceptance criteria established in Section 7.1.3 for the radiological protection of the environment. The High Geosphere Diffusivity sensitivity case is selected because its dose rate is considerably higher than that of the Reference Case. Similarly, the All Containers Fail at 10,000 years is a relatively high dose rate Disruptive Scenario.

Table 7-44 shows this comparison for the Reference Case for the set of potentially significant radionuclides identified in the screening analysis (Section 7.6) for which interim acceptance criteria are available (Section 7.1.3). Similar to the dose results presented in Section 7.8.2, these are the maximum values reached over a 10 million year time period.

Because there is no lake or river in the system models used for the safety assessment calculations, sediment values are generated using sorption coefficients taken from Gobien et al. (2013) and contaminant concentrations in the well. The resulting values are expected to be very conservative for the situation in which a lake or river is present because of the much greater dilution that would be available.

The comparison shows very large margins to the interim acceptance criteria. It is therefore concluded that the radiological effects on the environment associated with the Reference Case of the Normal Evolution Scenario are negligible.

Table 7-44: Comparison of Reference Case Concentrations with Interim Acceptance Criteria for the Radiological Protection of the Environment

Radionuclide	Media					
	Water* [Bq/L]			Soil [Bq/kg]		
	Calculated	Criteria	Ratio	Calculated	Criteria	Ratio
Cl-36	3.8×10^{-10}	2.8	1.4×10^{-10}	1.4×10^{-10}	3.8×10^{-1}	3.7×10^{-10}
I-129	9.8×10^{-6}	3.2	3.0×10^{-6}	1.1×10^{-4}	2.4×10^{3}	4.7×10^{-8}
Cs-135	4.2×10^{-9}	2.1×10^{-3}	2.0×10^{-6}	8.8×10^{-6}	8.5	1.0×10^{-6}
Tc-99	4.7×10^{-11}	8.0×10^{-1}	5.9×10^{-11}	7.9×10^{-11}	4.3×10^{1}	1.8×10^{-12}
Ra-226	0	5.9×10^{-4}	0	0	2.5×10^{2}	0
Np-237	0	5.8×10^{-2}	0	0	5.0×10^{1}	0
U-238	0	2.3×10^{-3}	0	0	4.2×10^{1}	0
Pb-210	0	4.3	0	0	3.7×10^{3}	0
Po-210	0	7.0×10^{-3}	0	0	3.0×10^{1}	0

Radionuclide	Sediment** [Bq/kg]		
	Calculated	Criteria	Ratio
Cl-36	8.3×10^{-4}	4.1×10^{4}	2.0×10^{-8}
I-129	7.4×10^{-1}	1.2×10^{6}	6.2×10^{-7}
Cs-135	1.1×10^{-3}	3.5×10^{5}	3.2×10^{-9}
Tc-99	7.1×10^{-8}	3.0×10^{6}	2.4×10^{-14}
Ra-226	0	9.3×10^{2}	0
Np-237	0	1.1×10^{3}	0
U-238	0	1.1×10^{4}	0
Pb-210	0	6.3×10^{3}	0
Po-210	0	5.6×10^{3}	0

Notes: *Well water: **Generated from well water concentrations

Table 7-45 shows this comparison for the High Geosphere Diffusivity sensitivity case of the Normal Evolution Scenario.

The comparison shows large margins to the interim acceptance criteria. It is therefore concluded that the radiological effects on the environment associated with this sensitivity case of the Normal Evolution Scenario are negligible.

Table 7-45: Comparison of High Geosphere Diffusivity Sensitivity Case Concentrations with Interim Acceptance Criteria for the Radiological Protection of the Environment

Radionuclide	Media					
	Water* [Bq/L]			Soil [Bq/kg]		
	Calculated	Criteria	Ratio	Calculated	Criteria	Ratio
Cl-36	3.4×10^{-6}	2.8	1.2×10^{-6}	1.2×10^{-6}	3.8×10^{-1}	3.3×10^{-6}
I-129	1.3×10^{-4}	3.2	4.0×10^{-5}	1.5×10^{-3}	2.4×10^{3}	6.1×10^{-7}
Cs-135	8.4×10^{-8}	2.1×10^{-3}	4.0×10^{-5}	1.8×10^{-4}	8.5	2.1×10^{-5}
Tc-99	4.4×10^{-7}	8.0×10^{-1}	5.6×10^{-7}	7.4×10^{-7}	4.3×10^{1}	1.7×10^{-8}
Ra-226	1.0×10^{-18}	5.9×10^{-4}	1.7×10^{-15}	5.6×10^{-17}	2.5×10^{2}	2.2×10^{-19}
Np-237	0	5.8×10^{-2}	0	0	5.0×10^{1}	0
U-238	0	2.3×10^{-3}	0	0	4.2×10^{1}	0
Pb-210	1.0×10^{-18}	4.3	2.4×10^{-19}	8.8×10^{-17}	3.7×10^{3}	2.4×10^{-20}
Po-210	1.0×10^{-18}	7.0×10^{-3}	1.5×10^{-16}	8.9×10^{-17}	3.0×10^{1}	3.0×10^{-18}

Radionuclide	Sediment** [Bq/kg]		
	Calculated	Criteria	Ratio
Cl-36	7.4	4.1×10^{4}	1.8×10^{-4}
I-129	9.6	1.2×10^{6}	8.0×10^{-6}
Cs-135	2.3×10^{-2}	3.5×10^{5}	6.5×10^{-8}
Tc-99	6.7×10^{-4}	3.0×10^{6}	2.2×10^{-10}
Ra-226	4.8×10^{-14}	9.3×10^{2}	5.2×10^{-17}
Np-237	0	1.1×10^{3}	0
U-238	0	1.1×10^{4}	0
Pb-210	2.3×10^{-11}	6.3×10^{3}	3.6×10^{-15}
Po-210	7.5×10^{-12}	5.6×10^{3}	1.3×10^{-15}

Notes: *Well water: **Generated from well water concentrations

Table 7-46 shows this comparison for the All Containers Fail Disruptive Scenario.

The comparison shows reduced margins as compared to the Normal Evolution Scenario, as would be expected due to the significantly greater source term.

Given the low values, it is concluded that the All Containers Fail Scenario will not result in an exceedance of the interim acceptance criteria.

Table 7-46: Comparison of All Containers Fail at 10,000 years Disruptive Scenario Concentrations with Interim Acceptance Criteria for the Radiological Protection of the Environment

Radionuclide	Media					
	Water* [Bq/L]			Soil [Bq/kg]		
	Calculated	Criteria	Ratio	Calculated	Criteria	Ratio
Cl-36	5.8×10^{-7}	2.8	2.0×10^{-7}	2.1×10^{-7}	3.8×10^{-1}	5.6×10^{-7}
I-129	4.2×10^{-2}	3.2	1.3×10^{-2}	4.8×10^{-1}	2.4×10^{3}	2.0×10^{-4}
Cs-135	5.2×10^{-6}	2.1×10^{-3}	2.5×10^{-3}	1.1×10^{-2}	8.5	1.3×10^{-3}
Tc-99	8.4×10^{-5}	8.0×10^{-1}	1.0×10^{-4}	1.4×10^{-4}	4.3×10^{1}	3.3×10^{-6}
Ra-226	0	5.9×10^{-4}	0	0	2.5×10^{2}	0
Np-237	0	5.8×10^{-2}	0	0	5.0×10^{1}	0
U-238	0	2.3×10^{-3}	0	0	4.2×10^{1}	0
Pb-210	0	4.3	0	0	3.7×10^{3}	0
Po-210	0	7.0×10^{-3}	0	0	3.0×10^{1}	0

Radionuclide	Sediment** [Bq/kg]		
	Calculated	Criteria	Ratio
Cl-36	1.3	4.1×10^{4}	3.1×10^{-5}
I-129	3.2×10^{3}	1.2×10^{6}	2.6×10^{-3}
Cs-135	1.4	3.5×10^{5}	4.0×10^{-6}
Tc-99	1.3×10^{-1}	3.0×10^{6}	4.2×10^{-8}
Ra-226	0	9.3×10^{2}	0
Np-237	0	1.1×10^{3}	0
U-238	0	1.1×10^{4}	0
Pb-210	0	6.3×10^{3}	0
Po-210	0	5.6×10^{3}	0

Notes: *Well water: **Generated from well water concentrations

7.11.3 Protection of Persons and the Environment from Hazardous Substances

This section considers the potential non-radiological effects of contaminants arising from the used fuel bundles and from the container on the health and safety of persons and the environment.

The approach compares results obtained for the Reference Case of the Normal Evolution Scenario, its associated High Geosphere Diffusivity sensitivity case and the All Containers Fail Disruptive Scenario against the interim acceptance criteria shown in Table 7-1. The High Geosphere Diffusivity sensitivity case is selected because its dose rate is considerably higher than that of the Reference Case. Similarly, the All Containers Fail at 10,000 years is a high dose rate Disruptive Scenario.

Table 7-1 shows different acceptance criteria for background groundwater and potable groundwater. For the purpose of this assessment, groundwater concentrations are taken to be those in the well of the SYVAC3-CC4 model. These concentrations are compared against the background groundwater values and if an exceedance occurs, the exceeding concentration is then compared against the potable groundwater value with a supporting justification provided.

Because there is no lake or river in the nearby biosphere, well water concentrations are used as a proxy for surface water concentrations, with the well water concentrations reduced by a factor of 10 to account for anticipated dilution (MoE 2011b). Sediment values are similarly generated using well water concentrations reduced by a factor of 10 and then multiplied by sorption coefficients taken from Gobien et al. (2013).

The ratio determined by dividing an element concentration by its acceptance criterion is called the ‘Concentration Quotient’. Concentration Quotients less than 1.0 indicate the interim acceptance criterion is not exceeded.

7.11.3.1 Contaminants from the Used Fuel Bundles

Table 7-47 shows the Concentration Quotients computed for the Reference Case.

All concentration quotients are well below 1.0, indicating that wide margins are available to the interim acceptance criteria.

Table 7-47: SYVAC3-CC4 - Concentration Quotients for the Reference Case

Element	Groundwater	Surface Water*	Soil	Sediment*
Ag	1.1×10^{-5}	3.4×10^{-6}	1.4×10^{-6}	8.0×10^{-5}
Al	-	2.6×10^{-7}	6.4×10^{-7}	-
Ba	3.6×10^{-7}	5.5×10^{-6}	6.5×10^{-7}	-
Be	4.4×10^{-12}	2.0×10^{-14}	1.3×10^{-12}	-
Bi	-	5.5×10^{-9}	2.9×10^{-7}	-
Cd	4.1×10^{-9}	1.2×10^{-8}	1.4×10^{-9}	1.4×10^{-8}
Ce	-	1.2×10^{-7}	1.2×10^{-5}	1.1×10^{-6}
Co	1.9×10^{-7}	8.0×10^{-8}	2.4×10^{-8}	1.9×10^{-6}
Cr	1.8×10^{-7}	2.0×10^{-7}	8.7×10^{-6}	2.3×10^{-7}
Cs	-	2.1×10^{-14}	-	-
Cu	5.7×10^{-8}	5.7×10^{-9}	8.7×10^{-10}	1.8×10^{-7}
Eu	-	1.2×10^{-8}	1.8×10^{-8}	1.1×10^{-8}
Hg	5.8×10^{-7}	1.4×10^{-6}	3.6×10^{-8}	1.9×10^{-6}
La	-	1.3×10^{-7}	2.8×10^{-7}	1.7×10^{-7}
Mo	1.6×10^{-6}	9.2×10^{-8}	1.9×10^{-6}	-
Nd	-	2.4×10^{-6}	1.3×10^{-6}	4.7×10^{-7}
Ni	1.7×10^{-7}	9.6×10^{-9}	5.1×10^{-8}	4.5×10^{-6}
P	-	6.0×10^{-8}	-	-
Pb	1.9×10^{-8}	3.6×10^{-9}	5.2×10^{-10}	1.9×10^{-6}
Pd	-	5.1×10^{-10}	-	-
Pr	-	1.3×10^{-7}	1.6×10^{-7}	7.5×10^{-8}
Sb	9.6×10^{-8}	7.2×10^{-10}	4.1×10^{-8}	7.2×10^{-7}
Se	7.1×10^{-10}	3.6×10^{-10}	1.3×10^{-10}	-
Sm	-	7.7×10^{-8}	1.9×10^{-6}	-
Sr	-	0	0	-
Te	-	2.7×10^{-8}	1.9×10^{-8}	-
U	0	0	0	-
V	2.0×10^{-7}	1.3×10^{-8}	1.9×10^{-8}	-
Y	-	7.2×10^{-8}	1.1×10^{-7}	2.4×10^{-7}
Zr	-	5.3×10^{-29}	8.5×10^{-29}	-

Note: * Values are estimated using the well concentration as described in Section 7.11.3.

The Concentration Quotients for the High Geosphere Diffusivity sensitivity case are shown in Table 7-48. In this sensitivity case, the concentrations of all species have increased and the concentrations of many of the chemical elements have peaked in the 10 million year simulation time.

All Concentration Quotients are well below 1.0, indicating that wide margins are available to the interim acceptance criteria.

Table 7-48: SYVAC3-CC4 - Concentration Quotients for the High Geosphere Diffusivity Sensitivity Case

Element	Groundwater	Surface Water*	Soil	Sediment*
Ag	1.5×10^{-4}	4.5×10^{-5}	1.9×10^{-5}	1.1×10^{-3}
Al	-	3.2×10^{-6}	7.8×10^{-6}	-
Ba	9.9×10^{-7}	1.5×10^{-5}	1.8×10^{-6}	-
Be	7.9×10^{-10}	3.6×10^{-12}	2.4×10^{-10}	-
Bi	-	1.2×10^{-7}	6.1×10^{-6}	-
Cd	6.5×10^{-9}	1.9×10^{-8}	2.1×10^{-9}	2.2×10^{-8}
Ce	-	1.6×10^{-6}	1.6×10^{-4}	1.5×10^{-5}
Co	2.6×10^{-6}	1.1×10^{-6}	3.3×10^{-7}	2.5×10^{-5}
Cr	2.4×10^{-6}	2.7×10^{-6}	1.2×10^{-4}	3.1×10^{-6}
Cs	-	4.4×10^{-13}	-	-
Cu	1.9×10^{-6}	1.9×10^{-7}	2.9×10^{-8}	6.0×10^{-6}
Eu	-	1.6×10^{-7}	2.5×10^{-7}	1.5×10^{-7}
Hg	7.1×10^{-6}	1.8×10^{-5}	4.4×10^{-7}	2.3×10^{-5}
La	-	1.8×10^{-6}	3.8×10^{-6}	2.3×10^{-6}
Mo	2.1×10^{-5}	1.2×10^{-6}	2.6×10^{-5}	-
Nd	-	3.2×10^{-5}	1.7×10^{-5}	6.4×10^{-6}
Ni	2.3×10^{-6}	1.3×10^{-7}	7.0×10^{-7}	6.1×10^{-5}
P	-	8.0×10^{-7}	-	-
Pb	1.2×10^{-7}	2.4×10^{-8}	3.4×10^{-9}	1.2×10^{-5}
Pd	-	9.4×10^{-9}	-	-
Pr	-	1.8×10^{-6}	2.1×10^{-6}	1.0×10^{-6}
Sb	1.3×10^{-6}	9.7×10^{-9}	5.5×10^{-7}	9.7×10^{-6}
Se	1.3×10^{-7}	6.3×10^{-8}	2.4×10^{-8}	-
Sm	-	1.0×10^{-6}	2.6×10^{-5}	-
Sr	-	0	0	-
Te	-	3.7×10^{-7}	2.5×10^{-7}	-
U	0	0	0	-
V	2.7×10^{-6}	1.8×10^{-7}	2.6×10^{-7}	-
Y	-	9.9×10^{-7}	1.5×10^{-6}	3.2×10^{-6}
Zr	-	8.5×10^{-11}	1.4×10^{-10}	-

Note: * Values are estimated using the well concentration as described in Section 7.11.3.

Table 7-49 shows the Concentration Quotients for the All Containers Fail Disruptive Scenario.

The quotients are higher than in the Normal Evolution Scenario, as expected due to the significantly greater source term. Nevertheless, all Concentration Quotients remain below 1.0.

Table 7-49: SYVAC3-CC4 - Concentration Quotients for the All Containers Fail Case

Element	Groundwater	Surface Water*	Soil	Sediment*
Ag	4.8×10^{-2}	1.4×10^{-2}	6.1×10^{-3}	3.4×10^{-1}
Al	-	1.1×10^{-3}	2.7×10^{-3}	-
Ba	1.6×10^{-3}	2.4×10^{-2}	2.8×10^{-3}	-
Be	4.5×10^{-4}	2.0×10^{-6}	1.4×10^{-4}	-
Bi	-	2.3×10^{-5}	1.2×10^{-3}	-
Cd	5.2×10^{-6}	1.5×10^{-5}	1.7×10^{-6}	1.7×10^{-5}
Ce	-	5.1×10^{-4}	4.9×10^{-2}	4.8×10^{-3}
Co	8.0×10^{-4}	3.4×10^{-4}	1.0×10^{-4}	7.9×10^{-3}
Cr	1.0×10^{-3}	1.1×10^{-3}	5.0×10^{-2}	1.3×10^{-3}
Cs	-	2.7×10^{-11}	-	-
Cu	2.4×10^{-4}	2.4×10^{-5}	3.6×10^{-6}	7.5×10^{-4}
Eu	-	5.1×10^{-5}	7.9×10^{-5}	4.7×10^{-5}
Hg	2.5×10^{-3}	6.1×10^{-3}	1.5×10^{-4}	7.9×10^{-3}
La	-	5.6×10^{-4}	1.2×10^{-3}	7.0×10^{-4}
Mo	6.8×10^{-3}	3.9×10^{-4}	8.3×10^{-3}	-
Nd	-	1.0×10^{-2}	5.4×10^{-3}	2.0×10^{-3}
Ni	7.3×10^{-4}	4.1×10^{-5}	2.2×10^{-4}	1.9×10^{-2}
P	-	2.5×10^{-4}	-	-
Pb	2.6×10^{-5}	5.0×10^{-6}	7.3×10^{-7}	2.6×10^{-3}
Pd	-	2.2×10^{-6}	-	-
Pr	-	5.6×10^{-4}	6.7×10^{-4}	3.2×10^{-4}
Sb	4.3×10^{-4}	3.2×10^{-6}	1.8×10^{-4}	3.2×10^{-3}
Se	1.1×10^{-3}	5.6×10^{-4}	2.1×10^{-4}	-
Sm	-	3.3×10^{-4}	8.2×10^{-3}	-
Sr	-	0	0	-
Te	-	1.2×10^{-4}	7.9×10^{-5}	-
U	0	0	0	-
V	8.8×10^{-4}	5.7×10^{-5}	8.5×10^{-5}	-
Y	-	3.1×10^{-4}	4.6×10^{-4}	1.0×10^{-3}
Zr	-	8.6×10^{-22}	1.4×10^{-21}	-

Note: * Values are estimated using the well concentration as described in Section 7.11.3.

7.11.3.2 Copper Container Chemical Hazard Assessment

Chemical elements of potential concern could also be released from the copper containers and the engineered sealing materials. While the hazard from the sealing materials is expected to be very low because the components tend to be natural clay materials, an assessment is performed to determine the hazard associated with the copper containers.

The rate of release of contaminants from the copper metal depends on the copper corrosion or dissolution rate. Although reducing conditions are expected after closure, a small amount of copper corrosion can still occur as discussed in Chapter 5. As corrosion occurs, copper and any associated impurities are released into the buffer porewater.

In this assessment, a solubility-limited dissolution model is used to determine the rate of corrosion of the copper shell. In this model, the corrosion rate is controlled by the rate at which copper diffuses away from the container / buffer interface. FRAC3DVS-OPG is used to model the transport of copper to the biosphere and to calculate copper concentrations.

The transport of copper away from the container is simulated by applying a constant concentration boundary condition of 2.6×10^{-1} mol/m^3 at every grid node intersecting containers in the repository. This concentration corresponds to the copper solubility limit shown in Table 7-13 increased by a factor of 10 to account for uncertainties in the temperature and chemical conditions near the container. This results in a continuous input of copper into the model over the course of the 10 million year simulation.

Figure 7-100 shows the transport of copper to the surface as a function of time both with and without sorption.

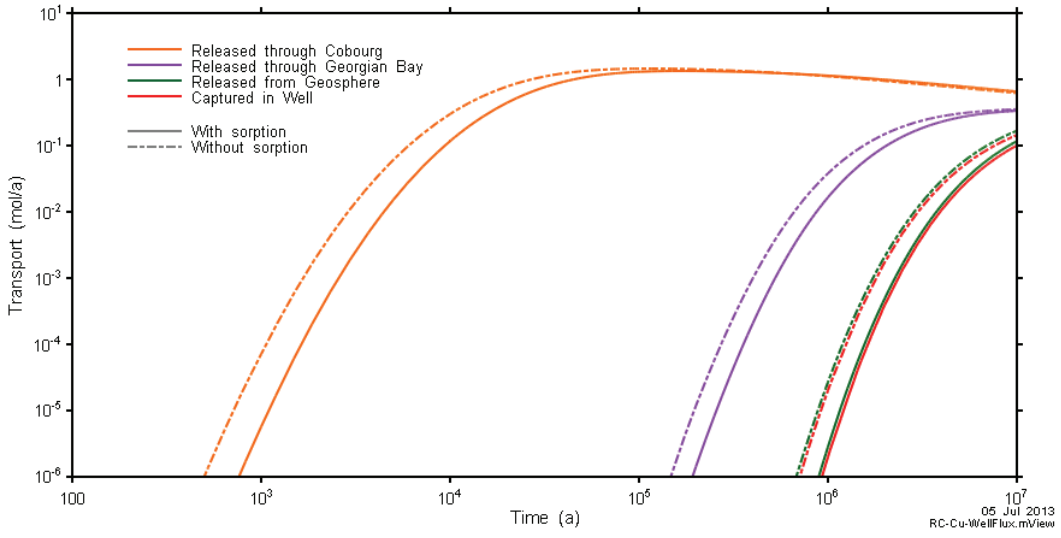

Figure 7-100: FRAC3DVS-OPG - Copper Transport to the Surface both With and Without Sorption

To determine the Concentration Quotient, the maximum total copper transport to the surface (i.e., 0.10 mol/a with sorption and 0.14 mol/a without sorption) is assumed to enter the well, with the well pumping at the reference rate of 1307 m^3/a. The resulting well water concentration (with sorption) is 7.65×10^{-5} mol/m^3 or 4.9 µg/L which is essentially equal to the background groundwater acceptance criterion of 5 µg/L (see Table 7-1). Because the well is the source of drinking water, a less conservative but appropriate comparison can also be made against the potable groundwater acceptance criterion of 69 µg/L (also see Table 7-1). For this comparison, the Concentration Quotient is 0.07 indicating a wide margin to the acceptance criterion.

Surface water concentrations are estimated by reducing the well water concentrations by a factor of 10 (see Section 7.11.3). The resulting maximum Concentration Quotient is about 0.1 which indicates the surface water concentration is well below the acceptance criterion.

To estimate the maximum soil and sediment concentrations, the well concentration of 7.65×10^{-5} mol/m^3 is reduced by a factor of 10 to generate a proxy for surface water (see Section 7.11.3) and this proxy is then conservatively multiplied by the respective soil and sediment sorption coefficients. For copper, the sediment K_d is 0.37 m^3/kg and the soil K_d is 0.03 m^3/kg resulting in maximum copper concentrations of 0.18 µg/g and 1.5×10^{-2} µg/g in sediment and soil, respectively. This results in Concentration Quotients of 2.4×10^{-4} for soil and 1.1×10^{-2} for sediment.

Chemical element impurities are present in the copper at the levels shown in Table 7-50 (SKB 2010b and SKB 1998). These impurities are also released as the copper corrodes. The calculation of copper impurity concentrations assumes the impurities are transported with the copper. Element specific K_d values in the buffer and geosphere for the impurities may produce some variation in the transport time and consequently the copper transport without sorption is used as a surrogate for impurity transport.

The well water and surface water Concentration Quotients for the impurity elements are shown in Table 7-50. Since these quotients are all well below 1.0, it is concluded that these elements would not pose a health and safety hazard to persons or to the environment.

Table 7-50: SYVAC3-CC4 - Concentration Maximum Impurity Levels in Copper and Estimated Impurity Element Concentration Quotients for Well Water

Element	Maximum Impurity Level (ppm)	Impurity Level [mol/mol Cu]	Estimated Maximum Element Conc in Well Water [mol/m^3]	Back-ground Ground-water Criteria [µg/L]	Surface Water Criteria [µg/L]	Groundwater Concentration Quotient	Surface Water Concentration Quotient
Cu	-	-	7.65×10^{-5}	5	5	9.72×10^{-1}	9.72×10^{-2}
Ag	25	1.47×10^{-5}	1.13×10^{-9}	0.3	1.2	4.05×10^{-4}	1.01×10^{-5}
As*	5	4.24×10^{-6}	3.24×10^{-10}	13	5	1.87×10^{-6}	4.86×10^{-7}
Bi	1	3.04×10^{-7}	2.33×10^{-11}	-	150	-	3.24×10^{-9}
Cd	1	5.65×10^{-7}	4.33×10^{-11}	0.5	0.017	9.72×10^{-6}	2.86×10^{-5}
Co	20	2.16×10^{-5}	1.65×10^{-9}	3.8	0.9	2.56×10^{-5}	1.08×10^{-5}
Cr	15	1.83×10^{-5}	1.40×10^{-9}	11	1	6.63×10^{-6}	7.29×10^{-6}
Fe*	10	1.14×10^{-5}	8.71×10^{-10}	-	300	-	1.62×10^{-8}
Hg	1	3.17×10^{-7}	2.42×10^{-11}	0.1	0.004	4.86×10^{-5}	1.22×10^{-4}
Mn*	0.5	5.78×10^{-7}	4.42×10^{-11}	-	200	-	1.22×10^{-9}
Ni	10	1.08×10^{-5}	8.28×10^{-10}	14	25	3.47×10^{-6}	1.94×10^{-7}
O*	5	1.99×10^{-5}	1.52×10^{-9}	-	-	-	-
P**	100	2.05×10^{-4}	1.57×10^{-8}	-	4	-	1.22×10^{-5}
Pb	5	1.53×10^{-6}	1.17×10^{-10}	1.9	1	1.28×10^{-5}	2.43×10^{-6}
S*	15	2.97×10^{-5}	2.27×10^{-9}	-	670	-	1.09×10^{-8}
Sb	4	2.09×10^{-6}	1.60×10^{-10}	1.5	20	1.30×10^{-5}	9.72×10^{-8}
Se	3	2.41×10^{-6}	1.85×10^{-10}	5	1	2.92×10^{-6}	1.46×10^{-6}
Si*	20	4.53×10^{-5}	3.46×10^{-9}	-	3200	-	3.04×10^{-9}
Sn*	2	1.07×10^{-6}	8.19×10^{-11}	-	73	-	1.33×10^{-8}
Te	2	9.96×10^{-7}	7.62×10^{-11}	-	20	-	4.86×10^{-8}
Zn*	1	9.72×10^{-7}	7.44×10^{-11}	160	20	3.04×10^{-8}	2.43×10^{-8}

Note: '-' indicates that there are no defined criteria for that element in the given medium.

*Element not included in Table 7-1. Detailed information on the individual source documents is available in Gobien et al. (2013).

** Impurity level for P is from SKB (2010b) others remain unchanged from SKB (1998).

7.11.3.3 Complementary Indicators

Natural processes carry small amounts of naturally occurring chemical elements from within the geosphere to the surface. Reference values for natural chemical element fluxes to the biosphere can be obtained using the elemental composition of Michigan Basin Sedimentary formations and the erosion rate of this formation over long time periods.

Soil erosion in the Michigan Basin can be due to a number of factors including the soil characteristics, rainfall frequency, rainfall intensity, topography, and land management practices. CSA (2008) recommends a soil erosion rate of 1.5 kg dw/m^2/a for clay soils. Erosion of the bedrock via glaciation is another potential concern for sedimentary formations and is expected to be the dominant form of erosion over the lifetime of the repository. Hallet (2011) recommends a conservative realistic glacial erosion rate of 100 m over 1 million years or 0.0001 m/a. Assuming the erosion rate is constant over a repository footprint area of 6 km^2 and using an average sedimentary rock density of 2750 kg/m^3, an erosion rate of about 1.65×10^6 kg/a can be determined. This rate is somewhat lower than the surface soil erosion rate for plowed soils of 9.0×10^6 kg/a estimated using the surface soil erosion rate from CSA (2008); however, the use of a lower erosion rate for calculating reference values for natural chemical element fluxes is conservative.

Table 7-51 lists the concentrations of the chemical elements of potential concern in Michigan Basin sedimentary rock. Using these values and the selected erosion rate, the natural chemical element transport rates from the geosphere to the biosphere can be calculated and compared with the transport rates associated with the All Containers Fail Disruptive Scenario. This comparison is shown in Table 7-51.

The results indicate that even under the conservative assumptions of the All Containers Fail Disruptive Scenario, transport to the biosphere is considerably less than the corresponding transport arising from natural erosion processes. This adds confidence to the conclusion that the potential chemical hazard from the repository is likely not significant even for the All Containers Fail Disruptive Scenario.

Table 7-51: Erosion Fluxes out of the Geosphere

Element	Michigan Basin Surface Bedrock* (g/Mg)	Michigan Basin Erosion Flux (mol/a)	All Containers Fail Flux to Surface** (mol/a)	Ratio of All Containers Fail Flux to Erosion Flux
Ag	4.67×10^{-2}	7.14×10^{-1}	1.73×10^{-4}	2.42×10^{-4}
Al	1.08×10^{4}	6.62×10^{5}	2.66×10^{-3}	4.02×10^{-9}
Ba	6.80×10^{1}	8.18×10^{2}	9.00×10^{-3}	1.10×10^{-5}
Be	2.50×10^{-1}	4.58×10^{1}	3.28×10^{-5}	7.16×10^{-7}
Bi	9.00×10^{-2}	7.11×10^{-1}	2.17×10^{-4}	3.05×10^{-4}
Cd	6.83×10^{-2}	1.00×10^{0}	3.02×10^{-8}	3.01×10^{-8}
Ce	9.13×10^{0}	1.08×10^{2}	1.04×10^{-3}	9.68×10^{-6}
Co	2.33×10^{0}	6.53×10^{1}	6.78×10^{-5}	1.04×10^{-6}
Cr	1.15×10^{1}	3.64×10^{2}	2.84×10^{-4}	7.80×10^{-7}
Cu	4.08×10^{0}	1.06×10^{2}	2.46×10^{-5}	2.32×10^{-7}
Eu	1.63×10^{-1}	1.76×10^{0}	4.41×10^{-5}	2.50×10^{-5}
La	4.41×10^{0}	5.23×10^{1}	5.37×10^{-4}	1.03×10^{-5}
Mo	1.13×10^{0}	1.95×10^{1}	2.12×10^{-3}	1.09×10^{-4}
Nd	4.13×10^{0}	4.72×10^{1}	1.65×10^{-3}	3.50×10^{-5}
Ni	9.33×10^{0}	2.62×10^{2}	2.28×10^{-4}	8.70×10^{-7}
P	8.22×10^{1}	4.38×10^{3}	4.29×10^{-4}	9.79×10^{-8}
Pb	2.55×10^{0}	2.03×10^{1}	3.17×10^{-7}	1.56×10^{-8}
Pr	1.10×10^{0}	1.28×10^{1}	4.76×10^{-4}	3.72×10^{-5}
Sm	7.65×10^{-1}	8.39×10^{0}	2.32×10^{-4}	2.77×10^{-5}
U	1.27×10^{0}	8.80×10^{0}	0.00×10^{0}	0.00×10^{0}
V	1.34×10^{1}	4.32×10^{2}	8.80×10^{-5}	2.04×10^{-7}
Y	2.82×10^{0}	5.24×10^{1}	2.90×10^{-4}	5.54×10^{-6}
Zr	1.26×10^{1}	2.28×10^{2}	4.95×10^{-22}	2.17×10^{-24}

Note: *: Data are average values for shallow rock layers in Wigston and Jackson (2010a, b) and Jackson and Murphy (2011).

**: 'Surface' is taken to be transport to the well. As discussed in Section 7.5.3.1, the well captures 93.7% of all contaminants entering the Guelph formation.

7.12 Summary and Conclusions

This section summarizes the postclosure safety assessment for liquid-borne contaminant transport.

Due to the very low hydraulic conductivity of the host rock and the dominance of diffusive transport, the dose rates arising in the one million year time period of interest are several orders of magnitude below the applicable interim acceptance criteria for all cases. Since the peak dose rate is not reached in this timeframe, results are quoted for a 10 million year period; however, even with this extension the peak dose rate is not reached for nearly all cases.

To put the quoted results into context, results obtained for the sensitivity case with geosphere diffusivities increased by a factor of 10 can be used. These results, illustrated in Figure 7-77 in Section 7.8.2.2, indicate that a peak dose rate of 2.6×10^{-8} Sv/a is reached at 5.6×10^{6} years. This shows that the long-term doses are expected to remain extremely low, even in cases where the peak rate is not reached in the 10 million year simulation time.

7.12.1 Scope Overview

The Normal Evolution Scenario represents the normal (or expected) evolution of the site and facility. Disruptive Scenarios consider the effects of unlikely events that lead to possible penetration of barriers and abnormal degradation and loss of containment.

Section 7.2 discusses the detailed scope of the assessment. Both Normal Evolution and Disruptive Scenarios are considered.

The containers are robust and there would be multiple inspection steps to ensure they are fabricated and placed correctly. However, given the large number of containers, it is possible that some containers could be placed with undetected defects. In particular, based on a simple estimate of the likelihood of failure in the copper shell welding and inspection process (i.e., 1/5000, Maak et al. 2001), statistically there could be three containers with undetected defects placed in the repository. For the assessment of the Normal Evolution Scenario, it is assumed that three containers with undetected defects are present at the time of repository closure.

Recognizing that the geosphere characteristics at a candidate site and the design of the repository may be different from the reference conditions assumed in this study, a number of sensitivity cases are also examined to illustrate the function of various engineered and natural barriers. Both deterministic and probabilistic simulations are conducted.

In the deterministic simulations, parameter variations are performed about a Reference Case of the Normal Evolution Scenario, where the Reference Case has the following attributes:

- Geosphere properties as per Chapter 2;
- Used fuel inventories as per Chapter 3;
- Repository design as per Chapter 4;
- Three containers each with an undetected defect placed in the repository at the location with the shortest groundwater transport time to the well;
- Defect radius = 1 mm, no evolution of the defect size with time;
- No other container failures occur;

- Groundwater fills the defective containers 10,000 years after the containers are placed in the repository (Gobien et al. 2013);
- Constant temperate climate and steady-state groundwater flow;
- Self-sufficient farming family growing crops and raising livestock on the surface above the repository;
- Drinking and irrigation water for the family obtained from a 219 m deep well that penetrates the entire thickness of the Guelph formation, and located along the main pathway for contaminants released from the defective containers;
- The well is pumping at a rate of 1307 m^3/a. This is sufficient for drinking water and irrigation of household crops;
- A small amount (tens of metres) of surface erosion occurs in the first one million years[6]; and
- Input parameters that are represented by probability distributions are set to either the most probable value (when there is one) or to the median value otherwise.

The deterministic sensitivity cases are:

- Fuel dissolution rate increased by a factor of 10;
- Instant release fractions set to 0.10 for all radionuclides;
- Container defect area increased by a factor of 10;
- No solubility limits in the container;
- No sorption in the EBS;
- Geosphere hydraulic conductivity increased by a factor of 10;
- Geosphere diffusivities increased by a factor of 10;
- No sorption in the geosphere;
- 100 m erosion occurring in the first one million years;
- Overpressure in the Shadow Lake formation;
- Hydraulic conductivity of the excavation damaged zone increased by a factor of 10; and
- Low sorption in the geosphere with coincident high solubility limits in the container.

For the probabilistic simulations, random sampling is used to simultaneously vary all input parameters for which probability distribution functions are available, including contaminant release, transport, and biosphere parameters. However, parameter values that could affect groundwater flow are not varied in these simulations.

These deterministic and probabilistic cases are described in detail in Table 7-3.

Results are generated for one complementary indicator of radiological safety.

Results are generated to address the radiological protection of the environment, and the protection of persons and the environment from hazardous substances. A complementary indicator of safety for hazardous substances is also evaluated.

[6] This is neglected in the analysis simulations due to its anticipated negligible effect.

The Disruptive Scenarios examined are:

- Inadvertent Human Intrusion;
- All Containers Fail at 60,000 Years (with a sensitivity case that has the failure occurring at 10,000 years); and
- Shaft Seal Failure.

These scenarios are described in detail in Table 7-4. All Disruptive Scenarios are analysed with deterministic methods only.

Some additional sensitivity cases were simulated in the course of the analysis as issues emerged that challenged the integrity of the simulations. These cases are listed below and further described in Table 7-5:

- Increased spatial resolution to confirm model convergence; and
- Increased temporal resolution to confirm model convergence.

Neither of the modelling choices had any material effect on the results and they are therefore not discussed further.

7.12.2 Results for the Normal Evolution Scenario

Reference Case

Section 7.8.2.1 reports the maximum dose rate for the Reference Case of the Normal Evolution Scenario is 2.0×10^{-9} Sv/a, occurring at 1.0×10^{7} years[7]. This is orders of magnitude below the average Canadian background dose rate of 1.8×10^{-3} Sv/a and is a factor of 150,000 times less than the 3×10^{-4} Sv/a interim dose acceptance criterion established in Section 7.1.1 for the radiological protection of persons.

The analysis shows that I-129 is the dominant contributor to dose rate. This is because I-129 has a sizeable initial inventory, a non-zero instant release fraction, a very long half-life, is non-sorbing in the buffer, backfill and geosphere and has a radiological impact on humans. All other fission products and actinides either decay away, or are released very slowly as the fuel dissolves and are thereafter sorbed in the engineered barriers and geosphere.

Section 7.10 discusses the effects of glaciation, and argues that only relatively minor effects are anticipated.

Section 7.11.1 discusses two complementary indicators that can be determined using radionuclide releases from the Reference Case. These indicators (i.e., radiotoxicity concentration in a water body and radiotoxicity transport from the geosphere) supplement the dose rate indicator using system characteristics that are much less sensitive to assumptions regarding the biosphere and human behaviour. Due to the absence of a lake or river in the nearby hypothetical biosphere model, results are reported only for the radiotoxicity transport

[7] The time of peak total dose is outside the 1 million year time frame of interest, and also outside the 10 million year period shown to illustrate model behaviour.

indicator. The discussion shows that this indicator is well below its reference value, thereby providing additional confidence that at long times the impact of the repository is likely to be very small.

Section 7.11.2 presents results addressing the radiological protection of the environment (i.e., on non-human biota). The discussion concludes that these effects are negligible for the Normal Evolution Scenario.

Section 7.11.3 discusses the protection of persons and the environment from hazardous substances. Such non-radiological hazards could arise due to release of copper and other potentially hazardous elements from the containers and used fuel. The discussion concludes that all contaminant concentrations are below their associated acceptance criteria.

Sensitivity Cases

Section 7.7.1.2 and Section 7.8.2 present radionuclide transport results for the deterministic sensitivity cases examining the effects of degraded physical barriers, degraded chemical barriers, and the geosphere sensitivity cases.

These results are summarized in Table 7-52 and discussed below. The table shows the maximum impacts (expressed in Bq/a I-129 or in Sv/a), the time of the maximum impact, the effect of the parameter variation on the Reference Case result and the factor by which the result is below the interim dose acceptance criterion for the radiological protection of persons. Results are shown in Bq/a I-129 for FRAC3DVS-OPG simulations because this model does not include representations of the biosphere and critical group. Inferences on dose impacts can be made from the I-129 transport results by comparison to cases for which both I-129 transport (in Bq/a) and dose rates (in Sv/a) are calculated.

Table 7-52: Result Summary

Case	Maximum Impact*		CC4 Result for Time of Maximum Impact (a)	Ratio to Reference Case+	Factor to Dose Limit
	I-129 (Bq/a)	Dose (Sv/a)			
Reference Case of the Normal Evolution Scenario	**7.4**	**2.0×10^{-9}**	**10,000,000**	**-**	**150,000**
Geosphere Sensitivity Cases					
Geosphere Conductivity 10 times Higher	6.2	-	10,000,000	0.8	180,000
EDZ Conductivity 10 times Higher	7.4	-	10,000,000	1.0	150,000
100 m Erosion in One Million Years**	7.4	2.0×10^{-9}	10,000,000	1.0	150,000
Shadow Lake Overpressure	8.3	-	10,000,000	1.1	134,000
Degraded Physical Barrier Sensitivity Cases					
Fuel Dissolution Rate 10 times Higher	-	5.9×10^{-9}	10,000,000	3.0	51,000
Container Defect Area 10 times Higher	-	2.0×10^{-9}	10,000,000	1.0	150,000
Instant Release Fraction set to 10%	-	2.2×10^{-9}	10,000,000	1.1	136,000
Geosphere Diffusivity 10 times Higher	-	2.6×10^{-8}	5,600,000	13	12,000
Degraded Chemical Barrier Sensitivity Cases					
No Sorption in the Geosphere	-	3.3×10^{-9}	10,000,000	1.7	91,000
No Solubility Limits	-	2.0×10^{-9}	10,000,000	1.0	150,000
No Sorption in the EBS	-	6.7×10^{-9}	10,000,000	3.4	45,000
Low Sorption in the Geosphere With Coincident High Solubility Limits	-	2.0×10^{-9}	10,000,000	1.0	150,000
Probabilistic Simulations					
All parameters varied: average dose	-	1.6×10^{-8}	5,600,000	8	19,000
All parameters varied: maximum dose rate, 95th percentile	-	7.5×10^{-8}	5,600,000	37	4,000
Disruptive Scenarios					
All Containers Fail at 60,000 Years	-	7.5×10^{-6}	10,000,000	N/A	133
All Containers Fail at 10,000 Years	-	8.4×10^{-6}	10,000,000	N/A	119
Shaft Seals Failure	7.4	-	10,000,000	N/A	500,000

Notes:

* Maximum impacts are determined from simulations performed with either the FRAC3DVS-OPG code or the SYVAC3-CC4 code. The FRAC3DVS-OPG model does not include biosphere and dose models and therefore results are presented for I-129 transport to the surface. This is a reasonable surrogate for dose because SYVAC3-CC4 simulations show that I-129 is the dominant dose contributor.

** A qualitative argument is used to show there is no significant effect on the Reference Case Results

+ N/A: not applicable

Geosphere Sensitivity Cases

These cases examine the individual effects of increasing the hydraulic conductivity of the host rock, increasing the hydraulic conductivity of the EDZ regions within the repository, 100 m of erosion occurring over one million years, and a 158 m overpressure in the Shadow Lake formation.

Table 7-52 shows that none of these cases have a material effect on the results.

Degraded Physical Barrier Sensitivity Cases

These cases examine the individual effects of increasing the fuel dissolution rate, increasing the container defect area, increasing the instant release fractions and increasing the geosphere diffusivity by a factor of 10. Key features to note are:

- Increasing the fuel dissolution rate by a factor of 10 increases the calculated dose rate by a factor of 3.0 compared to the Reference Case. Even with this increase, the dose consequence remains a factor of 51,000 times below the interim dose acceptance criterion;
- Increasing the geosphere diffusivity by a factor of 10 increases the maximum dose rate by a factor of 13. Even with this increase, the maximum dose rate for the high geosphere diffusivity case remains a factor of almost 12,000 times below the interim dose rate acceptance criterion.
- The other sensitivity cases have no material effect on the results.

Degraded Chemical Barrier Sensitivity Cases

These cases examine the individual effects of not crediting sorption in the geosphere, not crediting solubility limits, not crediting sorption in the EBS, and the combined effect of crediting low sorption in the geosphere with coincident high solubility limits.

Compared to the Reference Case, there is a 1.7 times increase in dose rate for the case with no sorption in the geosphere and a 3.4 times increase for the case with no sorption in the engineered barrier system.

The other cases show no material difference.

Probabilistic Cases

Table 7-52 also presents summary results for the probabilistic case. In this case 120,000 simulations are performed in which all parameters represented by probability distributions are simultaneously varied. The 95th percentile of the maximum dose rate is 7.5×10^{-8} Sv/a or 37 times that of the Reference Case. This is 4000 times less than the interim dose rate acceptance criterion.

7.12.3 Results for the Disruptive Scenarios

Table 7-52 also presents summary results for two Disruptive Scenarios. These scenarios examine the consequences of all containers failing and the effects of degraded shaft seals. Key features to note are:

- Failure of all containers at 60,000 years results in a maximum dose rate of 7.5×10^{-6} Sv/a while failure of all containers at 10,000 years results in a maximum dose rate of 8.4×10^{-6} Sv/a, indicating a slight sensitivity to the assumed failure time. These results are factors of 133 and 119 times below the interim dose rate acceptance criterion.
- The Shaft Seal Failure Scenario has no effect on the dose consequence. This is likely because the three failed containers are located some distance away from the degraded shaft seal (i.e., the failed container location was selected to maximize radionuclide transport to the well and not to the degraded shaft seal).

Section 7.9.1 presents a stylized analysis for the Inadvertent Human Intrusion Scenario. This scenario is not included in Table 7-52 because it is a special case, as recognized in CNSC Regulatory Guide G-320 (CNSC 2006). The assumed intrusion bypasses all barriers, and therefore the associated dose consequence exceeds the regulatory limit. The results show potential doses to the Drill Crew of about 1.06 Sv and to a site Resident of about 1.14 Sv/a conservatively assuming early intrusion, leaving contaminated material on the site, and a future resident living on the contaminated material. The risk of inadvertent human intrusion is minimized by placing the used fuel deep underground in a location with no viable mineral resources and no potable groundwater resources, and by the use of markers and institutional controls. The likelihood of this event occurring cannot be accurately determined; however, based on simple estimates of deep drilling rates, it is roughly estimated as 3×10^{-5} per annum, which implies a risk to the Resident of 2×10^{-6} per annum. This is less than the reference risk criterion 10^{-5} per annum.

7.12.4 Conclusion

The safety assessment shows, for the Normal Evolution Scenario and associated sensitivity cases, as well as for selected Disruptive Scenarios (excluding Inadvertent Human Intrusion), that all radiological and non-radiological interim acceptance criteria are met for liquid-borne contaminants during the postclosure period.

For the Inadvertent Human Intrusion Disruptive Scenario, Regulatory document G-320 (CNSC 2006) recognizes that this event could result in dose rates that exceed the regulatory limit and it states that reasonable efforts should be made to limit the probability of occurrence. The following repository characteristics have been adopted to minimize the likelihood of this event:

- A deep location;
- Site selection based on an absence of groundwater resources at repository depth that could be used for drinking or agricultural purposes;
- Site selection based on an absence of economically exploitable natural resources; and
- The use of records and markers to preserve institutional memory to the extent practicable.

7.13 References for Chapter 7

Amiro, B.D. 1992. Baseline concentrations of nuclear fuel waste nuclides in the environment. Atomic Energy of Canada Limited, AECL10454, COG 91231. Pinawa, Canada.

Amiro, B.D. 1993. Protection of the environment from nuclear fuel waste radionuclides: a framework using environmental increments. Science of the Total Environment 128: 157-89.

Becker, D.-A., D. Buhmann, R. Storck, J. Alonso, J.-L. Cormenzana, M. Hugi, F. van Gemert, P. O'Sullivan, A. Laciok, J. Marivoet, X. Sillen, H. Nordman, T. Vieno and M. Niemeyer. 2002. Testing of Safety and Performance Indicators (SPIN). European Commission Report FIKW-CT2000-00081. European Commission, Brussels, Belgium.

Berger, A. and M.F. Loutre. 2002. An exceptionally long interglacial ahead? Science 297, 1287-1288.

Brown, J.E., B. Alfonso, R. Avila, N.A. Beresford, D. Copplestone, G. Pröhl and A. Ulanovsky. 2008. The ERICA Tool. J. Environ. Radioactivity 99: 1371-1383.

CCME. 2002. Canadian Sediment Guidelines for the Protection of Aquatic Life, Summary Tables. Canadian Council of the Environment 2002 update. Accessed through website of the Canadian Environmental Quality Guidelines: http://st-ts.ccme.ca/

CCME. 2007a. Canadian Soil Quality Guidelines for the Protection of Environmental and Human Health, Summary Tables. Canadian Council of Environment 2007 update. Access through website of the Canadian Environmental Quality Guidelines: http://st-ts.ccme.ca/

CCME. 2007b. Canadian Water Quality Guidelines for the Protection of Agricultural Water Uses, Summary Tables. Canadian Council of Environment 2007 update. Accessed through website of the Canadian Environmental Quality Guidelines: http://st-ts.ccme.ca/

CCME. 2007c. Canadian Water Quality Guidelines for the Protection of Aquatic Life, Summary Tables. Canadian Council of Environment 2007 update. Accessed through website of the Canadian Environmental Quality Guidelines: http://st-ts.ccme.ca/

CNSC. 2006. Regulatory Guide G-320: Assessing the Long Term Safety of Radioactive Waste Management. Canadian Nuclear Safety Commission. Ottawa, Canada.

CNSC. 2011. Setting Radiation Requirements on the Basis of Sound Science: The Role of Epidemiology. Canadian Nuclear Safety Commission, INFO-0812. Ottawa, Canada.

CSA. 2008. Guidelines for Calculating Derived Release Limits for Radioactive Material in Airborne and Liquid Effluents for Normal Operation of Nuclear Facilities. Canadian Standards Association. N288.1-08. Toronto, Canada.

Curti E. and P. Wersin. 2002. Assessment of Porewater Chemistry in the Bentonite Backfill for the Swiss SF/HLW Repository. Nagra Technical Report 02-09. Wettingen, Switzerland.

DiCiccio, T.J. and B. Efron. 1996. Bootstrap Confidence Intervals. Statistical Science Volume 11(3), 189-228.

DOE. 2008. Final Supplemental Environmental Impact Statement for a Geologic Repository for the Disposal of Spent Nuclear Fuel and High-Level Radioactive Waste at Yucca Mountain. US Department of Energy Report DOE/EIS-0250F-S1. Nevada, USA.

EC/HC. 2003. Priority Substances List Assessment Report: Releases of Radionuclides from Nuclear Facilities (Impact on Non-Human Biota). Environment and Health Canada. Canadian Environmental Protection Act. Ottawa, Canada.

Ferry, C., J.-P. Piron, A, Poulesquen, and C. Poinssot. 2008. Radionuclides Release from the Spent Fuel under Disposal Conditions: Re-evaluation of the Instant Release Fraction. Material Research Society Symposium Proceedings 1107, 447-454.

Garisto, F. 1989. The Energy Spectrum of α-particles Emitted from Used CANDU Fuel, Annals of Nuclear Energy 16. 33-38.

Garisto, F. 2001. Radionuclide Screening Model (RSM) Version 1.1 Verification and Validation. Ontario Power Generation Report 06819-REP-01300-10029-R00. Toronto, Canada.

Garisto, F. and M. Gobien. 2013. SYVAC3-CC4 Verification and Validation Summary. Nuclear Waste Management Organization Report NWMO TR-2013-14. Toronto, Canada.

Garisto, F., T. Kempe, P. Gierszewski, K. Wei, C. Kitson, T. Melnyk, L. Wojciechowski, J. Avis and N. Calder. 2005. Horizontal Borehole Concept Case Study: Chemical Toxicity Risk. Ontario Power Generation Report 06819-REP-01200-10149-R00. Toronto, Canada.

Garisto, N.C., F. Cooper and S.L. Fernandes. 2008. No-effect Concentrations for Screening Assessment of Radiological Impacts on Non-human Biota. Nuclear Waste Management Organization Report NWMO TR-2008-02. Toronto, Canada.

Garisto, F., J. Avis., T. Chshyolkova, P. Gierszewski, M. Gobien, C. Kitson, T. Melnyk, J. Miller, R. Walsh and L. Wojciechowski. 2010. Glaciation Scenario: Safety Assessment for a Used Fuel Geological Repository. Nuclear Waste Management Organization Report NWMO TR-2010-10. Toronto, Canada.

Gierszewski, P., J. Avis, N. Calder, A. D'Andrea, F. Garisto, C. Kitson, T. Melnyk, K. Wei and L. Wojciechowski. 2004. Third Case Study - Postclosure Safety Assessment. Ontario Power Generation Report 06819-REP-01200-10109-R00. Toronto, Canada.

Gobien, M and F. Garisto. 2012. Data for Radionuclide and Chemical Element Screening. Nuclear Waste Management Organization Report NWMO TR-2012-11. Toronto, Canada.

Goodwin, B.W., P. Gierszewski and F. Garisto. 2001. Radionuclide Screening Model (RSM) Version 1.1 - Theory. Ontario Power Generation Report 06819-REP-01200-10045-R00. Toronto, Canada.

Grambow, B., J. Bruno, L. Duro, J. Merino, A. Tamayo, C. Martin, G. Pepin, S. Schumacher, O. Smidt, C. Ferry, C. Jegou, J. Quiñones, E. Iglesias, N. Rodriguez Villagra, J. M. Nieto, A. Martínez-Esparza, A. Loida, V. Metz, B. Kienzler, G. Bracke (GRS), D. Pellegrini, G. Mathieu, V. Wasselin-Trupin, C. Serres, D. Wegen, M. Jonsson, L. Johnson, K. Lemmens, J. Liu, K. Spahiu, E. Ekeroth, I. Casas, J. de Pablo, C. Watson, P. Robinson, and D. Hodgkinson. 2010. MICADO Model Uncertainty for the Mechanism of Dissolution of Spent Fuel in Nuclear Waste Repository. European Commission Report EUR 24597 EN. Brussels, Belgium.

Grasty, R.L. and J.R. LaMarre. 2004. The Annual Effective Dose from Natural Sources of Ionising Radiation in Canada. Radiation Protection Dosimetry 108, No 3, 215-226.

Guo, R. 2010. Coupled Thermal-Mechanical Modelling of a Deep Geological Repository using the Horizontal Tunnel Placement Method in Sedimentary Rock using CODE_BRIGHT. Nuclear Waste Management Organization Report NWMO TR-2010-22. Toronto, Canada.

Guttman, I. and S.S. Wilks. 1965. Introductory Engineering Statistics. John Wiley & Sons. New York, USA.

Hallet, B. 2011. Glacial Erosion Assessment, NWMO Report DGR-TR-2011-18, Toronto, Canada.

Hermann, O.W. and R.M. Westfall. 1995. ORIGEN-S - SCALE System Module to Calculate Fuel Depletion, Actinide Transmutation, Fission Product Buildup and Decay, and Associated Radiation Source Terms. In: SCALE: A Modular Code System for Performing Standardized Computer Analyses for Licensing Evaluations. Oak-Ridge National Laboratory NUREG/CR-0200, Rev.4 (ORNL/NUREG/CSD-2/R4) Volume II, Part I. Oak-Ridge, USA.

IAEA. 2006. Safety Requirements: Geological Disposal of Radioactive Waste. International Atomic Energy Agency Safety Requirements WS-R-4. Vienna, Austria.

ICRP. 1995. Age-dependent Doses to the Members of the Public from Intake of Radionuclides - Part 5 Compilation of Ingestion and Inhalation Coefficients. International Commission on Radiological Protection Publication 72, Annals of the ICRP 26(1). Vienna, Austria.

ICRP. 2007. The 2007 Recommendations of the International Commission on Radiological Protection. International Commission on Radiological Protection Publication 103, Annals of the ICRP (W2-4). Vienna, Austria.

ICRP. 2013. Radiological Protection in Geological Disposal of Long-lived Solid Radioactive Waste. International Commission on Radiological Protection Publication 122, Annals of the ICRP 42(3). Vienna, Austria.

Jackson R. and S. Murphy. 2011. Mineralogy and Lithogeochemical Analysis of DGR-5 and DGR-6 Core. Intera Engineering Technical Report TR-09-06. Ottawa, Canada.

JNC. 2000. H12: Project to Establish the Scientific and Technical Basis for HLW in Japan. Japan Nuclear Cycle Development Institute JNC TN1410 2000-004. Tokai, Japan.

King, F. and M. Kolar. 2006. Simulation of the Consumption of Oxygen in Long-term in situ Experiments and in the Third Case Study Repository using the Copper Corrosion Model CCM-UC.1.1. Ontario Power Generation Report 06819-REP-01300-10084-R00, Toronto, Canada.

Kitson C.I., T.W. Melnyk, L.C. Wojciechowski, T. Chshyolkova. 2012. SYVAC3-CC4 User Manual, Version SCC409. Nuclear Waste Management Organization Report NWMO TR-2012-21. Toronto, Canada.

Maak, P., P. Gierszewski and M. Saiedfar. 2001. Early Failure Probability of Used-Fuel Containers in a Deep Geologic Repository. Ontario Power Generation Report 06819-REP-01300-10022-R00, Toronto, Canada.

Medri, C. 2012. Human Intrusion Model for the Fourth and Fifth Case Studies: HIMv2.0. Nuclear Waste Management Organization Report NWMO TR-2012-04. Toronto, Canada.

MoE. 2011a. Soil, Groundwater and Sediment Standards for Use under Part XV.1 of the Environmental Protection Act. Ontario Ministry of the Environment. Toronto, Canada.

MoE. 2011b. Rationale for the Development of Soil and Groundwater Standards for Use at Contaminated Sites in Ontario. Ontario Ministry of the Environment. Toronto, Canada.

MoEE. 1994. Water Management Policies Guidelines Provincial Water Quality Objectives of the Ministry of Environment and Energy. Toronto, Canada.

Muurinen, A. and J. Lehikoinen. 1999. Porewater chemistry in compacted bentonite. Engineering Geology 54, 207-214.

Nagra. 2002. Project Opalinus Clay: Safety Report, Demonstration of the Disposal Feasibility for Spent Fuel, Vitrified HLW and Long-lived ILW. Nagra Technical Report 02-05. Wettingen, Switzerland.

NRC. 2006. Health Risks from Exposure to Low Levels of Ionizing Radiation: BEIR VII Phase 2. Committee on the Biological Effects of Ionizing Radiations (BEIR). The National Academies Press, Washington, DC, USA.

NWMO. 2011. Geosynthesis. Nuclear Waste Management Organization Report NWMO DGR-TR-2011-11 R000. Toronto, Canada.

NWMO. 2012. SYVAC3-CC4 Theory, Version SCC409. Nuclear Waste Management Organization Report NWMO TR-2012-22. Toronto, Canada

Oregon Department of Environmental Quality (ODEQ). 2001. Guidance for Ecological Risk Assessments, Levels I, II, III and IV:P Level II Screening Level Values. Portland, USA

Parkhurst, D.L. and C.A.J. Appelo. 1999. User's Guide to PHREEQC (Version 2) – A Computer Program for Speciation, Batch-Reaction, One-Dimensional Transport, and Inverse Geochemical Calculations. U.S Department of the Interior and U.S. Geological Survey Water-Resources Investigations Report 99-4259. Denver, USA.

Peltier, W.R. 2011. Long-term Climate Change. Nuclear Waste Management Organization Technical Report DGR-TR-2011-14. Toronto, Canada.

Sheppard, S.C. and B. Sanipelli. 2011a. Review of Environmental Radioactivity in Canada Nuclear Waste Management Organization report NWMO-TR-2011-17. Toronto, Canada.

Sheppard, S.C. and B. Sanipelli. 2011b. Environmental radioactivity in Canada - Measurements. Nuclear Waste Management Organization report NWMO-TR-2011-16. Toronto, Canada.

Shoesmith, D. 2008. The Role of Dissolved Hydrogen on the Corrosion/Dissoluton of Spent Nuclear Fuel. Nuclear Waste Management Organization Report NWMO TR-2008-19. Toronto, Canada.

SKB. 1998. Design Premises for Canister for Spent Nuclear Fuel. Swedish Nuclear and Waste Management Company Technical Report TR-98-08. Stockholm, Sweden

SKB. 2004. Interim Main Report of the Safety Assessment SR-Can. Swedish Nuclear Fuel and Waste Management Report SKB TR-04-11. Stockholm, Sweden.

SKB. 2010a. Handling of future human actions in the safety assessment SR-Site. Swedish Nuclear and Waste Management Company Technical Report TR-10-53. Stockholm, Sweden.

SKB. 2010b. Design, Production and Initial State of the Canister. Swedish Nuclear and Waste Management Company Technical Report TR-10-14. Stockholm, Sweden

SKB. 2011. Long-term Safety for the Final Repository for Spent Nuclear Fuel at Forsmark, Main Report of the SR-Site Project. Swedish Nuclear Fuel and Waste Management Company Report SKB TR-11-01. Stockholm, Sweden.

Tait, J.C., I.C. Gauld and A.H. Kerr. 1995. Validation of the ORIGEN-S Code for Predicting Radionuclide Inventories in Used CANDU Fuel. Journal of Nuclear Materials 223, 109-121.

Therrien, R., R. G. McLaren, E. A. Sudicky, S.M. Panday and V. Guvanasen. 2010 FRAC3DVS-OPG: A Three-Dimensional Numerical Model Describing Subsurface Flow and Solute Transport. User's Guide, Groundwater Simulations Group, University of Waterloo. Waterloo, Canada.

Vilks, P. 2011. Sorption of Selected Radionuclides on Sedimentary Rocks in Saline Conditions – Literature Review. Nuclear Waste Management Organization Report NWMO TR-2011-12. Toronto, Ontario.

Wigston, A., and R. Jackson 2010a. Mineralogy and Geochemistry of DGR-3 Core. Intera Engineering Technical Report TR-08-22. Ottawa, Canada.

Wigston, A., and R, Jackson. 2010b. Mineralogy and Geochemistry of DGR-4 Core. Intera Engineering Technical Report TR-08-23. Ottawa, Canada.

THIS PAGE HAS BEEN LEFT BLANK INTENTIONALLY

8. POSTCLOSURE SAFETY ASSESSMENT – GAS GENERATION AND TRANSPORT

This chapter, together with Chapter 7, presents an illustrative postclosure safety assessment for a used fuel repository located in the sedimentary rock of the Michigan Basin. The focus of this chapter is on gas generation and transport of volatile radionuclides. Chapter 7 addresses waterborne contaminant transport.

Exposure of the steel components of an engineered barrier system (EBS) to groundwater will result in the generation of gas due to corrosion processes. Microbial processes, if present, may also generate (or consume) gas. The fate of this gas, as it migrates through the repository, the excavation damaged zone (EDZ) and the surrounding host rock can affect both the internal repository pressure and the transport of gaseous radionuclides.

The assessment is arranged as follows:

- Section 8.1 – Interim Acceptance Criteria: presents the acceptance criteria against which the results of the gas generation and transport analysis are measured.
- Section 8.2 – Scope: describes the analysis case and the rationale for its selection.
- Section 8.3 – Conceptual Model: discusses the conceptualization of gas generation and migration.
- Section 8.4 – Computer Code: introduces T2GGM, the main computer code used.
- Section 8.5 – Analysis Methods and Key Assumptions: the computer code representations are described in detail.
- Section 8.6 – Results of Gas Generation and Transport Analysis: discusses simulations of gas generation and transport on the scale of an individual placement room and on the scale of the repository.
- Section 8.7 – Dose Consequences: postulates gas transport of volatile radionuclides to the biosphere and hypothetical dose consequences to a member of the critical group.
- Section 8.8 – Summary and Conclusions.

8.1 Interim Acceptance Criteria

For radiological consequences, the interim acceptance criteria are identical to those adopted for the waterborne contaminant transport assessment described in Chapter 7.

For pressure, the target acceptance criterion is that pressure in the intact host rock surrounding the repository should remain below 80% of lithostatic pressure (i.e., below 9.9 MPa).

Note that preliminary geophysical analysis indicates that lithostatic pressure must be exceeded before fracturing of the host rock can occur. If this latter criterion is met, the possibility that gas pressure build-up will lead to fracturing can be excluded.

8.2 Scope

This chapter considers the variant case of the All Containers Fail Disruptive Scenario in which all containers are assumed to fail at 10,000 years (see Chapter 6). This case assumes that an undefined event or process causes the copper cladding on all used fuel containers to fail, thereby exposing the entire carbon steel container surface area to anoxic, deep groundwater that has entered the repository following closure. This initiates carbon steel corrosion, gas generation and gas migration.

This is the bounding scenario, in that it has the largest potential for gas production and radiological impact from gas-borne radionuclides.

Additional gas sources, such as those arising from corrosion of rock bolts, degradation of trace organic materials in the backfill, and radiolysis of water are neglected on the basis that the amount of gas produced by such processes is much less than the amount of gas produced due to corrosion of all containers.

8.3 Conceptual Model

The generation and migration of gas is a coupled process, in which gas generation is dependent on the availability and transport of groundwater near the container. Gas can migrate through the repository by:

- Dilational flow, where gas pressure exceeds the local confining stress and physically displaces material, with gas moving through the resultant open pathway. Pathways are typically small scale and are localized. They will generally propagate until sufficient pathway volume has been opened to reduce the pressure. Dilational flow paths are typically unstable and will close once the pressure is reduced below the confining stress.

- Conventional two-phase flow, where gas pressure is sufficient to partially or completely displace water from the pore space of a material, allowing gas to travel through the connected porosity.

- Dissolving in groundwater, where dissolved gas can travel with groundwater flow or diffuse through groundwater.

The following sections describe the conceptual model for gas generation and transport applied in the analysis.

8.3.1 Gas Generation

In low-permeability sedimentary rock, saturation of the repository may take thousands of years. This leads to the definition of the following four phases in the evolution of the corrosion environment (see Chapter 5):

Phase 1: This is an early aerobic period that occurs prior to the onset of aqueous corrosion, immediately following closure of the repository. In this phase, saturation of the materials surrounding the container has not yet occurred, no liquid water is available for corrosion, and the material immediately adjacent to the container remains unsaturated due to high

temperatures. Oxygen is initially present in the unsaturated pore space. If relative humidity is also low, corrosion is limited to slow air oxidation.

Phase 2: This is an unsaturated aerobic phase that occurs following the condensation of liquid water on the steel surface. Steel corrosion is higher under these conditions.

Phase 3: This corresponds to an unsaturated anaerobic phase that occurs following the consumption of oxygen but prior to full saturation of the materials surrounding the container. Corrosion during this period is supported by the cathodic reduction of water accompanied by the evolution of hydrogen.

Phase 4: This is a saturated anaerobic phase that is entered once the materials surrounding the container have become fully saturated by groundwater. As with Phase 3, corrosion during Phase 4 is supported by the cathodic reduction of water accompanied by the evolution of hydrogen.

These four phases do not necessarily occur sequentially. Phases 1 and 2 both occur under aerobic conditions and the degree to which the Phase 1 and Phase 2 corrosion processes are active depends on the relative humidity. The Phase 3 and 4 corrosion processes proceed under anaerobic conditions after Phase 1 and Phase 2 and may occur concurrently. The Phase 3 process also depends on relative humidity.

There are a number of processes, such as methanogenesis, through which the quantity of gas in the repository may be reduced as discussed in Suckling et al. (2012). The gas modelling presented in this chapter takes no credit for these pressure mitigation processes.

Parameter values used in the corrosion calculations are discussed in Gobien et al. (2013).

8.3.2 Gas Migration and Transport

In this assessment, conventional two-phase flow and groundwater dissolution processes are considered sufficient for estimating gas migration through the repository. Whereas dilational flow describes transport through EBS materials that are near-fully saturated, in this system gas generation and migration are expected to desaturate different components of the EBS to varying degrees. This approach is consistent with other programs in which numerical modelling of gas migration has focussed primarily on conventional two-phase flow (Senger et al. 2011, Yu and Weetjens 2009, Marschall et al. 2005).

Two-phase flow gas migration modelling is based on the van Genuchten model for water retention (van Genuchten 1980, Mualem 1976). This model describes the relationship between the water content of a porous matrix and the suction, or capillary pressure. Capillary pressure is the difference in pressure across the interface between two immiscible fluids, and is defined here as the difference in pressure between the gas phase (non-wetting phase) and the water phase (wetting phase). The pressure difference is a function of the pore throat radius, with capillary pressure increasing as the wetting fluid is displaced into smaller and smaller pores. The model parameters have been fitted to the measured behavior of bentonites and also low permeability limestone and shale rocks.

The van Genuchten equations for capillary pressure as a function of liquid saturation are as follows.

$$P_c = -\frac{1}{\alpha}\left[S_{ec}^{-1/m} - 1\right]^{1/n} \tag{8-1}$$

$$S_{ec} = \frac{S_l - S_{lrc}}{1 - S_{lrc}} \tag{8-2}$$

where:

- P_c is the capillary pressure, Pa;
- α is a van Genuchten fitting parameter, Pa^{-1}. The inverse of α is analogous to the air entry pressure, but is often larger than the actual air entry pressure;
- S_{ec} is the effective saturation for the capillary pressure relationship (volume ratio);
- S_l is the liquid saturation (volume ratio);
- S_{lrc} is the residual liquid saturation for capillary pressure (volume ratio), the liquid saturation below which liquid does not flow, and capillary pressure is confined;
- m is a van Genuchten fitting parameter (unitless); and
- n is a van Genuchten fitting parameter (unitless).

Relative permeability of gas and liquid is described using the Luckner form of the van Genuchten-Mualem equations, as follows:

$$k_{rl} = S_{ek}^{1/2}\left[1 - (1 - S_{ek}^{1/m})^m\right]^2 \tag{8-3}$$

$$k_{rg} = (1 - S_{ek})^{1/3}\left[1 - S_{ek}^{1/m}\right]^{2m} \tag{8-4}$$

$$S_{ek} = \frac{S_l - S_{lr}}{1 - S_{lr} - S_{gr}} \tag{8-5}$$

where:

- k_{rl} is the liquid phase relative permeability (ratio);
- k_{rg} is the gas phase relative permeability (ratio);
- S_{ek} is the effective saturation for the relative permeability relationship (volume ratio);
- S_{lr} is the residual liquid saturation (volume ratio), the liquid saturation below which liquid does not flow; and
- S_{gr} is the residual gas saturation (volume ratio), the gas saturation below which gas does not flow.

Table 8-1 shows the two-phase flow properties used for each material.

Table 8-1: Two-Phase Flow Properties

Material	1/α(MPa)	n	m	S_{lrc}	S_{lr}	S_{gr}
Unit B and C	0.31	4.22	0.35	0.54	0.55	0.00
Unit A-2 Carbonate	0.76	3.06	0.50	0.00	0.00	0.00
Unit A-1 Upper Carbonate	0.04	4.89	0.15	0.24	0.25	0.00
Unit A-1 Carbonate	38.9	2.41	0.99	0.00	0.00	0.00
Unit A-1 Evaporite	2.06	2.28	0.99	0.00	0.01	0.10
Unit A0	2.06	2.28	0.99	0.00	0.01	0.10
Guelph	0.04	4.89	0.15	0.24	0.25	0.00
Fossil Hill	27.9	6.11	0.68	0.02	0.03	0.00
Cabot Head	14.6	6.82	0.24	0.00	0.00	0.05
Manitoulin	40.8	3.65	1.31	0.10	0.11	0.05
Queenston	35.6	4.45	1.13	0.08	0.09	0.06
Georgian Bay/Blue Mountain	30.1	3.82	1.10	0.16	0.17	0.04
Cobourg	61.7	3.13	1.69	0.05	0.06	0.03
Sherman Fall	28.2	2.33	1.00	0.16	0.17	0.11
Kirkfield	173	2.17	7.22	0.00	0.00	0.15
Cobokonk	66.2	1.82	1.73	0.00	0.00	0.03
Gull River	40.0	4.06	0.78	0.20	0.21	0.11
Shadow Lake	0.23	1.20	0.58	0.03	0.04	0.00
Cambrian	0.23	1.20	0.58	0.03	0.04	0.00
Upper Precambrian	0.23	1.20	0.58	0.03	0.04	0.00
Precambrian	0.23	1.20	0.58	0.03	0.04	0.00
Fossil Hill EDZ	5.57	6.11	0.68	0.02	0.03	0.00
Cabot Head EDZ	2.90	6.82	0.24	0.00	0.00	0.05
Manitoulin EDZ	8.16	3.65	1.31	0.10	0.11	0.05
Queenston EDZ	7.12	4.45	1.13	0.08	0.09	0.06
Georgian Bay EDZ	6.02	3.82	1.10	0.16	0.17	0.04
Cobourg EDZ	1.23	3.13	1.69	0.05	0.06	0.03
Repository Inner EDZ	2.47	3.13	1.69	0.05	0.06	0.03
Repository Outer EDZ	6.17	3.13	1.69	0.05	0.06	0.03
Placement Room Bentonite (Homogenized Bentonite)	20.6	1.06	0.61	0.03	0.40	0.00
Tunnel Seal Bentonite (HCB Seal)	34.6	1.36	0.67	0.03	0.40	0.00
Tunnel Dense Backfill	10.0	1.80	0.40	0.10	0.10	0.01
Concrete (LHHPC), degraded	1.00	2.00	0.50	0.20	0.20	0.10
Shaft Asphalt	-	-	-	-	0.00	0.00
Shaft Bentonite/Sand	10.0	1.80	0.40	0.01	0.01	0.01

Note: Data taken from Gobien et al. (2013)

The two-phase flow relationship between gas and liquid is based on a capillary pressure function and a relative permeability function. Figure 8-1 to Figure 8-3 show these functions for Placement Room Bentonite, Repository Inner EDZ, and the intact host rock of the Cobourg formation. These curves are formulated using the two-phase flow parameters associated with these materials.

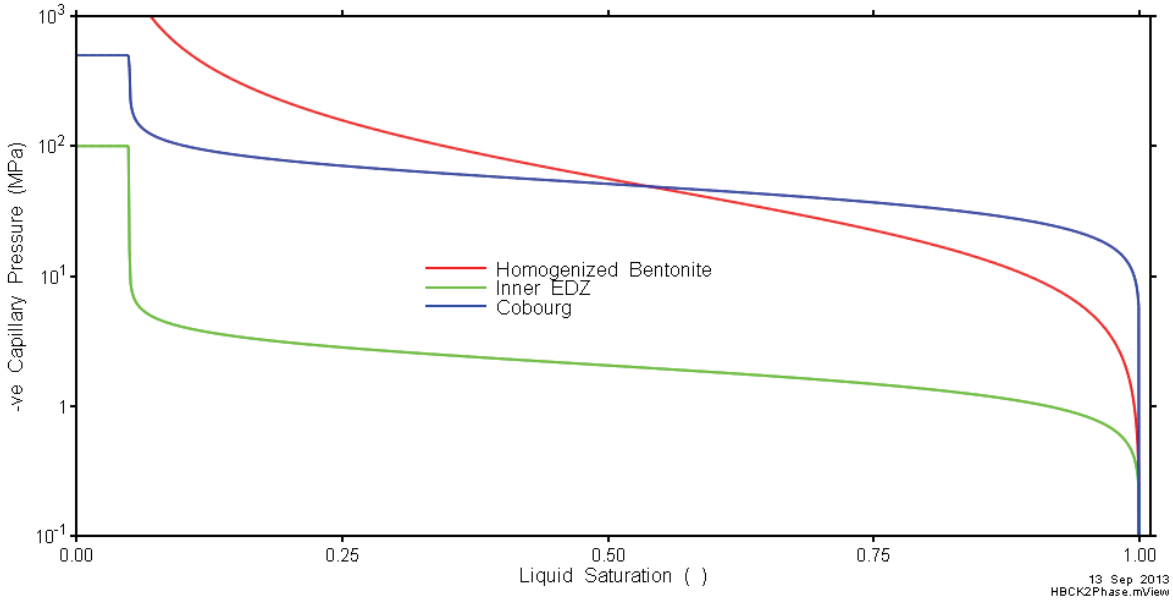

Figure 8-1: Capillary Pressure Curves for Placement Room Bentonite (Homogenized Bentonite), Repository Inner EDZ, and the Cobourg Formation

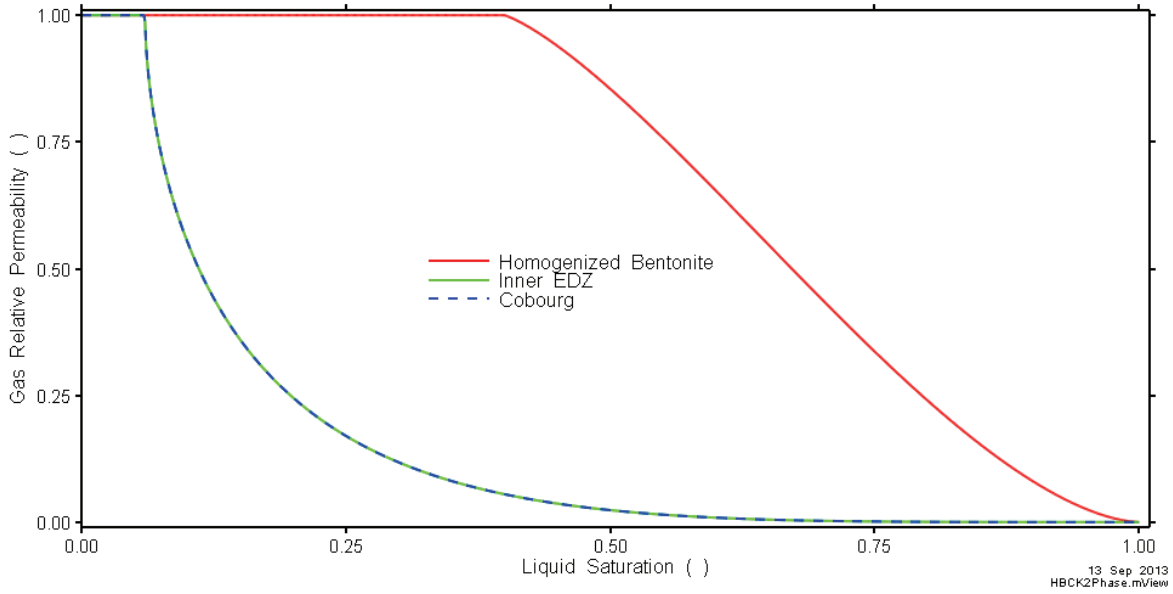

Figure 8-2: Relative Gas Permeability Curves for Placement Room Bentonite (Homogenized Bentonite), Repository Inner EDZ, and the Cobourg Formation

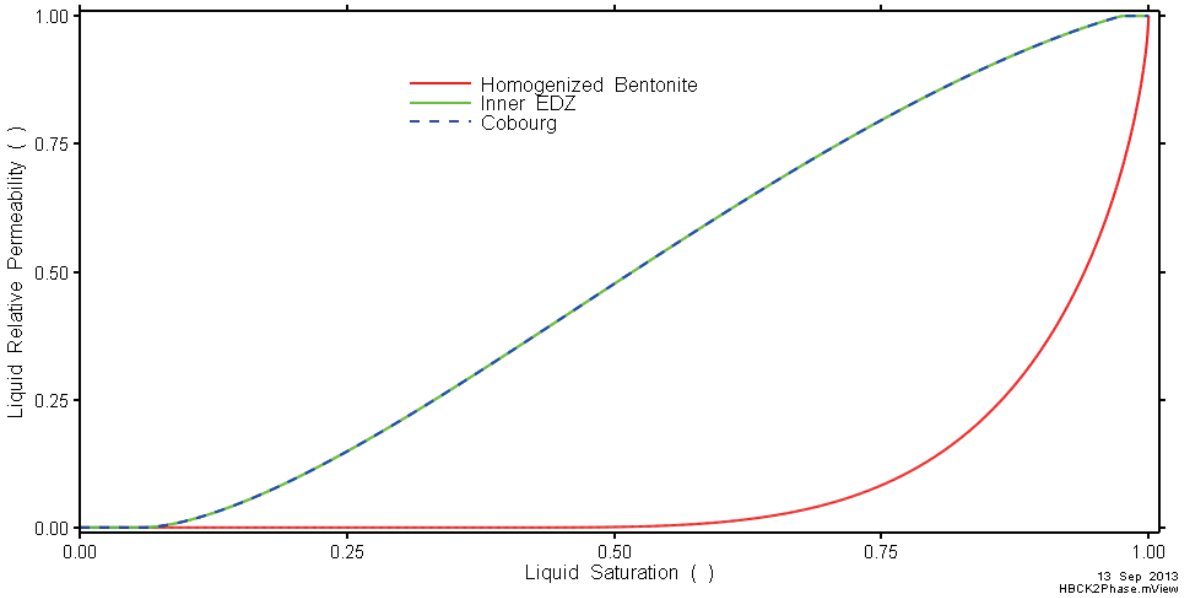

Figure 8-3: Relative Liquid Permeability Curves for Placement Room Bentonite (Homogenized Bentonite), Repository Inner EDZ, and the Cobourg Formation

Dissolution of gas in water is described by Henry's law, where the concentration of dissolved gas is proportional to the partial pressure of the gas. Salinity reduces the Henry's law coefficient, and a value of 4×10^{-11} mol fraction/Pa is used for hydrogen in this study (Quintessa and Geofirma 2011).

8.4 Computer Code

The conceptual model is numerically represented in the T2GGM computer code (Suckling et al. 2012).

Figure 8-4 identifies the interrelationship with repository parameters. Information from engineering design and site characterization is used to develop a site-specific system description.

T2GGM assesses the coupled behaviour between gas generation, temperature and the movement of gas and water. It is composed of two coupled models: the Gas Generation Model (GGM) used to describe the generation of gas due to corrosion of steel components, and the TOUGH2 model (Pruess et al. 1999) used to describe gas and water transport from the repository and within the geosphere. Key outputs are estimates of the repository pressure, repository saturation, and gas flow rates within the geosphere and repository system.

T2GGM has recently been used for gas modelling in support of the postclosure safety assessment for the Low and Intermediate Level Waste DGR proposed by Ontario Power Generation (Geofirma and Quintessa, 2011). T2GGM was used to calculate the generation and build-up of gas in the repository, the exchange of gas and groundwater between the repository and the surrounding rock, and between the rock and the surface environment.

The two coupled models are described below.

Table 8-2 provides more information on T2GGM.

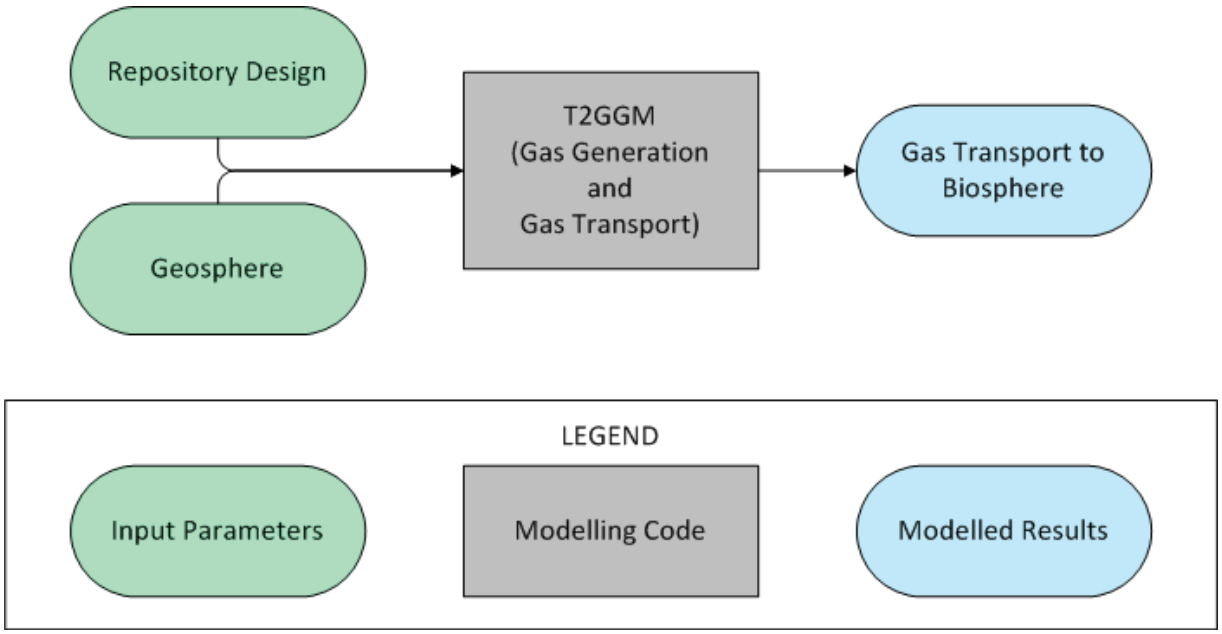

Figure 8-4: Main Computer Code

TOUGH2:

The TOUGH2 gas transport model is a widely used code for two-phase flow and gas transport in geological media, including for deep geological repositories (e.g., Talandier et al. 2006, Nagra 2008, FORGE 2010, Bate et al. 2012).

TOUGH2 is a multi-phase flow and heat transport program for fluid mixtures. T2GGM Version 3.1 includes TOUGH2 Version 2.0 with the EOS3 V1.01 equation-of-state module (ideal gas – air and water) (Pruess et al. 1999). The EOS3 module defines two-phase flow of water and air, or single-phase flow of water or air. Thermophysical properties of water are represented by steam-table equations, while the air is treated as an ideal gas. Dissolution of air in water is modelled with Henry's law. For T2GGM Version 3.1, an option is provided to represent the gas phase by an alternative gas, such as H_2.

GGM:

GGM is a gas generation model developed for NWMO (Suckling et al. 2012). It is implemented as a FORTRAN module that is used by TOUGH2 to incorporate gas generation due to corrosion and degradation processes. GGM includes a kinetic description of the various microbial and corrosion processes that lead to the generation and consumption of various gases. GGM can also be used to assess the effect of different gas-mitigation methods and other processes that can lead to the consumption of gas in the repository.

The GGM gas generation model is consistent with general literature and with approaches adopted in other waste management organizations for similar models.

Table 8-2: T2GGM, V3.1

Parameter	Comments
Components:	
TOUGH2	Core Code Version 2.0
EOS3	TOUGH2 Equation of State Module 3 Version 1.01
GGM	Gas Generation Component of T2GGM Version 3.1
Main Documents	T2GGM Version 3.1: Gas Generation and Transport Code (Suckling et al. 2012) TOUGH2 User Guide (Pruess et al. 1999)
Main Features:	- Temperature-dependent corrosion product and hydrogen gas generation from corrosion of steel and other alloys under aerobic and anaerobic conditions in the presence of a bentonite buffer - CO_2-enhanced corrosion of carbon steel and passive alloys - CO_2 and CH_4 gas generation from degradation of organic materials under aerobic and anaerobic conditions - H_2 gas reactions, including methanogenesis with CO_2 - Limitation of both microbial and corrosion reactions by the availability of water - Carbon, iron and water are mass balanced within repository reactions - Exchange of gas and water between the repository and the surrounding geosphere - Calculation of the generation and build-up of gas in each repository volume - Two-phase flow of water and gas within the geosphere with gas dissolution according to Henry's law - Heat flow coupled to two-phase flow of water and gas - 1D hydro-mechanical model to assess the effects of a uniformly applied glacial stress - Time-variable permeability, allowing the permeability properties of certain materials, such as engineered materials or EDZ, to evolve or degrade with time - Time-variable Dirichlet boundary conditions - The ability to stop and restart the simulations

8.5 Analysis Methods and Key Assumptions

Gas generation and transport are investigated using models at two different scales of resolution: Room-Scale and Repository-Scale.

The Room-Scale Model considers hydrogen gas generation from corrosion processes and two-phase flow with a simplified EBS geometry. It also considers thermal effects on groundwater flow and gas flow associated with heat transfer from the used fuel containers. The model domain extends to include a single full placement room and associated cross-cut drift.

Gas behaviour within each placement room is assumed sufficiently similar for Room-Scale results to be representative of gas behaviour in all placement rooms. Gas transport results are scaled to represent entire panels, each compromising either 27 or 28 placement rooms, with the scaled results used as input to the Repository-Scale Model. Gas transport data are provided to the Repository-Scale Model at locations where the cross-cut drifts intersect the main access tunnel. A constant pressure is specified at the cross-cut drift external boundary.

The Repository-Scale Model considers the transport of gas and water, without thermal effects, along the main drifts and shaft of the repository, using results from the Room-Scale Model to estimate the amount of gas reaching the drifts.

8.5.1 Overall Approach

During setup, the model is initially run for a sufficient period of time to allow the pre-construction conditions to equilibrate. Thereafter, simulations are conducted in three consecutive segments to account for the evolution of repository conditions. These are:

1. Preclosure – the engineered facilities are open to atmospheric pressure and are fully saturated with gas[1] for the operational period prior to closure. This is assumed to be seven years for placement rooms and 60 years for the main drift. Desaturation of the neighbouring rock is modelled and used to initialize the postclosure period.

2. Postclosure / pre-failure – the EBS is placed with specified gas saturations[2] at atmospheric pressure within the room and cross-cut drift (Room-Scale Model) or main drift and shaft (Repository-Scale Model) as the system is sealed. The system repressurizes and resaturates for 10,000 years with no gas generation taking place.

3. Post-failure – the steel container is exposed to the surrounding EBS and gas generation commences. Gas generation processes and rates are calculated as described in Section 8.3.1.

---

[1] Although the actual gas present in the pre-closure period is air, hydrogen is used in the simulations for consistency with the post-failure stage.

[2] Gas saturation is the volumetric fraction of a material's porosity that is filled with free-phase gas. Similarly, liquid saturation is the fraction of porosity filled with liquid. Within a pore's volume, the sum of the gas and liquid saturations is unity.

Pressure, gas saturation and dissolved gas content are continuous within the geosphere from one segment to the next.

The Room-Scale and Repository-Scale models are separate models and manual iteration is performed to ensure consistency between the model pressures at the interface location. A fully integrated model would allow time-dependent calculation of the interface pressure.

8.5.2 Detailed Transport Models

This section describes the Room-Scale and Repository-Scale Models.

Both models use the geosphere and repository material properties described in Chapter 2 and Chapter 4. Thermal processes are considered in the Room-Scale Model while the Repository-Scale Model is isothermal.

Within the host rock and the various engineered sealing materials, interactions between gas and liquid are modelled using the van Genuchten equations for water retention described in Section 8.3.2.

8.5.2.1 Room-Scale Model

The Room-Scale Model uses a simplified EBS geometry. The model domain consists of a full placement room and associated cross-cut drift. Gas generation, thermal effects and two-phase flow are simulated, with gas flow rates in the cross-cut drift calculated for input to the Repository-Scale Model.

The domain includes all 50 containers, the concrete and bentonite seals, and the access drift connecting it to the cross-cut drift. Horizontal symmetry is assumed and only one-half of the cross-section is modelled, including 10 m of host rock horizontally adjacent to the room. The plan section domain of 514.4 m × 10 m represents the full length of the single room located in the middle of the repository including one-half the intact rock separating the room from adjacent repository panels. The vertical extent of the model is from 1000 metres below the repository to the top of the Salina Unit B and C formations.

The 50 containers in the room are grouped into 10 combined containers where each combined container has the corrosion and heat generating characteristics of 5 individual containers. The combined containers have the length and volume of 5 individual containers so that the amount of bentonite is the same as in the actual system. Figure 8-5 illustrates the model.

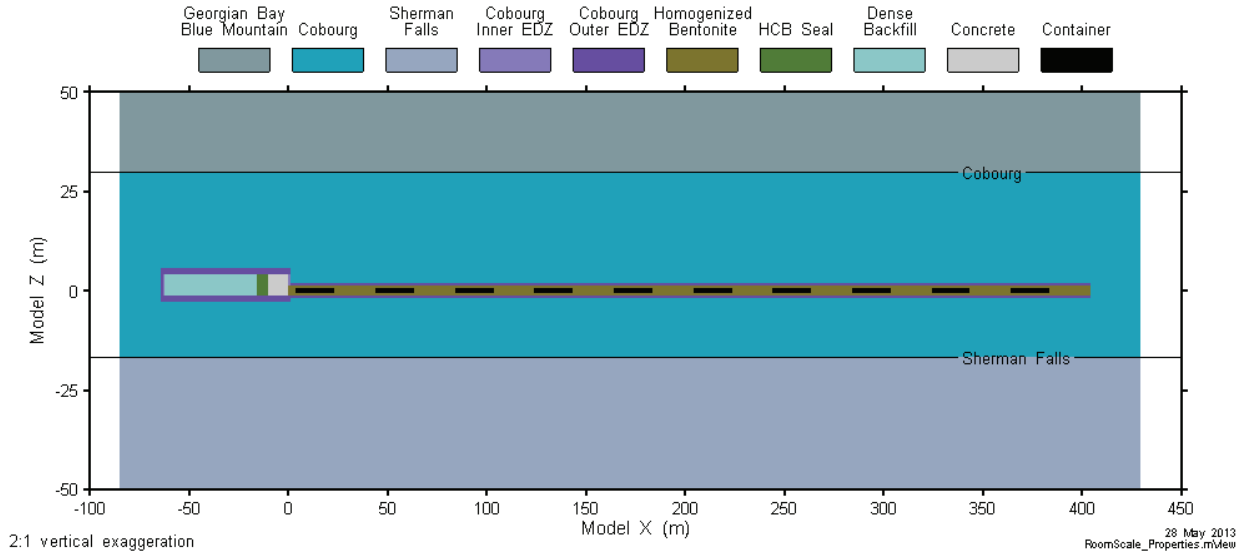

Figure 8-5: Room-Scale Model – Illustration

Figure 8-6 shows the drift end of the room. The drift is rectangular. Although the room is designed as circular with a radius of 1.25 m, it is implemented in the model as a square with equivalent cross-sectional area (i.e., 2.2 m width and height).

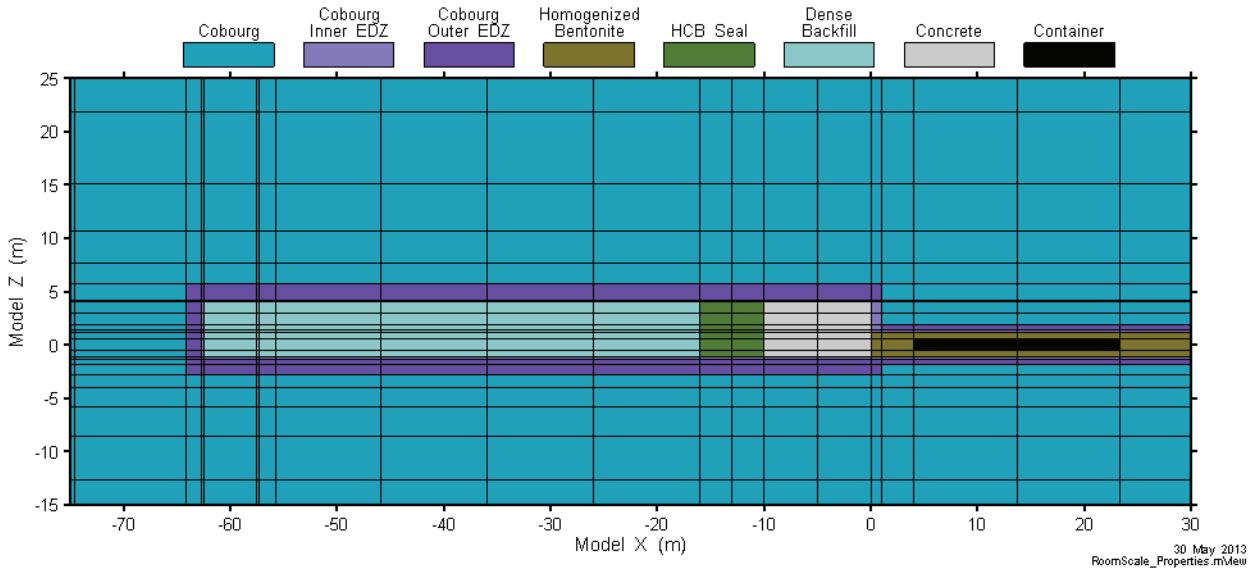

Figure 8-6: Room-Scale Model – Drift End of Room

Cross-sections through the first container and through the seal portion of the room entry drift are shown in Figure 8-7.

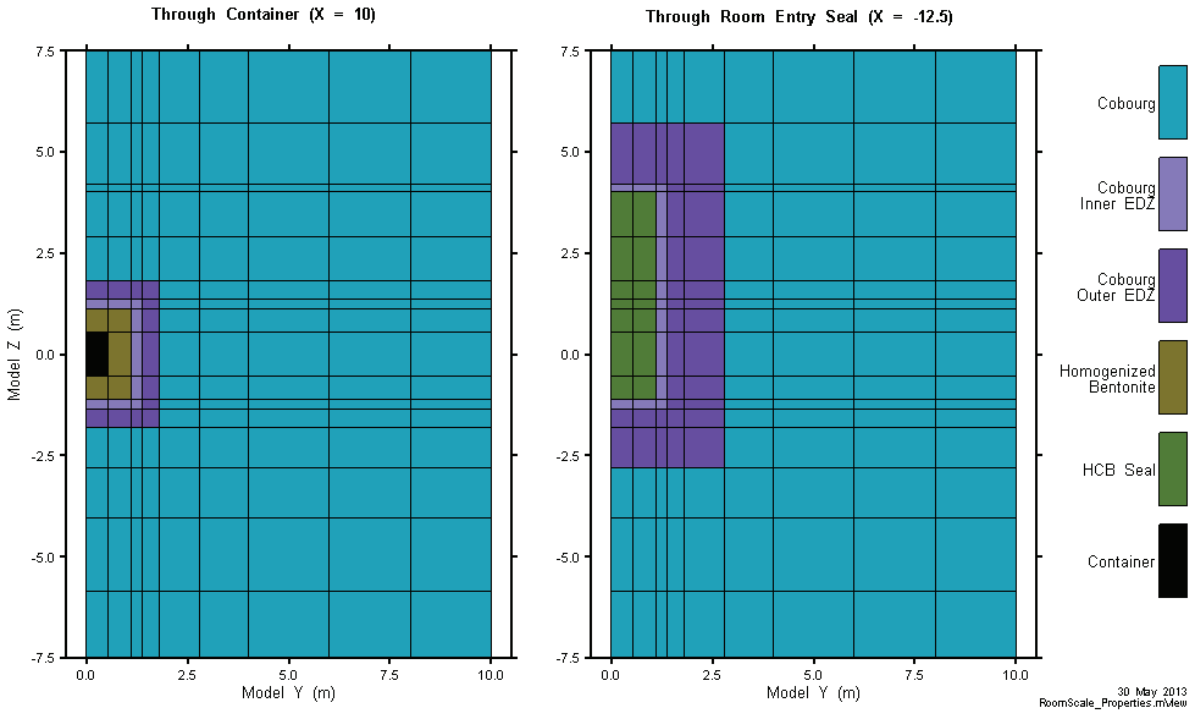

Figure 8-7: Room-Scale Model – Cross-Sections showing Container and Seal

Figure 8-8 is a plan section showing the container, room seal and cross-cut drift discretization. Some elements of the room dimensions and property assignments have been modified from the design specification to simplify the discretization. Specifically:

- The room entry drift is straight, rather than curved.
- The room entry drift width is 2.2 m (consistent with the simplified placement room) rather than 2 m, as specified in the design.
- The seal design is simplified in the model as it does not intersect the inner EDZ[3].
- The pedestal and surrounding bentonite pellets are combined into a single material with blended material properties.

These simplifications are not expected to materially affect model results.

The discretization contains 63 layers and 12,622 nodes.

[3] An additional smaller EDZ is associated with excavation of the seals and is assigned the same hydraulic conductivity as the EDZ surrounding all excavated spaces (see Section 7.3.2).

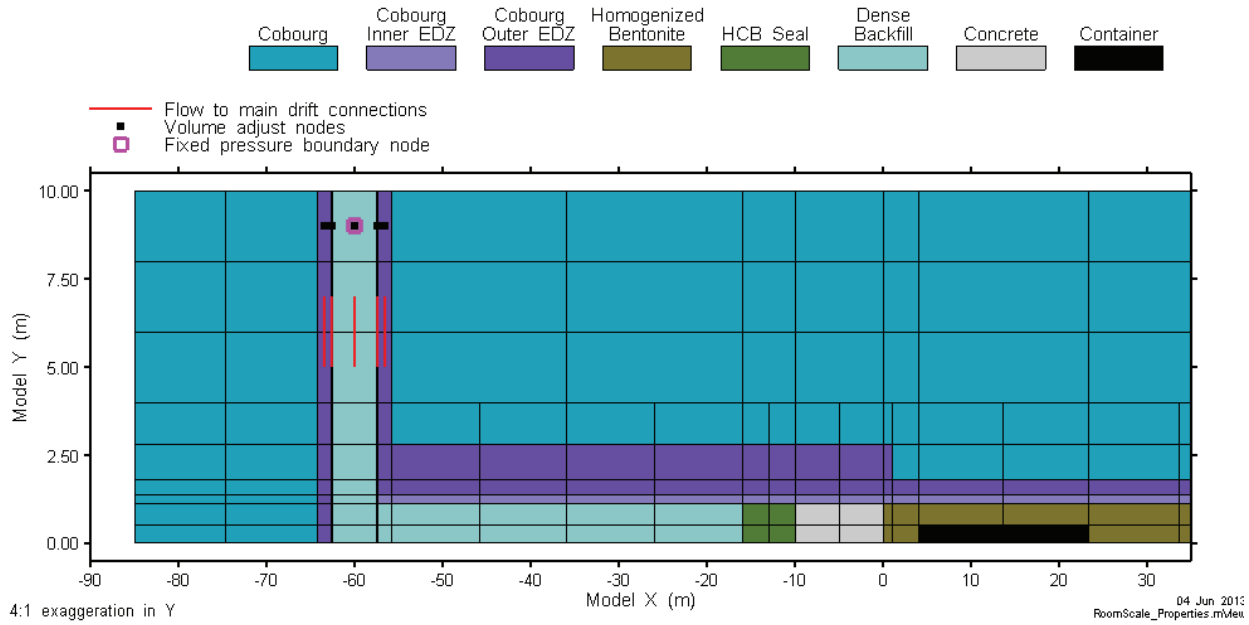

Figure 8-8: Room-Scale Model – Plan Section Cutting Middle of Placement Room

Boundary and Initial Conditions:

Pressure boundary conditions at the top and bottom of the model (i.e., the Salina Units B and C formations and 1000 m below the repository, respectively) are set to simulate a system at hydrostatic equilibrium. Initial pressures for all intact rock nodes are set to freshwater hydrostatic[4].

Highly compacted bentonite and dense backfill used in room seals and tunnels are assigned liquid saturations of 65% and 80% respectively. The bentonite around the containers was homogenized and initialized at 11% liquid saturation, representing the volumetrically averaged initial saturations of the pellet backfill (6%) and compacted block pedestal material (65%).

Thermal boundary conditions are defined according to Guo (2008). A temperature of 5°C was specified at the top of the model (ground surface). A temperature at the bottom of the model (1000 m below the repository) was defined based on a thermal gradient of 0.016°C/m through the sedimentary sequence, and a gradient of 0.012°C/m through the lower granite due to its higher thermal conductivity.

[4] Variations in fluid density will have negligible impact on the simulations, where pressures and flows are largely driven by processes occurring within the placement room. T2GGM has the ability to scale water density to simulate saline water; however, this feature was not used.

The thermal source term for heat released as a result of radioactive decay has been adopted from Guo (2008). Only heat generated by radioactive decay is considered. Although aerobic corrosion of steel is exothermic, the total heat generated would be negligible compared to the decay heat. Anaerobic corrosion of steel is endothermic. The watt-per-container values from Guo (2008) were multiplied by 50 to account for the 50 containers in the room, and then divided by two to reflect the half-room geometry. The resulting thermal source term was uniformly distributed among each of the two nodes in each of the ten combined containers.

Because the Room-Scale and Repository-Scale Models are each run independently, a fixed-pressure boundary node (see Figure 8-8) with pressure set to 6.8 MPa is used to couple the Room-Scale Model to the Repository-Scale Model. The 6.8 MPa value was determined by manual iteration of the two models. The node is defined to remain at 100% liquid saturation - this allows gas to exit the model, but does not allow gas to enter the model from the boundary.

Temperature at the boundary node is set to 14°C, determined by preliminary runs to be the long-term average temperature after 100,000 years. The fixed-temperature value is an approximation to simplify implementation. This affects the temperature in the drift, but has only a very small effect on the average temperature in the placement room.

GGM Implementation:

Preliminary scoping simulations indicated that the thermal state and resaturation profile did not vary significantly over the length of the room. Consequently, a single GGM compartment is used to simulate corrosion-generated gas from all containers in the room. The compartment consists of all homogenized bentonite nodes that are directly connected to a container node, as shown in Figure 8-9. The source term mass and surface areas are specified consistent with 50 half containers.

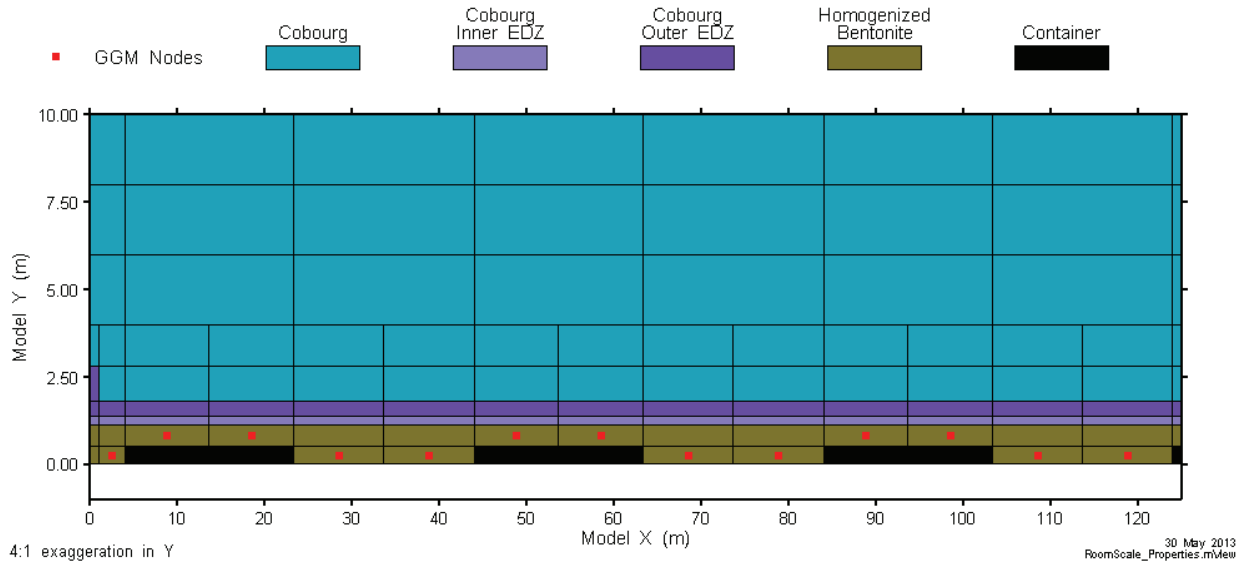

Figure 8-9: Room-Scale Model – Plan View Showing GGM Nodes

8.5.2.2 Repository-Scale Model

The Repository-Scale Model considers the transport of gas and water, without thermal effects, along the main drifts and shaft of the repository, using results from the Room-Scale Model to represent the amount of gas reaching the drifts. The model does not simulate any placement rooms.

The model domain consists of a single drift connecting the main and ventilation shafts. Horizontal symmetry is assumed; half the shafts are modelled. The model extends vertically from the bottom of the Coboconk formation up to the top of the Fossil Hill formation.

Figure 8-10 shows the model XY discretization, through the middle of the drift. Figure 8-11 shows an XZ slice through the middle of the drift intersecting one of the shafts. Figure 8-12 shows the shaft discretization in plan view. The outer EDZ is not represented.

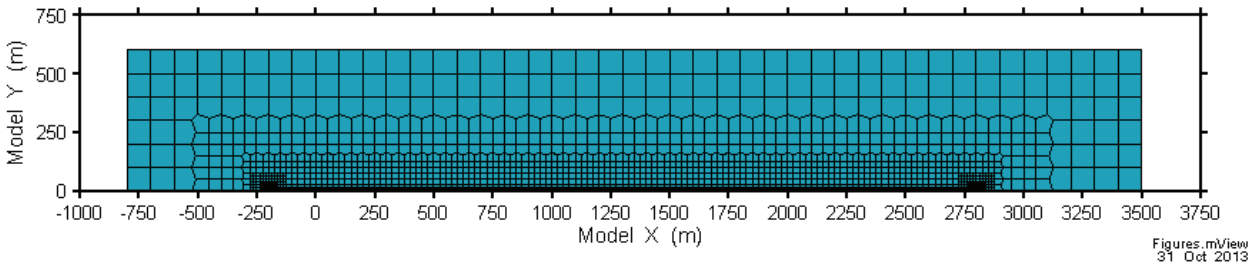

Figure 8-10: Repository-Scale Model – Plan View through the Main Drift

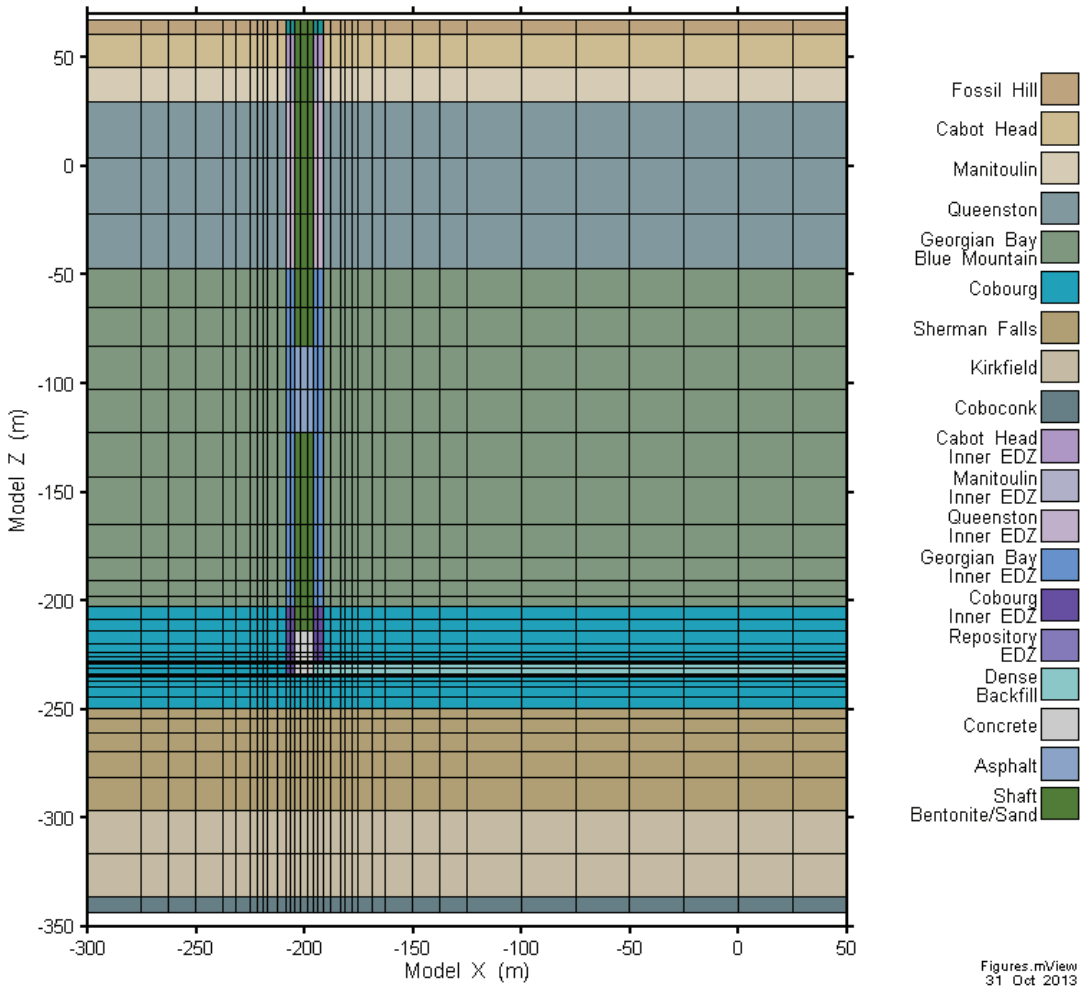

Figure 8-11: Repository-Scale Model – Drift and Shaft Discretization

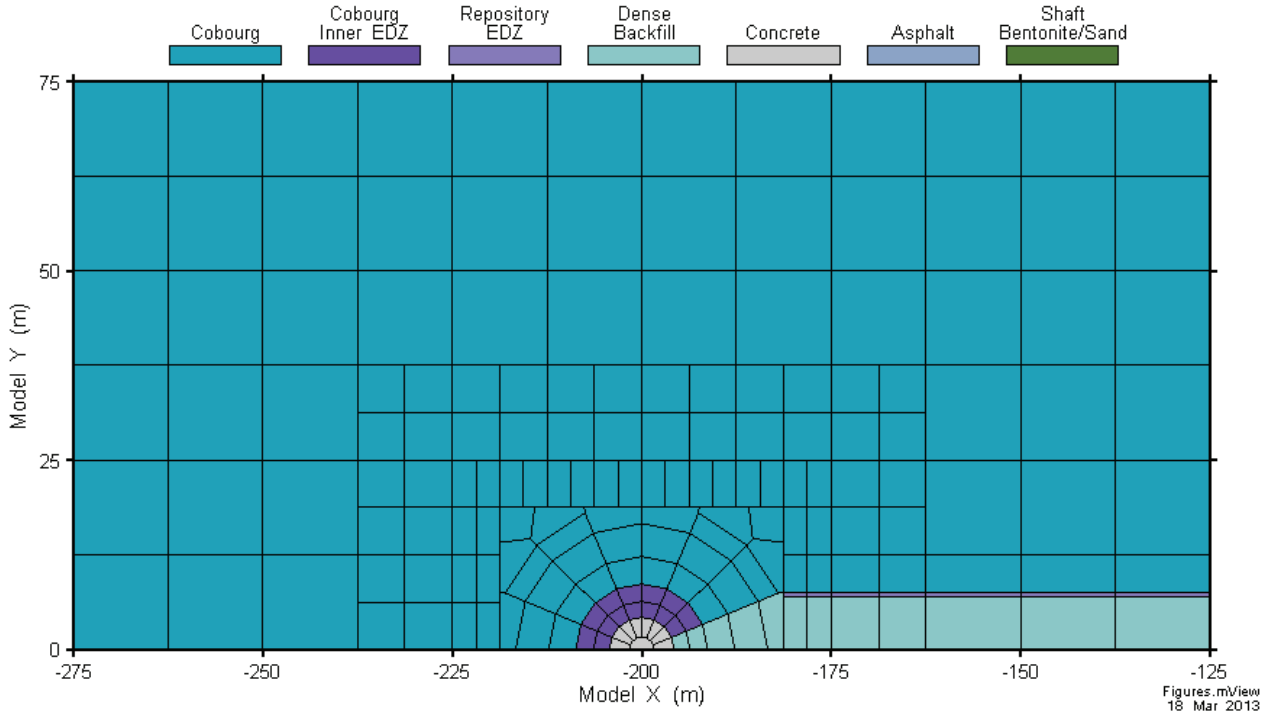

Figure 8-12: Repository-Scale Model – Plan View of Main Shaft Discretization

Boundary and Initial Conditions:

Pressure boundary conditions in the top and bottom layers of the model are calculated hydrostatic pressures based on a single point pressure obtained from the FRAC3DVS-OPG Site-Scale Model described in Chapter 7. This single point is located in the XY plane mid-way along the drift host rock, at the top of the Fossil Hill formation. The remaining sides of the model are no-flow boundaries.

Initially, the geosphere is assumed to be fully water-saturated. EBS materials have 80% saturation in the dense backfill and shaft seal at the start of the postclosure phase.

Gas is injected into the model at five locations, corresponding to intersections of the main access tunnel and the cross-cut drifts (Figure 8-13). The gas source term is calculated from results of the Room-Scale Model, multiplying the gas flow exiting a single room (i.e., from the end of the cross-cut drift segment, see Figure 8-8) by the average number of rooms in each panel[5]. This source term ignores the migration and accumulation of gas in the cross-cut drifts

[5] Half of the repository panels comprise 27 placement rooms while the other half comprise 28, providing an average of 27.5 placement rooms per panel. Multiplication factors are applied as required to account for the half-scale representation to ensure correct gas flows are used.

so that all gas leaving the Room-Scale Model is assumed to immediately reach the main access tunnel.

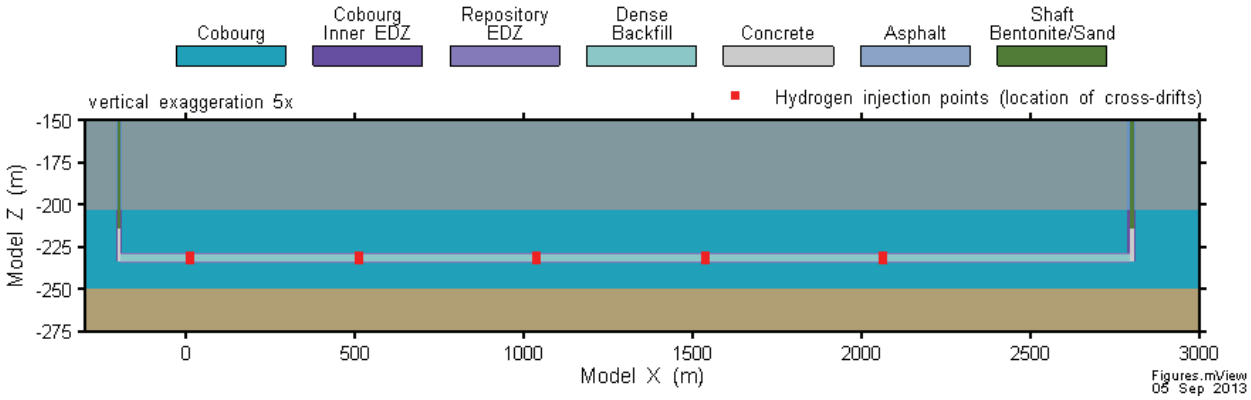

Figure 8-13: Repository-Scale Model – Gas Injection Locations

8.6 Results of Gas Generation and Transport Modelling

8.6.1 Room-Scale Model

Results from the Room-Scale Model simulation are shown in Figure 8-14 to Figure 8-20.

Figure 8-14 shows corrosion results in terms of container mass remaining (per container) and corrosion rates by process. The right hand axis shows the container mass remaining in terms of container wall thickness. The initial period of Phase 4 corrosion is caused by the high average liquid saturation (93%) within the EBS at the time of assumed failure. Phase 4 corrosion continues until the average gas saturation reaches 10%, after which only Phase 3 corrosion occurs. The corrosion rate decreases as temperature declines. Gas saturations near the container are relatively constant and remain high enough (greater than 10%) so that the criterion for resumption of Phase 4 corrosion is not reached until approximately 85,000 years. The container mass is exhausted by 440,000 years.

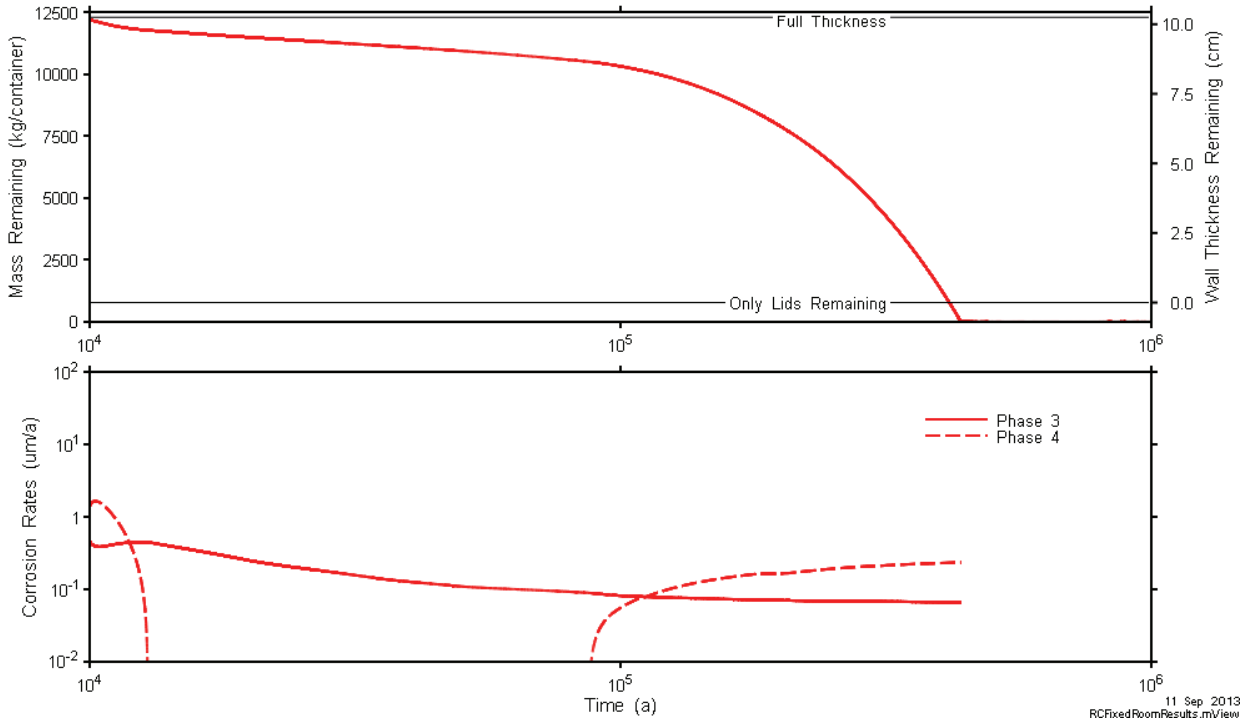

Note: the line labelled "Only Lids Remaining" indicates when the walls of the used fuel container have corroded. The lids are thicker than the walls.

Figure 8-14: Room Scale Model – Steel Consumption and Corrosion Processes

Figure 8-15 to Figure 8-18 show thermal profiles and gas saturation results for the following locations:

- Container – all nodes corresponding to the combined containers. These nodes have essentially no gas or liquid transport, but serve as thermal sources only.
- EBS – all engineered barrier system material (homogenized bentonite) for the nodes within the placement room beyond the concrete seal (i.e., Model X > 0).
- Inner EDZ – the inner EDZ of the placement room beyond the concrete seal.
- Intact rock – the closest intact rock nodes to the placement room beyond the concrete seal (i.e., nodes adjacent to the outer EDZ nodes).
- Intact rock 10 m – intact rock at the model boundary at Y =10 m.
- Cross-cut drift – the EBS material in the cross-cut drift.

The thin, lighter-coloured lines represent individual nodal values while the thicker, darker-coloured lines are the average of all nodes. For the intact rock and cross-cut drift, results are shown only for those nodes at the same elevation as the centre of the container (i.e., Model Z = 0.0).

Figure 8-15 and Figure 8-16 shows results for the first 10,000 years, or for the period of time prior to the assumed container failures. Figure 8-15 shows that the peak thermal pulse does not propagate to the drift, although drift temperatures have risen to near 50°C prior to the time of container failure. The placement room EBS and cross-cut drifts resaturate throughout the period and are approximately 90% saturated by 10,000 years. The inner EDZ does not start to resaturate until near the end of this time period, due in part to the high suction potential of the compacted bentonite within the placement room.

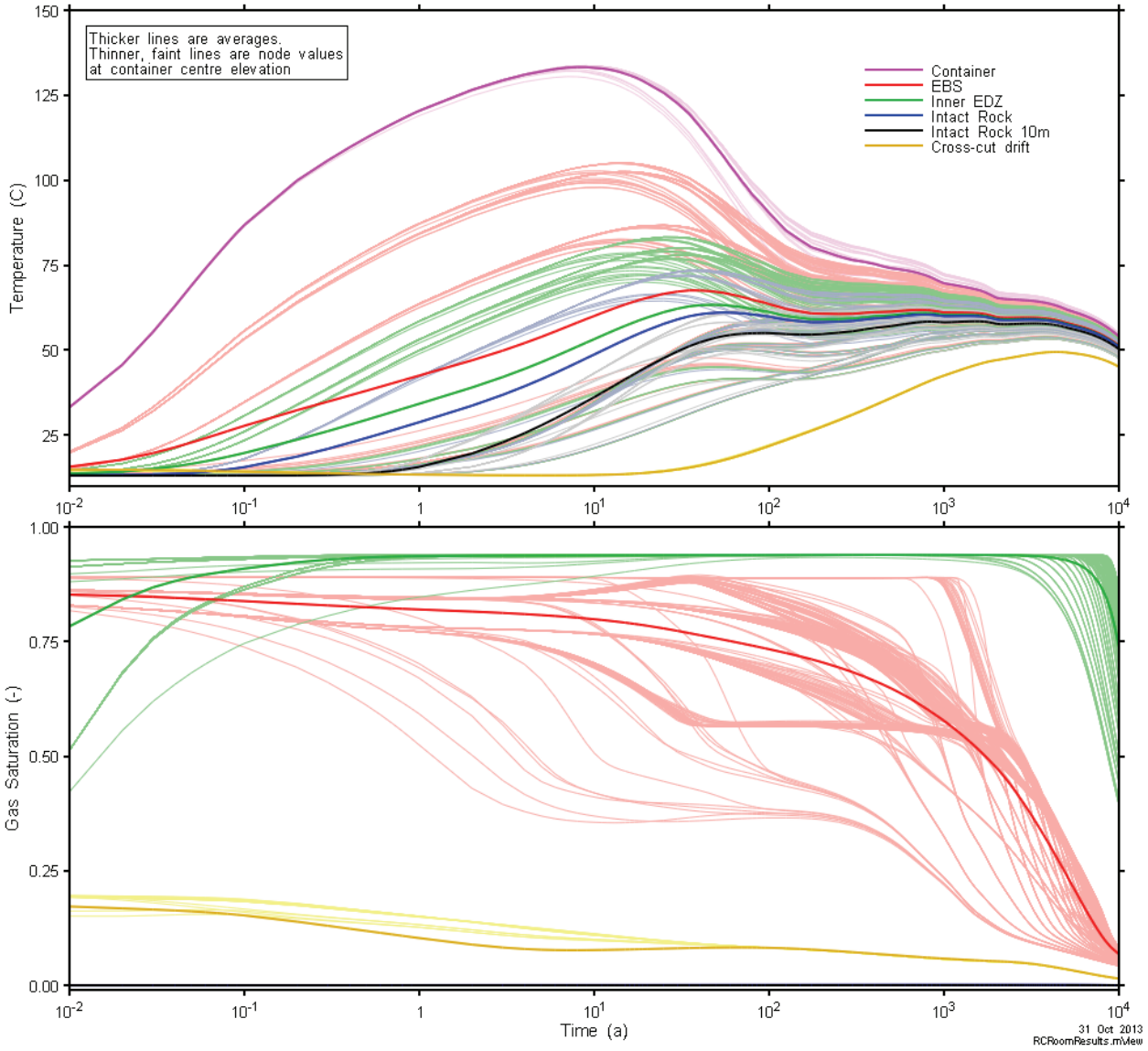

Figure 8-15: Room Scale Model – Conditions Prior to Container Failure

Figure 8-16 presents the gas, liquid and pore pressures[6] for the various locations. The figure shows that room and EBS pressures remain close to atmospheric (i.e., the pressure present when the repository is closed). Pressures in the intact rock at 10 m are initially hydrostatic but decrease in the 10 to 100 year period as fluid drains from the formation into the room during the resaturation process. The negative liquid and pore pressures represent suction pressures as calculated from the capillary pressure relationship.

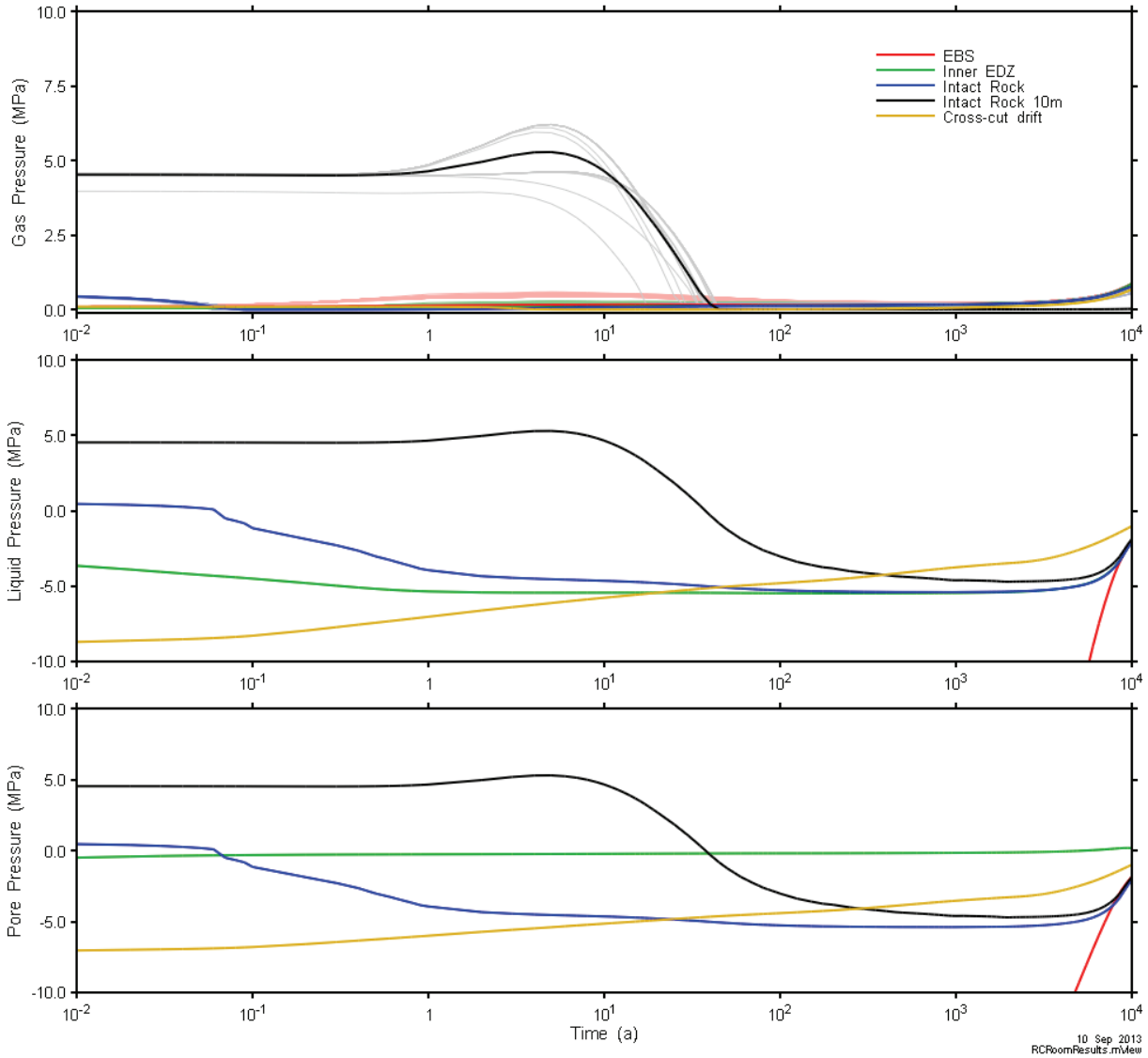

Figure 8-16: Room Scale Model – Nodal and Average Pressures Prior to Container Failure

[6] Pore pressure is calculated as the saturation-weighted average of gas and liquid pressures. The fluid volumetric saturations are used as a proxy for fluid surface areas on the contact surface. The resultant fluid pressure on the contact surface can be taken as a weighted average of the pressures in each of the two fluid phases (water and gas).

Figure 8-17 and Figure 8-18 show results for the period of time after the assumed container failures. Figure 8-17 shows that the thermal profile is uniform across the room, EDZ and intact rock, and that temperature declines to a near-steady state by 100,000 years. Gas saturations in the Inner EDZ reach 94% as generated gas moves from the EBS to the EDZ and porewater flows from the EDZ to the EBS due to the capillary pressure gradient. Gas saturations within the EBS and cross-cut drift increase slowly over the simulation with maximum gas saturations in the EBS reaching approximately 15%. Gas saturations in the intact rock at 10 m are essentially zero. The change in slope occurring at 440,000 years correlates with the time at which corrosion ceases because the entire mass of the container has corroded (Figure 8-14).

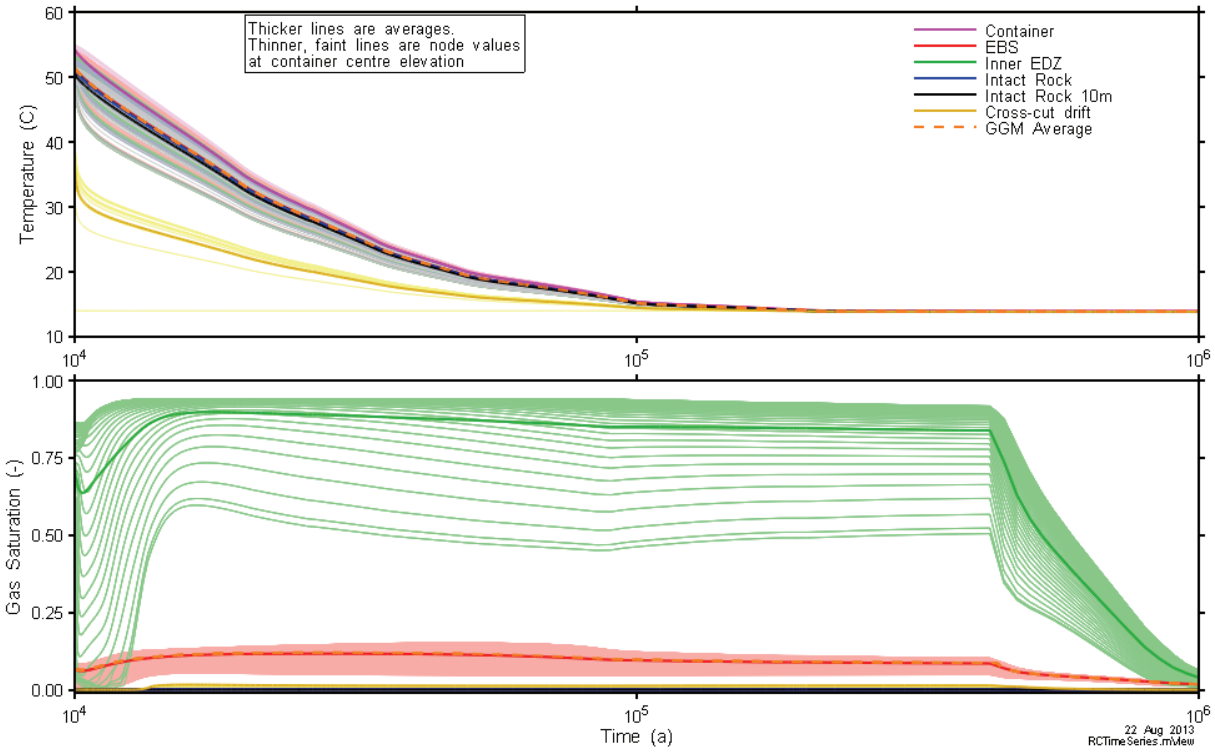

Figure 8-17: Room Scale Model – Conditions after Container Failure

Figure 8-18 presents the gas, liquid and pore pressures for the various locations. Pore pressures, shown in the bottom figure, represent the pressure experienced in the identified component. The results show that pore pressure in the intact rock (blue and black lines) remains well below 80% of lithostatic pressure (i.e., 9.9 MPa) throughout the simulation. Pressure in the cross-cut drift (yellow line) is constant because this is the imposed boundary condition, as discussed in Section 8.5.2.1. The change in slope occurring at 440,000 years correlates with the time at which corrosion ceases because the entire mass of the container has corroded (Figure 8-14).

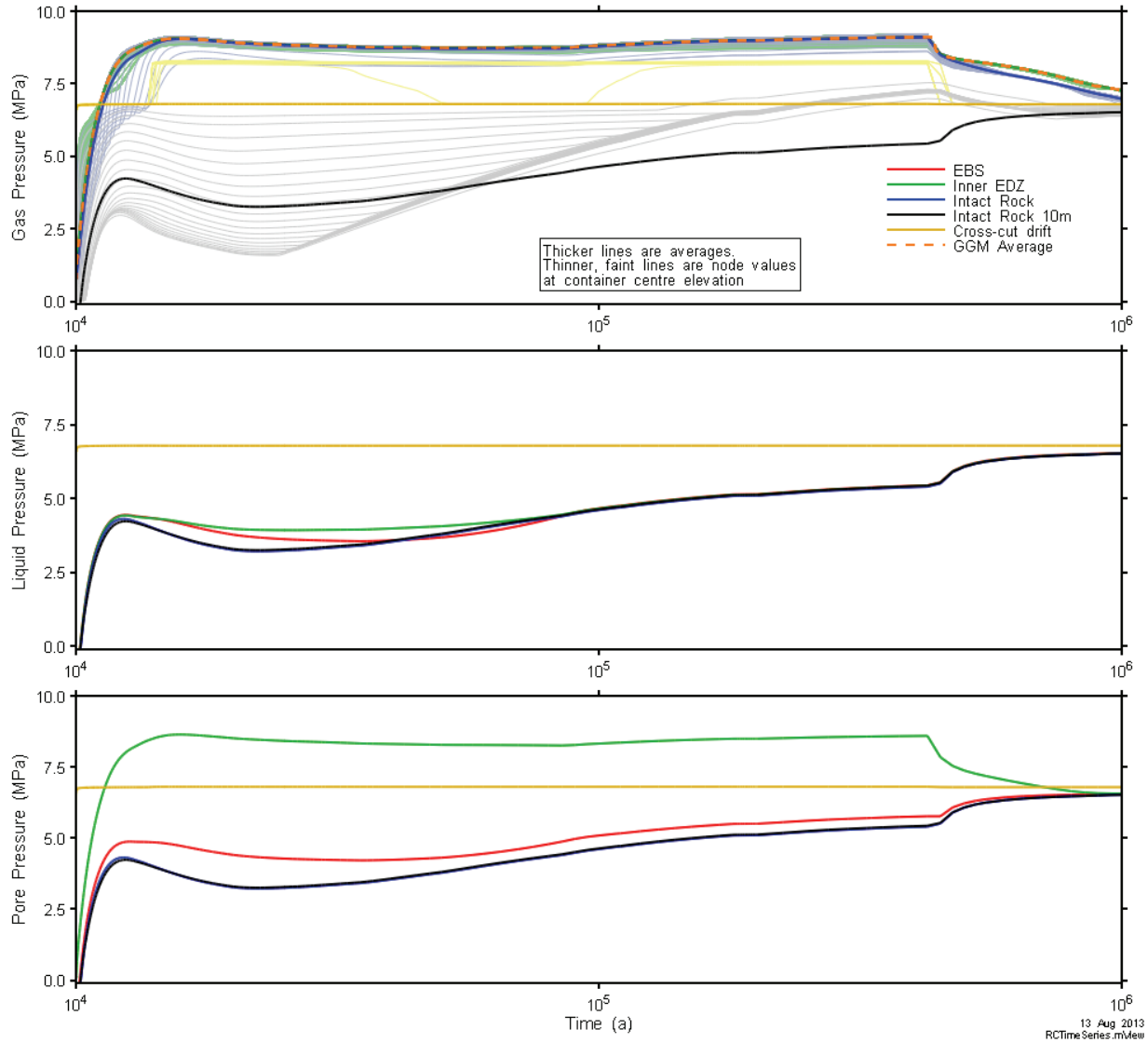

Figure 8-18: Room Scale Model – Nodal and Average Pressures after Container Failure

Figure 8-19 presents information on the gas distribution. The upper figure shows absolute distribution, while the lower figure presents the ratio by location of gas retained within the model. In general, nearly all generated gas leaves the room model through the cross-cut drift boundary. Of the gas retained, the placement room EBS contains the bulk of the generated gas, with the EDZ also containing a significant component for the first half of the simulation. The difference between the dashed line and the topmost solid line indicates the amount of gas that has exited the model domain and entered the Repository-Scale Model.

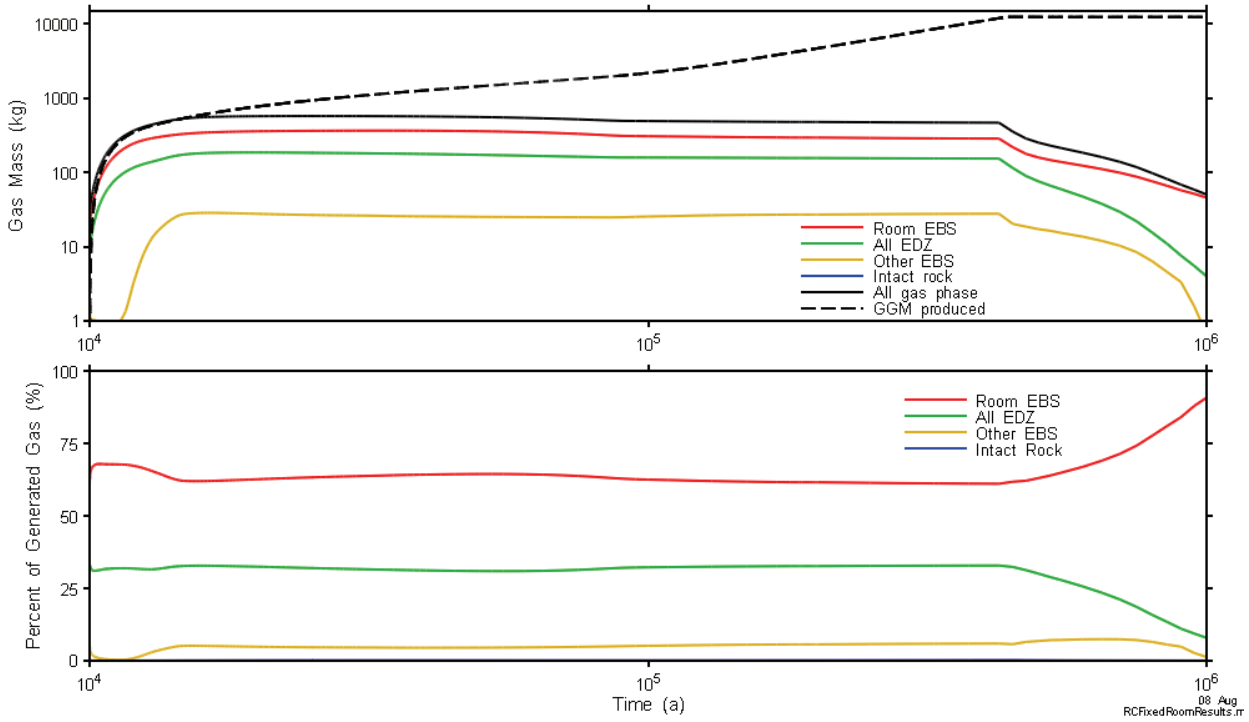

Figure 8-19: Room Scale Model – Gas Distribution

Figure 8-20 shows the gas generation rate within the placement room (red line) and the gas flow rate out of the placement room through the drift (blue line). The gas generation rate is computed using the GGM module and input at the locations shown in Figure 8-13. The flow rate out of the model corresponds to that at the flow location (red lines) in Figure 8-8.

The placement room buffers the initial pulse of gas until approximately 16,000 years, at which time gas begins to flow out of the model. The onset of Phase 4 corrosion (see Figure 8-14) is responsible for the change in slope that occurs just prior to 100,000 years. The Phase 4 period conservatively assumes that there is sufficient carbonate available to allow the reaction to proceed unabated (otherwise corrosion and gas generation would continue but at a slower rate). Gas flow ceases at 440,000 years when container mass is exhausted.

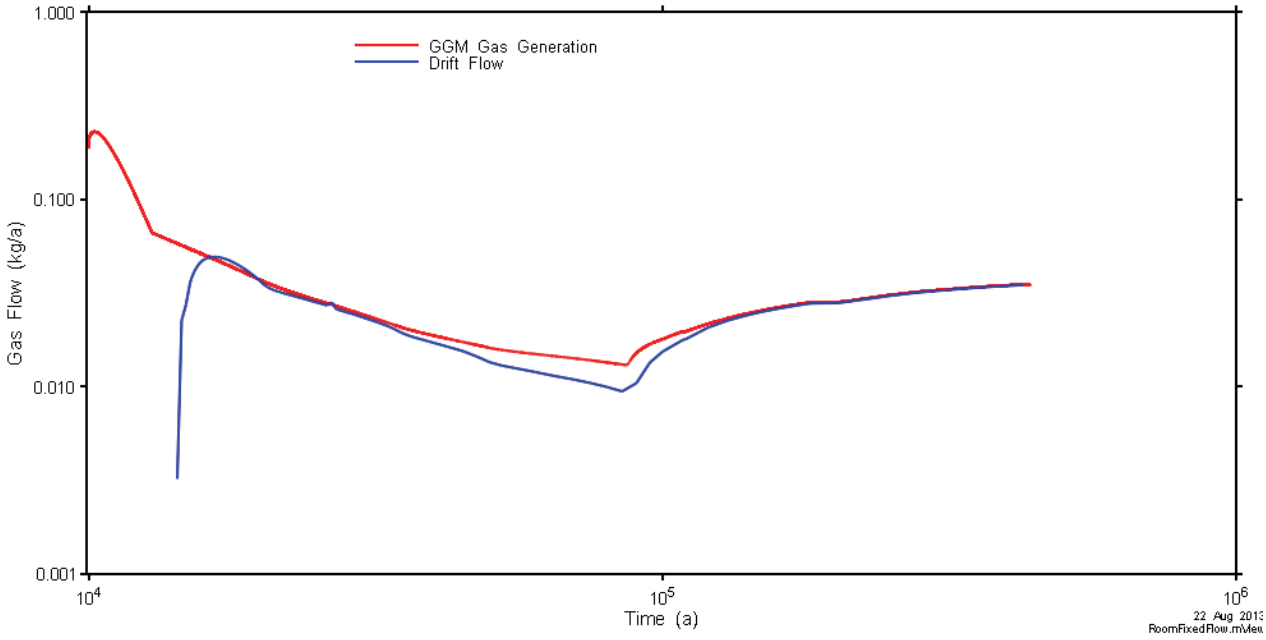

Figure 8-20: Room Scale Model – Gas Flow Rates

8.6.2 Repository-Scale Model

Results from the Repository-Scale Model are shown in Figure 8-21 to Figure 8-24.

Figure 8-21 shows the total amount of free-phase hydrogen gas within the Repository-Scale Model. Hydrogen gas is found mostly within the engineered sealing materials in the repository tunnels and shafts; however, significant amounts are also within the excavation damaged zone. Very little is in the host rock. The onset of Phase 4 corrosion (see Figure 8-14) is responsible for the change in slope that occurs just prior to 100,000 years.

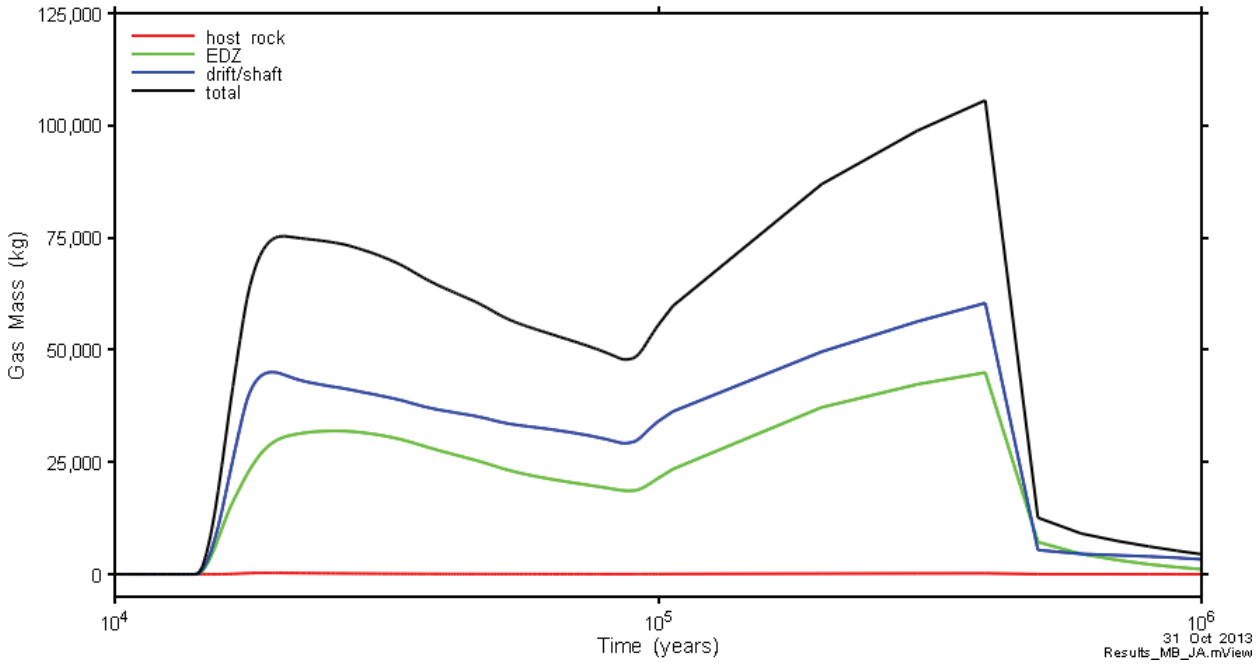

Figure 8-21: Repository-Scale Model – Distribution of Free-Phase Gas

Flow results shown in Figure 8-22 and Figure 8-23 illustrate the amount of hydrogen, in both a gas phase and as dissolved gas, leaving the top of the model. The grey line in Figure 8-22 represents the total rate at which gas enters the model from the placement rooms while the black line represents the total rate at which gas leaves the model via the shafts and, to a much lesser degree, the rock. The other colours indicate the exit pathways used by the gas. Because the Guelph formation has a much lower gas entry pressure than does the concrete seal and the bentonite / sand seal above the concrete, the rising hydrogen gas will exit the shafts and enter the Guelph formation.

Comparison of Figure 8-22 and Figure 8-23 shows that hydrogen is moving primarily in gaseous form, with dissolved hydrogen accounting for approximately 0.01% of hydrogen transport.

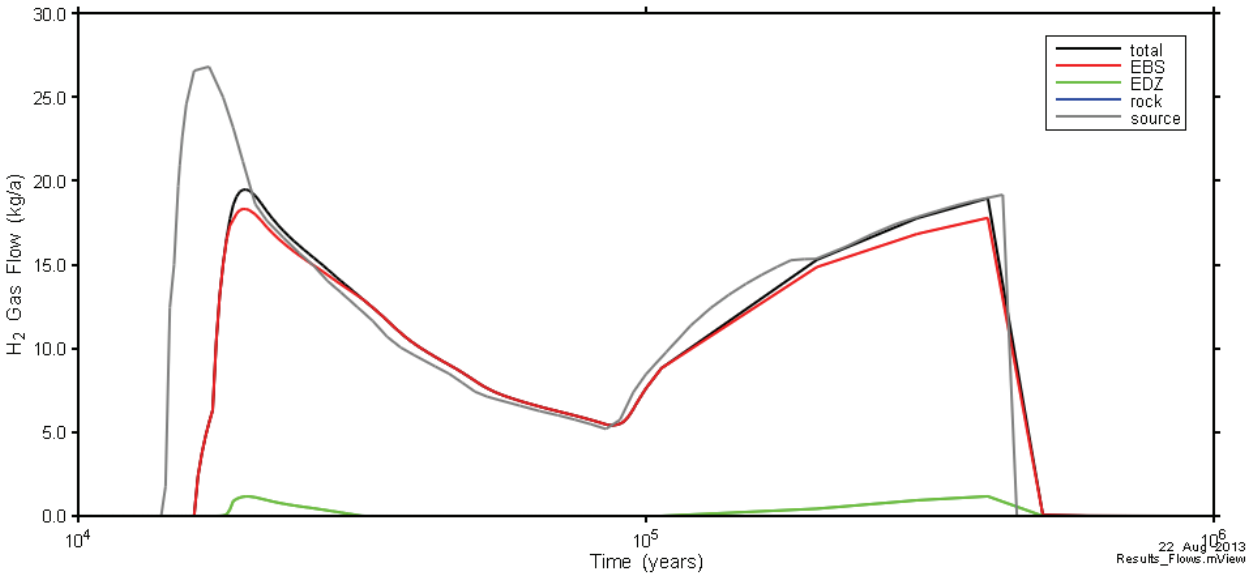

Figure 8-22: Repository-Scale Model – Gas flow Out of the Top of the Model

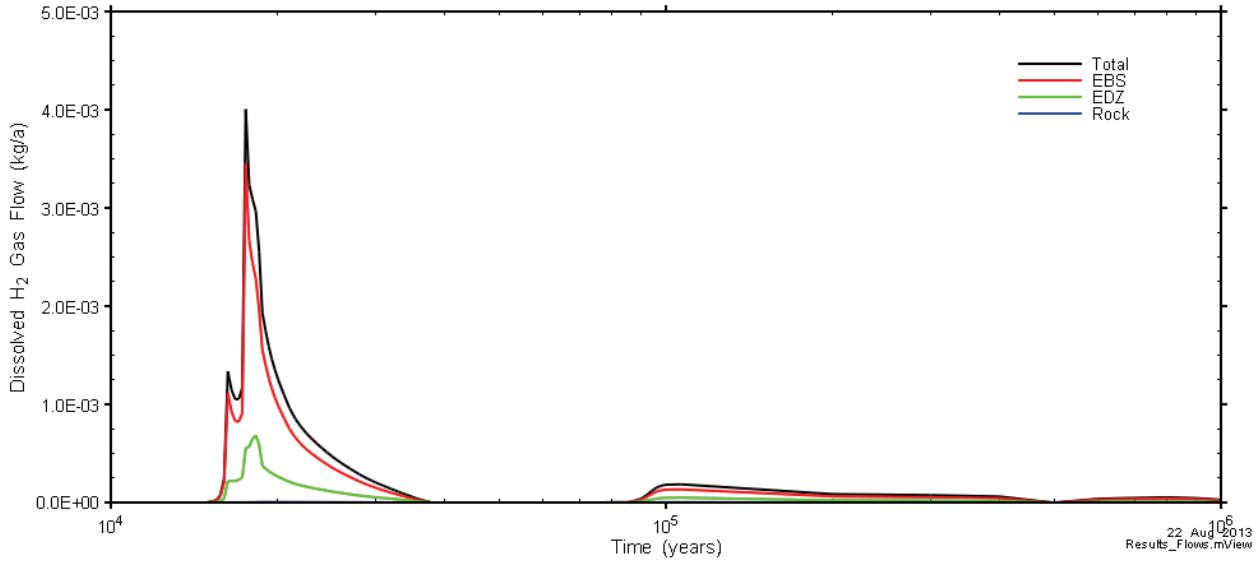

Figure 8-23: Repository-Scale Model – Dissolved Gas Flow Out of the Top of the Model

Model calculations indicate that pore pressures within the intact rock do not exceed 80% of lithostatic pressure over the 1 million year simulation period. As shown in Figure 8-24, pore pressure within the host rock neighbouring the repository reaches a maximum of 9.6 MPa at

15,700 years. As discussed in Section 8.1, this indicates the gas pressure is insufficient to fracture the rock.

While accounting for model / data uncertainties could result in higher pressures, the conservatism associated with the All Containers Fail at 10,000 Years analysis case provides confidence that the possibility of rock damage can be excluded. This will be further explored in future studies as modelling techniques improve and the knowledge base for gas generation and migration behaviour grows.

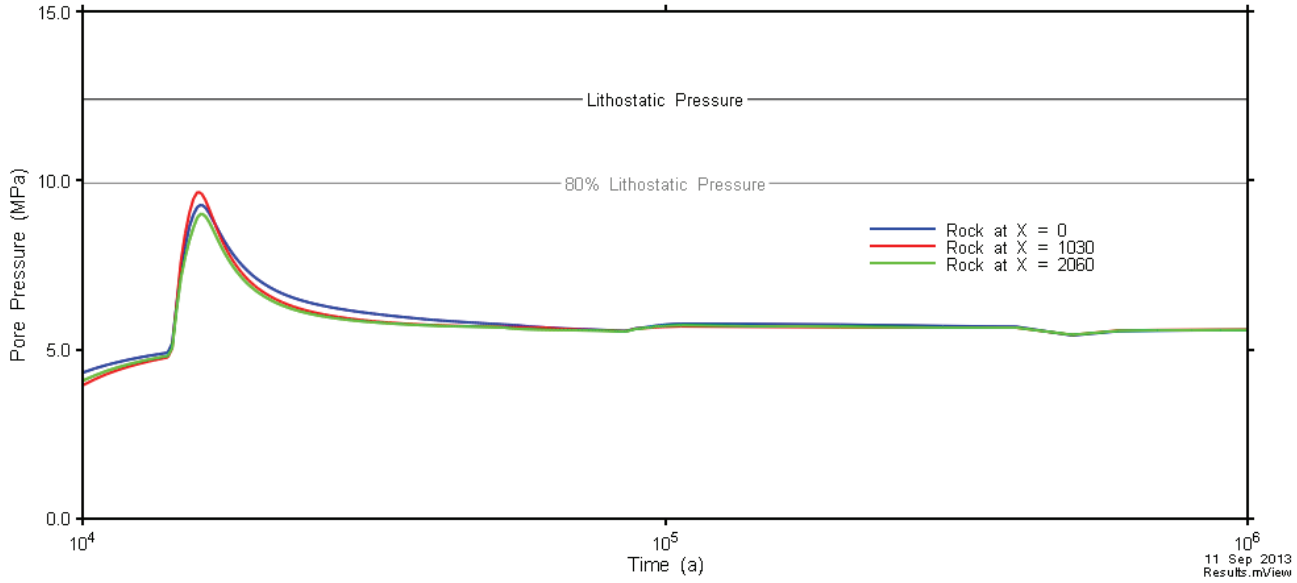

Figure 8-24: Repository-Scale Model – Pore Pressure

8.7 Dose Consequences

Of the radionuclide species present within the used fuel, very few are volatile or semi-volatile under repository conditions. Of these, only C-14, Cl-36, Se-79, and I-129 have half-lives sufficiently long to be of potential concern (Quintessa and Geofirma 2011, Gobien et al. 2013).

Table 8-3 shows the source term for each radionuclide together with their inhalation dose coefficients and Henry's law constants. The products of these three values are also shown to allow a comparison of the relative hazard. Because the product for C-14 is about four orders of magnitude greater than the others, only C-14 is considered further in the dose calculations.

Table 8-3: Comparison of Volatile, Long-lived Radionuclides

Nuclide	Half-Life (a)	Source*, 10,000 years (Bq/kgU)	Inhalation Dose Coefficient (Sv/Bq)	Henry's Law Constant (C_{gas}/C_{aq})	Product (Sv/kgU)
C-14	5700	4.7×10^{5}	6.2×10^{-12}	10^{2}	2.9×10^{-4}
Cl-36	301,000	1.8×10^{4}	7.3×10^{-9}	10^{-6}	1.3×10^{-10}
Se-79	295,000	1.9×10^{4}	6.8×10^{-9}	10^{-4}	1.2×10^{-8}
I-129	15,700,000	2.1×10^{4}	3.6×10^{-8}	10^{-4}	7.5×10^{-8}

Notes:

*The source term includes instant release from the fuel, instant release from the Zircaloy and congruent release from the fuel for the period of time between the assumed container failure (i.e., 10,000 years) and the time of maximum release to the Guelph aquifer (i.e., 18,000 years – Figure 8-25).

Data are taken or derived from Gobien et al. (2013), excepting the C-14 dose coefficient (Eckerman et al. 2012). The C-14 value is for CO_2.

The Repository-Scale Model results presented in Figure 8-21 and Figure 8-22 provide data needed to estimate the rate at which C-14 activity leaves the repository. Figure 8-21 shows the total amount of hydrogen gas in the repository while Figure 8-22 shows the rate at which hydrogen moves up the shafts.

As noted in Section 8.6.2, because the Guelph formation has a much lower air-entry pressure than the concrete seal and the bentonite / sand seal above the concrete, the rising hydrogen gas will exit the shafts and enter the more permeable Guelph formation. Once in the Guelph formation, the gas will most likely disperse and dilute laterally underground so there is no significant vertical flux upwards and no dose consequence to the critical group. Figure 8-25 shows the rate at which C-14 activity would enter the Guelph formation, taking into account radioactive decay of C-14.

A bounding estimate of the dose consequence can be conservatively obtained by assuming the gas is not dispersed in the Guelph formation and the critical group is exposed. This is done by assuming that all C-14 exits the repository via a single shaft, and that all C-14 in the shaft remains in the shaft until it reaches the surface. After reaching the surface, the C-14 then enters a house that is built directly on top of the shaft, exposing the occupants to an inhalation hazard. Under these assumptions, the rate information in Figure 8-25 also represents the rate at which C-14 activity enters the house. The maximum value is 320 kBq/hr.

The peak inhalation dose rate to the occupant is determined using data in Gobien et al. (2013). For a house volume of 228 m^3, an air exchange rate equivalent to a volume fractional turnover rate of 0.35 per hour (i.e., 7×10^{5} m^3/a), a dweller inhalation rate of 8400 m^3/a, an occupancy factor of 0.8, and an adult inhalation dose coefficient for C-14 (as CO_2) of 6.2×10^{-12} Sv/Bq (Eckerman et al. 2012), the peak dose rate is 0.17 mSv/a occurring at 18,000 years. Even with the extreme conservatism of assuming simultaneous failure of all containers at 10,000 years, this remains a factor of six below the interim Disruptive Event acceptance criterion of 1 mSv/a.

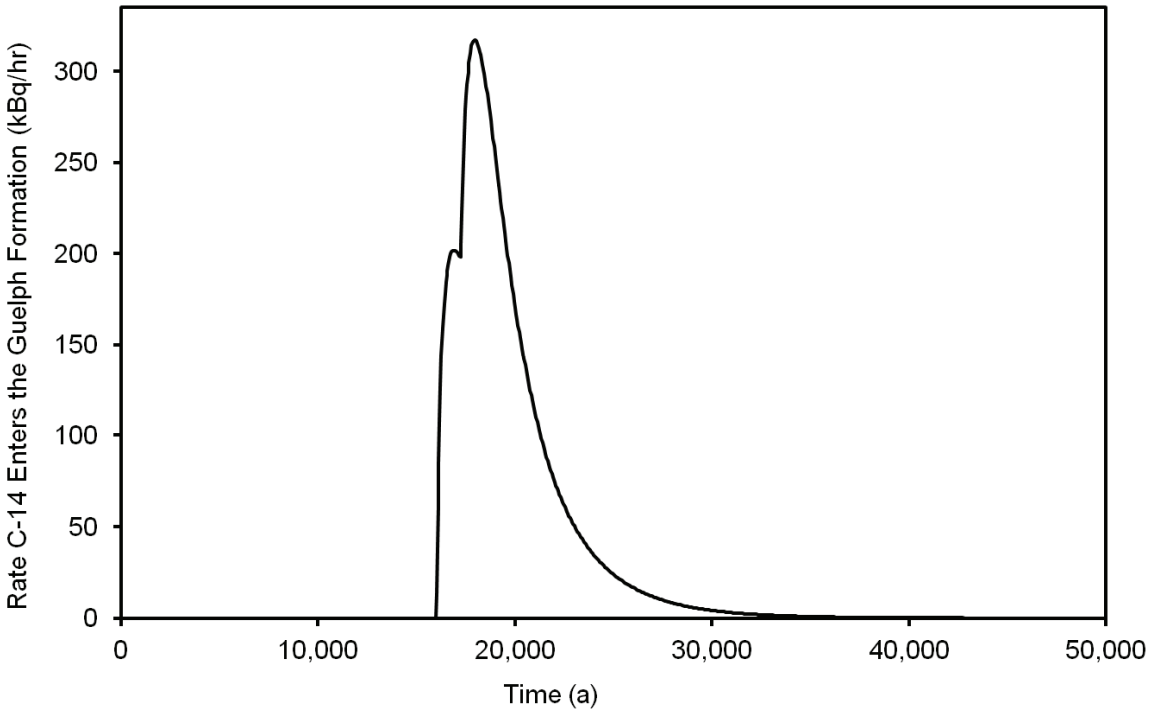

Figure 8-25: Rate at Which C-14 Enters the Guelph Formation

8.8 Summary and Conclusions

Exposure of the steel components of an engineered barrier system (EBS) to groundwater will result in the generation of gas due to corrosion processes. This gas can affect both the internal repository pressure and the transport of gaseous radionuclides.

Under the Normal Evolution Scenario, gas is not important because the rate of generation from the three defective containers is small, and because the primary gas-borne radionuclide (C-14) essentially decays away on a 60,000 year time frame (i.e., the half-life of C-14 is 5700 years).

A conservative assessment of the consequences of gas generation is determined by considering the variant case of the All Containers Fail Disruptive Scenario in which the container failures are all assumed to occur at 10,000 years. In this case, the steel in all containers is exposed and starts to corrode. Results indicate that gas is generated faster than it can leave through the rock, and it accumulates within the repository EBS and EDZ. The gas pressure builds sufficiently to allow gas to escape through the room seals and into the tunnels, where the pressure builds again and gas eventually escapes through the shaft seals.

Model calculations determine that pore pressure within the intact rock does not exceed 80% of lithostatic pressure over the 1 million year simulation period. Pressure within the host rock neighbouring the repository reaches a maximum of 9.6 MPa after 15,700 years.

Based on a set of extremely conservative assumptions, gas-borne dose consequences reach a peak dose rate of 0.17 mSv/a, which is a factor of six below the 1 mSv/a acceptance criterion for disruptive events. The peak occurs at 18,000 years. For a more realistic case of failure of copper containers over longer times, the dose rates would be lower. For example, if the copper containers all fail on time scales associated with the next glaciation or later, the associated dose rates would be well below 1 μSv/a due to decay of C-14.

8.9 References for Chapter 8

Bate, F., D. Roberts, A. R. Hoch, and C.P. Jackson. 2012. Gas migration calculations on the vault scale. Serco Assurance report SA/ENV-0924 Issue 3.1. Oxfordshire, UK (available at http://www.nda.gov.uk/documents/biblio/upload/Gas-Migration-calculations-on-the-vault-scale-report_I3_1.pdf).

Eckerman, K., J. Harrison, H.G. Menzel and C.H. Clement. 2012. ICRP Publication 119: Compendium of Dose Coefficients based on ICRP Publication 60. Annals of the ICRP, 41, 1-130.

FORGE. 2010. FORGE Milestone M15: Summary of Gas Generation and Migration. Current State-of-the-Art. Euratom 7th Framework Project, FORGE 2010. Deliverable D1.2-R.

Geofirma and Quintessa. 2011. Postclosure Safety Assessment: Gas Modelling. Geofirma Engineering Ltd. and Quintessa Ltd. report for the Nuclear Waste Management Organization NWMO DGR-TR-2011-31. Toronto, Canada.

Gobien, M., F. Garisto and E. Kremer. 2013. Fifth Case Study: Reference Data and Codes. Nuclear Waste Management Organization Technical Report NWMO TR-2013-05.

Guo, R. 2008. Sensitivity Analyses to Investigate the Influence of the Container Spacing and Tunnel Spacing on the Thermal Response in a Deep Geological Repository. Nuclear Waste Management Organization Report TR-2008-24.

Marschall, P., S. Horseman and T. Gimmi. 2005. Characterisation of gas transport properties of the Opalinus Clay, a potential host rock formation for radioactive waste disposal. Oil & gas science and technology, 60(1), 121-139.

Mualem, Y. 1976. A New Model for Predicting the Hydraulic Conductivity of Unsaturated Porous Media, Water Resour. Res., Vol. 12, No. 3, pp. 513 – 522, 1976.

Nagra. 2008. Effects of post-disposal gas generation in a repository for low- and intermediate-level waste sited in the Opalinus Clay of Northern Switzerland. Nagra Technical Report 08-07. Wettingen, Switzerland.

Pruess, K., C. Oldenburg and G. Moridis. 1999. TOUGH2 User's Guide, Version 2.0. Lawrence Berkeley National Laboratory LBNL-43134. Berkeley, USA.

Quintessa and Geofirma. 2011. Postclosure Safety Assessment: Data. Quintessa Ltd. and Geofirma Engineering Ltd. Report for the Nuclear Waste Management Organization. NWMO DGR TR-2011-32.

Senger, R., J. Ewing, , K. Zhang, J. Avis, P. Marschall and I. Gaus. 2011. Modeling approaches for investigating gas migration from a deep low/intermediate level waste repository (Switzerland). Transport in porous media, 90(1), 113-133.

Suckling, P., J. Avis, N. Calder, P. Humphreys, F. King and R. Walsh. 2012. T2GGM Version 3.1: Gas Generation and Transport Code. Quintessa Ltd. and Geofirma Engineering Ltd. Report for the Nuclear Waste Management Organization NWMO TR-2012-23. Toronto, Canada.

Talandier, J., G. Mayer and J. Croisé. 2006. Simulations of the Hydrogen Migration out of Intermediate-Level Radioactive Waste Disposal Drifts using TOUGH2. Proceedings, TOUGH Symposium 2006, Lawrence Berkeley National Laboratory. Berkeley, USA.

Van Genuchten, M. T. 1980. A Closed-Form Equation for Predicting the Hydraulic Conductivity of Unsaturated Soils. Soil Science Society of America Journal, 44(5), 892-898.

Yu, L. And E. Weetjens. 2009. Summary of gas generation and migration: current state-of-the-art. Extern. Rep. Belg. Nucl. Res. Cent. ER-106. Eur. Comm. FP7 FORGE. Fate Repos. Gases.

THIS PAGE HAS BEEN LEFT BLANK INTENTIONALLY

9. TREATMENT OF UNCERTAINTIES

All analysis calculations have an associated uncertainty. CNSC Regulatory Guide G-320 (CNSC 2006) expects that uncertainty will be taken into account.

9.1 Approach

Many organizations use the following three broad categories[1] to structure the analysis of uncertainties in postclosure safety assessments (e.g., Marivoet et al. 2008):

- **Scenario Uncertainty**: Arises from uncertainty in the evolution of the repository system and human behaviour over the time scales of interest.
- **Model Uncertainty**: Associated with uncertainty in the conceptual, mathematical and computer models used to simulate the behaviour of the repository system (e.g., due to approximations used to represent the system).
- **Data Uncertainty**: Arises from uncertainty in the data and parameters used as input in the modelling (e.g., due to incomplete site-specific data or due to parameter estimation errors from interpretation of test results).

The following briefly discusses the approach adopted for uncertainties in this pre-project review.

Scenario Uncertainty

Uncertainty in the future evolution of the site is addressed by assessing a range of scenarios that describe the potential evolution of the system. The scenario identification process, described in Chapter 6, ensures that key uncertainties are identified and scenarios are defined to explore their consequences.

The scenarios defined include the Normal Evolution Scenario (which describes the expected evolution of the repository) and a series of Disruptive Event Scenarios that postulate the occurrence of unlikely events leading to possible penetration of barriers and abnormal loss of containment.

To estimate potential future impacts, a stylized representation[2] of the biosphere and human receptors is used to allow illustrative estimates to be made. A stylized representation is adopted because it is unrealistic to predict human habits and behaviour over the time scale of relevance to the repository system, because major changes to the surface and near-surface environment are likely to occur as a result of natural changes such as ice sheet advance / retreat or as a result of future human actions, and because societal and technological changes are inherently unpredictable over such timescales.

---

[1] The boundaries between these categories can overlap. Depending upon how models are formulated, an uncertainty may be classed as a model or a data uncertainty.

[2] A stylized representation of the biosphere, and human habits and behaviour is a representation that has been simplified to reduce the natural complexity to a level consistent with the objectives of the analysis using assumptions that are intended to be plausible and internally consistent but that will tend to err on the side of conservatism.

In the stylized representation, it is assumed that future humans are generally similar to present day humans, and will adopt behaviors that would be consistent with current or past human practice. People are assumed to live on the repository site in the future in a manner that maximizes their potential dose from exposure to releases from the repository.

Since assumptions concerning the biosphere (e.g., climate), human lifestyles (e.g., critical group characteristics) and water flows in the near-surface environment become increasingly uncertain with time, two complementary long-term indicators are also used to supplement the dose rate indicator using system characteristics that are much less sensitive to such assumptions.

Model Uncertainty

Conceptual and mathematical model uncertainties are identified in the model development process. Key uncertainties are addressed by using alternative conceptual representations of the system. This is facilitated by the availability of a range of computer codes (e.g., FRAC3DVS-OPG and SYVAC3-CC4) that are capable of representing different conceptualizations and mathematical descriptions of the system.

Some conceptual and mathematical model uncertainties are amenable to representation with parameter values, and these are investigated using the methods applied to data uncertainties. For example, uncertainties in the representation of sorption are treated by considering bounding cases in which the sorption values are set to zero.

Data Uncertainty

Data uncertainties are identified in Gobien et al. (2013). These are accounted for through:

- Deterministic Calculations – alternative sets of parameter values, each providing a self-consistent representation of the system. Results are compared to the Reference Case and the differences explored. A limitation of this approach is that there is often no systematic or complete coverage of the uncertainty space in parameter values.

  Sensitivity cases in this pre-project review (identified in Section 7.2.1) explore the effect of variations in key parameters affecting the performance of various physical and chemical barriers.

- Probabilistic Calculations – parameters are assigned probability distribution functions that describe their inherent uncertainty. The model is evaluated a large number of times, with each case using input values randomly selected from the distribution functions. The model output is a distribution of results. The strength of the probabilistic approach lies in its ability to be comprehensive in exploring the space of the phenomena considered, and their associated model parameters. Its weakness is the need to make use of simplified models.

Conservatisms

Throughout the assessment process, it is necessary to make various assumptions relating to scenarios, models or data. Assumptions are often categorized as 'realistic'[3] or 'conservative'[4], although care needs to be taken when using such terms. The key is to ensure that each major assumption used in the assessment is considered and documented, and that the potential implications are understood.

While it may appear sensible to adopt a conservative approach to ensure that potential impacts are not under-estimated, care is needed because the net effect of many conservative assumptions can be an unrealistic estimate of impacts. Thus, the postclosure safety assessment adopts scientifically informed, physically realistic assumptions for processes and data that are understood and can be justified on the basis of the results of research and / or site investigation. Where there are high levels of uncertainty, conservative assumptions are adopted to allow the impacts of uncertainties to be bounded.

In particular, the following conservative assumptions are incorporated in the Normal Evolution Scenario:

- The defective containers fill with water in the first 10,000 years;
- No credit is taken for the presence of the fuel sheath in maintaining fuel integrity and in preventing contact of the fuel matrix with water that may enter the container;
- No credit is taken for the effect of H_2 (produced by corrosion of the defective container) on the dissolution rate of the UO_2 fuel;
- No credit is taken for the effect of iron oxides (produced by corrosion of the defective container) providing a high surface area for adsorption of some of the radionuclides released from the fuel;
- No credit is taken for the likely filling of the defect with bentonite and / or corrosion products which could significantly increase the transport resistance of the defect;
- The defective containers are positioned in the repository location with the shortest contaminant travel time to the surface;
- Adoption of a 219 m deep well penetrating to the bottom of the Guelph layer located in the position with the shortest transport time to the surface;
- Positioning the well so that it maximizes the capture of radionuclides released from the defective containers; and
- Defining conservative properties of the critical group (e.g., use of 90th percentile food ingestion rates; obtaining all food, fuel, water and building material locally; and all drinking and irrigation water taken from the well).

---

[3] Realism is defined as "the representation of an element of the system (scenario, model or data), made in light of the current state of system knowledge and associated uncertainties, such that the safety assessment incorporates all that is known about the element under consideration and leads to an estimate of the expected performance of the system attributable to that element" (IAEA 2006).

[4] Conservatism is defined as "the conscious decision, made in light of the current state of system knowledge and associated uncertainties, to represent an element of the system (scenario, model or data) such that it provides an under-estimate of system performance attributable to that element and thereby an over-estimate of the associated radiological impact (i.e., dose or risk)" (IAEA 2006).

9.2 Key Uncertainties

The postclosure safety assessment summarized in Section 7.12 and Section 8.8, indicates that the deep geological repository in geologic settings similar to the assumed site could tolerate large changes in the properties of key chemical and physical barriers without challenging the interim dose acceptance criteria.

The key uncertainties in terms of their importance to modify potential impacts are:

- **Chemical Reactions**: Under the highly saline conditions of the deep geosphere, several aspects of the chemistry in the repository are uncertain due to the limited database. These include the sorption of contaminants on seal materials and host rocks, as well as mineral precipitation / dissolution reactions. These uncertainties have been addressed in the pre-project review through the adoption of conservative values, the analysis of various sensitivity cases, and the identification of appropriate disruptive scenarios such as the Container Failure Scenario.

- **Gas Pressure and Repository Saturation**: The presence of robust copper containers ensures gas generated from potential corrosion of the steel inner containers is not a significant issue for the Normal Evolution Scenario. However, gas behaviour becomes increasingly important when large number of containers are assumed to fail, such as in the All Containers Fail Disruptive Scenario. This report includes a detailed study of the expected gas evolution for this event.

- **Glaciation Effects**: Although geological evidence at a real site is expected to indicate the deep geosphere has not been affected by past glaciation events and that the deep groundwater system has remained stagnant, glaciation will have a major effect on the surface and near-surface environment that is not entirely predictable. Glaciation is not likely to occur before 60,000 to 100,000 years, at which point the remaining hazard will be long-lived radionuclides and potentially hazardous chemical elements.

- **Fracture Characterization**: For a real site, there will be some uncertainty in the nearby fracture network. However, in principle a sedimentary rock site may have features that provide high confidence that there are no significant fractures nearby. These uncertainties can be reduced through site selection and repository location and depth, and any residual uncertainties can be handled through the adoption of conservative assumptions and / or Disruptive Scenarios (such as the Undetected Fault Scenario) within the postclosure analysis.

9.3 References for Chapter 9

CNSC. 2006. Regulatory Guide G-320: Assessing the Long Term Safety of Radioactive Waste Management. Canadian Nuclear Safety Commission. Ottawa, Canada.

Gobien, M., F. Garisto, E. Kremer and C. Medri. 2013. Fifth Case Study: Reference Data and Codes. Nuclear Waste Management Organization Report NWMO TR-2013-05. Toronto, Canada.

IAEA. 2006. Safety Requirements: Geological Disposal of Radioactive Waste. International Atomic Energy Agency Safety Requirements WS-R-4. Vienna, Austria.

Marivoet, J., T. Beuth, J. Alonso and D.-A. Becker. 2008. Safety Functions, Definition and Assessment of Scenarios, Uncertainty Management and Uncertainty Analysis, Safety Indicators and Performance/Function Indicators. PAMINA Deliverable D-No. 1.1.1, European Commission. Brussels, Belgium.

THIS PAGE HAS BEEN LEFT BLANK INTENTIONALLY

10. NATURAL ANALOGUES

Natural analogues are natural features (materials or processes) that are similar to those expected in some part of a deep geological repository. Natural analogues can include both natural and man-made materials provided the processes that affect them are natural. They provide understanding or demonstration of how a repository may behave over time scales ranging to many millions of years. Analogues exist for most features of the repository system, including the used fuel, engineered and natural containment systems, and key processes such as transport of contaminants.

The use of natural analogues in supporting key assumptions in safety assessment and adding credibility to its findings is recommended in IAEA (1999) and in Regulatory Guide G-320 (CNSC 2006). G-320 states: "*Natural analogue information should be used to build confidence that the system will perform as predicted by demonstrating that natural processes will limit the long-term release of contaminants to the biosphere to levels well below target criteria.*"

The natural analogues presented here can assist in understanding many of the underlying principles relevant to the long-term isolation and containment of used nuclear fuel.

10.1 Analogues for Used Nuclear Fuel

10.1.1 Natural Uranium Deposits

Natural uranium is relatively abundant. Like all other elements, it is cycled through biological and geological systems and tends to concentrate in some locations by natural processes. Uranium will slowly dissolve under oxidizing conditions and precipitate under reducing conditions. Most uranium ore bodies form by this process. Once formed, until local conditions change, a uranium deposit will remain in place. Uranium ore bodies that are being mined today were formed hundreds of millions of years ago.

Used fuel consists predominantly of uranium dioxide, with about 2% of the total being fission and activation products resulting from the nuclear reactions occurring in the fuel during power production. These are mostly incorporated within the solid matrix of the used fuel. Natural uranium minerals are comparable in that they consist of uranium dioxide along with uranium decay products.

One gram of natural uranium, as it is extracted from the earth in equilibrium with its progeny contains a little less than 2×10^5 Bq of radioactivity. In comparison, after discharge from a reactor and 30 years of cooling, used fuel has an inventory of 2.7×10^9 Bq per gram of uranium, principally in the form of fission and activation products (Tait et al. 2000), and is considerably more radioactive than the original uranium ore. Due to the rapid decay of most of the fission product isotopes present in used fuel, radioactivity decreases to 2.3×10^7 Bq per gram after 1000 years while after approximately one million years, radioactivity decreases to a level similar to that in natural uranium.

The Cigar Lake uranium deposit found in Northern Saskatchewan (Figure 10-1) provides a Canadian example of an analogue for geological placement of used nuclear fuel. The Cigar Lake deposit is under development as a uranium mine and has been well studied as a natural analogue (Cramer and Smellie 1994, Miller et al. 2000).

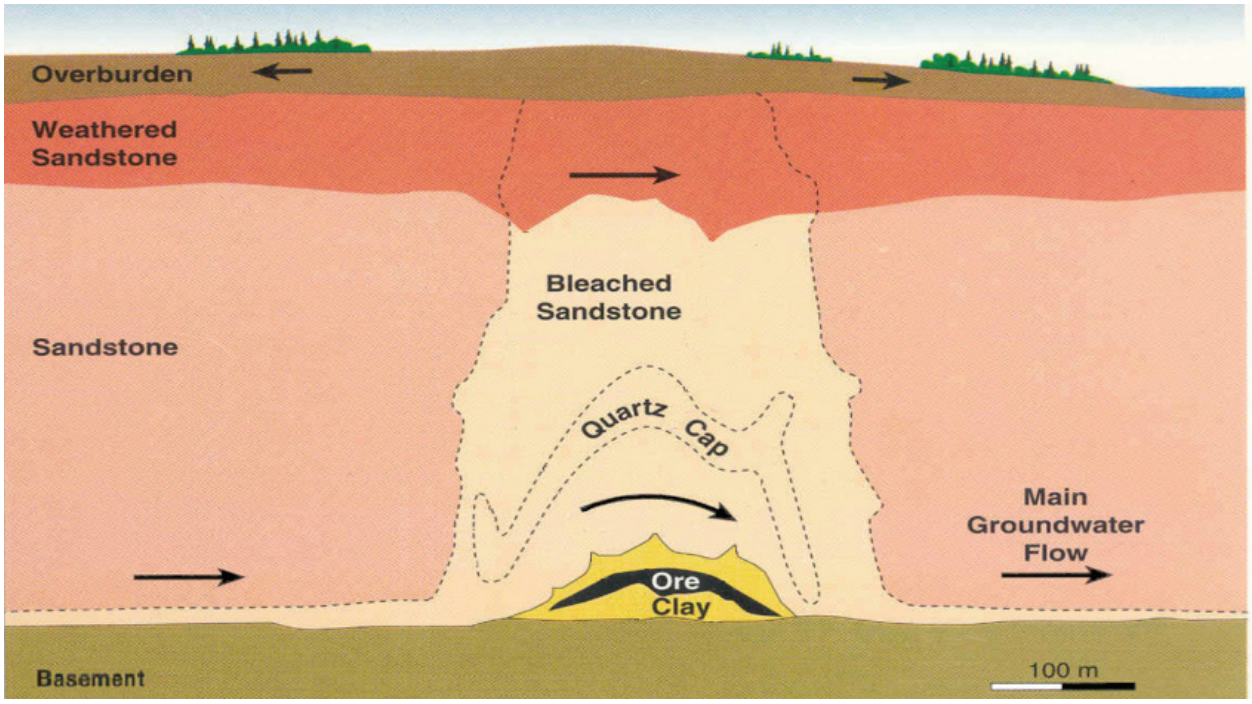

Figure 10-1: Cigar Lake Ore Deposit

The Cigar Lake uranium deposit is located about 430 m below surface, similar in depth to the repository considered in this pre-project review (i.e., 500 metres underground). The ore body formed about 1.3 billion years ago. It is similar in general composition to used fuel, and the ore is surrounded by a clay envelope somewhat similar to the clay buffer specified in the repository design. It can be considered analogous to a “worst case” simulation, as it lacks any specially designed used fuel containers and the host rock above the ore body is highly fractured sandstone.

Based on the Cigar Lake natural analogue study (Cramer and Smellie 1994), it was concluded that:

- uranium dioxide will remain stable over 100 million year time scales under the chemically-reducing conditions found adjacent to the Cigar Lake ore body, with very little uranium migrating from the deposit;
- the natural clay surrounding the ore has provided an effective long-term seal, preventing migration of radionuclides from the deposit (see Section 10.2.2);
- dissolved organic matter in groundwater migrating past the ore has not played a significant role in mobilizing radionuclides from the deposit; and
- natural hydrologic barriers and appropriate geochemical conditions found at the site are effective in preventing significant radionuclide migration from the deposit.

Insufficient radionuclide migration has occurred to produce any detectible concentration anomalies in the soil, surface water and lake sediments and waters overlying the ore body. Environmental and geological exploration in the area has shown no surface expression of the ore body, and it had to be discovered by geophysical techniques. Indeed, on a map of surface radioactivity in Canada, the area of the Saskatchewan deposits generally shows up as having below-average surface radioactivity (McKee and Lush 2004).

Reducing conditions are expected in the repository due to buffering by the rock and engineered sealing materials; however, radiolysis of groundwater may produce oxidizing conditions locally. Redox conditions are critical because the geochemical behaviour of many elements strongly depends on their redox state. The long-term performance of the repository is therefore strongly dependent on the redox conditions assumed.

In some parts of the world, uranium found in permeable rocks is mined by “in-situ” mining methods. Some of the ore bodies mined in this manner are called roll-front ore bodies, as they are continuously migrating or rolling through the permeable host rock. The front of the ore body is in a reduced state, while the rear of the ore body is in a more oxidized state as a consequence of oxidizing groundwaters that are slowly driving the ore body through the rock formation. This creates a condition at the rear of the ore body in which the uranium becomes soluble and migrates to the front of the ore body where it again precipitates.

A well-studied example of a roll-front uranium deposit is the Osamu Utsumi mine in Brazil (Hofmann 1999). Measuring reducing materials such as iron or organic carbon provides an indication of how uranium and other radionuclides in used fuel will be immobilized in the repository. Hoffman reported that migration of uranium, along with palladium and selenium, was strongly inhibited at a redox front, causing immobilization. Results indicated that reducing conditions inhibit transport of these elements under most natural low-temperature conditions.

Roll-front uranium deposits illustrate how migration of used fuel through locally oxidizing conditions in the container (assuming groundwater infiltration of used fuel containers and subsequent radiolysis) would be effectively suppressed by the reducing conditions of the placement rooms and repository host rock.

10.1.2 Natural Fissioned Uranium

Nuclear fission occurred naturally on Earth over two billion years ago. In Gabon, Africa, there are 15 deposits of uranium ore that have acted as natural nuclear reactors (Miller et al. 2000), sometimes referred to as the Oklo fossil reactors (Figure 10-2). The remnants of natural uranium fission provide the closest natural analogue for used nuclear fuel over long time periods in a geologic environment.

The quantity of U-235 present in natural uranium ore bodies today is low at 0.7%. However, approximately two billion years ago, when the Oklo ore bodies formed, the fraction of U-235 present in natural uranium was much greater, comprising just over 5%. The Oklo reactors operated at low power over about one million years. Results of material sampling infers that approximately 6 to 12 tonnes of U-235 underwent fission, producing plutonium and generating temperatures in the natural reactors of up to 600°C.

Oklo reactor studies provide data regarding the stability of uranium dioxide in the presence of other fission products and the transport of radionuclides within the surrounding shale and sandstone formations. These studies indicate that more than 90% of the uranium “fuel” present in the reactors 2 billion years ago has remained in place, including transuranic elements, most of the fission products and their decay products. The plutonium generated has moved less than 3 metres over two billion years. This is in the absence of the engineered barriers incorporated into a geological repository. The surrounding rock has proved to be a well-sealed vault.

The stability of the Oklo used fuel has lasted through two billion years of continental drift and groundwater movement. This is additionally impressive considering the present day near-surface location of these natural reactors.

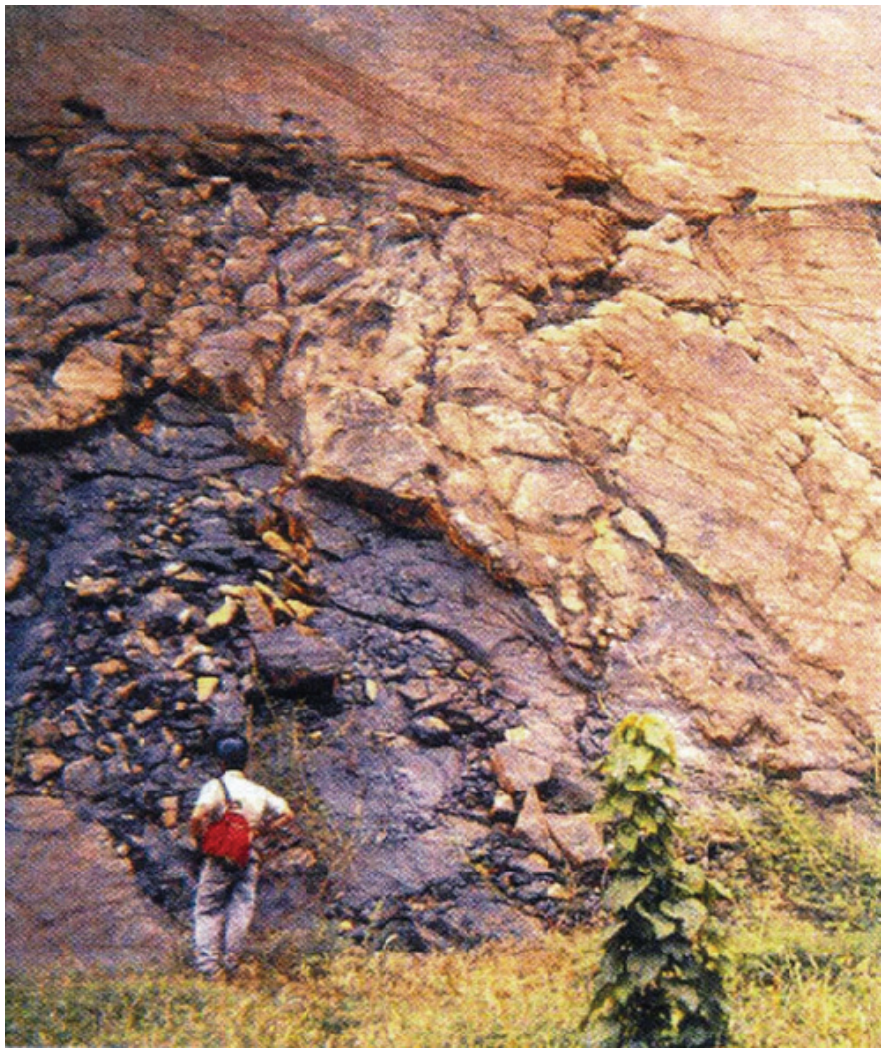

Notes: In Oklo, Gabon, the remains of an ancient natural nuclear reactor indicate the resulting plutonium has moved less than 3 metres over two billion years. From Miller et al. (2000).

Figure 10-2: Naturally Occurring Fission Reactor

The Oklo fossil reactors provide a snapshot in time of the condition of a natural used fuel repository two billion years after decommissioning. Information is obtained through indirect evidence such as the quantity and location of fission products and their decay products, and the actinides that can still be found in association with these natural reactors. This evidence indicates that careful selection of the host rock formation for a used fuel deep geological repository can render many fission products and actinides largely immobile.

10.1.3 Fractured Uranium Deposits

The Tono uranium ore body, located near Tokyo, has been the subject of analogue studies relating to transport of uranium (Miller et al. 2000). The ore body lies within a sedimentary formation containing significant quantities of carbonaceous material and pyrite, making it a highly reducing environment; as such, it provides an opportunity to evaluate radionuclide migration through sedimentary rocks under reducing conditions. The ore body is approximately 3.4 km long; however, the area is tectonically active and between 5 and 10 million years ago, the ore body was split by a fault. This displaced a portion of the ore body 30 m upward. Despite this large fault, many other nearby faults, and the occurrence of frequent tremors, Yoshida (1994) found that no significant uranium transport occurred from the ore body to the adjacent environment. The rock provided substantial opportunity for matrix diffusion and very large surface area for sorption of radionuclides. Consequently, no substantial remobilisation of the uranium has occurred, despite the faulting history of the area.

The preferred location for a used fuel repository will be tectonically inactive, providing even greater physical stability and security than seen at this site.

10.2 Analogues for Barriers

The repository design uses multiple barriers, including materials such as iron, copper, clays, concrete and asphalt to inhibit or prevent movement of radioactive elements and other materials from the facility into the surrounding environment.

10.2.1 Metals

In the current study, used fuel bundles are placed into large, durable containers designed to hold 360 fuel bundles each. For the reference container design, the inner vessel is made from 100 mm-thick carbon steel which provides the mechanical strength to withstand the pressures of the overlying rock and future glacial loading. The outermost layer of the container is corrosion-resistant copper, 25 mm thick, of which a few mm is required for corrosion resistance over one million years.

The used fuel container prevents water from contacting the used fuel bundles, thereby preventing radionuclides in the fuel from escaping into the underground environment. The used fuel container is engineered to remain intact for at least 100,000 years, and is expected to last much longer, keeping the used fuel completely isolated from the surroundings.

10.2.1.1 Copper

Copper is one of the relatively few metals that naturally occurs in its metallic state. Solid pieces of native copper have been found containing more than 99% copper. The largest known

deposit of metallic copper is in the Keweenaw Peninsula of Michigan (Crissman and Jacobs 1982), where large pieces of almost pure copper were either mined or found in glacial outwash. Data from these natural analogues provide copper corrosion rates for both reducing and oxidizing environments, which are useful in assessing the longevity of the used fuel containers.

Copper "plates" found in the mudstones from South Devon in England (Figure 10-3) provide a natural analogue for the corrosion of used fuel containers placed in a clay backfill. These copper plates were formed 200 million years ago (lower Jurassic period) and show little corrosion since that time, due in part to the protection of the clay-rich mudstone (Milodowski et al. 2000).

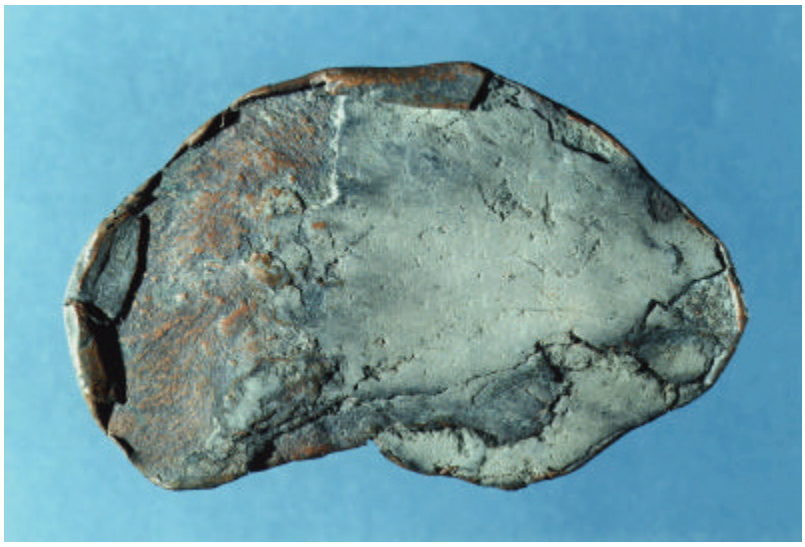

Note: From Milodowski et al. (2000).

Figure 10-3: Copper Analogues

10.2.1.2 Iron

Recorded use of iron dates to Egypt in 1900 BCE (Miller et al. 2000). Johnson and Francis (1980) studied the corrosion of artifacts under a wide range of environmental conditions and reported annual corrosion ranging from 0.1 to 10 microns.

The large amounts of iron (carbon steel) in the used fuel containers may buffer redox conditions in the repository, preventing oxidizing conditions near the used fuel. The Inchtuthil Roman nails found in Scotland provide an interesting analogue for this. At a Roman fortress that was abandoned in 87 CE (Angus et al. 1962; Pitts and St. Joseph 1985), over 1 million nails were buried in a 5-m deep pit under 3 m of earth. When the nails were unearthed in the 1950s, the nails on the outside of the mass were found to have corroded and formed a solid crust of iron oxides (rust) around the remaining mass of nails. The outside layer of nails formed a sacrificial redox sink, consuming oxygen before it could penetrate to the interior of the mass of nails. The physical expansion of the rust also served to self-seal the remaining nails from intruding

groundwater and water vapour. As a result, the nails inside the rusty barrier experienced minimal-to-no corrosion over nearly 2,000 years.

In Greenland, on Disko Island, magmatic conditions within a crystalline rock formation (basalt) promoted deposition of native iron over a period of volcanism spanning from about 63 to 30 million years ago. An estimated 10 million tons of iron were deposited. Mass transport limitations (low diffusivity of reactants combined with high redox capacity) favoured preservation of the native iron. Native iron has survived millions of years in the rock matrix (Hellmuth 1991).

The natural redox buffering capacity of the bentonite and rock surrounding the Cigar Lake ore body is due mainly to ferrous compounds in the mafic mineral phases (Smellie and Karlsson 1996). These reducing conditions have suppressed transport of uranium and other oxidising species, playing a major role in preserving the stability of the ore. The outer clay in contact with groundwater migrating past the ore body is a light reddish colour, indicating that the iron in the clay has oxidized. Deeper within the clay, the reddish colour disappears, suggesting that oxygen has been precluded and reducing conditions maintained (Miller et al. 2000). The result is a very stable ore body.

10.2.2 Clays

The primary sealing material within the engineered containment systems is the swelling clay component of bentonite, usually referred to as smectite or, more specifically, montmorillonite. Bentonite (Figure 10-4) is a group of naturally occurring clays. Bentonite swells when exposed to water, minimizing water seepage and making an excellent sealing material when physically confined. It also has a high chemical sorption capacity, able to bind many elements to its crystalline surfaces, which greatly slows the migration of radionuclides. Bentonite is also very stable, typically formed millions to hundreds of millions of years ago. Clay materials can act as a very robust physical and chemical barrier, as illustrated in the discussion above of Cigar Lake where naturally formed clays acted as a protective barrier for geological time periods. Laine and Karttunen (2010) recently produced a wide-ranging review of natural analogues for bentonite.

Each used fuel container is surrounded by compacted bentonite clay and all excavated spaces are filled with mixtures of clay, sand, and crushed rock. As the closed and sealed repository is slowly infiltrated by groundwater, the bentonite will swell and fill any remaining void spaces. Radionuclides will only be able to move through the bentonite by diffusion, greatly restricting their migration. In addition, the clay's high adsorption capacity for many elements will significantly inhibit their movement.

Note: Figure from EUBA (2011)

Figure 10-4: Bentonite Clay

The Dunarobba Forest in Italy (Figure 10-5) provides a natural analogue of the effectiveness of clays in minimizing groundwater movement (Benvegnú et al. 1988; Ambrosetti et al. 1992). The sequoia-like Dunarobba trees were buried in clay for 1.5 million years. The clay minimized the flow of water to the trees and prevented oxygen from reaching the wood. This maintained reducing conditions around the wood, protecting the wood from bacterial or fungal decay or chemical oxidation. As a result, the trees did not decay. They also did not fossilize - they are still made of wood.

Similar analogues have been found in the Canadian Arctic on Axel Heiberg Island (Greenwood and Basinger 1994) and at the Strathcona Fiord on Ellesmere Island (Francis 1988), where shale deposits over 40 million years old were found to contain preserved specimens of redwood, walnut, elm, birch and alder; also, gingko and katsura, now native to eastern Asia. The shale, which is consolidated clay, provided an effective barrier to oxygen and preserved the wood such that the wood grain and bark are preserved without chemical alteration – the cellular structure and most of its molecular structure remain intact.

Note: Retrieved Aug 1 2013 from http://it.wikipedia.org/wiki/File:Dunarobba.jpg.

Figure 10-5: 1.5 Ma Sequoia-like Tree Stumps at Dunarobba, Italy

Sensitivity to Temperature

Thermal alteration of bentonite has been studied, with a focus on higher temperatures that are of relevance to the near field. These studies indicate little reaction or degradation of bentonite physical properties below 150°C (Wersin et al. 2007). This compares well with repository temperatures (see Section 5.2.4), where the temperature at the surface of the container is predicted to peak at less than 120°C within 10 years of closure, then steadily decrease to 90°C after 100 years and ultimately return to ambient temperature by approximately 100,000 years.

The bentonite beds at Kinnekulle in Southern Sweden were exposed to temperature of 140-160°C over a period of about 1000 years as a result of a basaltic intrusion (Pusch et al. 1998). The measured swelling pressures are still substantial and hydraulic conductivities are reasonably low. Wersin et al. (2007) reviewed natural analogue data on thermally-exposed bentonite to assess its stability, concluding that even for an extended heating period with resulting cementation and illitization, the hydraulic properties of the bentonite remain favourable.

Laine and Karttunen (2010) report on the Ishirini bentonite body in Libya. Some of the bentonite formations were crosscut by basaltic intrusions about 20.2 million years ago, causing local thermal alteration near the intrusions. Kolařiková and Hanus (2008) found that the minimum

temperature experienced by the bentonite during the intrusions was probably higher than 190°C. The impact of raised temperatures, however, appears minimal: while some local cementation occurred, the majority of the bentonite remains unaltered.

Sensitivity to Salinity:

Under postclosure conditions, high salinity of the groundwater is expected to affect the swelling properties of the bentonite; however, it is not expected to alter the mineral stability of the bentonite.

Alexander and Milodowski (2013) observe that the Perapedhi bentonites studied under the Cyprus Natural Analogue Project likely remained in a marine, saline environment until the formation of Cyprus and the initiation of fresh groundwater circulation.

Figure 10-6 compares the swelling pressure of the Cyprus bentonite with a range of industrial bentonites (plus one other natural bentonite from Avonlea), indicating that exposure of the Perapedhi bentonite to marine saline conditions for nearly 90 million years had no significant impact on its swelling capacity.

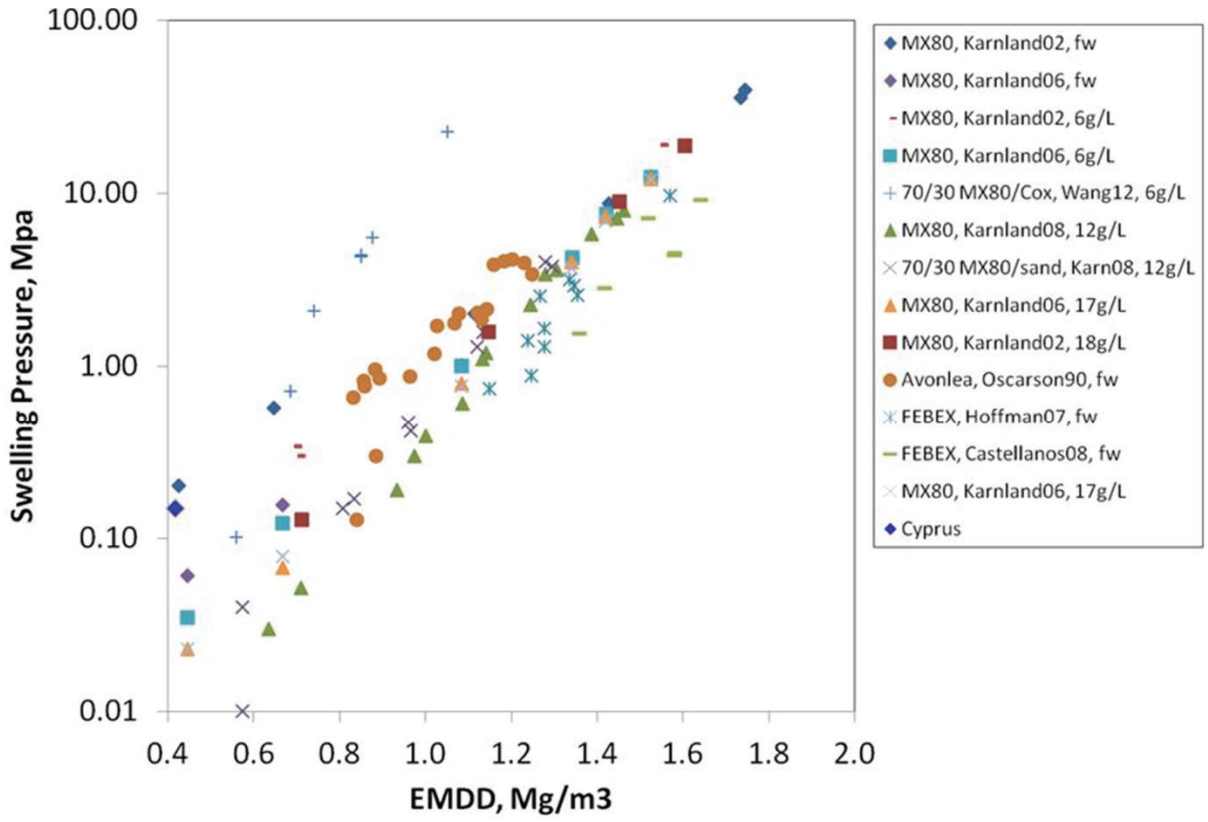

Note: The legend indicates that saturation waters range in salinity from fresh water (fw) to 18 g/L of dissolved salt.

Figure 10-6: Swelling Pressures of Various Bentonites across a Range of Equivalent Montmorillonite Dry Densities (EMDD)

Sensitivity to Alkalinity

Bentonite, particularly the swelling clay component (smectite), is unstable under high pH conditions. In the repository, concrete may produce alkaline conditions locally, affecting adjacent bentonite. However, as the low-heat high-performance concrete leachates will have a lower pH (10 - 11) than Ordinary Portland Cement, it is expected that any reaction with the bentonite will be local. Furthermore, the concrete plugs are placed at a distance from the bentonite buffer around the containers.

Significant degradation of smectite under alkaline groundwater has been observed in conditions with large amounts of alkaline groundwater; however, in natural analogue systems with limited groundwater flow, the reaction is limited. For example, although the International Philippines Natural Analogue Project is at an early stage (Fujii et al. 2010), results to date show that reaction with alkaline water (pH ~11) in the bentonite is restricted to the contact interface, with the width of the reaction zone a maximum of 5 cm. In another example, at the Cyprus Natural Analogue Project (Alexander and Milodowski, 2013), the groundwater ($10 < pH < 11$) appears to have been circulating under the bentonite for approximately 100,000 years. In this time, less than 1% of the smectite in the bentonite has reacted, indicating very slow reaction times. The authors note that sufficient swelling pressure remains in the reacted bentonite to minimize further reaction due to pore throat reduction (see also Wilson et al. 2011).

10.2.3 Concrete

Low-heat, high-performance concrete may be used to close container placement rooms. The concrete bulkheads will counteract the swelling pressure of the bentonite components and maintain the tunnel backfill materials in their intended position. Concrete bulkheads could also be used to provide structural support and confinement to the column of shaft sealing materials. Low-heat high-performance concrete is designed to minimize effects on the adjacent clay (Dixon et al. 2001).

Analogue studies of natural cements suggest that, within stable systems, the material is durable, with the oldest reported cements at Maqarin in north Jordan being some 2 million years old (Alexander 1992). Milodowski et al. (1989) also reported the presence of unreacted natural cements from the Scawt Hill and Carneal Plug sites in Northern Ireland. These cements were produced during the thermal metamorphism of the host limestone and are estimated to be some 58 million years old. In both examples, the natural cements are effectively impermeable and remain unchanged until accessed by groundwaters (through tectonic damage, for example). If damaged, the tendency is for these systems to reseal, either with secondary calcium silicate hydrate phases (Linklater 1998) or carbonates (Clark et al. 1994).

Of the natural analogue studies reported to date on cements, it is important to note that the natural cements examined are more akin to Ordinary Portland Cement, not low-heat high-performance cement (Gray and Shenton 1998). Low-heat high-performance cement is essentially the same as the pozzolanic cements developed by the Romans in the 3rd century BCE, or perhaps in Tiryns and Mycenae a millennium earlier (Middleton 1888). Recent studies of Roman cements exposed to marine salinities for about 2000 years tend to suggest little degradation of the cement (Oleson et al. 2004, Vola et al. 2011).

10.2.4 Asphalt

Bitumens are meltable substances distilled from fossil fuels while asphalts are solid bitumens containing various mineral materials[1]. The shaft seal design concept includes a layer of asphalt, providing a redundant low-permeability seal. The reference asphalt is the same as proposed for use in the Waste Isolation Pilot Plant (WIPP 2009).

Natural asphalts and bitumens have been used as glue or mastic for water-proofing for many thousands of years. In almost all cases where archaeological artifacts have been found coated in asphalt, they have been well preserved when mechanical disruption of the bitumen has not occurred: one example is provided by Babylonian buildings from 1300 BCE, where asphalt was used to coat floors and as a building material in river banks and piers (Hellmuth 1989); another comes from remains within the caves of Lascaux in France, approximately 15,000 years old (NAGRA 1988).

Natural asphalts are found in a number of geological environments and in all climatic zones. Examples include the asphalt lakes of Trinidad and Guanoco, Venezuela, impregnated sandstones and limestones in Athabasca (Canada), Utah (USA), Val de Travers (Switzerland), and Hannover (Germany), and hydrothermal veins in Derbyshire (England).

The Athabasca oil sands located in the McMurray Formation in Athabasca are the largest known reservoir of crude bitumen in the world. The host formation is of early Cretaceous age and composed of numerous lenses of unconsolidated oil-bearing sand. Isotopic studies show the oil deposits to be about 112 million years old (Selby and Creaser 2005). The study by Longstaffe (1993) indicates that the bitumen has remained stable for over 10 million years.

The bitumen deposits in sandstone rocks in the Uinta Basin in Utah are believed to be from the late Cretaceous to Eocene period, 70 to 30 million years ago (Schamel 2009), formed under basin waters that were likely comparable to marine salinity. This natural analogue provides another example of the long-term stability of bitumen under likely saline conditions.

Also within the Uinta Basin in Utah, extensive veins of another natural asphalt called gilsonite were formed by hydrothermal fluids during the Eocene period, 56 to 34 million years ago, and have subsequently remained little altered for several tens of millions of years (Boden and Tripp 2012).

Drake et al. (2006) report natural asphalt (asphaltite) in open and closed fractures at the Forsmark site in Sweden. This asphalt was exposed to brines (45 g/L at present) for at least several million years, suggesting very long-term stability of asphalt under saline conditions.

10.3 Analogue for Geosphere

The site itself is an important analogue for the future behaviour of the geosphere. In particular, geoscientific evidence of the past history of the site provides a direct analogue for future behaviour. This will be gathered for a real site as part of the site characterization, and

[1] Local preference may reverse this terminology (e.g., United Kingdom vs. United States); similarly, common usage may not align with preferred geological terminology.

presented in the geosynthesis. While this is not available for this hypothetical site, the Michigan Basin in general has low seismicity and no volcanism, with evidence that oxygen does not penetrate to any great depth during glaciation.

10.4 Natural Analogue Summary

Performance of repositories cannot be verified by experiment for time scales relevant to their long-term safety. Natural analogues provide qualitative and quantitative illustrations of long-term behaviour, providing support for key model assumptions and for the identification of processes that need to be represented and those that can be excluded. The natural analogues identified here provide additional understanding of the materials and processes that influence the behaviour of radionuclides in a deep geological repository. They provide confidence in the long-term performance of the repository.

10.5 References for Chapter 10

Alexander, W.R. (ed). 1992. A natural analogue study of cement-buffered, hyperalkaline groundwaters and their interaction with a sedimentary host rock - I: Source-term description and geochemical code database validation. NAGRA Technical Report Series NTB 91-10. NAGRA, Wettingen, Switzerland.

Alexander, W.R. and A.E. Milodowski (eds). 2013. Cyprus Natural Analogue Project (CNAP) Phase IV Final Report. Posiva Working Report. Posiva, Eurajoki, Finland.

Ambrosetti, P., G. Basilici, S. Gentili, E. Biondi, Z. Cerquaglia and O. Girotti. 1992. La Foresta Fossile di Dunarobba. Ediart, Todi, Italy.

Angus, N.S., G.T. Brown and H.F. Cleere. 1962. The Iron Nails from the Roman Legionary Fortress at Inchtuthil, Perthshire. Journal of Iron and Steel Institute 200, 956-968.

Benvegnú, F., A. Brondi and C. Polizzano. 1988. Natural Analogues and Evidence of Long-term Isolation Capacity of Clays Occurring in Italy: Contribution to the Demonstration of Geological Disposal Reliability of Long-lived Wastes in Clay. CEC Nuclear Science and Technology Report EUR 11896. Luxembourg.

Boden, T. and B.T. Tripp. 2012. Gilsonite veins of the Uinta Basin, Utah. Utah Geological Survey, Special Study 141. Utah Dept. of Natural Resources, Salt Lake City, USA.

Clark, I.D., R. Dayal and H.N. Khoury. 1994. The Maqarin (Jordan) natural analogue for 14C attenuation in cementitious barriers. Waste Management 14, 467-477.

CNSC. 2006. Regulatory Guide G-320: Assessing the Long Term Safety of Radioactive Waste Management. Canadian Nuclear Safety Commission. Ottawa, Canada.

Cramer, J.J. and J.A.T. Smellie. 1994. Final Report for the AECL/SKB Cigar Lake Analog Study. Atomic Energy of Canada Limited Report AECL-10851, COG-93-00147, SKB-TR-94-00004. Pinawa, Canada.

Crissman, D. and G Jacobs. 1982. Native Copper Deposits of the Portage Lake Volcanics, Michigan: Their Implications with Respect to Canister Stability for Nuclear Waste

Isolation in Columbia River Basalts beneath the Hanford Site, Washington. Rockwell Hanford Operations Technical Report RHO-BW-ST- 26P. Hanford, USA.

Dixon, D.A., N.A. Chandler and P.M. Thompson. 2001. The selection of sealing system components in AECL's 1994 Environmental Impact Statement. Ontario Power Generation Report 06819-REP-01200-10074-R00. Toronto, Canada.

Drake, H., B. Sandström and E-L. Tullborg. 2006. Mineralogy and geochemistry of rocks and fracture fillings from Forsmark and Oskarshamn: Compilation of data for SR-Can. SKB R-06-109. SKB, Stockholm, Sweden.

EUBA. 2011. Fact Sheet on Bentonite. The European Association of the Bentonite Producers (EUBA: Member of IMA-Europe). Brussels, Belgium.

Francis, J.E. 1988. A 50 million-year old fossil forest from Strathcona Fiord, Ellesmere Island, Arctic Canada: evidence for a warm polar climate. Arctic. 41 314-318.

Fujii, N., C.A. Arcilla, M. Yamakawa, C. Pascua, K. Namiki, T. Sato, N. Shikazono and W.R. Alexander. 2010. Natural analogue studies of bentonite reaction under hyperalkaline conditions: overview of ongoing work at the Zambales Ophiolite, Philippines. Proc. ICEM 2010 Conference, ASME, Washington, USA.

Gray, M.N. and B.S. Shenton. 1998. For better concrete, take out some of the cement. In Proc. 6th ACI/CANMET Symposium on the Durability of Concrete, Bangkok, Thailand.

Greenwood, D.R. and J.F. Basinger. 1994. The paleoecology of high latitude Eocene swamp forests from Axel Heiberg Island, Canadian High Arctic. Review of Palaeobotany and Palynology. 81 83-97.

Heikola, T., S. Kumpulainen, U. Vuorinen, L. Kiviranta and P. Korkeakoski. 2013. Influence of alkaline (pH 8.3-12.0) and saline solutions on chemical, mineralogical and physical properties of two different bentonites. Clay Minerals. 48 (2) 309-329.

Hellmuth, K-H. 1989. Natural analogues of bitumen and bitumenized waste. Finnish Centre for Radiation and Nuclear Safety, STUK-B-VALO 58, Helsinki, Finland.

Hellmuth, K-H. 1991. The existence of native iron – Implications for nuclear waste management. Helsinki, Finland: Finnish Centre for Radiation and Nuclear Safety. Report STUK-B-VALO 68.

Hofmann, B.A. 1999. Geochemistry of Natural Redox Fronts – A Review. NAGRA Technical Report NTB 99-05. Wettingen, Switzerland.

IAEA. 1999. Use of Natural Analogues to Support Radionuclide Transport Models for Deep Geological Repositories for Long Lived Radioactive Wastes. International Atomic Energy Agency TECDOC-1109. Vienna, Austria.

Johnson, A.B. and B. Francis. 1980. Durability of Metals from Archaeological Objects Metal Meteorites and Native Metals. Battelle Pacific Northwest Laboratory PNL-3198. Hanford, USA.

Kolaříková, I. and R. Hanus. 2008. Geochemistry and mineralogy of bentonites from Ishirini (Libya). Chemie der Erde-Geochemistry. 68 (1) 61-68.

Laine, H. and P. Karttunen. 2010. Long-Term Stability of Bentonite: A Literature Review. Posiva Working Report WR 2010-53, Posiva, Eurajoki, Finland.

Linklater, C.M. (ed). 1998. A natural analogue study of cement buffered, hyperalkaline groundwaters and their interaction with a repository host rock II. Nirex Science Report, S-98-003, NDA-RWMD, Harwell, UK.

Longstaffe, F. 1993. Meteoric Water and Sandstone Diagenesis in the Western Canada Sedimentary Basis, in SG36: Diagenesis and Basin Hydrodynamics. American Association of Professional Geologists AAPG Special Volume. Tulsa, USA.

McKee, P. and D. Lush. 2004. Natural and Anthropogenic Analogues - Insights for Management of Spent Fuel. Nuclear Waste Management Organization Report APM-REF-06110-24105. Toronto, Canada.

Middleton, J.H. 1888. On the chief methods of construction used in ancient Rome. Archaeologie LI, 41 – 60.

Miller, W., R. Alexander, N. Chapman, I McKinley and J. Smellie. 2000. Geologic Disposal of Radioactive Wastes & Natural Analogues Volume 2. Elsevier/ Pergamon Press. Oxford, UK.

Milodowski, A.E., P.H.A. Nancarrow and B. Spiro. 1989. A mineralogical and stable isotope study of natural analogues of Ordinary Portland Cement (OPC) and CaO–SiO2–H2O (CSH) compounds. United Kingdom Nirex Safety Studies Report, NSS/R240, NDA, Moor Row, UK.

Milodowski, A.E., M.T. Styles and V.L. Hards. 2000. A Natural Analogue for Copper Waste Canisters: The Copper-uranium Mineralised Concretions in the Permian Mudrocks of South Devon, United Kingdom. Swedish Nuclear Fuel and Waste Management Company Report SKB TR-02-09. Stockholm, Sweden.

NAGRA. 1988. Solidification of Swiss Radioactive Waste with Bitumen. National Cooperative for the Disposal of Radioactive Waste (NAGRA). NTB 85-28. Baden, Switzerland (in German).

Oleson, J.P., C. Brandon, S.M. Cramer, R. Cucitore, E. Gotti and R.L. Hohlfelder. 2004. The ROMACONS Project: a Contribution to the Historical and Engineering Analysis of Hydraulic Concrete in Roman Maritime Structures. Intern. J. Nautical Archaeol., 33.2, 199–229. doi: 10.1111/j.1095-9270.2004.00020.x

Pitts, L. and A. St. Joseph. 1985. Inchtuthil Roman Legionary Fortress Excavation 1952-1965. Society for the Promotion of Roman Studies. Britannia Monographs Series 6. London, England.

Pusch, R., H. Takase and S. Benbow. 1998. Chemical processes causing cementation in heat-affected smectite – the Kinnekulle bentonite. SKB Technical Report TR-98-25, Stockholm, Sweden.

Schamel, S. 2009. Strategies for in situ recovery of Utah's heavy oil and bitumen resources. Utah Geological Survey, Open File Report 551. Salt Lake City, USA.

Selby D. and R.A. Creaser. 2005. Direct Radiometric Dating of Hydrocarbon Deposits Using Rhenium-Osmium Isotopes. Science 308, 1293-1295.

Smellie, J.A.T. and F. Karlsson. 1996. A reappraisal of some Cigar Lake issues of importance to performance assessment. SKB Technical Report TR 96-08, SKB, Stockholm, Sweden.

Tait, J.C., H. Roman and C.A. Morrison. 2000. Characteristics and Radionuclide Inventories of Used Fuel from OPG Nuclear Generating Stations Volumes 1 and 2. Ontario Power Generation Report 06819-REP-01200-10029-R00. Toronto, Canada.

Vola, G., E. Gotti, C. Brandon, J.P. Oleson and R.L. Hohlfelder. 2011. Chemical, mineralogical and petrographic characterization of Roman ancient hydraulic concretes cores from Santa Liberata, Italy, and Caesarea Palestinae, Israel. Periodico di Mineralogia 80, 317–338.

Wersin, P., L.H. Johnson and I.G. McKinley. 2007. Performance of the bentonite barrier at temperatures beyond 100°C: A critical review. Physics and Chemistry of the Earth 32 780-788.

Wilson, J., D. Savage, A. Bond, S. Watson, R. Pusch and D. Bennett (2011). Bentonite: a review of key properties, processes and issues for consideration in the UK context. Quintessa Report QRS-1378ZG-1.1 for the NDA-RWMD, Quintessa, Henley - on - Thames, UK.

WIPP. 2009. Waste isolation pilot plant hazardous waste facility permit renewal application September 2009: Appendix I2, Appendix A, Material specification shaft sealing system compliance submittal design report. Waste Isolation Pilot Plant, U.S. Department of Energy, Carlsbad, USA.

Yoshida, H. 1994. Relation between U-series nuclide migration and microstructural properties of sedimentary rocks. Applied Geochemistry, 9 (5), 479-490.

11. QUALITY ASSURANCE

11.1 Introduction

This chapter describes how project activities important to safety in the APM Used Fuel Repository Conceptual Design and Postclosure Safety in Sedimentary Rock were conducted under an appropriate quality assurance framework.

11.2 Used Fuel Repository Conceptual Design and Postclosure Safety

11.2.1 APM Safety Case Project Quality Plan

The APM Safety Case Project Quality Plan (PQP) APM-PLAN-00120-0002-R002 (NWMO 2012a) was prepared by the NWMO Director, Quality Assurance and approved by the Project Manager for use during the preparation of the Used Fuel Repository Conceptual Design and Postclosure Safety in Sedimentary Rock. This APM Safety Case PQP meets the requirements of both CSA N286-12 and ISO 9001:2008.

The quality program applies to all organizational units with responsibilities for the preparation of the Used Fuel Repository Conceptual Design and Postclosure Safety in Sedimentary Rock project. The following processes implement the program:

- A managed system consisting of governing documents that prescribe controls and responsibilities to ensure activities are carried out in a quality assured, effective manner by qualified personnel;
- Individual accountability for implementing and adhering to the managed system elements;
- A specific APM Safety Case Project Execution Plan indentifying project scope, work breakdown, responsibilities and controls, and
- Evaluation and enhancement of the program elements through continuous improvement processes.

Selected vendors and suppliers are required to be qualified to appropriate quality assurance standards defined by the NWMO. Each of these vendors and suppliers selected is required to submit a detailed quality assurance and inspection plan, consistent with the APM Safety Case PQP, for review and subsequent approval.

The quality program includes provisions for systematic planned audits and assessments designed to provide a comprehensive, critical and independent evaluation of project activities. These audits and assessments cover the overall quality program, sub-tier programs, and interfaces between programs. The audits and assessments monitor compliance with governing procedures, standards and technical requirements, and confirm that quality program requirements are being effectively implemented. Audit and assessment results are documented, reported to and evaluated by a level of management having sufficient breadth of responsibility to assure actions are taken to address the findings.

Additional oversight of activities is provided through regular project monitoring and reporting, self-assessment and the non-conformance and corrective action program. In particular, the corrective action program assures that non-conformance conditions are identified, documented, reported, evaluated and corrected in a timely manner.

The APM Safety Case PQP is supported by NWMO governance that establishes expectations for engineering and design, safety assessment, procurement, occupational health and safety, environmental protection, product and services approval, document control and record keeping.

The following are key elements of the APM Safety Case PQP:

- Project specific quality objectives are established.
- Each person working on the project is responsible for achieving and maintaining quality and management is responsible for providing adequate resources and evaluating the quality of the work.
- APM project work is performed in accordance with applicable NWMO governing documents and established processes and procedures.
- Specific requirements for design, safety assessment and technical studies involving computer modeling are described.
- All work is conducted by qualified individuals.
- When work within the scope of the APM project is performed by another organization, the consultant/contractor performs work in compliance with ISO 9001:2008 or CSA N286-12 as appropriate and in compliance with an approved work specific quality plan and APM project-specific governing documents. When a consultant/contractor provides a specialized technical service, and their quality management system is not based on a recognized system, their quality management system may be accepted if it meets internal quality objectives and requirements.
- APM work is verified via verification processes and procedures. Furthermore for work conducted by contractors, project quality plans are approved and include appropriate verification procedures for deliverables including verification process documentation.
- Experience from related industries is obtained through planned activities including information exchanges with other nuclear waste management organizations, participation in technical conferences, contracting with organizations and obtaining independent expert review and input.
- NWMO APM project personnel have access to observe and verify consultants/contractors' quality processes and examine quality assurance documentation.
- Documents considered to be quality assurance records as per APM-LIST-08133-0001, Quality Assurance Documents (NWMO 2011), are transmitted into NWMO records.
- Targeted periodic assessments of work are performed on the APM project. Work performed by NWMO project personnel is assessed for compliance with the APM PQP and applicable procedures. Work performed by consultants/contractors and their subcontractors are assessed to confirm that it is being performed in compliance with their work specific quality plans.

11.2.2 Examples of Peer Review and Quality Assurance

Experienced contractors worked with NWMO to carry out the illustrative postclosure safety assessments for the APM project under approved project specific quality plans. The contractors committed to provide high quality work through effective application of a quality system that fostered best practice and included processes for continual improvement. Safety assessments were conducted consistent with NWMO's governance, NWMO-PROC-EN-0003 Safety Assessment Procedure (NWMO 2012b). For this illustrative safety case formally accepted data clearance forms were used between the geosciences, engineering and safety assessment

teams. Software and reference datasets were procured, developed and maintained consistent with NWMO's governance, NWMO-PROC-EN-0002 Technical Computer Software Procedure (NWMO 2010). The confidence in the software models used for this illustrative safety assessment is reinforced by the consistency in terms of nuclide transport observed between the models as described in Section 7.8.

NWMO and independent peer review of key results and conclusions in the illustrative postclosure safety assessment was planned by the NWMO and completed. The comments and suggested improvements provided by the independent reviewers have been addressed and incorporated as appropriate into the illustrative safety assessment prior to submission to the regulator.

11.2.3 Future Safety Case Quality Assurance

Once an actual repository site is selected, on-site work will commence to characterize the site in terms of its geophysical and environmental properties. Simultaneously, the conceptual design will progress towards the detailed design required for licensing and ultimately container manufacture and facilities construction. The project quality assurance plan will necessarily expand in scope to ensure that the site characterization, detailed design, associated preclosure and postclosure safety assessment and environmental assessment are prepared under a comprehensive and robust quality assurance regime. At an appropriate time in the future, specific quality assurance plans will be prepared and implemented for the manufacturing and qualification of containers and the construction and commissioning of the used fuel transfer facility and the repository.

11.3 References for Chapter 11

CSA N286-12. Management System Requirements for Nuclear Facilities. Canadian Standards Association. Canada.

ISO 9001:2008. Quality Management Systems Requirements. International Organization for Standardization.

NWMO. 2010. Technical Computer Software Procedure. Nuclear Waste Management Organization Procedure NWMO-PROC-EN-0002. Toronto, Canada.

NWMO. 2011. APM Deep Geological Repository Project Quality Assurance Documents. Nuclear Waste Management Organization List APM-LIST-08133-0001. Toronto, Canada.

NWMO. 2012a. APM Safety Case Project Quality Plan. Nuclear Waste Management Organization Plan APM-PLAN-00120-0002-R002. Toronto, Canada.

NWMO. 2012b. Safety Assessment Procedure. Nuclear Waste Management Organization Procedure NWMO-PROC-EN-0003. Toronto, Canada.

THIS PAGE HAS BEEN LEFT BLANK INTENTIONALLY

12. SUMMARY AND CONCLUSIONS

12.1 Purpose of the Pre-Project Report

As stated in Chapter 1, this report presents an illustrative case study of a postclosure safety assessment methodology applied to examine the long-term safety of a reference multi-barrier deep geological repository design for Canada's used nuclear fuel within a hypothetical sedimentary rock setting. The purpose of this case study is to present a postclosure safety assessment methodology to illustrate how CNSC expectations, documented in CNSC Guide G-320 (CNSC 2006), subsequently referred to as G-320, are satisfied. Table 1-4 provides links between G-320 and sections of this report.

It should be recognized that this report is not intended to provide a full deep geological repository safety case as described in G-320. Aspects of G-320 that are relevant to this case study are extracted from this guidance document and included in grey 'text' boxes throughout this chapter. This text is intended to be complementary to this summary and to highlight how key aspects of G-320 have been addressed by the postclosure safety assessment methodology. In this regard, the work presented has focused on describing the appropriate selection and application of assessment strategies.

Developing a long-term safety case, G-320 Section 5.0:

Demonstrating long term safety consists of providing reasonable assurance that waste management will be conducted in a manner that protects human health and the environment. This is achieved through the development of a safety case, which includes a safety assessment complemented by various additional arguments...

It is noteworthy that in the context of a postclosure deep geological repository safety case, this illustrative case study does not include a Geosynthesis. The purpose of a Geosynthesis is to provide an understanding of the geosphere proposed to enclose the repository and its evolution as it relates to establishing confidence in a repository safety case. In the absence of a specific site, a hypothetical sedimentary site was established using geologic information consistent with a location in southern Ontario.

Licensing considerations, G-320 Section 4.3:

It is up to the applicant to determine an appropriate methodology for achieving the long term safety of radioactive waste based on their specific circumstances; however, applicants are encouraged to consult with CNSC staff throughout the pre-licensing period on the acceptability of their chosen methodology.

This summary chapter is intended to highlight the means by which a safety assessment methodology has been applied to evaluate the long-term safety and associated uncertainty surrounding the performance of a repository for nuclear used fuel in a sedimentary setting. The strategy adopted is based, in part, on a defence-in-depth approach consistent with current best

international practice. The results of the safety assessment provide useful insight into the performance of the multi-barrier repository design and specific features of the design that could most influence long-term performance.

The request for a CNSC review of this repository design and illustrative safety assessment is consistent with the G-320 licensing considerations on determining methodology.

12.2 Repository System

System description, G-320 Section 7.3:

It is recognized that the system description may be less complete and rigorous early in the licensing lifecycle, and that the information used in long term assessments of safety for the purpose of design optimization or to support an environmental assessment or a licence application may therefore need to use some default or generic data. As licensing progresses through the facility's lifecycle, as-built information and operational data are acquired, and the site characteristics become better understood. It is expected that assessments of long term safety that are made later in the licensing lifecycle will be based on updated and refined models and data, with less reliance on default, generic, or assumed information, resulting in more reliable model results.

Section 4 of G-320 identifies several methods for long-term waste management, including surface facilities, near-surface facilities and deep geological facilities. As previous mentioned, this report describes the currently envisioned deep geological multiple barrier repository design for the long-term safe management of used nuclear fuel in a sedimentary rock setting. This design and waste management approach is commensurate with the waste's radiological, chemical, and biological hazard to the health and safety of persons and the environment.

The deep geological repository system is described in Chapters 2 through 5 of this report where:

- Chapter 2 describes the hypothetical geosphere setting;
- Chapter 3 describes the characteristics of the used nuclear fuel;
- Chapter 4 describes the repository design concept; and
- Chapter 5 describes how key components of the system will interact with each other and with the environment in the long term.

The key points from these chapters are summarized in this section along with parameters identified in the safety assessment as being influential to repository performance.

12.2.1 Geologic Description of the Hypothetical Site

Information related to the geologic characteristics of the site for the purpose of this illustrative safety assessment is presented in Chapters 1 and 2. Site-specific characterization activities at a candidate site would be designed to gather information on a broad range of geologic characteristics that would be used to develop a Descriptive Geosphere Site Model and support a repository safety case. For the purpose of this illustrative case study several key attributes

have been assumed for the hypothetical site as listed in Chapter 1 (Section 1.6.3.1). Such attributes that would be verified through site-specific investigation include:

- The repository is located in an area of low seismic hazard;
- The repository location is not associated with potable groundwater resources;
- The repository location is not associated with economically viable natural resources;
- The groundwater system at repository depth is reducing;
- No large-scale transmissive fractures are in close proximity to the repository site;
- The host rock formation can withstand transient thermal and mechanical stresses; and
- The rate of site uplift and erosion are sufficiently small not to influence repository safety.

Specific site characteristics for the case study are described in Chapter 2. In particular, this chapter describes a conceptual geosphere model for the site assessed. The properties assigned to the various bedrock formations within the sedimentary sequence has been informed by work conducted in Southern Ontario. Information presented in Chapter 2 describes the long-term behaviour of the groundwater system as relevant to developing an understanding of postclosure repository safety. In addition to a reference case geosphere, alternative conceptual models are described with the purpose of illustrating a range of possible characteristics and groundwater system behaviours. The uncertainty associated with these alternative models is explored through sensitivity, bounding and 'what-if' simulations performed as part of the safety assessment.

12.2.2 Used Fuel

The characteristics of the used fuel are described in Chapter 3. The durability of used fuel and distribution of radionuclides within the fuel are identified as characteristics of the multi-barrier system. These characteristics contribute to the low dissolution rate of the fuel and hence the low release rate of radionuclides from the fuel matrix.

12.2.3 Design Concept

Licensing considerations, G-320 Section 4.3:

The design of a nuclear facility should be optimized to exceed all applicable requirements. In particular, a radioactive waste management facility should more than meet the regulatory limits, remaining below those limits by a margin that provides assurance of safety for the long term.

The repository design concept is presented in Chapter 4. As part of the multi-barrier system, two engineered barriers are included in this concept: a copper-shell container and a clay-based sealing system. Appendix A summarizes a comparison of this engineered barrier system design to internationally proposed repository concepts. A notable difference in this case study with those presented in Appendix A is the copper-shell container design as opposed to a steel-only design. The container and clay-based sealing system designs will be further refined and optimized in advance of a future licence application. This approach is consistent with G-320, which identifies that the repository should more than meet the regulatory limits and remain below those limits by a margin that provides assurance of safety in the long term.

Waste management system, G-320 Section 4.1:

Waste management system for long term storage and disposal of waste refer to the combination of natural and engineered barriers and operational procedures that contribute to safely managing the waste. Long term assessment of these systems can provide information that can be used when making decisions concerning:

1. *Selection of an appropriate site;*
2. *Site characterization;*
3. *Selection of suitable design options during planning;*
4. *Optimization of selected design(s), including minimization of operational and post-operational impacts; and*
5. *Development of construction, operation, and decommissioning strategies and plans.*

Key assumptions in this case study include:

- The repository was positioned arbitrarily at a depth of 500 m. In an actual siting process, the repository location and layout geometry would be designed to improve passive safety based on site-specific host rock conditions.
- A long-lived container with a 25 mm copper corrosion barrier. Research indicates that 1.3 mm would be sufficient for corrosion protection for 1 million years under reducing conditions. The assumed thicker copper-shelled containers provide a much greater margin of safety and facilitate container manufacturing and handling.
- Highly compacted low permeability bentonite surrounds the containers.
- Low permeability clay-based repository sealing systems.

The influence of these design features on repository performance is explored through the safety assessment summarized in Section 7.12. For example, sensitivity and complementary bounding analyses are used to illustrate the effects of an increased fuel dissolution rate, increased container failure rate, increased bedrock hydraulic conductivity, increased geosphere diffusivities and decreased sorption.

Chapter 5 describes the repository system, and how key components of the system will interact with each other and the environment in the long-term, consistent with the G-320 guidance.

The long-term safety assessment presented in this report provides information that can be used to support and inform future decision making as described in G-320.

12.3 Safety Assessment

A structured approach is used to conduct the postclosure safety assessment where two classes of scenarios are assessed, consistent with Sections 5 and 7 of G-320. More specifically, the expectation to demonstrate the understanding of the system through a well structured, transparent, and traceable methodology is described in this report.

Performing long term assessments, G-320 Section 7.0:

The CNSC expects the applicant to use a structured approach to assess the long term performance of a waste management system. Although long term assessments are done with different levels of detail and rigor for different purposes, the overall methodology for performing them should include the following elements:

1. *Selection of appropriate methodology;*
2. *Assessment context;*
3. *System description;*
4. *Timeframes;*
5. *Assessment scenarios; and*
6. *Development of assessment models.*

The approach uses a systematic scenario identification process that acknowledges the timeframes of interest and that identifies features, events, and processes, which could have an impact on the repository's safety features, as described in Chapter 6. The different assessment strategies, including key assumptions and rationale, are described and complementary indicators are presented in Chapter 7, and summarized in this section.

The **Normal Evolution Scenario** is based on a reasoned extrapolation of the hypothetical site and repository features, events and processes. It accounts for the expected degradation of the site and repository over time, and addresses the effects of anticipated events. The computer models and key assumptions are discussed in Chapter 7, which includes a description of analyses of impact for a Reference Case and a range of variant cases in which the effects of changes in postulated physical and chemical conditions are examined.

Disruptive Event Scenarios examine the occurrence of unlikely events leading to the circumvention of barriers and loss of containment. Chapters 7 and 8 present the methods, assumptions and results associated with the analysis of disruptive events.

Criteria for protection of persons and the environment, G-320 Section 6.2:

The regulatory requirements for protection of persons and the environment from both radiological and non-radiological hazards of radioactive wastes lead to four distinguishable sets of acceptance criteria for a long term assessment:

1. *Radiological protection of persons;*
2. *Protection of persons from hazardous substances;*
3. *Radiological protection of the environment; and*
4. *Protection of the environment from hazardous substances.*

The results from the Normal Evolution and Disruptive Events Scenarios are compared against interim acceptance criteria consistent with the guidance of G-320. The interim acceptance criteria selected for comparison were proposed to the CNSC for the purpose of this pre-project report in the following categories:

- Radiological protection of persons;
- Protection of persons from hazardous substances;
- Radiological protection of the environment; and
- Protection of the environment from hazardous substances.

The interim acceptance criteria are described in Section 7.1 for this case study.

12.3.1 Assessment Strategies

Use of different assessment strategies, G-320 Section 5.2:

The strategy used to demonstrate long term safety may include a number of approaches, including, without being limited to:

1. *Scoping assessments to illustrate the factors that are important to long term safety;*
2. *Bounding assessments to show the limits of potential impact;*
3. *Calculations that give a realistic best estimate of the performance of the waste management system, or conservative calculations that intentionally over-estimate potential impact; and*
4. *Deterministic or probabilistic calculations, appropriate for the purpose of the assessment, to reflect data uncertainty.*

Any combination of these or other appropriate assessment strategies can be used in a complementary manner to increase confidence in the demonstration of long term safety.

Key activities that are included in the approach to assess long-term safety are described in Sections 7.5 and 8.5. These include:

- Performing a screening exercise to identify potentially significant dose contributing radionuclides so that subsequent assessments can focus on these radionuclides.
- Conducting 3-dimensional hydrogeological modelling of the groundwater system(s) hosting the repository.
- Performing deterministic and probabilistic calculations of radionuclide transport from fuel to surface. This includes analysis of both normal and disruptive scenarios accompanied by sensitivity cases and bounding assessments.
- Estimating dose consequences for a critical group assumed to be farming on the surface biosphere directly above the repository.
- Investigating gas generation and transport at two different scales of resolution (room-scale and repository-scale) to determine impact on dose consequence.

12.3.2 Modelling Tools and Computer Codes

As discussed in Sections 7.3, 7.4 and 8.3, appropriate modelling tools and computer codes are applied to assess key aspects of the repository's components and specific scenarios, consistent with the expectations in Section 7.6 of G-320.

The main computer models used to assess water-borne contaminant transport are FRAC3DVS-OPG v1.3 and SYVAC3-CC4 v4.09. These codes and their reference datasets are maintained under a NWMO software quality assurance system. They are the current generation of codes that have been in use for Canadian repository assessments for many years, with FRAC3DVS being a commercially available code.

Developing and using assessment models, G-320 Section 7.6:

An assessment model should be consistent with the site description, waste properties, and receptor characteristics, and with the quality and quantity of data available to characterize the site, waste, exposure pathways, and receptors. A systematic process should be used to ensure that the set of data used for developing the assessment model is accurate and representative. Complex models should not be developed if there is not sufficient data to support them. The use of generic or default data in place of site-specific data in developing the conceptual and computer models may be acceptable when there is no site-specific data available, such as in early stages of development; however, with the acquisition of as-built information and operational data, and increased understanding of site characteristics throughout the facility lifecycle, site-specific data should be used.

Confidence in assessment models:

Confidence in the assessment model can be enhanced through a number of activities, including (without being limited to):

1. *Performing independent predictions using entirely different assessment strategies and computing tools;*
2. *Demonstrating consistency between the results of the long term assessment model and complementary scoping and bounding assessments;*
3. *Applying the assessment model to an analog of the waste management system;*
4. *Performing model comparison studies of benchmark problems;*
5. *Scientific peer review by publication in open literature; and*
6. *Widespread use by the scientific and technical community.*

The codes are used in a complementary manner, with FRAC3DVS-OPG providing detailed 3-dimensional flow and mass transport results for a limited number of cases, and SYVAC3-CC4 extending the results to a broader range of nuclides and sensitivity cases. The simplified SYVAC-CC4 model for this case study is derived with help from the detailed FRAC3DVS-OPG transport results for I-129. This model was then verified by comparing the I-129 mass flow results from the two models at various locations in the geosphere, including the Cobourg and Georgian Bay formations. Further similar comparisons were performed for other specific

radionuclides that represented a range of decay and transport parameters (i.e., Cs-135, U-234 and U-238).

To explore uncertainties arising from data variability, SYVAC3-CC4 is used to conduct a probabilistic safety assessment of the entire repository system. Over 100,000 simulations are performed in which hundreds of input variables are simultaneously varied according to defined parameter distributions.

The main computer code used to assess gas-borne transport is T2GGM. It assesses the coupled behaviour between gas generation, temperature and the movement of gas and water. It is composed of two coupled models: the Gas Generation Model (GGM) used to describe the generation of gas due to corrosion of steel components, and the TOUGH2 model used to describe gas and water transport from the repository and within the geosphere, as described in Section 8.3.

12.3.2.1 Key Assumptions and Conservatisms in Modelling

Conservative over-estimates, G-320 Section 5.2.2:

A *conservative approach should be used when developing computer codes and models, and assumptions and simplifications of processes to make them more amenable for inclusion in computer models should not result in under-estimation of the potential risks or impacts*.

Chapter 7 describes the key attributes for the Reference Case of the normal evolution scenario. The illustrative assessment presented in this report uses different strategies consistent with expectations in G-320. The assessment of the Reference Case includes the following conservatisms as described in Chapter 9:

- The defective containers fill with water 10,000 years after the containers are placed in the repository;
- No credit is taken for the presence of the fuel sheath in maintaining fuel integrity and in preventing contact of the fuel matrix with water that may enter the container;
- No credit is taken for the effect of hydrogen gas (H_2) (produced by corrosion of the defective container) on the dissolution rate of the uranium oxide fuel (UO_2) fuel;
- No credit is taken for the effect of iron oxides (produced by corrosion of the defective container) in providing a high surface area for adsorption of some of the radionuclides released from the fuel;
- No credit is taken for the likely filling of the defect with bentonite and/or corrosion products which could significantly increase the transport resistance of the defect;
- Positioning the 3 defective containers in a repository location associated with the shortest travel time to the surface;
- A very deep well (219 m) is included in the assessment. It is positioned at the bottom of the Guelph formation layer, at about the deepest point where potable water may occur. This is

a position that would maximize dose consequence (i.e., it penetrates the entire thickness of the Guelph Formation and is located along the main pathway for contaminants released from the defective containers); and

- Conservative properties for the critical group (e.g., use of 90th percentile food ingestion rates; obtaining all food, fuel, water and building material locally; and all drinking and irrigation water taken from the well, etc.).

Since this Reference Case assumes a constant temperate climate, Section 7.10 also discusses the anticipated effects of glaciation on the assessment.

Analyzing uncertainties, G-320 Section 8.2:

A formal uncertainty analysis of the predictions should be performed to identify the sources of uncertainty. This analysis should distinguish between uncertainties arising from:

1. *Input data;*
2. *Scenario assumptions;*
3. *The mathematics of the assessment model; and*
4. *The conceptual models.*

These conservatisms are further described as part of the approach to assess uncertainties in Chapter 9. The division of uncertainties into scenario, model and data uncertainties is consistent with the guidance of G-320.

12.3.3 Normal Evolution Scenario

Normal evolution scenario, G-320 Section 7.5.1:

A normal evolution scenario should be based on reasonable extrapolation of present day site features and receptor lifestyles. It should include expected evolution of the site and degradation of the waste disposal system (gradual or total loss of barrier function) as it ages.

Depending on site-specific conditions and the timeframe for the assessment, a normal evolution scenario may need to include extreme conditions such as climate shifts or the onset of glaciations.

The Normal Evolution Scenario is based on a reasoned extrapolation of the site and repository, consistent with the expectations in Section 7.5 of G-320. The containers are designed to be durable over very long times, and will be fabricated and placed under careful quality control.

For the Reference Case, the primary dose contributor from the defective containers is determined to be I-129. This is because a fraction of the I-129 is instantly released from the gap and grain boundary inventory in the fuel when water first contacts the fuel. Also, it is long-lived and unretarded in the sub-surface environment. Other radionuclides, in particular

actinides, are only released as the fuel slowly dissolves and are then subsequently sorbed by the enclosing barrier systems.

Figure 12-1 illustrates how radionuclides from the assumed defective containers are expected to be transported through the system's barriers over time. Two timeframes (i.e., 15,000 years and 1 million years) are used to illustrate the changes in activity for the following three types of radionuclides:

- I-129 is non-sorbing in the buffer, backfill and geosphere and is therefore expected to eventually be released to the surface biosphere, with a predicted peak contribution to dose occurring at around 10 million years.

- Cs-135 is an intermediate sorbing fission product that is delayed by the buffer and backfill and hence it's released to the surface biosphere is delayed.

- U-238 is strongly sorbing to the buffer and backfill and is never expected to be released to the surface biosphere.

The calculated peak total dose for this case is determined to be about 0.000002 mSv per year (2 nSv/a) and occurs at the modelling cut-off time of 10 million years. As shown in Figure 7-73, I-129 is responsible for the dose consequence. The dose applies to a person living in the surface biosphere directly above the repository. It is about 150,000 times less than the dose constraint of 0.3 mSv per year, and is a small fraction of the average natural background dose (more than one million times lower). The peak dose occurs after 10 million years and is captured in the sensitivity analysis of increasing the rock diffusivity by a factor of 10, as described in Section 12.3.3.1.

The radiological impact on non-human biota is discussed in Section 7.11.2 and the assessment concludes that the effects are negligible for the Normal Evolution Scenario.

Chapter 7 also addresses the protection of persons and the environment from hazardous substances such as copper and other elements released from the used fuel and the containers. Section 7.11.3 concludes that all contaminant concentrations are below their associated acceptance criteria.

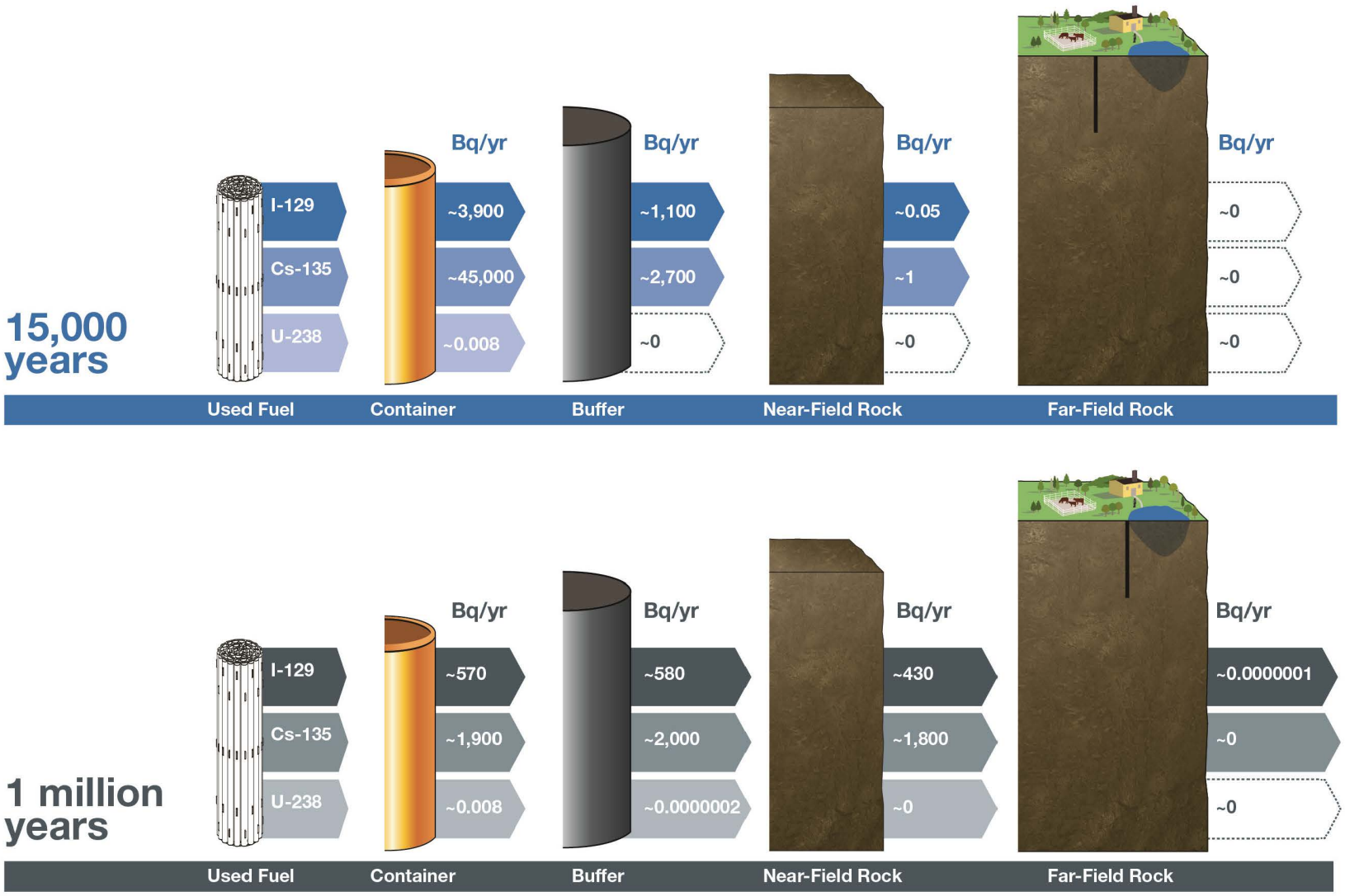

Figure 12-1: Illustration of Radionuclide Transport in the Repository System

12.3.3.1 Results from Sensitivity Analyses and Bounding Assessments

Deterministic calculations, G-320 Section 5.2.3:

The mathematical approach to analyzing the scenarios in the safety case is guided by the purpose of the long term assessment. A deterministic model uses single-valued input data to calculate a single-valued result that will be compared to an acceptance criterion. Variations in input data values are taken into account in these calculations. To account for data variability, individual deterministic calculations must be done using different values of input parameters.

This is the approach used for performing sensitivity analyses (determining the response of model predictions to variations in input data) and importance analyses (calculating the range of predicted values that corresponds to the range of input values) of deterministic models.

To account for the variation in the key input data values used in the Reference Case, a number of sensitivity analyses are completed for key parameters as described in Section 7.2. Some parameters are also pushed beyond their reasonable range of variations by setting their values to zero or by removing limits and running a set of bounding assessments, where a specific parameter is completely ignored. The identified parameters, the variation in their values and the rationale for selecting these cases are summarized in Chapter 7, Table 7-3.

The impacts are determined from simulations performed with either the FRAC3DVS-OPG or the SYVAC3-CC4 codes. The FRAC3DVS-OPG code does not have a biosphere model and therefore its results are presented in terms of I-129 transport to the surface. This provides a reasonable estimate of potential impacts by comparison with the I-129 transport to surface for the Normal Evolution Scenario, since SYVAC3-CC4 simulations show that I-129 dominates the dose consequence.

A summary of the cases, a comparison against the interim acceptance criterion and the key findings are presented in Table 12-1. This comparison of assessment results with interim acceptance criteria is consistent with the guidance in Section 8 of G-320.

The sensitivity analyses show that the impact on dose is small when key parameters are varied. The sensitivity analysis showing the largest effect on the calculated impacts is when the rock diffusivity is increased by a factor of 10. In this case, the peak dose is 13 times greater than in the Reference Case and occurs at 5.6 million years. This remains 12,000 times below the interim dose acceptance criterion. Increasing the dissolution rate of used fuel is also observed to have an impact. The dose consequence when the fuel dissolution rate is increased by a factor of 10 is 3 times greater than in the Reference Case. This remains approximately 51,000 times below the interim dose acceptance criterion with the maximum dose during the simulation occurring at the same time as in the Reference Case, i.e., at the modelling cut-off time of 10 million years.

Some sensitivity analyses are found to have a negligible impact on dose in this case study. When the hydraulic conductivity of the rock mass enclosing the repository is increased by a

factor of 10, the maximum dose consequence relative to the Reference Case is slightly lower. When a 158 m overpressure is used in the Shadow Lake Formation, which is located below the repository at a depth of approximately 675 m, the maximum dose consequence is 1.1 times greater than the Reference Case. Similarly, when the fuel's instant release fraction is increased, the maximum dose consequence is 1.1 times greater than the Reference Case. In all cases, the maximum dose occurs at the same time as the Reference Case, i.e., at the modelling cut-off time of 10 million years.

Some sensitivity analyses are found to have no impact on dose in this case study and these include: increasing the hydraulic conductivity value of the excavation damaged zone, increasing the container defect area, and reducing sorption in the geosphere at the same time as increasing solubility limits.

As noted above, a set of bounding assessments are included to explore the effects of varying some parameters beyond the reasonable range of variations.

The bounding assessments with an effect on dose are for the sensitivity cases where sorption is ignored. When sorption in the near field is ignored, the dose consequence is assessed to be 3.4 times greater than in the Reference Case. This remains approximately 45,000 times below the interim dose acceptance criterion, with the maximum dose occurring at the same time as the Reference Case, i.e., at the modelling cut-off time of 10 million years. When sorption in the geosphere is ignored, the dose consequence is assessed to be 1.7 times greater than in the Reference Case. This remains approximately 91,000 times below the interim dose acceptance criterion, with the maximum dose occurring at the same time at the Reference Case.

There is no impact on dose when radionuclide solubility limits are ignored.

12.3.3.2 Results from the Probabilistic Analysis

Probabilistic calculations, G-320 Section 5.2.3:

Probabilistic models can explicitly account for uncertainty arising from variability in the data used in assessment predictions. Such models may also be structured to take account of different scenarios (as long as they are not mutually exclusive) or uncertainty within scenarios. Probabilistic models typically perform repeated deterministic calculations based on input values sampled from parameter distributions, with the set of results expressed as a frequency distribution of calculated consequences. Frequency multiplied by consequence is interpreted as the overall potential risk of harm from the waste management system.

The results from the probabilistic cases are presented in Chapter 7, consistent with the expectations of G-320 in Section 5.2 on the use of different assessment strategies, where all parameters represented by probability distributions are simultaneously varied. In this case study, relevant parameters for contaminant release and mass transport (in the repository, geosphere and biosphere) were varied whereas the parameters associated with groundwater flow were not.

The probabilistic analysis uses a Monte Carlo random sampling strategy that considers the full range of possible parameter values. A total of 120,000 simulations are performed and examined to identify an average and 95th percentile peak dose rates. The results are summarized in Table 12-1. The average dose for all simulations is 8 times greater than the Reference Case, as shown in Figure 7-85. Whereas, the 95th percentile dose consequence is assessed to be 37 times greater than in the Reference Case. This remains 4,000 times below the interim dose acceptance criterion. The results also show that there are no simulations that exceed the interim dose acceptance criterion.

Table 12-1: Summary and Key Findings from Sensitivity Analyses, Bounding Assessments and Probabilistic Analysis

Case	Description	Key Findings
Reference Case	Reference Case parameters	• Peak dose occurs after 10 million years • Maximum dose occurs at 10 Ma and is 150,000 times lower than normal evolution dose acceptance criterion of 0.3 mSv per year
Degraded Physical Barrier Sensitivity Cases		
Fuel dissolution rate	Fuel dissolution rate increased by a factor of 10	Impact of variation is minimal • Maximum dose rate occurs at the same time • Dose consequence is 3 x Reference Case
Container defect area	Container defect area increased by a factor of 10	No impact • Maximum dose rate occurs at the same time • Dose consequence is equal to Reference Case
Fuel instant release fraction	Instant release fraction increased to 10%	Impact of variation is negligible • Maximum dose rate occurs at the same time • Dose consequence is 1.1 x Reference Case
Geosphere Sensitivity Cases		
Rock Mass Hydraulic Conductivity	Hydraulic conductivity increased by approximately a factor of 10	Impact of variation is negligible • Maximum dose rate occurs at the same time • Dose consequence is 0.8 x Reference Case
Conductivity of excavation damaged zone	Hydraulic conductivity value increased by a factor of 10	No impact • Maximum dose rate occurs at the same time • Dose consequence is equal to Reference Case
Rock diffusivity	Diffusivity increased by a factor of 10	Impact of variation is noticeable • Peak dose rate occurs at 5.6 million years • Dose consequence is 13 x Reference Case

Case	Description	Key Findings
Shadow Lake overpressure	158 m overpressure in the Shadow Lake Formation	Impact of variation is negligible • Maximum dose rate occurs at the same time • Dose consequence is 1.1 x Reference Case
Degraded Chemical Barrier Sensitivity Case		
Coincident sorption and radionuclide solubility limits	Low sorption in the geosphere with coincident high solubility limits	No impact • Maximum dose rate occurs at the same time • Dose consequence is equal to Reference Case
Bounding Assessments		
Sorption in the geosphere	Sorption in the geosphere is ignored	Impact of variation is negligible • Maximum dose rate occurs at the same time • Dose consequence is 1.7 x Reference Case
Radionuclide solubility limits	Radionuclide solubility limits are ignored	No impact • Maximum dose rate occurs at the same time • Dose consequence is equal to Reference Case
Sorption in the near field	Sorption in the near field is ignored	Impact of variation is minimal • Maximum dose rate occurs at the same time • Dose consequence is 3.4 x Reference Case
Probabilistic Simulations		
All parameters varied	Average dose	• Dose rate occurs at 5.6 million years • Dose rate is 19,000 times lower than normal evolution dose acceptance criterion of 0.3 mSv per year
All parameters varied	Maximum dose rate, 95th percentile	• Dose rate occurs at 5.6 million years • Dose rate is 4,000 times lower than normal evolution dose acceptance criterion of 0.3 mSv per year

12.3.3.3 Results from Complementary Indicators

Complementary indicators of safety, G-320 Section 5.4:

Several other safety indicators, such as those that reflect containment barrier effectiveness of site-specific characteristics that can be directly related to contaminant release and transport phenomena, can also be presented to illustrate the long term performance of a waste management system. Some examples of additional parameters include:

1. *Container corrosion rates;*
2. *Waste dissolution rates;*
3. *Groundwater age and travel time;*
4. *Fluxes of contaminants from a waste management facility;*
5. *Concentrations of contaminants in specific environmental media (for example, concentration of radium in groundwater); or*
6. *Changes in toxicity of the waste.*

Complementary indicators other than dose to an assumed human group are described in Section 7.11.1. Two indicators considered in this study are:

- Radiotoxicity concentration in a water body, for medium time scales; and
- Radiotoxicity transport from the geosphere, for longer time scales.

Due to the absence of a lake or river in the nearby hypothetical biosphere model, results are reported only for the radiotoxicity transport indicator. Chapter 7 shows that this indicator is well below its reference value, thereby providing additional confidence that at long times the impact of the repository is likely to be very small.

12.3.4 Disruptive Events Scenarios

Disruptive event scenarios, including human intrusion, G-320 Section 7.5.2

Disruptive event scenarios postulate the occurrence of unlikely events leading to possible penetration of barriers and abnormal loss of containment.

Disruptive scenarios are assessed where barriers are assumed to fail due to unlikely failure mechanisms, as described in Section 6.2 of this report and consistent with Section 7.5 of G-320.

Chapter 6 also includes a review of the scenarios considered in assessments of deep repositories in other countries. The results, summarized in Table 6-5 of this report, show that most assessments have identified a limited number of additional scenarios that consider the degradation / failure of engineered and natural barriers by external processes (e.g., earthquakes, climate change) and human actions (e.g., drilling, poor quality control). Although there are some scenarios identified that are not considered in the current study, these

are either not relevant to a sedimentary rock site or were identified as relevant but not analyzed in this case study.

The scenarios considered in this study and key findings are summarized in Table 12-2.

The impacts are determined from simulations performed with either the FRAC3DVS-OPG or SYVAC3-CC4 codes. The FRAC3DVS-OPG code does not have a biosphere model and therefore its results are presented in terms of I-129 transport to the surface. This provides a reasonable estimate of potential impacts by comparison with the I-129 transport to surface for the normal evolution scenario, since SYVAC3-CC4 simulations show that I-129 dominates the dose consequence.

Table 12-2: Summary of Key Findings from Disruptive Events

Scenario	Key Findings
All Containers Fail at 60,000 Years	• Maximum dose rate occurs at 10 million years • Dose consequence is 130 times below the disruptive events dose acceptance criterion of 1 mSv per year
All Containers Fail at 10,000 Years	• Maximum dose rate occurs at 10 million years • Dose consequence is 120 times below the disruptive events dose acceptance criterion of 1 mSv per year
Shaft Seal Failure	• Maximum dose rate occurs at 10 million years • Dose consequence is 500,000 times below the disruptive events dose acceptance criterion of 1 mSv per year

The results from the All Container Failure Scenarios, identified in Table 12-2, indicate that the containers are an important part of the multiple barriers in sedimentary rock, but also that there is sufficient redundancy in the system that safety is not compromised even in the unexpected event of simultaneous failure of all the containers at 10,000 years or later. The maximum impact is roughly proportional to the number of failed containers (a little less, as radionuclides released from some containers take a long time to reach the well location). However the maximum results are not highly sensitive to the time of container failure beyond 10,000 years. This occurs since the container failure time in both cases is longer than the short-lived fission product decay time, meaning that fuel dissolution rates are not influenced by these short-lived fission products. The remaining actinides and most of the remaining long-lived fission products are retained and delayed in the other engineered and natural barriers so that the maximum dose rate does not substantially change between these two cases.

Chapter 8 further examines the variant case of the All Containers Fail at 10,000 years Scenario in a bounding assessment that considers the largest potential for gas production (from the corrosion of steel within the copper container) and determines the radiological impact from gas-borne radionuclides. The model shows that gas generated within the repository could travel upward to the Guelph Formation.

Model calculations determine that pore pressure within the intact rock does not exceed 80% of lithostatic pressure over the one million year simulation period.

Gas-borne dose consequences are further assessed in Chapter 8 using a set of extremely conservative assumptions to bound the potential dose consequences. A peak dose rate of 0.17 mSv per year is obtained when all the Carbon-14 is assumed to discharge into a house above the repository. This remains a factor of six below the 1 mSv per year acceptance criterion. The peak occurs at 18,000 years. For a more realistic case of failure of copper containers over longer times, the dose rates would be substantially lower. For example, if the copper fails on time scales associated with the next glaciation or later, the corresponding dose rates would be well below 0.001 mSv per year due to decay of Carbon-14.

The Shaft Seal Failure Scenario shows negligible effect on the predicted dose consequence in this study due to the distance between the three defective containers and the shafts. The location of the defective containers relative to shaft will be further assessed in a future safety case.

Disruptive event scenarios, including human intrusion, G-320 Section 7.5.2

Scenarios assessing the risk from inadvertent intrusion should be case-specific, based on the type of waste and the design of the facility, and should consider both the probability of intrusion and its associated consequences. Surface and near-surface facilities (e.g., tailings sites) are more likely to experience intrusion than deep geological facilities.

Scenarios concerning inadvertent human intrusion into a waste facility could predict doses that are greater than the regulatory limit. Such results should be interpreted in light of the degree of uncertainty associated with the assessment, the conservatism in the dose limit, and the likelihood of the intrusion. Both the likelihood and the risk from the intrusion should therefore be reported.

As described in Chapter 7, Section 7.9.1 presents a stylized analysis for the Inadvertent Human Intrusion Scenario. This scenario is a special case, as recognized in Section 7.5.2 of G-320, since it bypasses all the barriers put in place, and therefore the associated dose consequence could exceed the regulatory limit.

The results from the human intrusion assessment show a potential maximum acute dose to the drill crew of about 1,100 mSv, and a potential chronic dose to a site resident (i.e., someone farming on the site) of about 1,100 mSv per year, assuming early intrusion and improper management of the drill site.

The likelihood of inadvertent human intrusion is addressed in the siting of a deep geological repository; in part through placing the used fuel deep underground in a geologic setting with low mineral resource potential, poor prospects for potable groundwater resources, and by the use of institutional controls.

The likelihood of this event occurring is roughly estimated as $3x10^{-5}$ per year, which implies a risk of serious health effects of $2x10^{-6}$ per year. This is less than the annual risk criterion of $1x10^{-5}$ per year.

12.4 Future Work

The conceptual design and illustrative postclosure assessment presented in this report for a hypothetical site represent a single case study in sedimentary rock. Other design concepts and other site conditions have been explored in other Canadian and international case studies. Most recently, the NWMO completed a similar study for a used fuel repository in crystalline rock (NWMO 2012).

Since this report is prepared for a hypothetical site and thus is not a full safety case, a number of aspects are not covered in detail. These are noted in Chapter 1. Also, the postclosure safety assessment illustrated the method and approach, but did not assess all scenarios or aspects of relevance for a full safety case (see Section 7.2.4).

There is ongoing work at NWMO to improve our understanding of key processes and uncertainties in both crystalline and sedimentary rock settings. These are described in the NWMO RD&D report (Villagran et al. 2011).

12.5 Conclusion

The purpose of the NWMO request for a review of this pre-project report is to obtain CNSC feedback on meeting general overall expectations of CNSC Guide G-320, Assessing the Long Term Safety of Radioactive Waste Management. The current case study work, done at a very early stage in the APM Project, supports the continuing development of a deep geological repository for used fuel in sedimentary rock. The illustrative postclosure safety assessment methodology is included for review.

12.6 References for Chapter 12

CNSC. 2006. Regulatory Guide G-320: Assessing the Long Term Safety of Radioactive Waste Management, Canadian Nuclear Safety Commission, Ottawa, Canada.

NWMO. 2012. Used Fuel Repository Conceptual Design and Postclosure Safety Assessment in Crystalline Rock, Pre-Project Report. Nuclear Waste Management Organization NWMO TR-2012-16. Toronto, Canada.

Villagran, J., M. Ben Belfadhel, K. Birch, J. Freire-Canosa, M. Garamszeghy, F. Garisto, P. Gierszewski, M. Gobien, S. Hirschorn, N. Hunt, A. Khan, E. Kremer, G. Kwong, T. Lam, P. Maak, J. McKelvie, C. Medri, A. Murchison, S. Russell, M. Sanchez-Rico Castejon, U. Stahmer, E. Sykes, A. Urrutia-Bustos, A. Vorauer, T. Wanne and T. Yang. 2011. RD&D Program 2011 – NWMO's Program for Research, Development and Demonstration for Long-Term Management of Used Nuclear Fuel. Nuclear Waste Management Organization Report NWMO TR-2011-01. Toronto, Canada.

THIS PAGE HAS BEEN LEFT BLANK INTENTIONALLY

13. SPECIAL TERMS

13.1 Units

a	annum
Bq	becquerel
^{o}C	degree Celsius
cm	centimetre
d	day
dm	decimetre
g	gram
Gy	gray
GPa	gigapascal
h	hour
K	Kelvin
kg	kilogram
kgU	kilogram of Uranium
kJ	kilojoule
km	kilometre
kW	kilowatt
L	litre
m	metre
Ma	million years
mASL	metres above sea level
mBGS	metres below ground surface
mg	milligram
Mg	megagram
MJ	megajoule
mL	millilitre
mm	millimetre
mol	mole
MPa	megapascal
mSv	millisievert
mV	millivolt

mW	milliwatt
MW	megawatt
n	neutron (associated with neutron fluence)
nm	nanometre
nSv	nanosievert
Pa	pascal
ppm	parts per million
s	second
Sv	sievert
W	watt
wt%	mass percentage
µg	microgram
µm	micrometre
µSv	microsieverts

13.2 Abbreviations and Acronyms

1D	One Dimensional
2D	Two Dimensional
3D	Three Dimensional
ADS	Adsorbed
AECL	Atomic Energy of Canada
ALARA	As Low as Reasonably Achievable
APM	Adaptive Phased Management
AQ or (aq)	Aqueous
BCE	Before Common Era
BSB	Bentonite-Sand Buffer
CANDU	CANada Deuterium Uranium
CANLUB	Thin graphite coating between the fuel pellet and the fuel sheath
CC4	Canadian Concept Generation 4
CC	Constant Climate
CCME	Canadian Council of the Environment
CCM-UC	Copper Corrosion Model for Uniform Corrosion

CE	Common Era
CEAA	Canadian Environmental Assessment Act
CFU	Colony Forming Units
CNSC	Canadian Nuclear Safety Commission
CRT	Container Retrieval Test
C-S-H	In the C-S-H term, the “C” stands for Ca, “S” for Si, and “H” for H_2O. The hyphens indicate that no specific solid phases or proportions are implied.
CSA	Canadian Standards Association
C Steel	Carbon Steel
DBF	Dense Backfill
DDW	Dry Density Weight
DEM	Digital Elevation Model
DFN	Discrete Fracture Network
DGR	Deep Geological Repository
DGSM	Descriptive Geosphere Site Model
EA	Environmental Assessment
EBS	Engineered Barrier System
EBW	Electron-Beam Welding
EC	Environment Canada
E_{CORR}	Corrosion Potential
EDZ	Excavation Damage Zone
Eh	Oxidation Potential
EIS	Environmental Impact Statement
EMDD	Effective Montmorillonite Dry Density
ENEVs	Estimated No Effect Values
EPM	Equivalent Porous Media
ERICA	Environmental Risks from Ionising Contaminants Assessment
FEPs	Features, Events and Processes
FP	Fission Product
FSW	Friction-Stir Welding
GGM	Gas Generation Model
GLFA	Glycol-Lipid Fatty Acid
GM	Geometric Mean

GSD	Geometric Standard Deviation
GSM	Glacial Systems Model
HC	Health Canada
HCB	Highly-Compacted Bentonite
HEPA	High-Efficiency Particulate Air
HIM	Human Intrusion Model
HM	Hydromechanical
IAEA	International Atomic Energy Agency
ICRP	International Commission on Radiological Protection
ID	Inner Diameter
Imp	Impurity
ISO	International Organization for Standardization
LBF	Light Backfill
LGM	Last Glacial Maximum
LHHPC	Low-Heat, High-Performance Concrete
MIC	Microbiologically Influenced Corrosion
MLE	Mean Life Expectancy
NDT	Non-Destructive Testing
NEA	Nuclear Energy Agency
NLFA	Neutral-Lipid Fatty Acid
NOAA	National Oceanic and Atmospheric Administration
NTS	National Topographic System
NWMO	Nuclear Waste Management Organization
OD	Outer Diameter
OFP	Oxygen-Free Phosphorus-doped
O/M	Oxygen/Metal
OPG	Ontario Power Generation
PDF	Probability Density Function
PLFA	Phospho-Lipid Fatty Acid
PPT	Precipitate
PQP	Project Quality Plan
PWR	Pressurized Water Reactor
RH	Relative Humidity

RSM	Radionuclide Screening Model
SCC	Stress Corrosion Cracking
SKB	Swedish Nuclear Fuel and Waste Management Company (Svensk Kärnbränslehantering AB)
SRTM	Shuttle Radar Topography Mission
SSM	Swedish Radiation Safety Authority
STP	Standard Temperature and Pressure
SYVAC3	System Variable Analysis Code
TDS	Total Dissolved Solids
TDZ	Thermal Damage Zone
THM	Thermal-hydraulic-mechanical
TWI	The Welding Institute
UFC	Used Fuel Container
UFPP	Used Fuel Packaging Plant
UFTP	Used Fuel Transportation Package
UofT GSM	University of Toronto Glacial Systems Model
URL	Underground Research Lab
WRA	Whiteshell Research Area

THIS PAGE HAS BEEN LEFT BLANK INTENTIONALLY

APPENDIX A – DESIGN OPTIMIZATION

A.1. Introduction

This report presents an illustrative postclosure safety assessment for a deep geologic repository for used nuclear fuel in a Canadian sedimentary rock geosphere.

Previous Canadian case studies have focussed on crystalline rock settings. The present study is the first detailed postclosure safety assessment of a Canadian repository in sedimentary rock. These results together with other NWMO studies will help support an optimized design that caters specifically to the features of Canadian sedimentary rock environments. Such features include the absence of water conducting features, high groundwater salinity and an extremely low rock hydraulic conductivity limiting water, gas and radionuclide transport.

Information to guide potential design optimization studies is also available from international experience in sedimentary rocks.

A.2. International Sedimentary Rock Concepts

Several countries are considering disposal of used fuel or high level waste in sedimentary rock formations. Some, such as Japan and the UK, are considering both crystalline and sedimentary rock sites. Presently, Switzerland, France and Belgium are well advanced in terms of sedimentary rock design concepts, and have operating underground research facilities. The repository design features considered by Switzerland, France and Belgium are described further below.

A.2.1 Switzerland (Nagra)

Switzerland is presently in a repository siting process. Nagra is proposing to dispose of spent fuel, high level waste and long-lived intermediate level waste in a repository in an Opalinus Clay rock formation (Figure A-1) in Switzerland. The safety concept, described in Nagra (2002), uses a multiple-barrier system to isolate radionuclides from the environment. The components of the system are:

- a stable, durable waste form;
- long-lived containers;
- low-permeability backfill (bentonite clay); and
- low-permeability self-sealing host rock.

The reference sedimentary host rock formation is Opalinus Clay. This rock has a high clay content with low hydraulic conductivity. It will self-seal in the presence of water.

In the reference design concept (Nagra 2012), placement tunnels are aligned in parallel and accessible by a ramp. The tunnel walls are stabilized with rock bolts and steel mesh, with the possibility that a cement-based liner will also be used. Used fuel containers are to be placed horizontally in tunnels, on bentonite blocks with the remaining space backfilled with bentonite pellets.

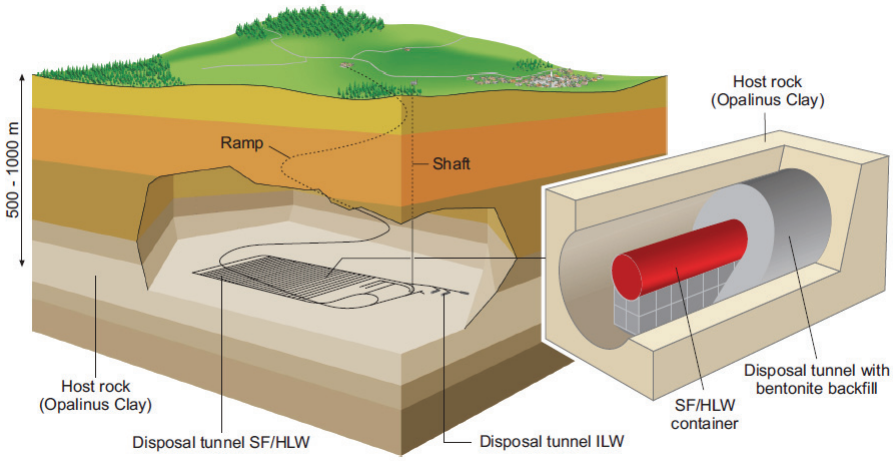

Note: From Nagra (2009).

Figure A-1: The Swiss Repository Concept in Opalinus Clay

The reference spent fuel containers are cast iron containers about 5 m long and 1.05 m diameter, with a 0.14 m wall thickness (Nagra 2012). The minimum required container lifetime is 1000 years; however, their design life is 10,000 years (Nagra 2012). Hydrogen gas produced from the corrosion of iron is assumed to disperse along the repository access structures through gas-permeable seals and also into the surrounding Opalinus Clay, in part through the porosity and in part through dilation-and-resealing in this high clay-content material (Nagra 2009).

Nagra is also considering a copper container with a steel insert as an alternative container concept (Nagra 2009, 2012).

A.2.2 France (Andra)

The French program is presently preparing a repository license application. Andra is proposing to dispose of spent fuel, vitrified high-level waste and long-lived intermediate-level waste in a deep geologic repository in a Callovo-Oxfordian clay formation. Like other organizations, Andra implements a multiple-barrier safety approach.

The main used fuel waste form (C waste) is in vitrified glass as a result of reprocessing. The reference C waste containers are made from P235 non-alloyed steel, about 1.6 m long × 0.6 m diameter, and 0.055 m thick. The container is expected to last at least 4,000 years (Andra 2005). The containers are placed horizontally in steel-lined tunnels within the clay. France will also have unreprocessed spent fuel (CU wastes). The reference CU waste containers for UO_2 fuel are 5.99 m long × 1.25 m diameter, and 0.110 m thick unalloyed steel. These are designed to be leak tight for 10,000 years. Figure A-2 shows the C waste container and placement concept, and Figure A-3 shows the CU waste container and placement concept (Quintessa 2007).

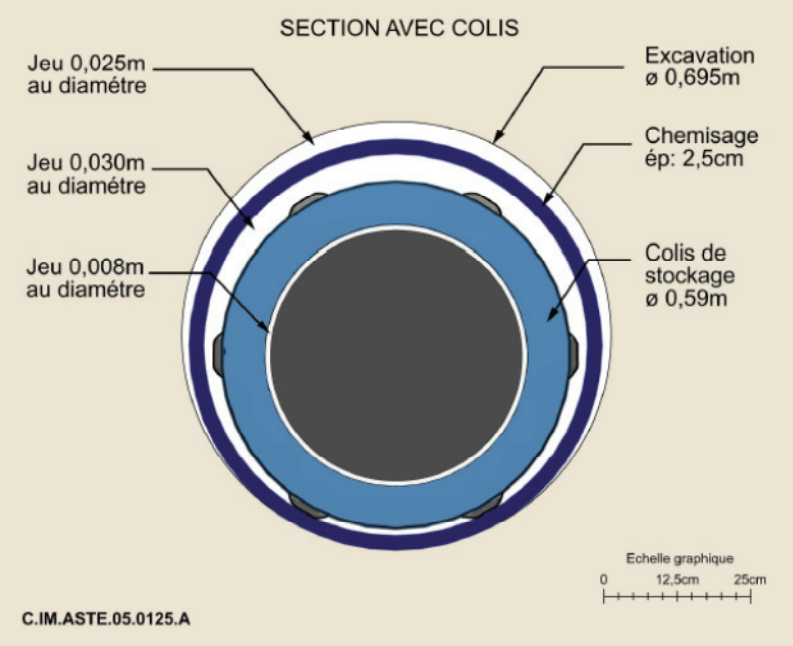

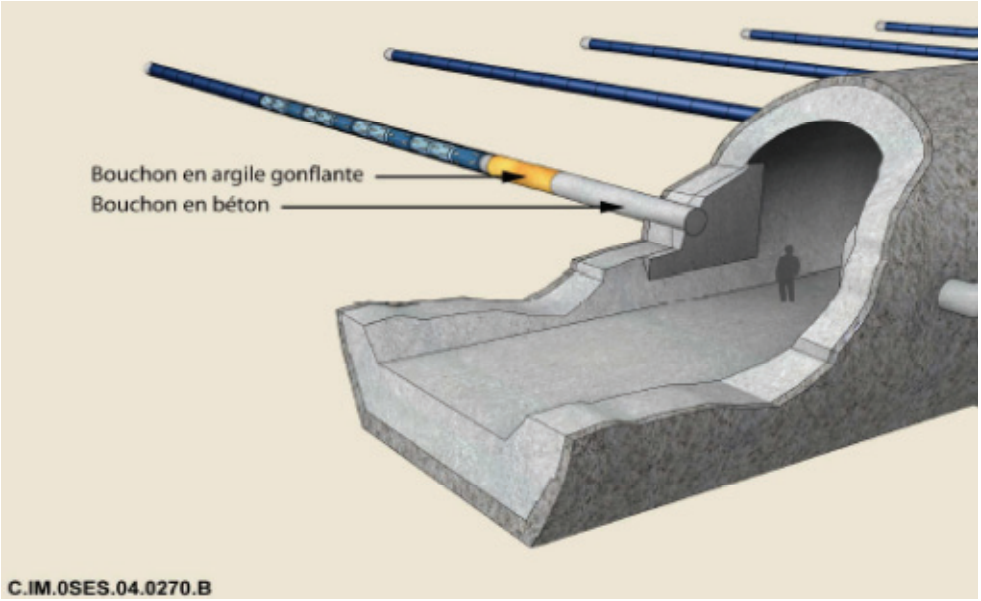

Note: From Andra (2005).

Figure A-2: The French Repository Concept for Vitrified HLW in Callovo-Oxfordian Clay

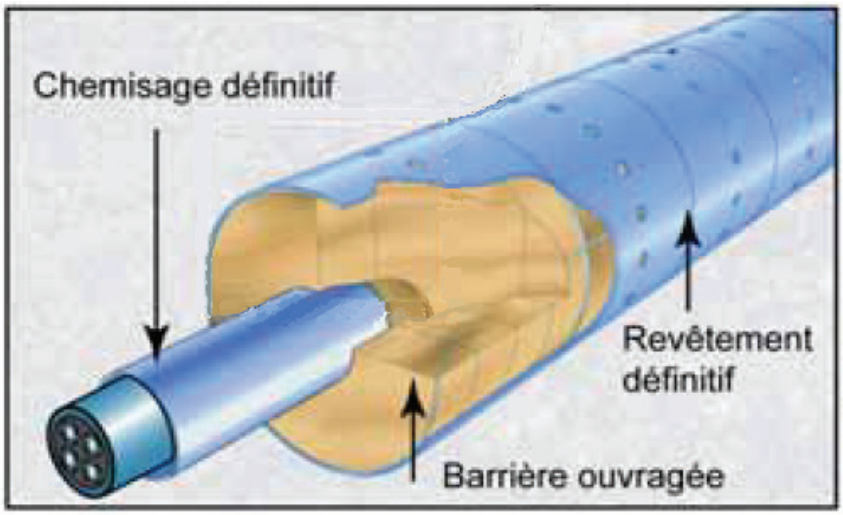

Note: From Andra (2005).

Figure A-3: The French Repository Concept for Spent Fuel in Callovo-Oxfordian Clay

A.2.3 Belgium (ONDRAF/NIRAS)

In Belgium there is no identified repository site. However, the potential host formations studied by ONDRAF/NIRAS for a geological repository are currently limited to poorly indurated argillaceous formations, with the Boom Clay as a reference host formation and Ypresion clays as an alternative. Geological conditions in the Boom Clay are being investigated at the underground research laboratory at SCK·CEN in Mol.

The repository concept also relies on multiple barriers. The reference design concept is referred to as the "supercontainer" (Yu and Weetjens 2009). The container stores both vitrified waste canisters and spent fuel assemblies (Figure A-4).

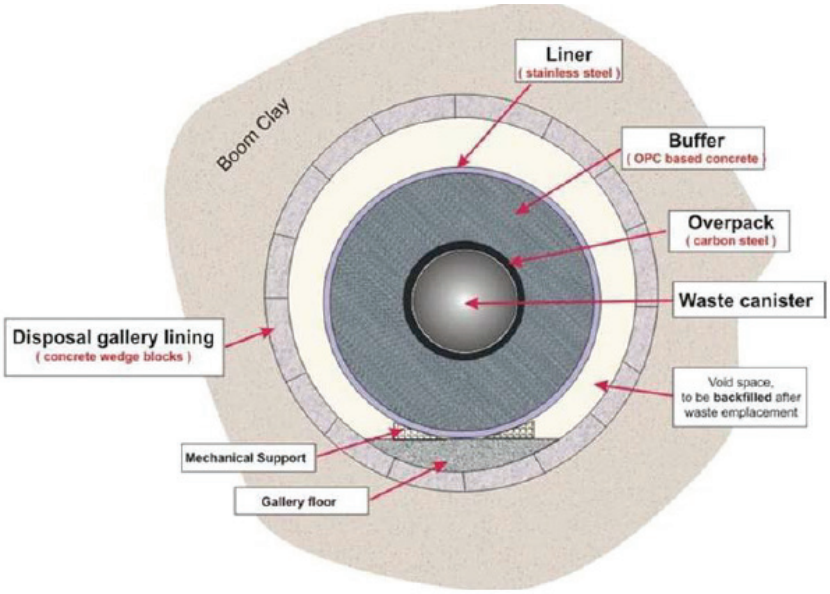

Note: From Mallants and Jacques (2004)

Figure A-4: Cross Section View of the Belgian Supercontainer Concept for HLW

The supercontainer design consists of a carbon steel overpack surrounded by a Portland cement-based concrete buffer and a stainless steel outer liner. Concrete has been chosen for the buffer because, under the high-pH conditions due to the surrounding concrete, the carbon steel overpack will undergo uniform and slow corrosion. This supercontainer has a minimum lifetime covering at least until the end of the thermal phase.

In the long term, hydrogen gas will be produced from steel corrosion. Experiments suggest the gas is released via preferential pathways opened in the Boom Clay. Since this is a soft clay, these pathways can be created at relatively low pressures, and they will close up and disappear after the gas passes (Yu and Weetjens 2009). The Boom Clay self-seals, with the clay returning to its original low-transport properties.

A.3. Key Differences

The above discussion indicates that the overall conceptual approach for sedimentary rock in other countries is the same as that adopted in Canada, that is, deep disposal in a multiple-barrier repository.

Although all of these cases involve low-permeability sedimentary rock, there are important differences in the rock properties. In particular, these European clay formations are softer than the shales and limestones under consideration in Canada. Furthermore, the Canadian sedimentary rock groundwaters are more saline.

Another difference is the container design. All containers rely on steel for structural support. However, the conceptual design considered in this study has a copper outer shell for corrosion resistance, whereas the other sedimentary rock countries are primarily considering steel-only

containers. The very low permeability and lack of fractures in sedimentary rocks supports their container design basis.

The use of steel-only containers has potential benefits. The main advantages cited are: well-understood and generally uniform corrosion under repository conditions; well-understood and readily available engineering material, leading to ease of manufacture, welding, and cost-effectiveness; and the ability of the thick steel overpack to provide a radiation shield (Quintessa 2007). The main disadvantage is that the predicted lifetime of steel containers is less than that predicted for copper shell containers. Generation of hydrogen gas may require accommodation within the design of the repository, depending on the rate of generation.

International experience indicates that robust safety cases that exceed regulatory requirements can be developed for steel-only containers. Work is underway to assess whether this is possible in relevant Canadian sedimentary rock formations. Other design optimizations are also under study, including use of copper coatings, alternative container size and alternative container placement methods.

A.4. References for Appendix A

Andra. 2005. Safety Evaluation of a Geological Repository. Agence Nationale Pour La Gestion. Dossier 2005 Argile. Paris, France.

Mallants, D. and Jacques, D., 2004. Performance assessment for deep disposal of low and intermediate level short-lived radioactive waste in Boom Clay, SCK•CEN-R-3793. Mol, Belgium

Nagra. 2002. Project Opalinus Clay, Safety Report. Nagra Technical Report 02-05. Nagra Wettingen, Switzerland.

Nagra. 2009. A Review of Materials and Corrosion Issues Regarding Canisters for Disposal of Spent Fuel and High-Level Waste in Opalinus Clay. National Cooperative for the Disposal of Radioactive Waste Technical Report 09-02. Wettingen, Switzerland.

Nagra. 2012. Canister Design Concepts for Disposal of Spent Fuel and High Level Waste. Nagra Technical Report TR-12-06. Wettingen, Switzerland.

Quintessa. 2007. International Precedents for HLW/SF Iron Canister Concepts; Review and Consideration of Applicability in the UK Context. Quintessa Limited report for Nirex. QRS-1376A-1 v2.0. Henley-on-Thames, UK.

Yu, L. and E. Weetjens. 2009. Summary of Gas Generation and Migration. SCK-CEN External Report SCK-CEN-ER-106. Mol, Belgium.